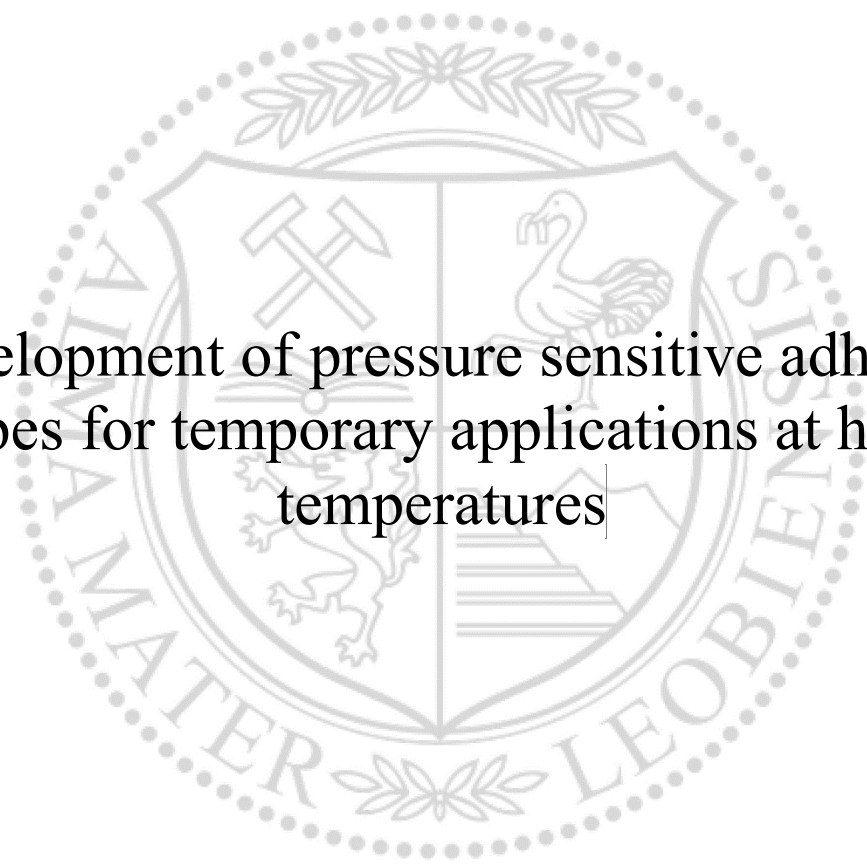




|Chair of Chemistry of Polymeric Materials|

Doctoral Thesis



|Development of pressure sensitive adhesive
tapes for temporary applications at high
temperatures|

|Dipl. Ing. Christine Bandl, BSc|

|September 2019|

Affidavit

I declare on oath that I wrote this thesis independently, did not use other than the specified sources and aids, and did not otherwise use any unauthorized aids.

I declare that I have read, understood, and complied with the guidelines of the senate of the Montanuniversität Leoben for "Good Scientific Practice".

Furthermore, I declare that the electronic and printed version of the submitted thesis are identical, both, formally and with regard to content.

Leoben,

(Date)

.....

(Signature)

Es gibt kein größeres Hindernis des Fortgangs in den Wissenschaften als das Verlangen, den Erfolg davon zu früh verspüren zu wollen.

Georg Christoph LICHTENBERG

Acknowledgements

Firstly, I thank Univ.-Prof. Mag. rer. nat. Dr. Wolfgang Kern for the academic support and the opportunity to write my thesis about this interesting and manifold topic. Furthermore, I owe thanks to my supervisor Priv.-Doz. Dipl.-Ing.Dr techn. Sandra Schlögl for her great support and all the inspiring discussions as well as for her patience while answering all my questions.

I want to thank Dr. Hannes Voraberger and Dr. Gerald Weidinger from AT&S, who set up the underlying research project and kindly provided access to machines and materials required for my experiments. In addition, I thank Gerald for his helpful advices and his support throughout my stays at the company partner and the whole AT&S team for the friendly and cooperative atmosphere.

Moreover, I thank my colleagues from the PCCL and the Montanuniversitaet Leoben for an inspiring and motivating atmosphere as well as for all the nice lunch breaks and conversations. In particular, I want to thank Andrea for our detailed discussions about work and her readiness to listen me. Special thanks go to my dear friend Simone, who believed in me and built me up whenever I was desperate or about to give up.

Also, I want thank my colleagues and friends from VSC and the DK-team for all the amazing moments we had on the volleyball court and the funny afternoons and evenings we spent. This was exactly the balance I needed during writing my thesis. Especially, I thank Eveline for all the good advices, encouraging words and our daily messages.

Furthermore, I owe thanks to my family, who always supports me unconditionally. Special thanks I dedicate to my mum for all the patience and understanding and for reminding me what I am capable of. Deep gratitude I direct to my dad, for all the advice and honest discussions we had and for making every effort to guide me the right way and show me future perspectives. I also want to thank my sister Katharina, who is always there for me and believed in me when I doubted myself.

Finally, I thank my love Christopher, with whom I can be myself and who brought a smile back to my face. In particular, I want to thank him for encouraging me and understanding that I had to spend so many hours on writing instead of being with our little family.

Abstract

Besides their application as decorative films, tapes and sticky notes in household and office, pressure sensitive adhesive (PSAs) tapes are widely used in various industries. Typical applications include surface protection, labeling, packaging, the assembly of automotive parts, the construction of printed circuit boards (PCBs) and the manufacture of electronic devices. In general, PSAs are based on elastomers and visco-elastic polymers such as natural and synthetic rubbers, polyacrylates, polysiloxanes, etc., which may be formulated with additives such as tackifiers, plasticizers, stabilizers, fillers and pigments.

In the present work, a PSA tape for temporary applications in the microelectronic industry is designed. The adhesive has to provide high initial tack and adhesive strength during use, while easy and clean removability after exposure to high temperatures (200 °C) and pressures (20 bar) are required in the end of the application. These requirements are met by adjustment of the adhesive properties of the PSA and the incorporation of a release function, enabling debonding on demand. The latter is realized by UV-triggered crosslinking, which decreases adhesion but increases cohesion and the glass transition temperature (T_g) of the adhesive.

Firstly, adhesive polymers based on polyacrylics and epoxides are synthesized. The composition of the polymers is varied in order to adjust the adhesive properties. Moreover, aromatic monomers are incorporated to increase the thermal stability of the adhesives, while vinyl and acryl groups are introduced to the side chains to provide photo-reactive moieties for UV-crosslinking. The synthesized polymers are characterized by IR- and NMR-spectroscopy as well as by GPC, TGA and DSC.

In the second part of this thesis, PSA tapes are prepared by coating the adhesive polymers onto PET carriers. Based on first adhesion experiments, it was decided to use acrylic polymers, which are blended with multifunctional acrylic monomers and a photoinitiator in order to generate semi-interpenetrating networks (semi-IPN) upon UV-irradiation. The photocuring kinetics of the adhesive layers in dependence of the PSA formulation is characterized by IR-spectroscopy. Moreover, DSC and TGA measurements provide information about the T_g and the thermal stability of the respective adhesive layers. The performance of the prepared PSA tapes and their removability after exposure to temperature ≤ 240 °C is evaluated by the use of optical light microscopy. In the course of these experiments, the impact of the substrate surface quality, the PSA composition, different processing parameters and the preparation method was examined. To summarize the most important findings, the removability of the PSA tape is improved by the use of high T_g adhesive polymers and highly functional acrylic monomers, which yield highly crosslinked semi-IPN with high cohesion. This is advantageous with regard to

-Abstract-

interactions with the adherent, which is influenced by both, the chemistry and the topography of the substrate. Moreover, corona treatment of the carrier and the application of adhesion promoters significantly improved the anchorage of the PSA to the carrier and in turn the removability of the PSA tape. Two methods for tape preparation were elaborated, providing different crosslinking gradients, which influence the performance in dependence of the surface quality of the substrate.

The developed photo-sensitive PSA tape meets all requirements stated above providing sufficient adhesive strength during application and clean peel from roughened and adhesion promoted surfaces (BondFilm® treated copper) without leaving residues after application at 180 °C for one hour.

Kurzfassung

Neben der Verwendung von Haftklebstoffen in Haushalt und Büro, wo sie in Form von Klebebändern, Dekorfilmen und Haftnotizen eingesetzt werden, gibt es auch eine Vielzahl an industriellen Anwendungen. Diese umfassen den Schutz von Oberflächen, das Etikettieren und Verpacken, die Montage von Autoteilen, sowie den Einsatz in der Mikroelektronikindustrie. Als Basis für Haftklebstoffe werden (visco-) elastische Polymere wie z.B. Kautschuke, Polyacrylate oder Polysiloxane verwendet. Diesen können beim Formulieren des Klebstoffes Additive wie Klebrig- oder Weichmacher, Stabilisatoren, etc. hinzugefügt werden. In der vorliegenden Arbeit wird ein Klebeband für temporäre Anwendungen in der Mikroelektronikindustrie entwickelt. Dabei muss das Klebeband zunächst eine hohe Klebkraft aufweisen, und am Ende des Prozesses, bei dem hohe Temperaturen und Drücke (bis 200 °C, 20 bar) herrschen, rückstandslos entfernt werden können. Diese widersprüchlichen Anforderungen werden einerseits über die Anpassung der Klebeeigenschaften des Haftklebers und andererseits über die Einführung einer Release-Funktion, realisiert. Letztere wird mittels UV-induzierter Vernetzung des Klebstoffes umgesetzt, die zur Verringerung der Klebkraft sowie zur Erhöhung der Kohäsion und der Glasübergangstemperatur (T_g) des Klebstoffes führt.

Zunächst werden Acrylat-Copolymere und Epoxy-Harze synthetisiert und als Basis für den zu entwickelnden Haftklebstoff verwendet. Die Klebeeigenschaften der Polymere werden über ihre Zusammensetzung variiert. Außerdem werden aromatische Monomere eingebaut, um die thermische Stabilität des Klebstoffs zu erhöhen. Vinyl- bzw. Acryl-Gruppen in den Polymerseitenketten dienen als photo-reaktive Einheiten, welche während dem UV-induzierten Release vernetzen. Die hergestellten Polymere werden mit Hilfe von IR- und NMR-Spektroskopie als auch mit GPC, TGA und DSC charakterisiert.

Der zweite Teil dieser Arbeit befasst sich mit der Herstellung und der Funktionsprüfung des entwickelten Klebebands. Dazu werden PET-Trägerfolien mit Lösungen der synthetisierten Polymere beschichtet und auf unterschiedlichen Substraten appliziert. Erste Ergebnisse zeigen einen deutlichen Vorteil der Acrylat-Klebstoffe. Weitere Entwicklungsschritte führen zum Einsatz von Klebersystemen, die sich aus einem Acrylat-Copolymer, multifunktionellen Monomeren und einem Photoinitiator zusammensetzen und unter Bestrahlung mit UV-Licht „semi-interpenetrating networks“ (semi-IPN) ausbilden. Die Kleberschichten werden hinsichtlich ihrer Reaktionskinetik (IR), ihres T_g (DSC) und ihrer thermischen Stabilität (TGA) untersucht. Die Funktion und die Ablösbarkeit der Klebebänder nach Anwendung bei Temperaturen bis 240 °C werden mit Hilfe von Lichtmikroskopie beurteilt. Dabei werden der Einfluss der Substratoberfläche, der Klebstoffzusammensetzung und der Herstellungsmethode, sowie die Auswirkung

verschiedener Prozessparameter untersucht. Die Ergebnisse zeigen, dass die Ablösbarkeit durch den Einsatz von Polymeren mit hohem T_g und hoch funktionellen Monomeren verbessert wird, da diese Formulierungen unter UV-Bestrahlung in hohem Grad vernetzen. Dies ist vorteilhaft bezogen auf Wechselwirkungen zwischen Kleber und Substrat, welche sowohl von der chemischen Zusammensetzung als auch von der Topographie des Substrats beeinflusst werden. Zusätzlich verbessern Corona-Behandlung des Trägers und die Anwendung von Haftvermittlern die Anbindung des Klebstoffes an den PET-Träger und in Folge dessen auch die Ablösbarkeit des Klebebands. Es wurden zwei Methoden zur Herstellung von Klebebändern entwickelt, aus denen sich unterschiedliche Vernetzungsgrade der Kleberschicht ergeben.

Der entwickelte UV-reaktive Haftklebstoff erfüllt alle genannten Anforderungen und bietet somit ausreichende Klebkraft während der Anwendung, sowie einfache und rückstandsfreie Entfernung nach Prozessierung bei 180 °C auf rauen und adhäsionsbegünstigten Oberflächen.

List of abbreviations

Abbreviation	Meaning
AA	acrylic acid
AIBN	azobisisobutyronitrile
ATR	attenuated total reflection
3-APTMS	3-acryloxypropyl trimethoxysilane
BA	butyl acrylate
BHT	butylated hydroxytoluene
CDCl₃	deuterated chloroform
DPEPHA	dipentaerythritol penta/hexaacrylate
DSC	differential scanning calorimetry
DTMPTA	di(trimethylolpropane) tetraacrylate
EGPEA	ethylene glycol phenyl ether acrylate
2-EHA	2-ethylhexyl acrylate
2-EHGE	2-ethylhexyl glycidyl ether
EtAc	ethyl acetate
EtOH	ethanol
FT-IR	Fourier transformed infrared spectroscopy
GIPE	glycidyl isopropyl ether
GMA	glycidyl methacrylate
GPC	gel permeation chromatography
HDPE	high density polyethylene
HQ	hydroquinone
H₂SO₄	sulfuric acid
IBA	isobornyl acrylate
LDPE	low density polyethylene
MA	methyl acrylate
3-MAPTMS	3-methacryloxypropyl trimethoxysilane
MEHQ	hydroquinone monomethyl ether
MeOH	methanol
MF	melamine- formaldehyde adhesive/resin
M_n	number average molecular weight
M_w	weight average molecular weight
[M₀]	initial monomer concentration
NaPS	sodium persulfate
NBR	nitrile butadiene rubber
NMR	nuclear magnetic resonance
NR	natural rubber
p(AA)	polyacrylic acid

-List of abbreviations-

PAG	photo acid generator
PC	polycarbonate
PCB	printed circuit board
PDI	polydispersity index
PE	polyethylene
PET	polyethylene terephthalate
PETA	pentaerythritol tetraacrylate
PF	phenol-formaldehyde adhesive/resin
PP	polypropylene
PS	polystyrol
PSA	pressure sensitive adhesive
PSP	pressure sensitive product
PUR	polyurethane
PVC	polyvinyl chloride
R_p	rate of polymerization
rt	room temperature
RTV	room temperature vulcanizing
S_a	average roughness
SBR	styrene-butadiene rubber
S_q	root mean square roughness
T_g	glass transition temperature
T_{gON}	onset of glass transition
TGA	thermogravimetric analysis
THF	tetrahydrofuran
TMAB	tetramethylammonium bromide
TMESi² BAPO	bis(acylphosphane)oxide-4-(trimethoxysilyl)butyl-3-[bis(2,4,6-trimethylbenzoyl)phosphinoyl]-2-methyl-propionate
T_{MID}	point of maximum degradation/decomposition
TMPTA	trimethylolpropane triacrylate
T_{END}	end of degradation/decomposition
T_{ON}	onset of degradation/decomposition
UF	urea- formaldehyde adhesive/resin
VMA	vinyl methacrylate
VOC	volatile organic compounds
VP	1-vinyl-2-pyrrolidone
XPS	X-ray photoelectron spectroscopy

Table of Contents

Affidavit	II
Acknowledgements	IV
Abstract	V
List of abbreviations	IX
Table of Contents	XI
1. Introduction.....	1
2. Scope of the thesis	3
3. Theoretical background.....	5
3.1. History of adhesives.....	5
3.2. Adhesion and adhesives.....	6
3.2.1. Definition of adhesion and cohesion	6
3.2.2. Adhesion theories	7
3.2.3. Adhesion performance	11
3.2.4. Adhesion enhancement	12
3.2.5. Classification of adhesives.....	19
3.3. Pressure sensitive adhesives and products	35
3.3.1. Pressure sensitivity	35
3.3.2. Characterization of PSAs.....	37
3.3.3. Basic materials for pressure sensitive adhesives	38
3.3.4. Manufacture of pressure sensitive products	40
3.4. Photochemistry.....	43
3.4.1. Definition and importance of photochemistry	43
3.4.2. Photopolymer technology and photo-polymerization.....	44
3.5. Printed circuit boards	53
3.5.1. The history of printed circuit boards	53
3.5.2. Construction of printed circuit boards.....	54
4. Strategies and approaches	60
5. Experimental part.....	62

-Table of Contents-

5.1.	Chemicals and materials.....	62
5.2.	Machines and devices	66
5.3.	Synthesis of adhesive polymers.....	71
5.4.	Physico-chemical characterization of the synthesized polymers	75
5.5.	Preparation of UV-curable PSA tapes	76
5.6.	Characterization of the PSA tapes	79
5.7.	Characterization of the substrates and carrier materials.....	82
6.	Results and discussion.....	84
6.1.	Synthesis and characterization of the adhesive copolymers	85
6.1.1.	Acrylic Copolymers	85
6.1.2.	Polyethers.....	96
6.1.3.	Conclusion about the synthesis of adhesive copolymers.....	100
6.2.	Design of photo-curable PSA tapes.....	101
6.2.1.	Characterization of the adhesive layer.....	103
6.2.2.	Basic steps of tape preparation.....	118
6.2.3.	Conclusion about the impact of the chemical composition and summary of the basic steps in PSA development.....	124
6.3.	Performance of the designed PSA tapes.....	126
6.3.1.	Impact of the surface quality of the joint substrate.....	126
6.3.2.	Influence of the adhesive composition	132
6.3.3.	Impact of process parameters	141
6.3.4.	Influence of the preparation method.....	146
6.3.5.	Conclusion about the adhesion performance.....	148
6.1.	Improvement of the removability by the use of adhesion promoters.....	152
6.1.1.	Modification of the PET carrier – application of adhesion promoters	155
6.1.2.	Covalent attachment of the adhesive layer to the modified carriers	160
6.1.3.	Adhesion strength of the PSA tapes.....	160
6.1.4.	Performance of tapes with modified carriers	161
6.1.5.	Conclusion about the application of adhesion promoters and their impact on the removability of the tapes.....	167

-Table of Contents-

7. Conclusion	169
8. Outlook	173
9. List of Figures.....	174
10. List of Tables	179
11. Literature	181
12. Curriculum Vitae.....	196
13. Publications.....	197
14. Appendix.....	199

1. Introduction

Nowadays, adhesion is an important phenomenon in nature as well as in technology. Adhesives may be applied as solutions in organic solvents or water, as emulsions or dispersions, as reactive systems or 100 % solids such as hot melts for example. Adhesive bonding plays an important role in many industries, including packaging, building and construction, automotive and commercial vehicles, electronics, the medical and paper sector [1] as well as in office and household. A large portion is applied in form of pressure sensitive adhesive (PSA) tapes.

In 2015, 43.3 billion square meters of PSA tapes were produced worldwide. [2] According to market analysis, the global market of PSA tapes amounted to 50.12 billion USD in 2017 and is forecast to grow with a compound annual growth rate (CAGR) of 6.22 % from 2017 to 2022, reaching 67.76 billion USD at the end of this period. While the Asia Pacific holds the biggest market share of 42 %, also Europe (33 %) and North America (17 %) are important for the PSA tape industry. The market growth is driven by the high demand in various application fields, including packaging, electrical & electronics, transportation, construction as well as the medical & healthcare sector. The highest increase is estimated for the Asia Pacific due to fast growing industrialization in this region. In terms of industry segments, the electric and electronic sector is expected to grow at the highest CAGR rate in 2017-2022. Here, PSA tapes are applied to mount components to printed circuit boards (PCBs), in the manufacture of consumer electronic devices (mobile phones, cameras, etc.) and for electrical interconnections and assemblies. [3,4]

Furthermore, PSA tapes are used for temporary surface protection (masking tape), packaging, labeling, the assembly of automotive parts and toys as well as in medical products such as plasters, surgical drapes, dermal dosage systems and biomedical electrodes. Another important sector is represented by household and office, where PSAs are applied as decorative films, double or single sided adhesive tapes or in form of sticky notes. [1,5–12]

For temporary applications tapes are required to exhibit high holding power in order to ensure reliable bonding during use and simultaneously easy and clean peel in the end of the application. [13] This can be achieved by precise adjustment of the chemical composition of the adhesive and/or by the incorporation of a release function, which leads to the reduction of the adhesive strength by exposure to an external trigger. One example is the use of increased temperatures, which weaken the adhesive joint by heating above the T_g of the adhesive (softening). [14,15] Moreover, thermally induced decomposition can be utilized to degrade the polymer backbone of the adhesive and/or to initiate the development of gases, which consequently reduce the adhesive bond strength at the

interface. [15] Also, thermally responsive compounds can be added, which cause swelling of the adhesive, undergo phase changes or decompose upon heating. Molten additives act as plasticizers, which dilute, swell or even break crosslinking sites in the adhesive matrix, while their decomposition leads to the development of gases or water vapor, weakening the bondline by the related expansion pressure. [16] Another approach is the incorporation of expandable fillers or foaming agents. Debonding is achieved by volumetric expansion of the compounds, which must be sufficiently high to overcome elastic modulus and toughness of the adhesive. [15,17] Along with thermally triggered systems, also cooling can be applied to detach adhesive sheets. In one approach, an acrylic based adhesive containing a side chain crystallizable polymer (acrylic acid alkyl esters with 16-22 carbon atoms), which reduces its adhesive strength by cooling below the melting transition temperature ($\sim 35\text{ }^{\circ}\text{C}$), was developed. [18]

Another important and widely used external stimulus is represented by irradiation with UV- or visible light. The adhesive strength is either reduced by photo-crosslinking of the adhesive formulation, photo-induced degradation of the adhesive polymer or photo-triggered phase changes. [19] Photo-induced crosslinking is related with an increase of the molecular weight, cohesion and T_g as well as reduced wetting and adhesive strength. [20–28] Typical UV- or Vis-switchable adhesives are based on (meth)acrylic compounds [22,27–34] and employ the formation of interpenetrating or semi-interpenetrating networks [22,32,33] or the reversible dimerization of coumarine derivatives [35,36]. On the contrary, photo-labile groups such as *o*-acyloxime [19] or *o*-nitrobenzyl compounds [36–38] can be incorporated to enable photo-triggered degradation of the adhesive polymer. Alternatively, photo-induced phase changes based on *cis-trans*-isomerization of multi-azobenzene sugar-alcohol derivatives can be utilized to fix and unfix adhesive joints via reversible liquefaction (UV) and solidification (Vis). [39–41]

Externally induced debonding can also be induced electrically, as realized with an amine cured epoxy resin, which comprises ionic conductivity. Debonding at the adhesive-anode bondline is achieved upon application of a low power current inducing polarization of the adhesive boundary layer. [15,42,43] Further possibilities to realize debonding on demand include the use of shape memory polymers, which can be fixed to temporary shapes and recover upon external stimuli such as elevated temperatures or UV-irradiation. [44] Also, magnetism can be employed as an external trigger. Therefore, nano-scaled fillers of iron oxide, which are embedded in silicon dioxide, are admixed to the adhesive. Upon the action of a rapidly alternating magnetic field the particles start to oscillate and thus generate heat, which in turn starts heat induced debonding. [15,45–47] In addition, there are dual cure systems, which require a combination of UV-irradiation and heat to trigger the debonding mechanism. [48–52]

2. Scope of the thesis

A pressure sensitive adhesive (PSA) tape for temporary application in the production of printed circuit boards (PCBs) was designed. More precisely, the tape will be used in the embedding process to hold small microelectronic components in position until the full curing of the epoxy resin. PCBs consist of alternating layers of copper and epoxy prepregs, which are joined by the application of high temperatures and pressures (see chapter 3.5.2 for more details). Components such as microelectronic chips are incorporated by placing them into cavities of a copper core and subsequent joining with epoxy prepregs and copper foils. During pressing, the epoxy resin cures and consequently fixes the component to the desired position after cooling. However, it is important to ensure an accurate position of the chip until it is fixed by the epoxy resin. For this purpose, the following procedure was pursued (see Figure 1): Firstly, a PSA tape is applied to one side of the copper core, which comprises a void. The component is then placed in the cavity, where it is held in position by the PSA tape. After joining with an epoxy prepreg and a copper foil, the tape is removed. Finally, the second side is joined with epoxy and copper during a second pressing step. Due to the harsh conditions of the joining process, high thermal stability is required of the PSA tape. The adhesive must not decompose or soften at temperatures up to 200 °C. In order to ensure that the component is fixed reliably to the desired position even at high temperatures and pressures (20 bar), the tape must comprise dimensional stability as well as high initial tack and adhesive strength during application. On the contrary, clean removability is required in the end of the application since adhesive residues on the copper core or on microelectronic components would lead to delamination throughout further layer construction and processing.

The aim of this work, was to develop an adhesive system, which comprises the required thermal stability and to find a solution for the contradictory demands of high initial tack and residue-free removability, which is related to low adhesion strength. This was realized by the design of a photo-curable acrylic PSA, which reduces its tack upon UV-irradiation.

-Scope of the thesis-

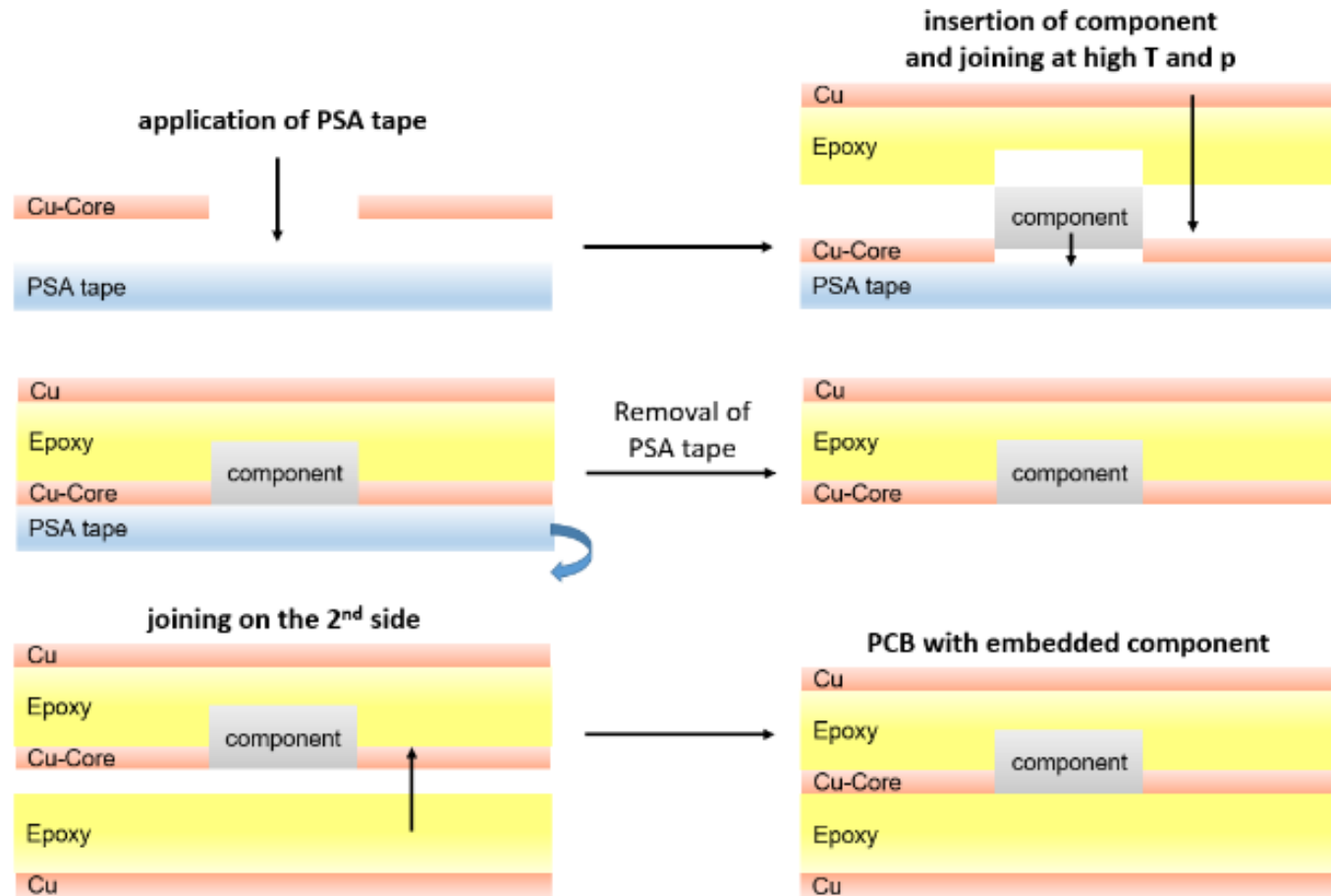


Figure 1: Process for embedding microelectronic components in a PCB by the use of a PSA tape

3. Theoretical background

3.1. History of adhesives

The history of adhesives goes back to the beginning of mankind, where humans observed nature and learned to utilize sticky plants and asphaltic materials to entrap insects, birds and small mammals. Primitive composites of straw or other vegetable material with mud and clay were used to build habitations, which were sealed with mud, clay or snow. Further early adhesives included beeswax, rosin, rubber, shellac, tars and vegetable gums. [53] In 4000 BC asphalt and bitumen were used for constructions by the Mesopotamians and the Babylonians. [1,53,54] The Egyptians utilized a paste of starch and water to build papyrus by joining layers of reed [54] and to manufacture primitive tapes by applying this paste onto cloth strips. [5,53] Moreover, they laminated furniture with animal and casein glues [53] and used gum Arabic from the acacia tree and animal glues as an adhesive. [1,54] As already did the Egyptians, also the Greeks and Romans used resins, pitches, tars and beeswax in ship and boat manufacturing and sealing. [5,53,54] Furthermore, they produced pozzolanic cement from slaked lime with volcanic ash and sand, which was used in the construction of the Pantheon and the Colosseum. [53]

The development of modern bonding industry started in the 17th and 18th century. [1] During the 19th century, casein glues played an important role in aircraft industry and starch adhesives were used on postage stamps. [53] With the development of tires for bicycles and cars the rubber industry began to flourish and adhesives based on natural rubber (NR) were introduced. [5,53] Other important adhesives developed throughout the 20th century include phenolic resins (1930s) and epoxy resins (~1934), which are in use for metal bonding, polyurethanes and acrylates (1937), which represent widely used adhesive classes today, poly(vinyl acetate) (1940s), silicon adhesives (1944) [1,53], which are suitable for applications at both high and low temperatures [5], polyester resins (1950) and polyethylene (PE), which is nowadays the most important hot melt material. (1954). [1,53] Since the 1950s research about adhesive materials accelerated rapidly. In the 1970s, a shift from natural to petroleum derived raw materials was observed and further new materials and products were developed (1980s). In order to answer the arising environmental concerns related to solvent based systems, 100 % solids, water based adhesives and radiation curable systems were developed. [5] In the beginning, industrial application of adhesives relied on solvent based systems [20] until hot melts were introduced in 1940. [5] The industrial use of PSA tapes dates back to the 1920s and 1930s [1,5,53], where a masking tape was firstly applied in the automobile sector. [1] The first PSA tape was based on NR [1,5] and the first transparent tape was made from cellophane. [1] Then, the introduction of self-adhesive labels followed in 1935. [20]

3.2. Adhesion and adhesives

3.2.1. Definition of adhesion and cohesion

According to literature, **cohesion** is defined as the forces, which act between *same* molecules. Thus, it describes the interactions within the *bulk* phase of a solid material (internal strength). [55,56] On the contrary, **adhesion** is defined as the sum of all interatomic and intermolecular forces along an *interface*, resulting in the joining of *dissimilar* materials. Adhesion and cohesion are caused by chemical and physical interactions, including Van der Waals forces, hydrogen bonds, Keesom forces (dipole-dipole) and Debye forces (induced dipole-dipole) as well as covalent bonds, acid-base complex formation and mechanical interactions such as entanglement and interpenetration. [55–57] Since the operating distance of these intermolecular forces is typically lower than 1nm (see Table 1), the atoms and molecules of the adhesion partners have to be brought in close contact for a strong assembly. Therefore, good wetting of the substrate by the adhesive is a prerequisite for good adhesion (see also chapter 3.2.2). [1,55,56] Moreover, it is important to select a proper adhesive system and to clean the substrate surface from dust, greases, oils, moisture, rust, scale, miscellaneous dirt, weak oxides and other foreign materials before joining to ensure that the substrate-adhesive interaction is not disturbed. [1,57]

Table 1: Overview of intermolecular forces, the associated binding energies and operating distances [56,58–60]

type of intermolecular force	binding energy [kJ/mol]	operating distance [nm]
Van der Waals forces	≤ 40	0.3-0.5
Keesom forces	20	0.3-0.5
Debye forces	2-10	0.3-0.5
London forces	0.1-40	0.3-0.5
hydrogen bonds	≤ 50	0.3-0.5
acid-base interactions	20-190	0.3-0.5
metallic interactions	110-260	0.2-0.3
covalent bonds	60-680	0.1-0.2
ionic interactions	560-1000	0.1-0.2

3.2.2. Adhesion theories

Historically, different theories were developed to explain the phenomenon of adhesion. However, each theory explains parts of the relevant adhesion mechanism, but none can universally be applied to all adhesive systems. Thus, in most cases, more than one concept is used to describe the numerous processes contributing to bond formation. Which theory is appropriate, depends on the chemistry of the adhesive and the curing process as well as on the surface composition and morphology of the substrate. [1,6,57]

The classical adhesion theories are summarized in Figure 2. Essentially, there are the mechanical and specific adhesion theories. The latter include adhesion due to chemical bonds, physical interactions as well as diffusion, polarization and electrostatic interactions. [1]

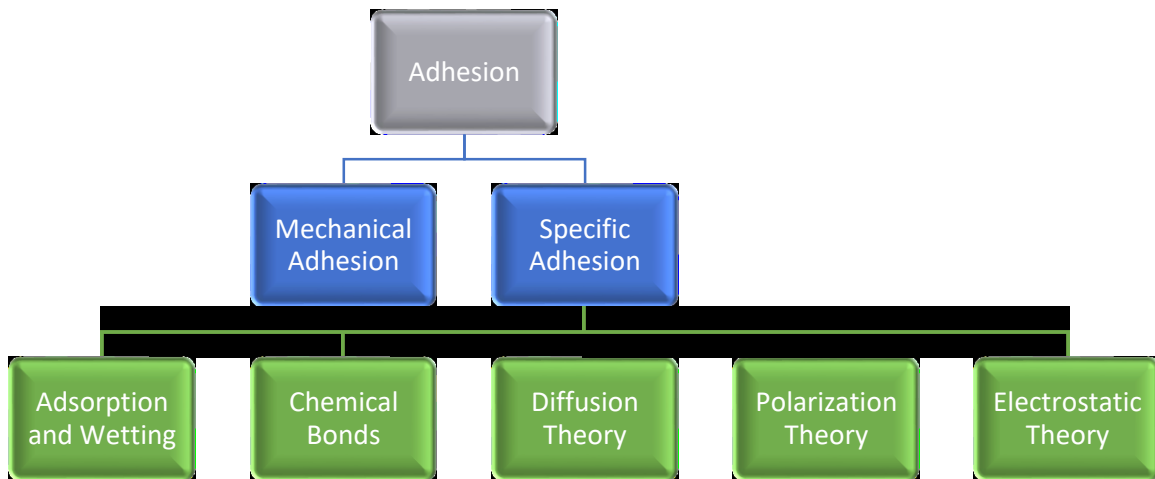


Figure 2: Classical adhesion theories

Mechanical interlocking

The mechanical theory is the oldest of all adhesion theories. It describes adhesion due to mechanical interlocking or keying, which arises from penetration of the adhesive into the morphology of the adherent (pores, cavities, irregularities). The extent of interlocking depends on the porosity of the substrate, the viscosity of the adhesive and the application pressure and duration. This theory is mainly applied to explain bonding of porous

substrates such as wood, paper, textiles and metal-oxide layers (aluminum!). On the contrary, it is not suitable to describe adhesion to smooth surfaces. According to the established view, the effect of mechanical interlocking is of limited importance, though certainly present to some extent. Enhanced adhesion on roughened and abraded surfaces was observed and may be due to (i) improved mechanical interlocking, (ii) cleaning of the surfaces, (iii) the formation of highly reactive surfaces or (iv) an increase of the adhesive-substrate contact area. Basically, it is debated whether mechanical interlocking or the increase of the effective contact area, which enhances other mechanisms, is responsible for strong adhesion on rough surfaces. [1,6,53,55,57,59,61–63]

Physical adsorption and wetting (thermodynamic model of adhesion)

Zisman, Fowkes, Good and Wu (1963) postulated that adhesion via physical adsorption underlies Van der Waals forces acting between the substrate and the adhesive. These secondary valence forces have three components, which contribute to the formation of adhesive joints: the dipole orientation effect by Keesom (between molecules with permanent dipoles), the induced dipole effect by Debye (between a molecule with permanent dipole and a non-polar molecule) and the dispersion effect by London (between non-polar molecules). Since molecular distances are required for these forces to become active, good adhesion is achieved if the adhesive spreads over the surface and wets the substrate completely. Therefore, adhesion is determined by the surface free energies of the adherent and the adhesive. Substrates comprising high or medium surface energy such as metals, wood or paper, can be bonded comparatively easily. In contrast, joining of polymers is more difficult, especially when their surface energy is low. To overcome this restriction, the surface can be pretreated before joining to increase the surface energy of the polymer. Although adhesion via adsorption is the widest applicable theory, it is not universal since PSAs adhere to substrates comprising various chemistries. [6,53,55,57,59,61–63]

Chemisorption

Besides Van der Waals forces, primary valence forces, such as ionic or covalent bonds, can act across the adhesive joints. Typically, the adhesive strength is higher than bond strength achieved by physisorption. In the chemisorption process the adhesive is irreversibly adsorbed to the substrate. The heat of adsorption presumably provides the activation energy required for bond formation. Adhesive bond strength depends on the reactivity of the adhesive and the adherent. The chemisorption theory (since 1960) is used to describe

adhesion of chemically reactive adhesives and the functionality of coupling agents such as organosilanes, while its importance for nonreactive adhesives is not proven. [1,53,55,57,59,62,63]

Diffusion theory

The diffusion theory by Vojutskii (1960) relies to the mutual penetration of adhesive and substrate, generating an adhesive joint. It is mainly used to describe bonding of (viscoelastic) polymers, which inherently offer the required mobility by their chainlike structure. Interdiffusion of polymer chains can be enhanced by heat ($> T_g$; heat welding) or the use of a solvent (solvent-welding) and depends on the applied pressure, the application time and temperature as well as on the viscosity, the molecular size or weight and the reciprocal solubility of the used materials. Typically, the thickness of the diffuse interfacial layer amounts to 1-100 nm. Moreover, this theory is important to understand the adhesion mechanism of pressure sensitive adhesives (PSAs), which offer high molecular mobility. On the contrary, the diffusion theory is not useful to explain adhesion to substrates, which comprise low molecular mobility, such as metals, glass or crystalline and highly crosslinked polymers. [1,6,53,55,57,59,61–63]

Polarization theory

The polarization theory proposed by De Bruyne (1935) is the forerunner of the electrostatic theory. It considers interactions between permanent and induced dipoles and the related electrostatic attraction forces, which are stated to contribute to all adhesion processes of specific adhesion. Thus, the focus is set to Keesom and Debye forces acting between polymers, which comprise heteroatoms such as O, N or F. [1,56,63]

Electrostatic theory

Electrostatic adhesion was introduced by Derjaguin (1950), who describes the formation of an electric double layer at the adhesive-substrate interface resulting from the different electronic band structures of the two materials. Thus, the adhesive system is considered as a plate capacitor. As the adhesive and the substrate get in close contact, electrons are transferred to balance the Fermi levels (potential difference). Adhesion is accomplished by Coulomb attraction forces acting across the electric double layer. While this theory plausibly explains polymer-metal adhesion, it does not (primarily) contribute to the

adhesive strength in non-metallic adhesive systems. However, one has to bear in mind that electrostatic adhesion is a temporary phenomenon since the charge transfer compensates the potential difference, which is responsible for the attractive forces between adhesive and adherent. [6,53,56,57,59,61–63]

Besides the classical adhesion theories, also special cases are discussed in literature. **Liquid adhesion** is used to interpret the mechanism of pressure sensitive adhesion and the initial tack of liquid adhesives. It considers a thin film of a highly viscous liquid, generating adhesion in a process, in which separation of adhesive and adherent results in a flow in the narrow gap and is required to overcome a considerable resistance. [6]

Another special theory deals with the formation of **weak boundary layers** and their impact on adhesion performance. The theory of weak boundary layers proposes that clean surfaces give rise to strong adhesive joints, while the presence of contaminants such as rust, oil and greases, which concentrate near the adhesive-substrate interface, disturbs adhesion by the formation of cohesively weak layers in either the adhesive or the adherent. [55,57] According to Bikermann, physical, physicochemical or chemical phenomena at the adhesive-substrate interface lead to the formation of an altered or modified interphase, which comprises properties different to those of the bulk materials (lower cohesion strength). This so called weak boundary layer ranges from the molecular level to the microscopic scale and originates from the adhesive, the adherent, the environment or combinations of these factors. It develops upon (i) orientation of chemical groups or over-concentrations of chain ends at the adhesive-substrate interface, (ii) migration of low molecular weight fractions or additives towards the interface, (iii) growth of trans-crystalline structures, (iv) formation of pseudo-glassy zones, which result from the reduction of the chain mobility by strong interactions or (v) modification of the thermodynamics or kinetics of polymerization or the crosslinking reaction at the interface via preferential adsorption of reactants or catalytic effects. Examples for weak boundary layers are (i) air, which is trapped between adhesive and adherent if the surface is not wetted properly, (ii) contaminants such as impurities, additives or pollutants, (iii) low molecular weight compounds, which moved towards the interface or (iv) products of reactions between air and the adhesive/the adherent (development of loosely bound metal oxides). The cohesive strength of this weak boundary layer is seen as the main factor determining the level of adhesion. Adhesion loss is more favorable to occur due to cohesive failure within the weak material layer than via fracture propagation along the adhesive-substrate interface. Although there is some criticism against this theory, the creation of interfacial layers has attracted much attention in the recent years. [53,56,57]

3.2.3. Adhesion performance

To get an idea about the adhesion performance, the adhesion strength and the prevalent failure mode have to be considered. The adhesion strength between a surface coating and a substrate can be analyzed by over 300 test methods, which can either be destructive (majority) or nondestructive. With destructive methods a load is applied to the coating in some manner and the resulting damage is analyzed. With nondestructive methods a specific portion of energy, which allows for conclusions about mechanisms at the interface, is identified after applying an energy pulse to the joined system. In this chapter, a short overview of the most important test methods for the determination of adhesion strength is summarized:

The most prominent adhesion test method is the **peel test**. It employs a tensile test apparatus and a suitable hardware to apply the peel force load and to maintain the peel rate and angle. [64] Thereby, the interfacial region is subjected to tensile and shear load and a force plot allowing for conclusions about the adhesive strength of the joined system is obtained. [6,64] In general, any peel angle is possible, but typical setups use peel angles of 90° or 180°. Moreover, climbing drum or T-peel setups are used to test rubber coatings or two flexible films, respectively. [1,21,64] Another important test method is the **pull test**, where a test stud, which is fixed to the coating by an epoxy adhesive, is pulled off under controlled conditions by a tensile test apparatus. [64] Again, the obtained force plot allows for conclusions about the strength of the adhesive joint. [6,64] Furthermore, **indentation debonding tests** can be done to determine the adhesive strength. Therefore, an indenter with a semispherical tip is thrust into the coating until it is penetrated. The **scratch test** can be seen as a kind of extension to this method, since it involves penetration and dragging of an indenter through the applied coating. The load, which is required to remove the coating, is taken as a measure of coating adhesion. Other methods for the determination of adhesive strength are the **blister test**, where a blister is generated in the coating along which delamination is observed, **beam bending tests** such as the three- or four point bend tests, where load versus deflection data are produced, the **Brazil nut test**, where a solid cylinder is cut across its diameter and glued back together and the **wedge test**, where tensile stress is induced to a sandwich laminate by forcing a wedge into one end of the adhesive joint and the resulting crack growth under aggressive conditions (high temperature and humidity) and the failure mode are evaluated. [1,21,64] However, it has to be mentioned that the determined value for the adhesive strength is always influenced by the substrate material and the testing conditions (testing speed, peel angle/direction of load), independent on the test method. [6]

Besides adhesion strength, also the prevalent failure mechanism provides information about the quality of the adhesive joint. [6,64] There are mainly two modes according to which an adhesive joint can fail. The failure mode is independent of the substrate material and adhesive system applied. [6,60] In case of **cohesive failure** mechanical separation occurs within the bulk of the adhesive. [6,55,56,65] This implies that the chemical bonds at the interface are equal or stronger than those within the bulk of the adhesive layer. [56] Cohesive failure originates from inhomogeneities in or changes of the adhesive layer caused by aging, and may follow ductile or brittle fracture (with or without deformation before rupture), depending on the load conditions including temperature and speed of load. [60] On the contrary, **adhesive failure** takes place at the adhesive-substrate interface [6,65], meaning that the atomic and molecular layers of the joined phases are separated perfectly. However, this describes an ideal situation, which - according to the research of Bikermann - is unlikely to reflect reality. Instead, he proposed the formation of a weak boundary layer, which fails cohesively. [55,60] Besides these two failure modes, also a combination of both or fracture of the adherent is possible. [6]

3.2.4. Adhesion enhancement

The cleanliness of the substrate, a proper choice of the adhesive system [57] and intimate contact between the substrate and the adhesive are prerequisites for good adhesion. The latter allows for the establishment of physical or chemical interactions and bond formation (see also chapters 3.2.1 and 3.2.2). [1,55] In order to ensure proper adhesion, different surface pretreatments can be employed to the substrates prior to adhesive bonding. Moreover, adhesion promoters (primers), which act as coupling agents between the adhesive and the adherent, may be applied to the substrate surfaces. The effect of surface pretreatments relies on (i) the removal or prevention of weak boundary layers and contaminations from the substrate surface, (ii) the establishment of an intimate molecular contact between the adhesive and the adherent as well as the formation of sufficiently high adhesion forces via adjustment of the surface energy of the substrate by either surface modification or roughening and (iii) the generation of a specific surface topography to increase the effective surface area and to support adhesion via mechanical interlocking. Other aspects of surface pretreatment include the protection of highly active surfaces such as metal substrates from undesired reactions with air contaminants or the assistance in the curing reaction of certain adhesives (e.g. cyanoacrylates). [55,59,60]

Surface pretreatment techniques

The major effect of all surface pretreatments is still based on the increase of the surface energy of the substrate [59], achieved by the introduction of superficial polar groups such as -OH, -C=O, -COOH groups, which enable intermolecular interactions of the adhesive and the adherent as well as improved wetting. In general, surface pretreatments are subdivided into mechanical, physical and chemical methods. [60]

Mechanical surface treatments

Mechanical surface treatments improve adhesion to the substrate by removal of interfacial layers, which hinder adhesion, and contaminants such as dust, oils, greases, lubricants and water. The surfaces are cleaned by wiping with or immersion into alkaline solutions or organic solvents or via steam degreasing. In a subsequent roughening step the substrate surface is activated and the effective surface area is increased by the use of wire brushes, sand and emery paper, abrasive pads and grit- or shot blasting. Thus, mechanical pretreatment is only appropriate for dimensionally stable substrates (e.g. metals). [59,60] The modified surface topography provides improved wetting and a higher surface area for bonding. Moreover, stress distribution in the adhesive near the interface is improved and mechanical interlocking of the adhesive in the roughened surfaces can contribute to adhesion to a certain extent. [59]

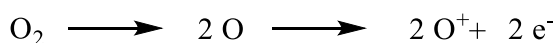
Physical surface treatments

Physical surface treatments induce chemical changes of the substrate via physical processes. This class of pretreatment includes plasma, corona and flame treatment as well as the application of lasers. [60]

Plasmas are defined as excited gases, consisting of atoms, molecules, ions, free radicals and free electrons as well as metastable species. They develop when a gas is fed high amounts of energy via high voltage discharge. [59,60] The energy input causes ionization of neutral gas atoms into electrons and ions



and dissociation of molecules into the corresponding atoms.



The typical emission during plasma treatment occurs when an excited particle returns to a lower energy state or the ground state. [60]

Plasma treatment activates the substrate surface with regard to higher reactivity. Different functional groups can be introduced, depending on the choice of the plasma gas. [60] Common process gases include air (usually for atmospheric plasma), hydrogen, oxygen and nitrogen as well as inert gases such as helium and argon. Moreover, fluorinated hydrocarbons (e.g. CF_4) or ammonia can be used. [59,60] There are numerous interactions between the plasma and the substrate, which can occur simultaneously in various combinations. The major effects include (i) cleaning of the substrate (ii) degradation and ablation, (iii) crosslinking, (iv) oxidation, (v) polymerization and grafting onto the substrate surface and (vi) ion implantation. [59,60] Due to their high kinetic energy, the excited species of the plasma remove contaminations from the surface of the substrates. Degradation and ablation is mostly observed for air and oxygen plasmas. In contrast, oxidation of the substrate surface and the related introduction of polar functional groups such as $\text{C}=\text{O}$ is achieved with all plasmas, because traces of oxygen in the treatment chamber are sufficient for this process. Besides these effects, the surface of unsaturated polymers can be crosslinked during plasma treatment and polymeric films, generated by polymerization of gas phase constituents (organic, organosilicone, organometallic, degraded species), may deposit and be grafted onto the substrate surface. Furthermore, foreign atoms may be implanted into the substrate surface. [59]

Plasmas can be classified according to the process temperature. Thermal plasmas are usually applied for heat transfer applications. They comprise a high energy density and are characterized by temperatures of several thousand Kelvin. As the high temperatures often cause material damage, the application of thermal plasmas is limited. In contrast, non-thermal or "cold" plasmas allow for treatment of heat sensitive materials and for tailored material processing, since the temperatures are in the range of 50-150 °C. Ionization is maintained via collisions of electrons with neutral gas particles, resulting in ions and further electrons. In addition, plasmas can be further divided according to application conditions such as process pressure and mode of energy impact. There are low-pressure plasmas (0.1-5 mbar) and atmospheric plasmas. Regarding the latter, the energy can be coupled in close proximity of the substrate surface, in a rather long distance to the surface (plasma approaches surface across flow processes) or via chemical processes such as flame treatment for example. [60]

In contrast to plasma beams, which are electrically neutral, corona discharge has an electric potential. [60] The corona discharge is generated by applying high voltage (AC of 10-20 kV, frequency of 10-40 kHz) to an electrode system. As a result, characteristically

luminous discharges develop, which ionize the air between the electrodes and give an atmospheric air plasma. [59,60] For surface treatment, the substrate is placed on the counter electrode (mass potential), which carries a dielectric layer to support homogeneous distribution of the micro discharges. However, the treatment is not completely homogeneous all over the surface, since higher positions are more prone to discharge striking. [60]

Corona discharge is the most widely used pretreatment method for polyolefins. [59] It increases the surface free energy of the substrate via introduction of polar functional groups in a free radical mechanism. [55,59] Surface treatment proceeds via contact of the electric arcs with the substrate. [60] On the one hand, the emitted electrons (discharge) transfer energy to oxygen (and nitrogen) molecules in the working gap, causing dissociation and ionization of these molecules. On the other hand, molecules at the substrate surface are cleaved, building active sites for adsorption of and reactions with the plasma particles. Since reactive oxygen species constitute a high portion of the formed plasma, surface modification is dominated by oxidation reactions. [60] Thus, polar groups including C-OH, C=O, COOH, C-O-C, epoxy, ester and hydroperoxide are introduced to the substrate surface. [66–68] In addition, the surface is roughened by ablation. [9,68] It is stated that both, surface modification and the changes in topography improve the wettability of the substrate and the adhesion properties. [60]

The efficiency of corona treatment mainly depends on the applied power output and the speed of sample throughput. Moreover, the air flow rate and the temperature of the polymer film are important parameters. An optimum corona treatment removes potential weak boundary layers and oxidizes the substrate in order to allow for proper wetting, improved superficial contact and thus increased intrinsic adhesion. An overtreatment, on the contrary, may generate a new weak boundary layer, which hinders adhesion [59], or may damage the substrate irreversibly. [60]

Though plasma and corona treatment are powerful methods to activate polymer surfaces, it is important to consider hydrophobic recovery. It is well known, that the superficial oxygen concentration of pretreated polymer surfaces decreases with time due to a thermodynamic effect. [60,69–71] Dipol-dipol interactions of the superficial polar groups with air initiate a rearrangement of the polymer chains (conformational movement, rotation) in order to minimize the surface free energy by orientation of the covalently attached functional groups towards the bulk. [69–71] It was shown that hydrophobic recovery proceeds rapidly during the first week [70] or even within hours [72] after corona treatment.

Another physical pretreatment method is flame treatment (Kreidl process). Similar to plasma and corona, the surfaces are chemically modified via surface oxidation. [1,59,60] The higher penetration depth of flame treatment, however, is advantageous for the activation and modification of huge and structured substrates. [60] Flame treatment is performed with burners consisting of a number of closely spaced jets, which are fed with an air- or oxygen-gas mixture. Examples for suitable burner gases are methane, propane or butane. The flame is passed over the sample (or vice versa) at a distance of 5-150 mm, causing thermal oxidation of the treated surface via a free radical reaction of the polymer chains of the substrate [59,60] Again, chemically active oxygen type species are implemented on the substrate. [55,60] For a short period of time (seconds) the surface is heated to temperatures of 200-400 °C. [60] In order to avoid thermal degradation, it is essential to optimize the process parameters. Important variables and influencing factors of flame treatment are the flame temperature, the exposure time, the gas-air ratio and the gas/air flow rate, the nature of the gas as well as the position and the distance of the substrate to the flame. [59,60] To provide an optimum treatment, the air-gas mixing ratio should contain slightly more oxygen than required for complete combustion. [1,59]

Besides the above mentioned physical surface treatments, different lasers, including excimer, CO₂, Nd-YAG and diode lasers, can be used for modification of the substrate morphology and surface chemistry. Photons of high energy hit the substrate surface, causing material abrasion and bond cleavage. If the laser treatment is performed in a reactive atmosphere (e.g. O₂) polar groups such as C-OH, C=O or COOH are introduced to the substrate surface. [60]

Chemical surface treatments

Typically, chemical surface treatments of polyolefins are carried out by immersion into solutions of sulfuric acid with sodium dichromate or into solutions of sodium hydroxide. [60] Moreover, etching with chromic acid is a common method. Chemical etching causes loss of material (roughening) on the one hand, and surface modification (oxidation and sulfonation) on the other hand. [59] It was proven that the adhesion promoting effect mainly relies on the introduction of polar functional groups such as C-OH, C=O, COOH, which improve wetting and interactions with the adhesive. [59,60] Moreover, mechanical interlocking of the adhesive on the roughened surface contributes to adhesion enhancement. The extent of oxidation and roughening depends on the etching time and the temperature applied during the chemical treatment. In addition, improved adhesion due to the removal of a potential weak boundary layer on the substrate surface was considered. However, it was found that this process is a minor aspect

and that surface oxidation still dominates adhesion promotion on weak boundary layer free surfaces. [59] Similar to polymeric substrates, the surface of metals can be treated with non-oxidizing acids (HCl, diluted H₂SO₄) or oxidizing acids (HNO₃, conc. H₂SO₄, H₃PO₄). The first remove metal oxides and other contaminants from the substrate and roughen the surface at a submicron level, while the latter additionally oxidize the substrate and introduce functional groups to the metal surface (nitrates, phosphates and sulfates). [60]

Another chemical pretreatment is the gas phase fluorination, where the polymer substrates are activated by the attachment of fluorine atoms. Due to the high reactivity of F₂, fluorine radicals are formed, which react with the hydrocarbon chains of the polymer in an exothermic radical chain mechanism. In order to avoid degradation by attack of C-C bonds of the substrate, the reaction conditions have to be adjusted. [60] A variation thereof is photobromination, where the substrate is simultaneously exposed to a saturated bromine vapor and light. [59]

Although limited to laboratory scale, also sulfonation can be applied from the gas phase. Therefore, 1 % of SO₃ is provided in a nitrogen atmosphere. As a result of sulfonation the surface energy of the substrate and consequently adhesion is significantly increased. [60]

Furthermore, the surface energy of the substrate can be increased via ozonization. Ozone is formed in a so called "ozonizator" via silent discharge. Since it is an instable compound, ozone decomposes to molecular oxygen and reactive oxygen:



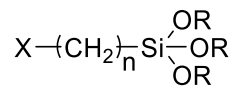
The latter acts as oxidizing agent and reacts with the hydrocarbon chains of the polymeric substrates. [60]

Adhesion promoters/primers

First of all, the difference of adhesion promoters (coupling agents) and primers has to be clarified: Primers are chemically reactive systems, which crosslink on the substrate surface and provide optimum conditions for good adhesion, while adhesion promoters are bifunctional molecules, which build a chemical bridge between the substrate and the adhesive. [60] Adhesion promoters and primers can be applied to the substrate either solely or as the last stage of a multistep pretreatment. [59]

-Theoretical background-

The most widely used class of adhesion promoters are based on organosilanes with the general formula



where RO is a hydrolysable group such as methoxy, ethoxy or β -methoxyl ethoxyl and X is an organofunctional group such as amino, hydroxyl, vinyl, methacryl or epoxy for example. [55,59,60] These molecules are also called coupling agents since they establish strong chemical bonds to both the adhesive and the substrate. [59] Organosilanes are usually applied from solution in water or water/ethanol mixtures, where they are hydrolyzed to the respective silanols. In a consecutive step the silanols adsorb onto the substrate and undergo condensation reactions with the superficial hydroxyl groups. As a result Si-O-linkages across the substrate are formed. Simultaneously the silanol groups of the coupling agents also react with each other, building a polysiloxane layer on the substrate surface. [55,59] Once attached to the substrate, organosilanes offer three mechanisms for adhesion enhancement: Firstly, the organofunctional group can react with the adhesive. Other modes of action rely on the penetration of the adhesive into the open porous structure of the polysiloxane layer, resulting in interpenetrating networks, or the limited interfacial diffusion of the polysiloxane layer and the adhesive may occur. [59] Besides organosilanes, also organotitanates, organozirconates, organozirconaluminates and chrome or cobalt complexes as well as mercaptoesters and benzotriazoles are applied as primers. While titanates and zirconates are commonly applied to improve adhesion between a polymer matrix and filler particles, cobalt compounds are employed to enhance adhesion between rubber and brass cords in tires. [55,59]

Besides the adhesion promoting effect, coupling agents and primers can also be applied as coatings, which reinforce the substrate surface and increase the service life of the joint via strong linkages. Moreover, they may build protective layers, which prevent undesired reactions of activated surfaces with the environment (e.g. air contaminants), corrosion and degradation by UV-light. [55,59]

3.2.5. Classification of adhesives

There are many different categories according to which adhesives are classified. Typical classification criteria are the chemical structure and composition, the setting mechanism and the form of application or processing. Additionally, adhesives are classified according to the solvent content, their application temperature, their thermal behavior, the field of application, their adhesive properties and the form of delivery. [1,6,60] In the following, the most important classification criteria are summarized and discussed.

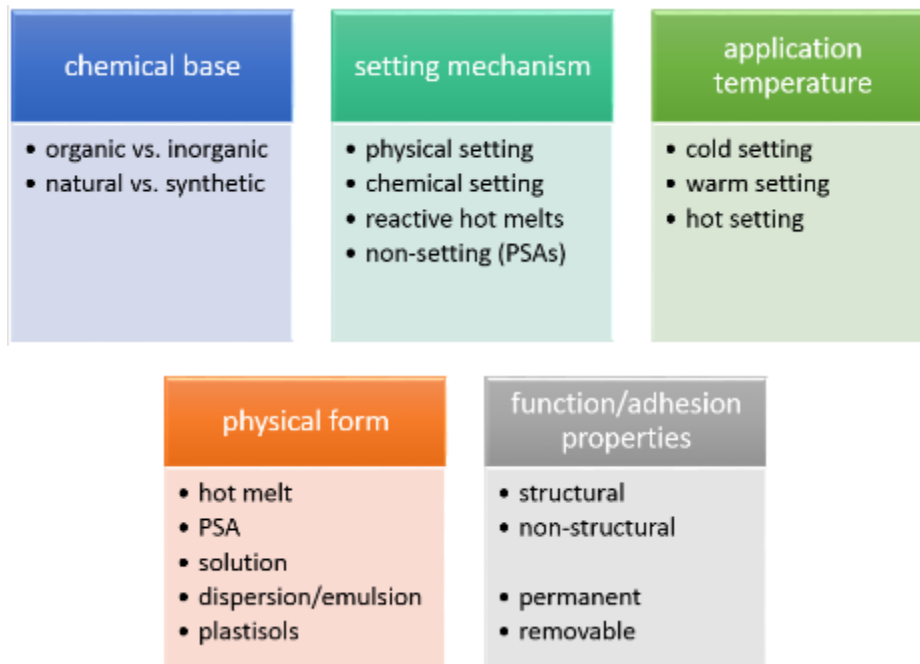


Figure 3: Classification of adhesive systems according to their chemical base, setting mechanism, application temperature and form of application

Classification according to the chemical base

In general, organic and inorganic as well as natural and synthetic adhesives are distinguished. Silicone based adhesives are seen as a hybrid form of inorganic and organic materials. The majority of adhesives applied today is based on synthetic organic polymers, which can be thermoplasts, duromers or elastomers. Independent on the mode of setting and form of application, adhesives are synthesized by radical polymerization, polyaddition or polycondensation. While the respective poly-reaction of chemically setting adhesives

takes place *after* application and during joining, physical setting adhesives are already present in their final molecular state (polymer) *before* application. [6,60]

The chemical composition of different synthetic adhesives is discussed in more detail in course of classification according to the setting mechanisms (see below).

Natural organic adhesives are further divided in animal glues and vegetable glues. [60] They are produced from proteins (e.g. elastin, collagen, keratin, casein), polysaccharides (e.g. cellulose, starch, gum arabic) or polyphenols such as lignin or lipids (terpenes or terpene rosins). [1] Compared to synthetic organic adhesives, their natural counterparts show low resistance against aging and bad long term stability, but are favorable with regard to environmental concerns and recycling. [1,60] They are applied in various forms including solvent containing contact adhesives, dispersions, water activated solids, hot melts and PSAs. Examples for industrial applications are the use of glutin adhesive in bookbinding and wooden composites and casein glues for wood processing. [1] Besides, there are also inorganic natural adhesives, which are based on inorganic glasses and show high thermal stability. Since inorganic adhesives are not as widely used as organic adhesives, they are not further discussed here. [60]

Classification according to the setting mechanism

Adhesives can be cured via physical or chemical processes. Thus, polymer formation according to radical polymerization, polyaddition or polycondensation can take place before or after application, respectively. [6,60] Moreover, there are reactive hot melts, which represent a hybrid of physically and chemically setting adhesive systems [60], and non-setting (pressure sensitive) adhesives (PSAs). [1]

Usually, **physically setting adhesives** are one component systems composed of polymers in their molecular end state, which are either dissolved or heated in order to provide the required wetting of the adherent during application. As the name suggests, they do not undergo chemical reactions during curing, but set by physical processes such as evaporation of the solvent, solidification after cooling or diffusion. [1,60]

Hot melt adhesives are 100 % solids and do not contain any solvent. They are provided as powders or foils consisting of thermoplastic polymers such as ethylene vinyl acetate, poly vinyl acetate, PE, amorphous polypropylene (PP), block copolymers, polyamides or polyesters, which are solid at temperatures up to ~ 80 °C. [1,6,60] Hot melts are applied in the molten state in order to provide good wetting of the adherent and set upon solidification by cooling. Therefore, the generated adhesive joints are thermally

reversible. [1,6] Diluents and additives including waxes, plasticizers, tackifiers, stabilizers and fillers may be added to adjust the flexibility of the adhesives, to lower their viscosity, and to enhance wettability and their adhesive strength. [6,60] Hot melt adhesives are applied in car manufacture, the building, textile, paper and packaging industry, as well as in sticky labels, bookbinding and the fabrication of hygienic products. As a variation, reactive hot melts were developed. These adhesives set by a combination of physical and chemical cure mechanisms and are therefore seen as a hybrid form of the two setting modes. [60] They are based on epoxy or polyurethane (PUR) hot melts and crosslinkable compounds, which undergo an additional post cure (chemical setting) after solidification by cooling (physical setting). Due to chemical crosslinking, the adhesives comprise increased durability and cohesion and cannot be remelted. [1] Reactive epoxy based hot melts are applied in automobile construction industry and in form of prepregs in the construction of printed circuit boards (PCBs). [60] Reactive PUR hot melt adhesives are used in bookbinding for adhesion of wood and in shoe manufacture. [6]

Another example for physically setting adhesives are plastisols, which consist of dispersions of polyvinyl chloride (PVC) or polymethyl methacrylate in a plasticizer. Upon heating to temperatures of 120–200 °C, the plasticizer diffuses into the polymer. Subsequent cooling leads to an irreversible transformation of the sol into a highly viscous gel. [1,6,60] Plastisol adhesives are cheap and show high adhesion and durability, which can be further improved by the addition of chemically curing components. [1] They are used to bond metals and silicate containing materials and are frequently applied in automobile construction. [1,6]

Furthermore, there are solvent based physically setting adhesive systems, where polymers including polyvinyl acetate and other copolymers, polyvinyl ethers, polyvinyl esters, polyacryl acid esters as well as nitrile butadiene rubber (NBR) or styrene-butadiene rubber (SBR) are dissolved in organic volatile solvent such as esters or ketones. The solvent is not part of the adhesive system but rather a processing aid, which is removed after application of the adhesive, either before or after joining, depending on the material properties of the substrate. While joining of dense adherents requires complete removal of the solvent in advance, porous substrates allow for solvent escape also after joining. [60] Hence, adhesion is achieved by evaporation of the solvent. Another approach employs dissolution and swelling of polymer substrates by solvent adhesives (pure solvent or solutions of styrene or PVC) and a subsequent migration process leading to interpenetration and mutual entanglement of the two adherents. Amongst others, solution based adhesives are used to bond paper, plastics, silicate containing materials and wood. [1,6] Besides dissolution in *organic* solvents, adhesive polymers can also be dissolved or dispersed in *water*. [6,60] Typically, emulsions of vinyl acetate homo- and

copolymers, polypropionate, polyacrylate and styrene copolymers as well as dispersions of rubber latices are used. Similar to solvent based adhesives, physically setting aqueous emulsions or dispersions cure by the evaporation of water. [6,60] Although they comprise low resistance against moisture, the importance of water based adhesive systems grows steadily due to environmental concerns (no volatile organic compounds (VOC)). [1,60]

Also, contact adhesives set by physical processes. They are applied to both adherents as polymer solutions or dispersions of chloroprene rubber, SBR, NBR, PUR, polyvinyl acetate, PE, PVC derivatives or phenol resins. [1,60] In case of porous substrates, drying does not have to be completed before further processing. During joining the adherents are pressed together [1], applying a short but high pressure. Setting of contact adhesives may occur according to three mechanisms. The first uses the formation of common crystallites between the two adhesive films, providing cohesion in the adhesive bondline. This requires a certain mobility of the polymer molecules and thus joining before the solvent is removed completely. The second mechanism is based on mutual diffusion of the two adhesive layers. Cohesion is provided by entanglement of the non-crystalline polymers applied to the adherents. The third possibility concerns the application of two component contact adhesives, where the adhesive can be applied to either one adherent (porous substrates) or both adherents (dense substrates). [60] In general, contact adhesives are not crosslinked and remain in the thermoplastic state after setting. Thus, their resistance against heat and creep is limited. As described for hot melts and plastisols, the durability and cohesion of adhesive can be improved by the addition of crosslinkable compounds. Moreover, additives such as tackifiers, anti-aging compounds or UV-stabilizers may be added. Typical application fields of contact adhesives are the textile industry, saddlery, the fabrication of mattresses and shoes, floor coverings and the manufacture of cars. [1]

In contrast to physically curing systems, **chemically setting adhesives** are applied as low molecular weight compounds. The adhesive polymer is formed during bonding according to chemical reactions following the mechanism of polymerization, polycondensation or polyaddition. [1,6,60] The kinetics of these reactions are influenced by temperature and pressure as well as reaction time and the concentration of the reactants. [60] The wide array of chemically curing adhesives can be further divided into one or two component systems. Generally, curing of *one component systems* is started by external factors such as heat, the presence of moisture, the catalytic effect of the substrate, absence of oxygen or irradiation. In contrast, *two component adhesives* consist of several compounds (monomer and hardener), which need to be mixed in a defined ratio. Since setting starts immediately after mixing, the pot life of two component adhesive is limited. The curing reaction is almost always exothermic. [1,6] Moreover, there are *cold, warm and hot setting adhesives*, which cure at room temperature or slightly elevated temperatures,

at 80-100 °C and 100-250 °C, respectively. Usually, cold setting adhesives require monomers with higher reactivity and achieve lower strength than warm and hot setting systems. [6,60]

Polymerization adhesives are generated by free radical or ionic polymerization. The reactive species (free radicals, cations or anions) attack C=C double bonds of the monomers, initiating a chain growth reaction (see Figure 12, chapter 3.4.2). The resulting polymers are usually thermoplastic. Typical examples for polymerization adhesives are acrylic copolymers, epoxy acrylates, urethane acrylates, polyester acrylates or polyether acrylates as well as different rubbers and saturated hydrocarbons. More precisely, polyvinyl acetate, polyvinyl alcohol, polyvinyl ether, ethylenvinylacetate, polystyrene, styrene block copolymers, PVC as well as NR, SBR, NBR, butyl rubber, chloroprene rubber, PE and PP are applied. Rather copolymers (statistic, alternating, block or graft copolymers) than homopolymers are applied in order to adjust the properties of the adhesive. Polymerization adhesives are further divided into one component and two component systems.

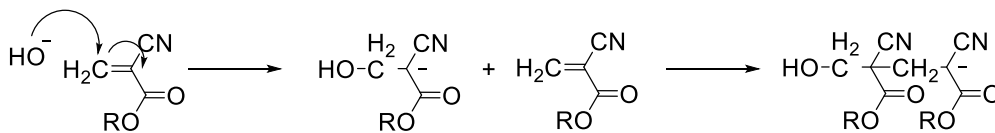
In *one component polymerization adhesives*, the monomers are stabilized for storing and the reaction is started by external factors during application and joining. Firstly, there are cyanoacrylate adhesives, which cure in the presence of water or alkalinity. Chain growth proceeds via anionic polymerization mechanism (see Figure 4) and is catalyzed by hydroxide ions (OH⁻). The resulting non-crosslinked high molecular weight polymer is used to bond metals, plastics, silicate containing materials as well as rubber and wood. Since joining occurs so quickly, cyanoacrylate adhesives are also known as superglues or instant adhesives. They are used to bond metals and plastics and are applied for tissue bonding in medicine. Another representative of one component polymerization adhesives are anaerobic adhesives, which require absence of oxygen and the presence of metal ions for curing. The adhesive system usually consists of methacrylic monomers and a peroxide initiator, which is decomposed to free radicals in a metal ion catalyzed reaction (see Figure 4). The adhesive stays liquid as long as it is in contact with oxygen and starts curing according to free radical polymerization as the metal substrates are joined and oxygen is displaced. Anaerobe adhesives show high resistance to temperature and media and are mainly used for screw locking systems. [1,6,60] In contrast, aerobe adhesives require the presence of oxygen to start polymerization. Here, compounds such as hydrazones, which build peroxides in the presence of oxygen, are used as an initiator. As with common peroxide initiators, free radical polymerization is initiated. Typical monomers are methacrylates and PU-methacrylates. [6,60,73] Moreover, there are radiation curable adhesive systems, where UV- irradiation, electron beams or lasers are used to initiate free radical or cationic polymerization of (meth)acryl or vinyl monomers. The initiating species,

-Theoretical background-

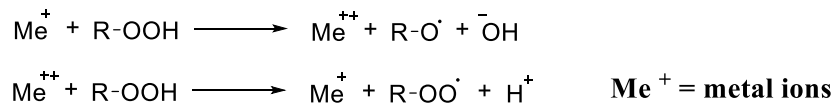
which are generated by photolysis of a photoinitiator (PI), attack the C=C double bonds of the monomers and thus start chain growth (compare Figure 12, chapter 3.4.2). [6,60]

Two component polymerization adhesives contain monomers and a hardener/accelerator system, which are mixed in a defined ratio to start the polymerization reaction. Typical monomers are methacrylates or unsaturated polyesters with monomeric vinyl compounds. Peroxide components are used as hardener and tertiary amines or metal salts as accelerator. The peroxide decomposes upon interaction with the accelerator, generating free radicals, which in turn start the polymerization reaction by attack of the C=C double bond of the monomers. Two component polymerization adhesives are used to bond metals, plastics and silicate containing materials. [6,60]

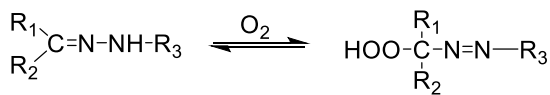
Curing reaction of cyanoacrylic adhesives



Anaerobic adhesives - metal catalyzed decomposition of peroxides



Aerobic adhesives - autooxidation of hydrazone



free radical polymerization of methacrylates with I = RÖ or RÖO

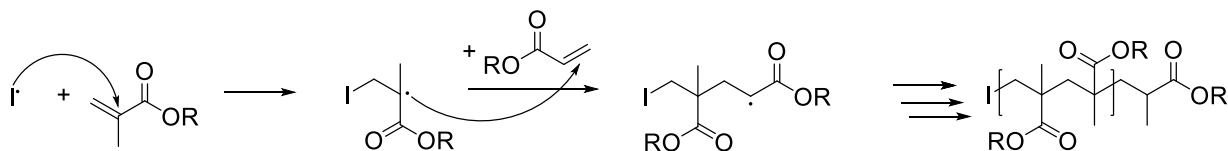


Figure 4: Reactions of one component polymerization adhesives [60]

In polyaddition adhesives polymer formation is based on the addition of reactive monomers and the migration transfer of a hydrogen atom from one component to another. The most important representatives are based on epoxides and PUR. Epoxides can be cured by mixing with amines (cold setting) or carboxylic acid anhydrides (warm setting) in a stoichiometric ratio or by exposure to UV-light. Less common systems employ carboxylic acids, organo-sulfur or hydroxyl compounds as a hardener. Typical monomers are the bisphenol A diglycidyl ether, aliphatic epoxides, cycloaliphatic diepoxides or epoxidized fatty acids. During the exothermic curing reaction, the hardener is added to the epoxy moiety of the monomer. Thereby, the epoxy ring is opened and a hydrogen atom is transferred from the hardener to the monomer, building a pendant hydroxyl group. The resulting free valences allow for addition of the respective molecule group (see Figure 5). [6,60] Besides polyaddition, epoxy adhesives can also be prepared by cationic ring opening polymerization, where the epoxy ring is activated by an initiator, starting the chain growth reaction (compare Figure 17, chapter 3.4.2). [1] Due to the hydroxyl groups in their structure, epoxy adhesives have high polarity and good adhesion to most substrates, including metals, plastics and silicate containing materials. Epoxides are among the most widely used structural adhesives and are characterized by good strength, high resistance against aging, temperature and chemicals, low shrinkage and low peel strength as well as long term durability. However, the high crosslinking density leads to brittleness, which can be overcome in toughened epoxy adhesives by adjusting the monomer structure or the incorporation of rubber-like particles. There is a huge variety of epoxy adhesives, encompassing one and two component systems as well as cold and warm setting adhesives. In two component systems the monomer resin and the hardener are packaged separately, while they are provided as a mixture in one component warm setting epoxy adhesives. [1,6,60] Typical application fields are the aircraft, automotive and construction industry. [1]

Curing reaction of polyaddition epoxy adhesives

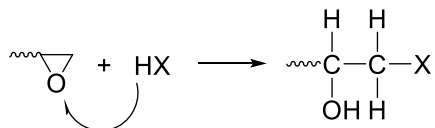


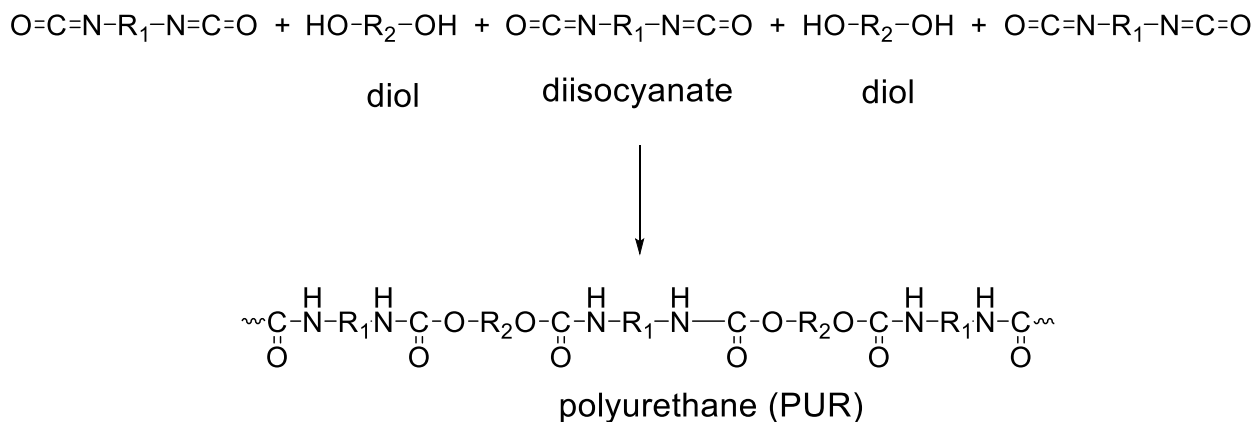
Figure 5: Curing reaction of polyaddition epoxy adhesives [60]

-Theoretical background-

The second group of polyaddition adhesives is based on PUR. *PUR adhesives* are generated by polyaddition reactions of diisocyanates and diols. As shown in Figure 6, the active hydrogen atom of the polyol is transferred to the nitrogen atom, while the RO remainder is attached to the carbon atom of the isocyanate group. [6,60] The reaction can be catalyzed by tertiary amines or metal salts. [1] PUR adhesives show good adhesion to various substrates, including metals, plastics and silicate containing materials, good resistance against abrasion, water, solvents, plasticizers, fats and oils, as well as high elasticity and flexibility. [6,60] However, compared to epoxides, the thermal stability of PUR adhesives is lower. [60] As with epoxides, there are one or two component systems as well as cold and warm setting adhesives. Usually, one component systems are composed of an isocyanate terminated polyether polyol, which cures upon the exposure to moisture (cold setting). [6,60] The isocyanate reacts with water instead of the polyol compound. In a two-step reaction carbamic acid is formed as an intermediate and CO₂ is released, giving the resulting amine, which in turn reacts with the isocyanate component (see Figure 6). In order to avoid foaming of the adhesive, high isocyanate contents are applied. Two component systems contain low molecular weight polyols and isocyanate compounds or a mixture of isocyanate terminated pre-polymers and polyols or polyamines [1,6,60], which can be cured either at room temperature or at elevated temperatures. Moreover, there are heat curable one component PUR adhesives, where the isocyanate component is blocked by a phenol. Upon heating the phenol is released and the polyaddition reaction with polyol is initiated. [6] PUR adhesives are widely used in furniture making and automotive industry as well as textile foam coatings. [1]

Curing reactions of polyaddition PUR adhesives

isocyanate + alcohol



isocyanate + water

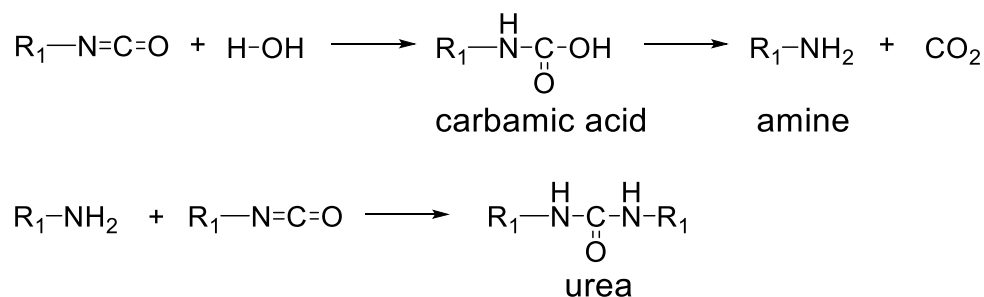


Figure 6: Curing reactions of PUR polyaddition adhesives [60]

Besides polymerization and polyaddition, also polycondensation can be utilized to generate and cure adhesive polymers. Typically, a low molecular weight byproduct such as water, alcohol or carboxylic acid is generated during polycondensation. The group of polycondensation adhesives encompasses formaldehyde condensates (phenol/urea/melamine formaldehyde adhesives), polyamides, polyesters, silicones, polyimides. *Formaldehyde condensates* or polyhydroxyl compounds are formed by polycondensation of formaldehyde and phenol, urea or melamine (see Figure 8). [6,60] These adhesives can be applied in pure form or as solution in water or an organic solvent. [6] *Phenol-formaldehyde adhesives* (PF) are formed by crosslinking of phenol, *o*-methylolphenol and other derivatives (kresols, resorcinols) via methylene and dimethylen ether bridges under the release of water. For the application of these adhesives, resols are preferred. The resulting PF resins are insoluble and infusible and can

be cured either by heat or catalytically. [60] In general, PF adhesives are cheap and show high resistance to biodegradation, hot water, high temperature and weathering. [6] The formation of *urea- and melamine-formaldehyde adhesives* (UF, MF) starts with an addition reaction between formaldehyde and the amine functionalities of urea or melamine. In a second step, the resulting alcohol compounds undergo a condensation reaction, giving an adhesive polymer, which is crosslinked by methylene and dimethylene ether bridges. In case of UF adhesives, the condensation reaction is pH-dependent and requires acidic conditions. Although melamine is able to react with a total of six formaldehyde molecules, usually a molar ratio of 1:3 (melamine : formaldehyde) is used. [60] All formaldehyde condensation adhesives (PF, UF, MF) are mainly applied as wood glue. [1,6,60]

Curing reactions of PF adhesives

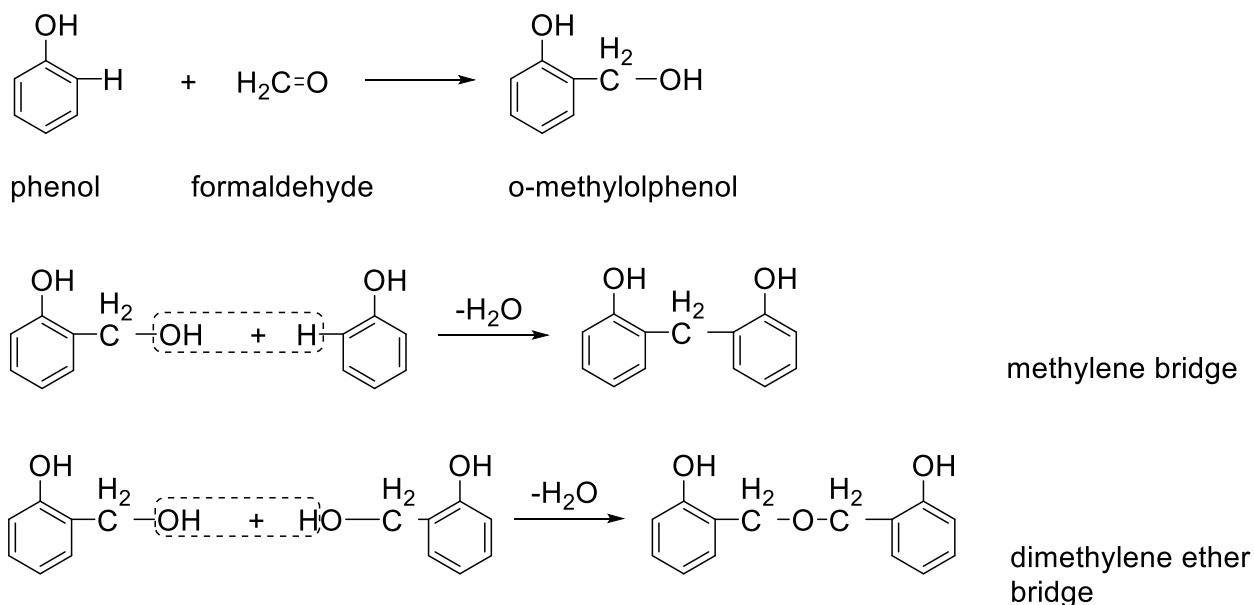
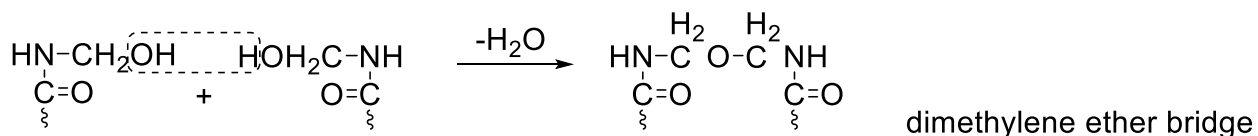
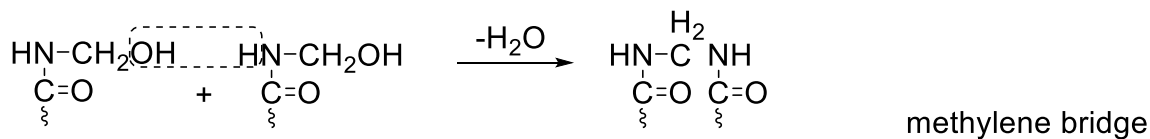
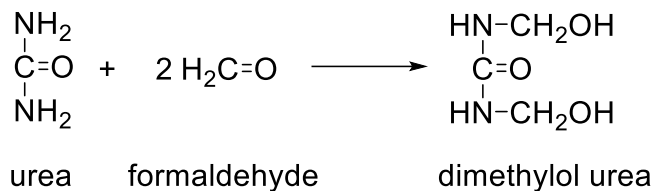


Figure 7: Curing reactions of phenol formaldehyde polycondensation adhesives [60]

Curing reactions of UF adhesives



Curing reactions of MF adhesives

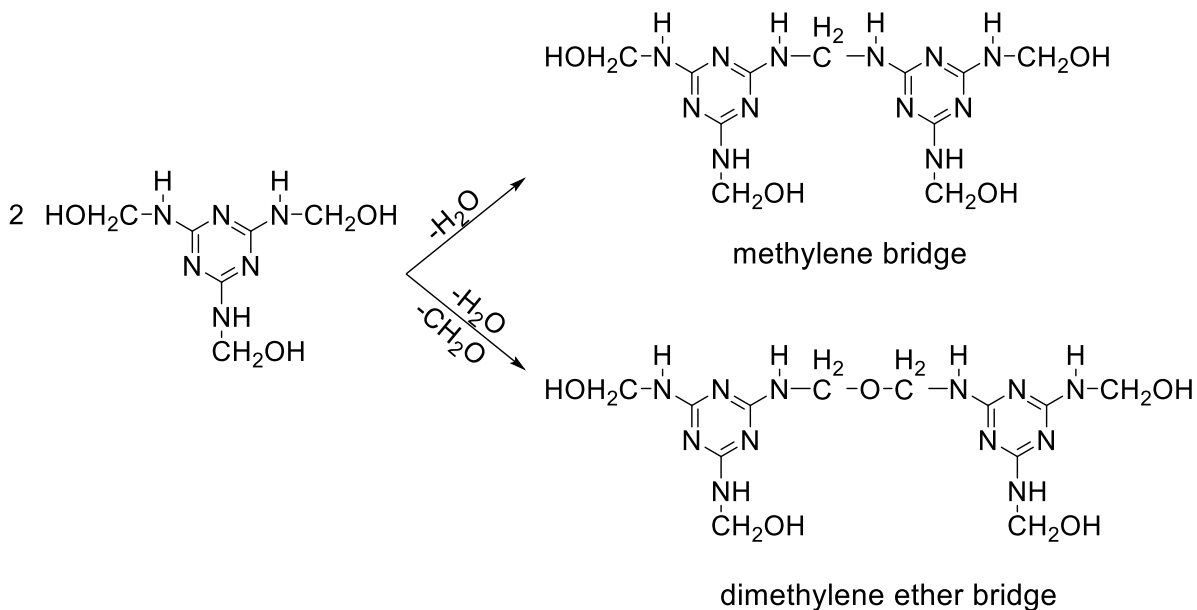
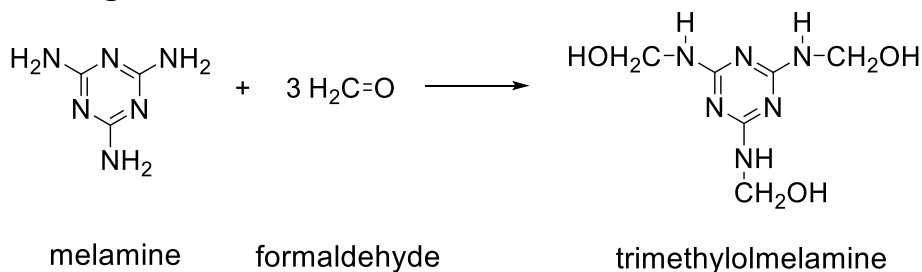


Figure 8: Curing reactions of melamine-formaldehyde polycondensation adhesives [60]

Another group of polycondensation adhesives is based on silicones, which are composed of an inorganic main chain (Si-O-Si) and organic substituents (hydrocarbons). [60] *One component RTV silicones* cure at room temperature in the presence of moisture. Polyorganosiloxanes are common starting materials. In order to prevent self-condensation via the terminal hydroxyl groups the siloxanes are blocked by a crosslinking agent, which is sensitive to hydrolysis. The curing reaction is initiated by hydrolysis of the crosslinking agent, yielding the corresponding silanols. In the subsequent condensation reaction siloxane polymers are built under the elimination of water (see Figure 9). In contrast, *two component RTV silicones* do not require moisture but rather a catalyst for curing. They are applied where curing of one component RTV silicones lasts too long due to low moisture concentration or high layer thicknesses. There are two pathways according to which two components RTV silicones can be cured: Firstly, silicic acid esters are crosslinked with hydroxyl polysiloxanes in an organo tin catalyzed condensation reaction under the elimination of alcohol. This reaction depends on the pH-value and the reaction temperature as well as on the catalyst concentration. The second mechanism is based on an exothermic addition reaction, where vinyl terminated siloxanes and siloxanes comprising a Si-H moiety react in the presence of a platinum catalyst. In the resulting polymers the silicon atoms are linked by oxygen and two methylene groups (see Figure 9). This polyvinylation reaction strictly depends on the reaction temperature. [1,6,60] In general, silicone adhesives are characterized by high thermal stability due to the stable Si-O-Si bonds building up the main chain. Moreover, they show good performance at low temperatures, high resistance to weathering, moisture, oxidation, hot water, weak acids and bases, polar solvents and soles. Silicones are elastic adhesives, which are used for medical applications as well as to bond various substrates including metals, glass, paper and plastics. [6,60]

Furthermore, polyimides are produced by polycondensation reactions, employing aromatic diamines and anhydrides of tetrafunctional carboxylic acids (see Figure 10). Firstly, the amine is added to the anhydride, followed by the cleavage of the anhydride ring. In a second step, thermally induced condensation leads to the formation of an imide ring under the elimination of water. The resulting polymers are insoluble and infusible. Due to the aromatic system they withstand high temperatures (up to 260 °C). However, they are comparatively expensive, difficult to handle, sensitive to moisture and require long cure times or harsh curing conditions (230-250 °C, 8-10 bar). Thus, their use is limited to special applications in the aircraft sector. [6,60]

Curing reaction of polycondensation polyamide adhesives

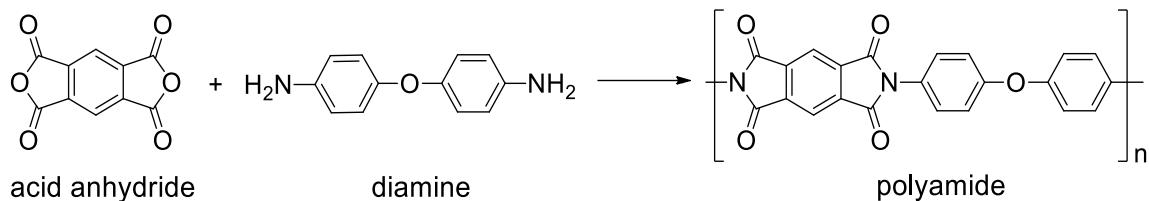


Figure 10: Curing reaction of polycondensation polyamide adhesives

In addition to the above discussed polycondensation adhesives, there are also polybenzimidazoles, which are condensation products of aromatic tetraamines and dicarboxylic acid esters. As with polyimides, the use of polybenzimidazoles is limited to special applications, where high thermal stability is required. [60]

Moreover, polyamide and polyester adhesives are produced by polycondensation. Since they are usually applied as physically setting adhesives, they are not discussed in detail here. Polyamides form by polycondensation of diamines and bifunctional carboxylic acids. They are thermoplasts and typically applied as hot melt adhesives. Polyesters are generated by crosslinking of multifunctional carboxylic acids and polyols. There are saturated and unsaturated polyesters. While saturated copolyesters are used as hot melts, unsaturated polyesters are dissolved in acrylic or vinylic monomers and are polymerized across their C=C double bonds in the presence of an initiator (peroxide). However, unsaturated polyesters are generally less important for the application as adhesive materials. [60]

As a supplement to chemical setting adhesives, blocked adhesive systems have to be mentioned. In order to prevent undesired reactions until application (increase of pot life) of two or more component systems, the monomers can be blocked chemically or mechanically. *Chemical blocking* is achieved by modification of highly reactive monomers. The curing reaction is initiated by defined conditions during joining. Examples are the oxygen inhibition of acrylic compounds and the modification of siloxane monomers with a crosslinking agent (see polycondensation adhesives). Moreover, thermally active systems can be used. Therefore, the basic adhesive polymer is modified with functional groups, which cleave off at high temperatures (high activation energy). For example chemical blocking is used with warm setting epoxy adhesives, phenol resins and thermally activatable PUR systems. Alternatively, the catalyst can be blocked instead of the

monomer. Secondly, the adhesive system can be *blocked mechanically*. The two components are packaged separately and curing starts immediately after mixing them together. [60] A comparatively new approach is the use of microencapsulation, which is mainly applied in screw locking systems. The components are applied as a latex solution and set free upon destruction of the capsules by mechanical pressure. The curing reaction is either based on anaerobic polymerization or initiated by mixing of two or more reactants (two/multi-component adhesives). [1,60]

Another supplement concerns irradiation curing. There are different adhesion systems, which can be cured by UV/VIS or electron beam irradiation. Examples are acrylic adhesives, epoxy adhesives, PUR as well as polyesters and polyethers. While in case of UV curing, a photoinitiator, which generates the reactive species upon irradiation, is required, the electrons of the electron beam directly start polymerization since they act as free radicals. Advantages of irradiation curable adhesives are the rapid cure and the possibility to bond to substrates, which are sensitive to heat as well as the replacement of solution based systems. After curing the adhesives show good resistance to heat, chemicals and are tough and dimensionally stable. Application fields of irradiation cured adhesives include the electronic, automotive and packaging industry as well as the medicine and tapes and labels sector. [6]

Besides physically and chemically setting adhesives, PSAs have to be mentioned separately. Since they do not change their physical or chemical state during application, they are considered as **non-setting adhesives**. [1,6,55,60,62] PSAs consist of high viscosity polymers such as NR, polyesters, polyacrylates, PUR or silicones, are permanently tacky and remain at least partially liquid in their final state. They are mainly applied as adhesive tapes and labels or as transfer systems, where the base is removed after application to the adherent. [1,6,60] More details about PSA systems are presented in chapter 3.3.

Classification according to physical form

As indicated in the classification according to the setting mechanism, adhesives can be applied in different physical forms. There are solid adhesives, which are provided as powders, films or tapes, and liquid or paste-like adhesives, which are available in their pure form or with a solvent. [74–76] More precisely, there are hot melts, PSAs (solids) and plastisol adhesives as well as solvent or water based solutions, dispersions and emulsions (liquids and pastes). The physical form of the adhesives influences the mode of application. Powders have to be molten or dissolved to provide satisfying wetting of the substrate during application. Films are either supplied solely or on a reinforcing carrier (tape/label). Liquids can easily be applied by spraying, brushing or roll coating, and pastes can also be applied to vertical surfaces due to their high viscosity. [77] In most cases, solvents serve as an application aid, which lowers the viscosity of the adhesives and thus enables good wetting of the substrate. Typically, they are removed after application. [60,76,78,79] Both, organic solvents and water can be used [79], whereof the latter is advantageous in terms of costs, toxicity, flammability and environmental issues. On the contrary, organic solvents dry more quickly and the formulation of dispersions is less complex compared to aqueous systems. [78,79]

Classification according to function and adhesion properties

Based on the function of the adhesives, structural and non-structural adhesives are distinguished. Structural adhesives are characterized by high cohesive strength, durability and resistance against aging and environment. Their primary purpose is to hold structures together permanently and to resist against high loads and stresses without loss of integrity. [57,74–77,80–82] These adhesives have to withstand shear strengths higher than 7 MPa at room temperature [57,74,77,80] and are used to bond high strength materials such as wood, metal, ceramics and reinforced plastics. [57,74] Typical representatives are epoxy, toughened epoxy, PUR, modified phenolics, polyaromatics, polyesters, anaerobic, cyanoacrylics, modified acrylics, nitrile and chloroprene rubber. [75,77,80] On the contrary, non-structural adhesives are used to hold lightweight materials in position. Hence, they are not required to withstand substantial loads. They are applied as PSAs, packaging and temporary adhesives. Moreover, they can be used for sealing, vibration damping and impact absorption as well as for the installation of thermal and electrical insulations. [57,76,77,80,82]

In addition, there is a particular classification for pressure sensitive adhesives, which distinguishes permanent and removable PSAs. Permanent PSAs provide high tack, peel adhesion, shear strength and cohesion and do not weaken with time. They bond quickly to various substrates and are supposed to resist against high stress rates and large forces (peel resistance > 9.0 N/25 mm). [7,20,60,83,84] Peel adhesion develops over time and is in the end higher than the mechanical resistance of the substrate. Therefore, permanent PSAs cannot be removed without destroying the adherent. [60,85] *Semi-permanent PSAs* are a variety of permanent PSAs, which remain removable and repositionable for some time before becoming fully permanent. [84] In contrast, removable PSAs comprise low peel strength (2.7- 9.0 N/25 mm), low-medium tack and cohesion but high shear strength. They can be removed without damaging the substrate or leaving residues even after an extended period of application. [7,20,60,84,85] Debonding occurs at the adhesive-substrate interface and depends on the debonding conditions (time and temperature) and the polymer rheology. [7,85] Polymers with limited molecular weight are preferred in order to provide the required fluidity for debonding (viscous flow). [20] Moreover, removability can be achieved by adjusting the PSA formulation and by regulation of the contact area between the adhesive and the adherent. Some removable PSAs can be relaminated after debonding. There are *repositionable PSAs*, which are characterized by time dependent relamination, and *readherable PSAs*, which show time independent relamination. However, repositionable and readherable PSAs should not be confused with semi-permanent PSAs, which cannot be relaminated. [7]

3.3. Pressure sensitive adhesives and products

3.3.1. Pressure sensitivity

Pressure sensitive adhesives (PSAs) are a special type of adhesives, which provide high and permanent tack at room temperature, adhere firmly to a variety of surfaces upon light pressure (finger/hand) and do not need any activation such as water, solvent or heat. [1,5,6,21,62] In contrast to other adhesives, PSAs do not change their physical or chemical state during the application. [1,6,55,62] Bonding and debonding processes are determined by the adhesive-substrate interface as well as by mechanical and rheological properties of the PSA. [1,6,62] Adhesion of PSAs can be explained by one or more of the theories described in chapter 3.2.2. Typically, physical adsorption plays an important role since wetting of the adherent is essential for adhesion build up. The quality of wetting is governed by the viscoelastic properties of the PSA and the interfacial energies. For complete spreading over the substrate surface and good adhesion, low surface energies

of the PSA, and high surface tension of the substrate are required. [1,6,55,62] Furthermore, adhesion is strongly dependent on application time and pressure. [6] The viscoelastic behavior of the PSA provides the required flow and deformability for proper adaption to the surface topography and the establishment of molecular interactions (like liquids at low deformation rates), and simultaneously enables the adhesive to sustain loads (like solids at high deformation rates). Besides good adhesion, PSAs must provide sufficient inner strength (cohesion) to withstand mechanical stress and to provide clean peel in case of removable tapes. Thus, a good balance between adhesion and cohesion is demanded to meet the partially contradictory requirements of PSA tapes for temporary applications. [1,5,6,62]

In general, the adhesion properties (tack, peel adhesion and cohesion) of PSAs are governed by the glass transition temperature T_g , which can be adjusted by variations of the chemical composition and structure (branching, crosslinking) of the adhesive. [1,6,10,20,34] More precisely, the kind of monomers, the type and amount of initiators and crosslinking agent as well as the polymerization method play an important role. Moreover, the number average molecular weight M_n , the polydispersity M_w/M_n , the average molecular weight between entanglements M_e , the molecular weight between junctions M_c of the basic adhesive polymer and the degree of branching have a strong impact on the mobility and the viscosity of the adhesive and hence on the mechanical and adhesive properties and the T_g . The addition of various additives, including tackifiers, antioxidants and fillers, allows further tuning of the adhesive performance. [1,10,20,62,86] Typically, the T_g of PSA is adjusted to 40-70 °C below the application temperature. [1,6,34]

PSAs are used in nearly all industries as well as in everyday life, including household, office, personal care and medical applications. In industry, this concerns temporary surface protection (masking tape), packaging, labeling and the assembly of automotive parts, toys or electronic circuit boards, while plasters, surgical drapes, dermal dosage systems and biomedical electrodes are representatives of the medical field. Moreover, PSAs are applied as decorative films, double or single sided adhesive tapes and with sticky notes in household and office. [1,5-12]

3.3.2. Characterization of PSAs

The behavior of PSAs is mainly described by three parameters: tack, adhesion (peel adhesion) and shear resistance (cohesion). **Tack** is defined as initial adhesion, which develops upon slight pressure and short application time. It enables the PSA to form a bond of measurable strength immediately after contact to the substrate and is a measure for the primary wetting of the substrate. It can be measured as the force required to separate adherend and adhesive at the interface, immediately after application. While tack describes *how quickly bonds are built*, **peel adhesion** is a measure of the *force required to separate* a PSA tape from a substrate at defined speed and peel angle (180 ° or 90 °). Both parameters are viscoelastic properties, which are influenced by the chemical composition (choice of monomers) and the structure of the adhesive (crosslinking degree, molecular weight). The determined values of tack and peel adhesion depend on the test method and conditions, including application time, temperature as well as the peel angle and speed. Moreover, the face stock material (carrier) and the coating weight have a significant impact. While tack is mainly influenced by the wetting behavior, peel is more dependent on the surface to which the PSA is applied. High peel adhesion requires a certain level of tack for bonding and proper cohesion for debonding. In contrast to tack and peel adhesion, **cohesion** (also called shear resistance or resistance to creep) is a bulk property and hence, describes adhesion within the substance (internal adhesion/strength, bulk property) rather than interactions between two different materials. It is defined as the force, which holds a substance together and is thus a measure of internal molecular forces. Cohesion is influenced by the molecular weight and the crosslinking density of the base polymer, whereas high molecular weights and high degrees of crosslinking result in high cohesion. However, it has to be considered that a certain molecular mobility is required for adhesion build up during bonding. In general, permanent adhesives require a higher level of cohesion than removable PSAs. For high cohesion, the molecular weight has to exceed the entanglement molecular weight M_e . On the contrary, cohesion is diminished by the addition of tackifiers, since they act as diluents and increase chain mobility. Besides these factors, also the coating weight, the face stock material, the substrate and the temperature during testing as well as the chemical composition and structure of the adhesive affect this parameter. [1,5,6,8,20,21,87]

The above described parameters can be determined by standardized tests, which are based on the methods described in chapter 3.2.3. Typically, peel adhesion, tack and shear resistance are investigated at room temperature. The standard ASTM method for the examination of *peel adhesion* is based on a peel test: The PSA tape is attached to a stainless steel test plate and subsequently lifted off at a speed of 15 cm/min and a peel angle of 180 °. The testing setup may be varied in order to provide better correlation to

usage conditions. The resulting force required for removing the tape from the test plate under given conditions is taken as the peel adhesion value. As already mentioned, peel adhesion is influenced by the temperature during testing, the application time and the backing material, which may alter the actual peel angle by deformation. [8] *Tack* is investigated using a pull test setup. Again, an adhesive bond is formed and broken during testing, but the bond was formed under comparatively light force and short application time. Usually, the tape is fixed and contacted by a probe or ball, which is subsequently pulled upwards under controlled conditions. [8,87] According to ASTM standards, the *shear holding power* is determined in a holding power test, where a fixed area (1.27 x 1.27 cm or 1.54 x 1.54 cm) of the tape is adhered to a vertical test panel. A weight of 0.5 or 1 kg is hung from the free end of the tape and the time required to pull the tape from the test panel is recorded (shear holding time). Although the shear holding power is mainly a property of the bulk, the test can be influenced by the backing and the surface interactions between the adhesive and the test panel. A variation of this method is the SAFT (shear adhesion fail temperature) test, which investigates the system under gradually rising temperatures (4.5 °C/min). The SAFT value is defined as the temperature at which the adhesive joint fails. [8]

3.3.3. Basic materials for pressure sensitive adhesives

While the first PSA tapes were based on NR and rosin, nowadays there is a huge variety of tapes which differ in their chemical base, the carrier material and their construction. [6,10] Typically, PSAs are based on (visco-)elastomers such as rubbers (natural and synthetic), polyacrylates and styrenic block-copolymers. Furthermore, polysiloxanes, polyurethans (PUR), polyesters, polyethers and ethyl vinyl acetate (EVA) polymers are used as basic adhesive material. [5,6,8,10,21,34,62] Adhesives based on rubber are the most cost-efficient PSA systems on the market. **Natural rubber** PSAs are characterized by a high molecular weight, low T_g (-70 to -40 °C), high tack and high peel adhesion. They are usually crosslinked to achieve the required cohesion and are applied from solution or as hot melts. However, these adhesives are not stable against long-term exposure to environmental conditions, as the unsaturated polymer backbone is prone to oxidative and radiation induced degradation causing yellowing and embrittlement. [1,5,6,21]

Block copolymers used in PSAs are mainly based on polystyrene in combination with isoprene or butadiene units and are composed of linear A-B-A, A-B, or branched (AB)_n sequences. Tack, peel and shear properties are controlled by the addition of tackifiers. They have moderate molecular weights and high cohesion due to phase separation, where

the domains act as physical crosslinkers. However, the unsaturation in isoprene or butadiene units causes oxidative instability as already discussed for NR. Block copolymer based PSAs are particularly applied as hot melts or high solids and packaging tapes. [1,6,8,10,21]

Another important class of PSAs is based on **polyacrylates**, which are obtained from random copolymers of (meth)acrylic esters and vinyl monomers. Polyacrylates are inherently pressure sensitive. Their adhesion properties and performance are mainly influenced by the chemical composition (choice of monomers) and the molecular weight of the acrylic polymers. Typical T_g s for polyacrylic PSAs are in the range of $-70\text{ }^{\circ}\text{C}$ to $-25\text{ }^{\circ}\text{C}$. [10,20,34] "Soft" acrylates with long side-chains such as *n*-butyl acrylate, 2-ethylhexyl acrylate or *iso*-octyl acrylate provide low T_g corresponding to high tack and peel adhesion. In contrast, "hard" short side-chain and polar monomers (e.g. acrylic acid and methyl methacrylate) increase the T_g and thus the peel force and the stiffness of the adhesive. Simultaneously, the internal strength increases due to the formation of intermolecular hydrogen bonds. In addition, acrylates with functional groups can be copolymerized to tailor interactions with selected substrates. For most applications polyacrylates are crosslinked to provide sufficient cohesion and stability. They are transparent and colorless and show excellent physiological properties as well as water, chemical and aging resistance (light, heat, oxidation) due to their saturated polymer backbone. [1,6,8,9] Along with aqueous emulsions or 100 %-systems (hot melts or low viscosity systems), acrylic PSAs are applied as organic solution of the copolymers. [5,6,11,88,89]

Typical **silicone PSAs** are based on poly(dimethylsiloxane) (PDMS) networks, which may be substituted with phenyl groups for increased surface tension, T_g ($-85\text{ }^{\circ}\text{C}$) and improved thermal stability. Usually, the long chain PDMS is crosslinked by addition of multifunctional siloxane resins. Moreover, vinyl, epoxy or acrylate functionalities may be introduced for crosslinking. The high costs of these niche products is often outweighed by high resistance to oxidative degradation, high chemical and weathering resistance and high thermal stability. In particular, the excellent temperature resistance ($> 500\text{ }^{\circ}\text{C}$) relies on the Si-O-Si backbone, which also provides high flexibility and thus low T_g . Hence, this class of PSAs can be applied in a wide temperature range ($-70\text{ }^{\circ}\text{C}$ to $250\text{ }^{\circ}\text{C}$) to both high and low energy surfaces. Peel can be improved by compounding the elastomers with silicon resins, which are attached via reaction of some free silanol groups, while crosslinking provides improved cohesion. [5,6,8,9,21,90] However, residual siloxane monomers present in the polymer matrix often remain on the surface of the adherend after tape removal, which compromises on product quality (e.g. decreased delamination resistance of composite structures) and thus limits the applicability of siloxane-based PSAs.

Besides silicones, also **polyurethane** adhesives comprise excellent bond strength durability and plasticizer resistance. PUR adhesives rely on urethane links, which are formed upon reactions of diisocyanates and di- or polyols. The viscoelastic properties are controlled by the chemical composition and structure of the monomers, whereas the structure of the diisocyanate has a high impact on the tack. Mostly, aliphatic diisocyanates are used. Alternating blocks of high and low T_g lead to segregated structures of hard and soft segments, which allow for thermoforming. PUR PSAs are mainly applied as laminating and mounting adhesives. [9,91]

Further PSAs are based on **polyvinyl (alkyl) ethers**. Unlike polyacrylates, these adhesives are not inherently pressure sensitive but rather comprise "dry tack". Consequently, blends of low and high molecular weight polymers are applied to ensure proper surface wetting as well as the required cohesion for PSA applications. [5,21] Crosslinking of di- or polyfunctional vinyl ethers provides the inner strength of the adhesive. [7] Since polyvinyl ethers comprise high moisture vapor permeability [5] and are non-irritating to skin, they are suitable for medical applications. [7]

3.3.4. Manufacture of pressure sensitive products

Common pressure sensitive products (PSPs) include tapes, labels or protective webs [1,7,8] and are wound to rolls, die cut or assembled on sheets. [6] PSA tapes represent the largest market share of all PSPs [1,8] and generally consist of a carrier coated with a PSA layer. [8] Furthermore, a release liner can be added to protect the adhesive layer until use. [7,8] The PSA is based on (visco)-elastomers (see chapter 3.3.3), which can be formulated with additives such as tackifiers, fillers, plasticizers, pigments, metal particles or carbon black (for electronic conductivity) or stabilizers against thermal oxidation (hindered phenols, phosphites, thioesters) or photo-induced degradation (hindered amines, UV-absorbers, pigments). [8] The carrier ensures the mechanical properties of the tape and may be any thin, flat and flexible material including plastic films (PET, LDPE, HDPE, PC, PVC, polyacrylates, PS and PP) or foams as well as papers and fabrics (woven/non-woven). [6,7,9] Also, the release liner consists of foils (PP, PE, PVC, PS, polyester) or coated papers. [6–9,88] Since it has to be removable without damaging the adhesive layer or deforming of the tape [8], the liner can be coated with a low energy material such as silicones based on PDMS, long alkyl-chain branched polymers or fluorinated polymers. In case of tapes, which are wound to rolls, this release coating is applied to the backside of the carrier. [6–8] Further approaches use rough surfaces to minimize the contact area

with the adhesive or consider the addition of low molecular weight materials, which build a weak boundary layer at the liner adhesive interface to ensure release properties. [8]

The classic way to manufacture PSA tapes is to coat the adhesive formulation onto the carrier. Alternatively, the adhesive can be applied to the carrier by extrusion coating or co-extrusion of adhesive and carrier. [9] The coating method depends on the physical state of the adhesive, the carrier material and the end use of the PSP. Typical techniques are roll-coating (knife over roll, reverse roll), (slot-) die coating, extrusion, calendaring as well as blade, casting, spray-coating and printing. [6,7,9] The adhesive is either coated directly onto the carrier or it is coated onto a release liner and subsequently transferred to the face stock material. [6,8,9,12] It can be applied (i) as solution or dispersion in organic solvents or water, (ii) in the molten state or (iii) as low molecular liquid components, which are polymerized directly on the carrier. [8] Before application the coated PSA layer (liquid state) has to be transferred to the solid state. In case of solutions or dispersions, the solvents are evaporated in air drying tunnels or festoon driers, while hot melts are simply cooled down. In addition, the adhesive layer might be crosslinked via thermal or irradiation curing (electron beam or UV-light) in order to control surface tack and adhesion strength. Finally, the prepared tape (continuous web) is converted to the desired geometry by cutting and slicing. [6,9] To ensure proper wetting and anchorage of the adhesive towards the carrier, the carrier surface might be modified by physical or chemical routes. [9,21] Therefore, primers or surface treatment techniques, including flame or corona discharge, are employed to increase the surface energy of the carrier (see chapter 3.2.4 for more details). [6,8,9]

According to their construction, PSA tapes are divided into single-sided and double-sided products. [7,8] Conventional single-sided tapes are composed of the following layers: carrier – primer – PSA layer (10-750 μm) - release liner (see Figure 11), whereof the primer and the release liner are optional. If the tape is wound to a roll, the release *liner* is replaced by a release *coating* on the backside of the carrier. [6-8] Double-sided tapes, in contrast, are coated on both sides of the carrier [6]. Thus, the construction includes the following layers: release liner - PSA 1 – primer – carrier – primer – PSA 2 – release liner (see Figure 11). Again, the primer is an optional component. In rolls only one intermediate release liner, which provides release properties on both sides, is required to prevent contact of the PSA layers. The two PSA layers can either be identical or different in order to adjust the adhesive properties to individual applications and requirements. [6] In transfer tapes, where the adhesive is transferred to the substrate as a free layer, the carrier is replaced by another release liner. [6,8]

-Theoretical background-

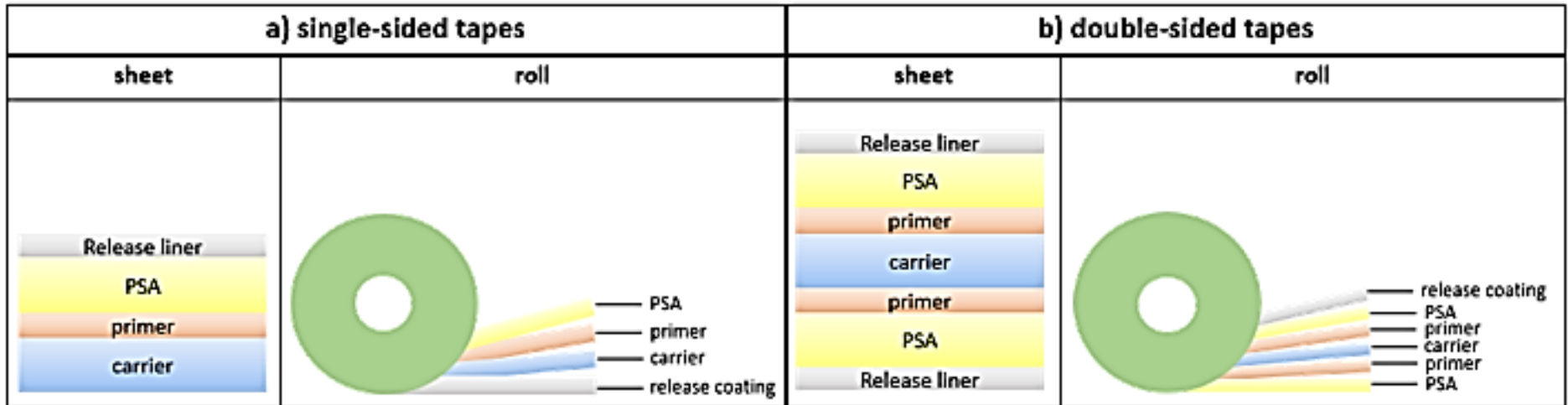


Figure 11: Construction of single- and double sided tapes

3.4. Photochemistry

3.4.1. Definition and importance of photochemistry

Photochemistry is the study of chemical reactions or physicochemical phenomena, which are induced by absorption of light (photons) by a material. Upon photon absorption a portion of molecules of the exposed material is transferred to the excited state and subsequently undergoes processes such as ionization, luminescence, radiation-less decay, quenching, excitation transfer or sensitization, photo-isomerization and rearrangements, photo-dissociation, decomposition, electron transfer, bimolecular reactions, addition reactions and photo-polymerization. [92,93] Typically, energies of 100-1000 kJ/mol are applied, which are in the right magnitude to break bonds or cause molecular rearrangement. These energies correspond to wavelengths in the range of 120-1200 nm, including the ultraviolet (UV; 10-400 nm), the visible (Vis; 400-750 nm) and the near infrared spectrum (NIR; 750-1500 nm). [92,94] Practically, radiation in the UV and VIS ($\lambda = 200-800$ nm) is applied to induce chemical reactions (electronic transitions), while NIR radiation causes changes of the vibrational and rotational energy levels of the molecules (movement). [92]

There are four laws, which describe the effect of light on chemical processes: The Grotthus-Drape's Law (1st law of photochemistry) was formulated independently by T. Grotthus (1818) and J. Draper (1839) and states that, light absorbed by matter can induce chemical changes in the material, while reflected and transmitted light do not cause any reactions. The Bunsen and Roscoe's Law declares that the number of moles changed photochemically is directly proportional to the product of the light intensity I and the duration of irradiation t ($n \sim I * t$). [92,95] In the Stark-Einstein's Law of photochemical equivalence light is considered as a stream of particles or quanta (photons) with an energy of $E = h * \nu$, where h is the Planck's constant and ν is the frequency of light. This law says, that for every quantum of light (photon) absorbed, one molecule of the irradiated substance reacts and undergoes a chemical change. Since the frequency is indirectly proportional to the wavelength ($\nu = 1/\lambda$), high energy is transferred to the irradiated material by the use of short wavelengths or a high frequency, respectively. [92,95,96] In contrast to the Stark-Einstein's Law, the Platnikow Law is more theoretical and proposes that if chemical changes take place in the dark and in the presence of light, the overall reaction will be the sum of effects, which occur due to darkness as well as due to light. [92,95]

Photochemistry has always been important since proteins and nucleic acids had been formed from CH_4 , NH_3 , H_2O and CO_2 under the impact of sunlight in the prebiotic era. Moreover, photosynthesis is a photo-chemical process, where chlorophyll, the green pigment in plants, absorbs irradiation in the VIS spectral region. The absorbed energy is then transferred to CO_2 and H_2O to give cellulose and carbohydrates. [92,93] Today, photo-chemical processes are also utilized in industry. For example, the photo-electric effect is used in solar cells, fluorescence and phosphorescence are used in tube lights and photochromic materials such as spiropyranes are part of photochromic sunglasses. Moreover, photochemical reactions are the basic for synthesis of organic compounds such as antioxidants, vitamin D_2 , caprolactam, halogenated aromatics, etc. [92] One advantage of photochemical reactions over thermally induced processes is their selectivity. [92,93] While it is possible to excite only one specific molecular species by selection of the proper wavelength, thermal activation increases the translational energy of all species in the exposed material. [92] Furthermore, photo-induced reactions are economically advantageous since they can be executed at room temperature without any solvent and because they are rapid and cost efficient and require comparatively low energy for initiation. [97] Photo-chemical reactions only take place during exposure to light, but stop when the irradiation source is turned off. Temperature has little effect on the reaction rate of photo-chemical processes. In contrast, the light intensity plays an essential role for the kinetics of photochemistry. [92]

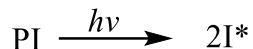
3.4.2. Photopolymer technology and photo-polymerization

Photopolymer technology deals with the action of light to form polymers and with photo-triggered reactions in polymer materials. This includes chemical and physical reactions of organic-based materials, which are induced by UV, IR or e-beam irradiation. First applications of photopolymer technology date back to the 1930s-1940s and emerged rapidly during the last five decades. Application fields encompass electronic materials such as photo-sensitive resists for PCB production (see 3.5.2 for more details), printing materials including printing plates and inks and optical and electro-optical materials (synthesis and alignment of liquid crystal polymers). Moreover, photopolymer technology is employed for the manufacture of devices, polymer materials, adhesives, sealants and coatings, including dental fillings, microporous gels and micro-particles, light sensitive adhesives, implantable bone prosthesis, contact lenses, hydrogels with controlled drug release properties and decorative and protective coatings. [98,99]

There are five mechanisms of photopolymer reactions: Photo-polymerization, photo-crosslinking, photo-molecular reactions, photo-degradation and photo/thermal reactions. Most commercial applications are based on the photo-triggered polymerization of monomers and oligomers yielding high molecular weight materials. [98] Typically, photo-polymer formulations contain reactive monomers and oligomers, a photoinitiator, a pre-polymer to provide the required physical properties for processing and additives. [98,99] In contrast, photo-crosslinking directs unsaturated moieties, which are already attached to a polymer and are crosslinked upon irradiation. One example is the [2+2] cycloaddition of ethylenic groups in poly (vinyl cinnamate). Another aspect of photo-polymer reactions is the modification of polymers. In photo-molecular reactions, small molecules undergo reactions with the polymer such as rearrangement and isomerization and are incorporated into the matrix. As a result, plasticization, tack and adhesion of the polymer are modified and color changes can be initiated. Moreover, polymers can be degraded upon the impact of light. The polymer may either contain photo-sensitive linkages, which are cleaved upon irradiation, or a light absorbing ingredient generating active species, which attack the polymer chain. Unlike the first four mechanisms, photo/thermal reactions are based on physical changes in the polymer matrix. One example is laser ablation of organic coatings in the production of printing plates. [98]

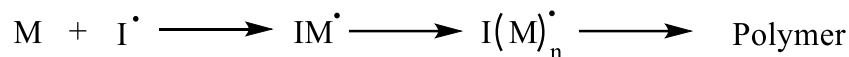
Here, **photo-polymerization** is discussed in more detail, since it represents an essential part of this work. In general, radical, cationic and anionic polymerizations can be started by exposure to light. [97–100] Since the formation of reactive species directly on the monomer is not efficient, photoinitiators (PI) are used. Upon exposure to light, the PI generates active species I^* , which in turn attack the monomer M and thus start polymerization (see Figure 12). [97,99,100] In addition, photosensitizers can be added to the formulation in order to extend the spectral sensitivity. Photosensitizers absorb light energy at wavelengths, where the PI is not able to operate, and transfer it to the PI. Typically, aromatic compounds such as benzophenone, acetophenone, naphthalene, anthracene, etc. are applied as photosensitizers. [97,99]

generation of active species

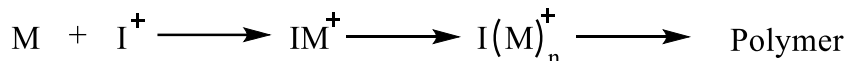


I* ... radical, cation, anion
M ... monomer

free radical polymerization



cationic polymerization



anionic polymerization

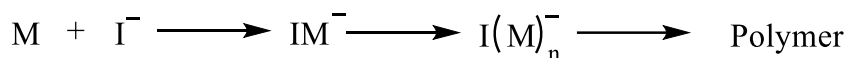


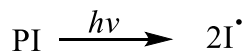
Figure 12: Schematic reaction mechanisms of radical, cationic and anionic polymerization

In the following the most important aspects of free radical and ionic polymerization are discussed:

Free radical polymerization either proceeds via free radical chain growth or via free radical addition, depending on the composition. The first utilizes C=C double bonds of unsaturated polyesters or styrene as well as multifunctional acrylates or methacrylates for curing. [98–100] The mechanism of free radical chain growth includes (i) initiation, where the initiating radicals are generated by photolysis of the PI and monomer radicals are formed, (ii) propagation, where monomers are successively added to the radical chain, chain transfer (iii), where hydrogen atoms transferred from a hydrogen donor stop propagation of the respective chain and start growth of another chain, and termination (iv), where chain growth is stopped by either recombination or disproportionation reactions of two radicals (see Figure 13). [99,100] Furthermore, the radicals can be trapped due to increasing viscosity and decreasing molecular mobility with proceeding polymerization. Since trapping is presumed to be permanent, these radicals are seen as inactive. [99] Another important aspect concerning free radical chain growth is oxygen inhibition. O₂ may disturb polymerization either by quenching the triplet state of the PI or by scavenging the initiating and chain radicals (see Figure 13). The generated peroxy radicals are inactive towards reaction with the monomers and thus retard or even stop polymerization. In contrast, they can react with hydrogen donors, building neutral hydro peroxides and a donor radical. In order to prevent oxygen inhibition, irradiation can be done under inert gas atmosphere (e.g. N₂, CO₂) or oxygen scavengers such as amines,

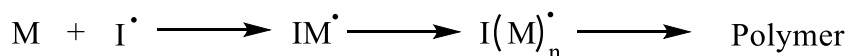
phosphines or thiols are added to the formulation. Moreover, paraffin waxes are added, building a protective layer at the surface. Also, the application of high PI contents and irradiation with high light intensity reduce the effect of oxygen inhibition. [99,100]

(i) initiation

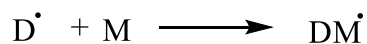
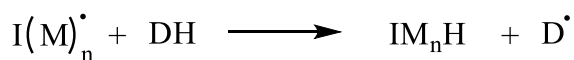


I^* ... radical, cation, anion
 M ... monomer

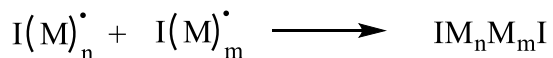
(ii) propagation



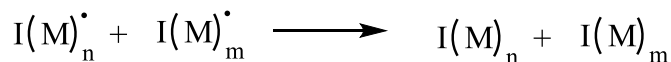
(iii) chain transfer



(iv) termination

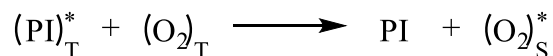
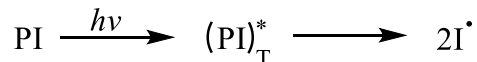


recombination

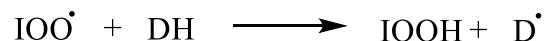
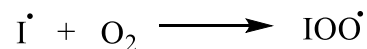


disproportionation

O₂ inhibition



quenching



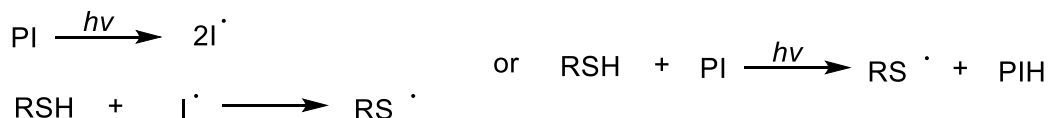
radical scavenging

Figure 13: Mechanism of free radical chain growth involving initiation, propagation and termination reactions as well as oxygen inhibition [99]

The second reaction type (free radical addition) utilizes thiol-ene reactions, where thiols are added to unsaturated compounds such as allylic functionalized resins, vinyl or allyl ethers as well as *n*-alkenes, (meth)acrylates and allylic urethanes. [99,100] Firstly, UV-irradiation is applied to cleave the PI (type I or type II) and generate initiating

radicals, which then abstract a hydrogen atom from the thiol. The resulting thiyl radical attacks the C=C double bonds of the olefinic monomers, building an alkyl radical, which in turn either adds to another C=C double bond or generates another thiyl radical by hydrogen abstraction (chain transfer). As for free radical chain growth, polymerization is terminated by recombination of two radicals (see Figure 14). In contrast, free radical addition reactions are not sensitive to oxygen inhibition, because peroxy radicals would only contribute to the formation of thiyl radicals via hydrogen abstraction and the related initiation of polymerization. [99,100] Although this mechanism is emerging in industry, it is limited to special applications so far. [100]

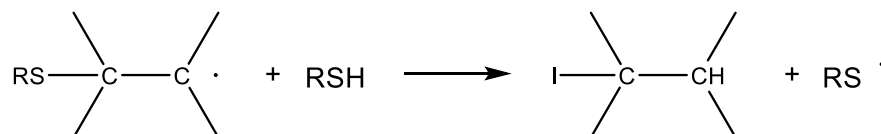
initiation



propagation



chain transfer



termination

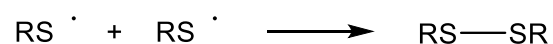
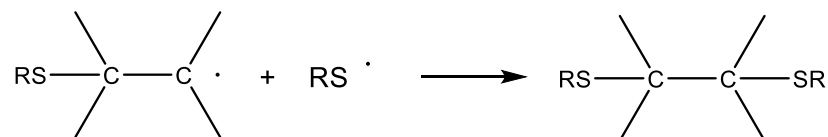
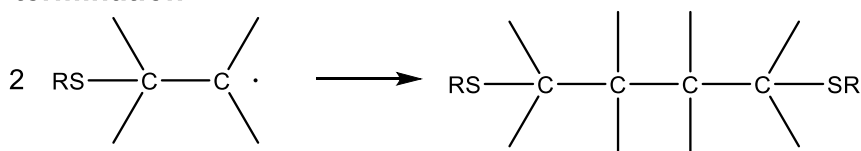
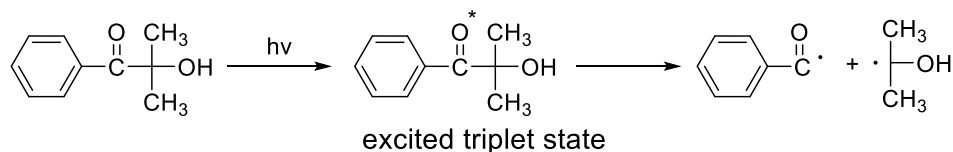


Figure 14: Mechanism of free radical addition involving initiation, propagation and termination reactions [99,100]

Typical initiators for radical photo-polymerization are peroxides, disulfates, azo compounds, ketones, aldehydes, whereof aromatic ketones are the common choice (compare Figure 15). [99,100] The generation of free radicals upon irradiation (initiation) follows two mechanisms, depending on the substitution of the ketone and the aromatic moiety. While R_1 directs the mechanism of degradation, R_2 influences the wavelength at which light is absorbed. When R_1 is an alkyl group, the PI is cleaved according to type I mechanism (scission; see Figure 15). The most common type I mechanisms are Norrish type I reactions, where absorption of UV-light leads to excited species in the triplet state, which form free radicals by the cleavage of the CO-alkyl bond. For type II mechanism (hydrogen abstraction), aryl groups are used in R_1 position. UV-light is of insufficient energy to cleave the CO-aryl linkage, and the PI remains in the excited state until it reacts with a hydrogen donor such as tertiary amines, ethers, esters or thiols. A hydrogen atom is abstracted by the PI in triplet state and low reactive ketyl and highly reactive donor radicals are formed. The two mechanisms are demonstrated in Figure 15 at the examples of an acetophenone derivative and benzophenone, which are typical representatives for type I and type II PIs. [100]

type I: scission



type II: hydrogen abstraction

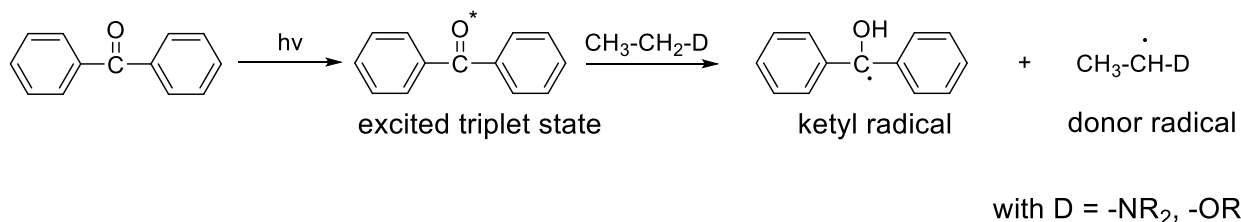


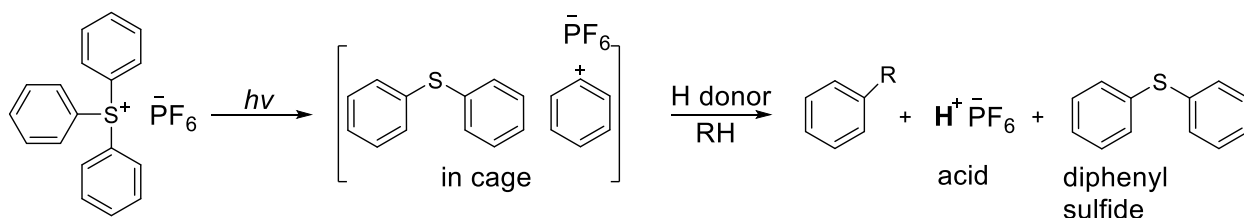
Figure 15: Generation of free radicals according to type I and type II processes [100]

Besides the formation of radicals according to type I or type II reactions, the triplet state may also decay from excitation in form of phosphorescence or may be quenched by monomers or oxygen. Since the life time of this transition state is much shorter for type I PIs, side reactions are less likely for this mechanism. The efficiency and speed of the

photo-reaction depends on the structure of the PI and the related stability of the transition state [99], the formulation (monomers, binders, etc.), the viscosity of the reaction mixture, the applied light intensity, the film thickness and the use of pigments and additives. [100]

In addition to the free radical mechanisms, photo-induced polymerization may also follow ionic pathways. Since anionic reactions are very sensitive to moisture and prone to O₂ inhibition, most available ionically cured systems are based on cationic polymerization. Typical monomers for **cationic photo-polymerization** are compounds containing epoxy, oxetane or vinyl ether moieties. [98–100] Polymerization starts with the UV-induced decomposition of a proper PI, yielding Brønsted or Lewis acids. There are three types of PIs, which can be applied to start cationic photo-polymerization: aryldiazonium salts, onium salts and organometallic complexes (ferrocenium salts), whereof onium salts are most commonly used. The most important representatives are triaryl sulfonium salts with counter ions such as PF₆⁻, SbF₆⁻, AsF₆⁻, BF₄⁻. These PIs either cleave homo- or heterolytically upon UV irradiation, generating “in-cage-intermediates” in the singlet state, which in turn form strong acids in the presence of hydrogen donors (see Figure 16). Therefore, PIs used for cationic polymerization are also called photo acid generators (PAG). Besides aryl and diphenyl sulfide, isomers of phenylthiobiphenyl (heterolytic) as well as benzene, biphenyl and other by-products (homolytic) are formed due to side reactions. [99,100]

heterolytic photo cleavage



heterolytic photo cleavage

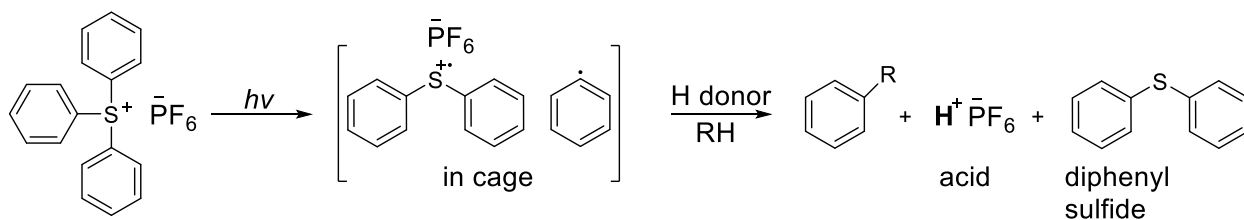


Figure 16: Formation of photo acid by heterolytic and homolytic cleavage of a triaryl sulfonium salt (PAG)

The generated proton reacts with a monomer and initiates ring opening polymerization of the cyclic ether group. A carbocation is formed, which attacks another monomer. Thus, propagation proceeds via cationic addition polymerization, resulting in a polyether chain or network (see Figure 17). In case of vinyl ether monomers, carbon chains with pendant ether groups are formed. [100] Termination may occur due to reactions with anions or hydroxyl groups or due to chain transfer. [99] Although initiation is UV-induced, the remaining polymerization process is thermally driven. [100]

cationic polymerization

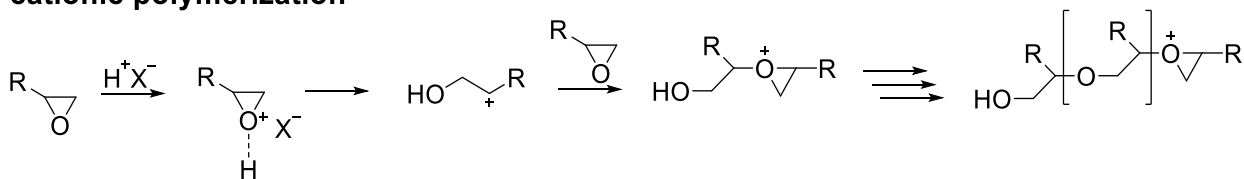


Figure 17: Reaction mechanism of cationic ring opening polymerization [100]

Cationic polymerization involves more expensive materials than free radical polymerization, and thus is less commonly used in industry. [100] Another difference is that cationic polymerization is not inhibited by oxygen, but by alkaline materials such as amines, urethanes or additives (fillers, pigments) and humidity. The latter may induce chain transfer reactions and thus reduces the average molecular weight of the formed polymer and slows down the cure speed. [99,100] Regarding the kinetics, there is also a strong impact of the viscosity of the starting material on the propagation rate and residual monomer content. [99] Moreover, the anion affects the strength of the photo acid. [100] Usually, epoxy cure is slower compared to free radical polymerization of acrylates. [99] However, post polymerization has to be considered here. Since the proton generated by cleavage of the PAG is very stable, it continues promoting the polymerization reaction even after the light source has been switched off. [99,100]

-Theoretical background, Photochemistry-

The main differences between free radical and cationic photo-polymerization are summarized in Table 2.

Table 2: Differences between free radical and cationic photo-polymerization

	free radical photo-polymerization	cationic photo-polymerization
reaction mechanism	free radical chain growth	cationic addition polymerization
monomers	(meth)acrylates, unsaturated polyesters, styrene or thiol-ene systems	epoxides, oxetanes, vinyl ethers
sensitivity	sensitive to oxygen not sensitive to alkaline components or humidity	not sensitive to oxygen sensitive to alkaline components or humidity
post reaction	no significant post reaction (stops when light switched off)	significant post reaction (dark reaction)
industrial aspects	many PIs available → cheaper	only few commercial PIs available → more expensive

3.5. Printed circuit boards

Nowadays, printed circuit boards (PCBs) are used in nearly all electronic products. PCBs provide mechanic support and electrical connection of electronic components via conductive tracks, pads and similar features. In general, PCBs consist of an insulating material, which carries conductive patterns. Therefore, thin copper foils are laminated to FR 4-epoxy prepregs and etched to create conductive paths. Depending on the number of copper layers, one can distinguish between single sided and double sided PCBs. For more complex circuits and high component densities, multi-layer PCBs are used. Components such as capacitors, resistors and active devices may be embedded in advanced PCBs. [101]

3.5.1. The history of printed circuit boards

PCBs how we use them today, only exist since a few decades. [102] Before PCBs were invented, wire wrapping or point-to-point constructions, which were extremely bulky and unreliable, had been used. [101,103] In the following, the most important milestones of PCB development are summarized:

A forerunner of modern PCBs was built by Albert Hanson in 1903. Foil conductors of brass or copper were cut or stamped out and adhesively bonded onto an insulating material (paraffined paper) in multiple layers. The bottom and the top conductor layers were connected via holes. [102,104,105] Moreover, Hanson already found that conductors can be built by electrodeposition and that a high packing density is crucial. At the same time, Thomas Edison was working on concepts of how to replace wires (1904). He proposed (i) selective application of glue, which was then dusted with conductive powders such as graphite and bronze, (ii) patterning of a dielectric with silver nitrate and a subsequent reduction of the salt to Ag^0 and (iii) the application of gold foil onto a patterned adhesive to build wireless circuits. [105] Another important development was the print and etch method, which was firstly described by Arthur Berry in 1913. [102,105] Electric tracks were produced by patterning the metal layer by a resist and etching the uncovered metal away. [105] In 1914, Max Schoop patented and later commercialized the flame spray method, where thick patterns of metal were deposited through a mask. [102,105] An early version of electroplating was developed in 1927 by Charles Durcase. Electric paths of copper, silver or gold were printed through a stencil, which allowed for direct application onto the insulating material [102,104,105] and thus eliminated complex wiring. [103] PCB invention dates back to John Sargrove (1936-1947), who sprayed metal

onto Bakelite. [101] However, the first contemporary PCB was developed by Paul Eisler in 1936 as part of a radio system. [101,102,104] His approach was based on photoetching, which is still the most popular manufacturing method. Eisler adopted photosensitive coatings, which were developed and well established in the 1800s, to the manufacture of circuits. [105] During World War II, Eisler's technology was used by the U.S. Army [102,104], who released it to the public in 1948 for the manufacture of commercial products. In 1949, Moe Abramson and Stanislaus F. Danko of the U.S. Army Signal Corps developed an auto-assembly process for PCB production, where component leads were passed through drilled holes and soldered to a PCB trace. [101,102] This concept was patented in 1956 [102–104] and became the standard of today after combining with the new inventions of board lamination and etching techniques. [101]

While in the 1920s almost everything was used as PCB material, including Bakelite, Masonite and even thin, plane pieces of wood [103], the materials were changed to resins in the 1950s to 1960s. However, printing was limited to one side of the PCB until 1947 and the 1960s, respectively, when the first double sided PCB with plated through-holes was produced and the first multi-layer (4+) board was developed. In the 1970s, PCBs started getting smaller and hot air soldering and the first photo imangible mask were developed, which were implemented in the standard production process. [103,104] Since the 1980s small parts were mounted to the PCB surface, replacing through-hole constructions. Moreover, the size of PCBs was further reduced, while providing the same level of functionality. Though the complexity of PCB construction increased continuously and miniaturization proceeded in the following years, automatization of PCB manufacture allowed for low costs. [101,103,104]

3.5.2. Construction of printed circuit boards

Materials

The basic materials used for the manufacture of PCBs are copper foils of different thicknesses (0.0007 or 0.00134 inches), prepregs (pre-impregnated bonding sheets) and inner-layer cores (copper foil – prepreg – copper foil). Among the different types of prepregs, FR 4 material is the most common in use. It consists of a woven glass fiber cloth pre-impregnated with an epoxy resin, which is cured to B-stage. Inner-layer cores, prepregs and copper foils are joined during the lamination process, where high temperatures and pressures “melt” or soften the epoxy resin. Consequently, the resin flows across the copper features and exposed laminate sites of the core, bonding them together

while cooling. In order to improve adhesion with the epoxy resin, the copper surfaces can be treated chemically and/or mechanically. [106] There are etching technologies and the black oxide treatment, which rely on mechanical adhesion only. In contrast, oxide replacement technologies additionally offer a certain extent of chemical adhesion. [107,108] One example for the latter is BondFilm® treatment, where the copper surface is roughened with an etchant of sulfuric acid and peroxide to enable good mechanical interlocking with cured epoxy prepregs (main adhesion mechanism). In addition, an organometallic layer containing benzotriazole derivatives is applied to provide some extent of chemical adhesion. [107–110] As described in reference [43], the coupling effect of the azole compounds is based on covalent bonds to copper (benzodiazolato Cu(I) or bis(benzotriazolato) Cu(II)) and its participation in the ring opening polymerization of the epoxy resin. [107–110]

Manufacturing process

In general, one distinguishes between single sided, double sided and multi-layer PCBs (see Figure 18). While single and double sided PCBs consist of a rigid prepreg base with copper on one or both sides, respectively, multi-layer PCBs are made from one or more inner-layer cores (depending on the design) with copper foils on the top and bottom. The number of layers corresponds to the number of copper foils incorporated.

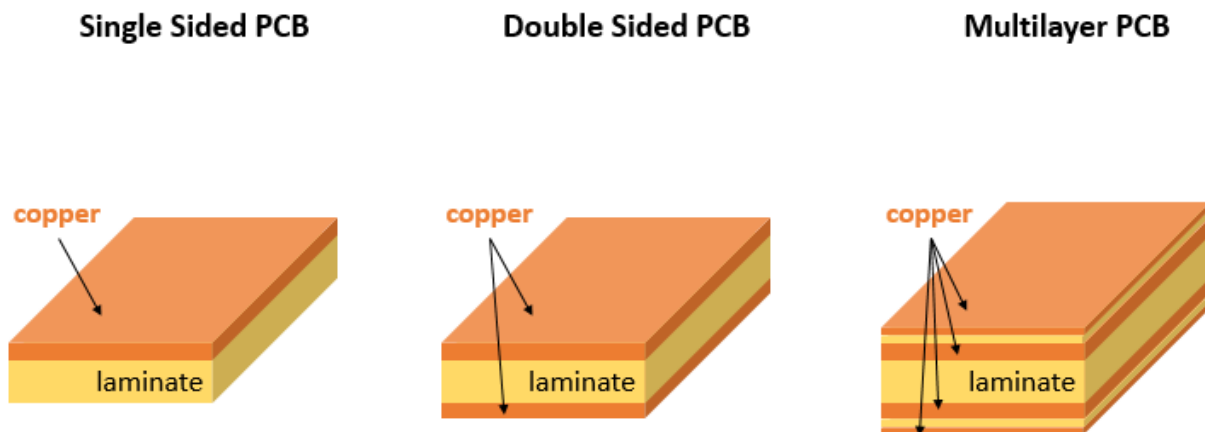


Figure 18: Construction of single-sided, double-sided and multilayer PCBs

The production of multi-layer PCBs (see Figure 19, Figure 20 and Figure 21) starts with the selection of an inner-layer core, which is subsequently covered with a photo-sensitive resist. The resist is cured under heat and pressure. Then the panels are exposed to high intensity UV-light through a patterned film, which depicts traces, pads and other copper features as well as the solder mask. The light can only pass through the clear areas of the film, where it cures the photo-sensitive resist. During image development, the non-polymerized areas of the resist are removed, giving in the negative image of the desired circuit pattern. In the next step, the copper, which is not covered by the resist, is chemically removed from the core (inner-layer etch) and the desired copper pattern is created. Finally, the remaining resist is removed chemically (resist strip), revealing a pattern of copper and exposed core laminate. The resulting inner-layer cores are then examined in an automated optical inspection, where defects are detected and - if possible - repaired. [106,111]

For multi-layer production, an adhesion promoting layer is applied to the exposed copper surfaces on the patterned core. Further layers of prepreg and copper foil are applied to the top and bottom of the inner-layer core via lamination under high temperature and pressure. Again, the copper surfaces are patterned by the use of a photo-sensitive resist and chemical etching (repeat steps 2-6). However, the final copper layers (top and bottom) of multi-layer PCBs remain unetched and do not comprise any pattern. [106,111]

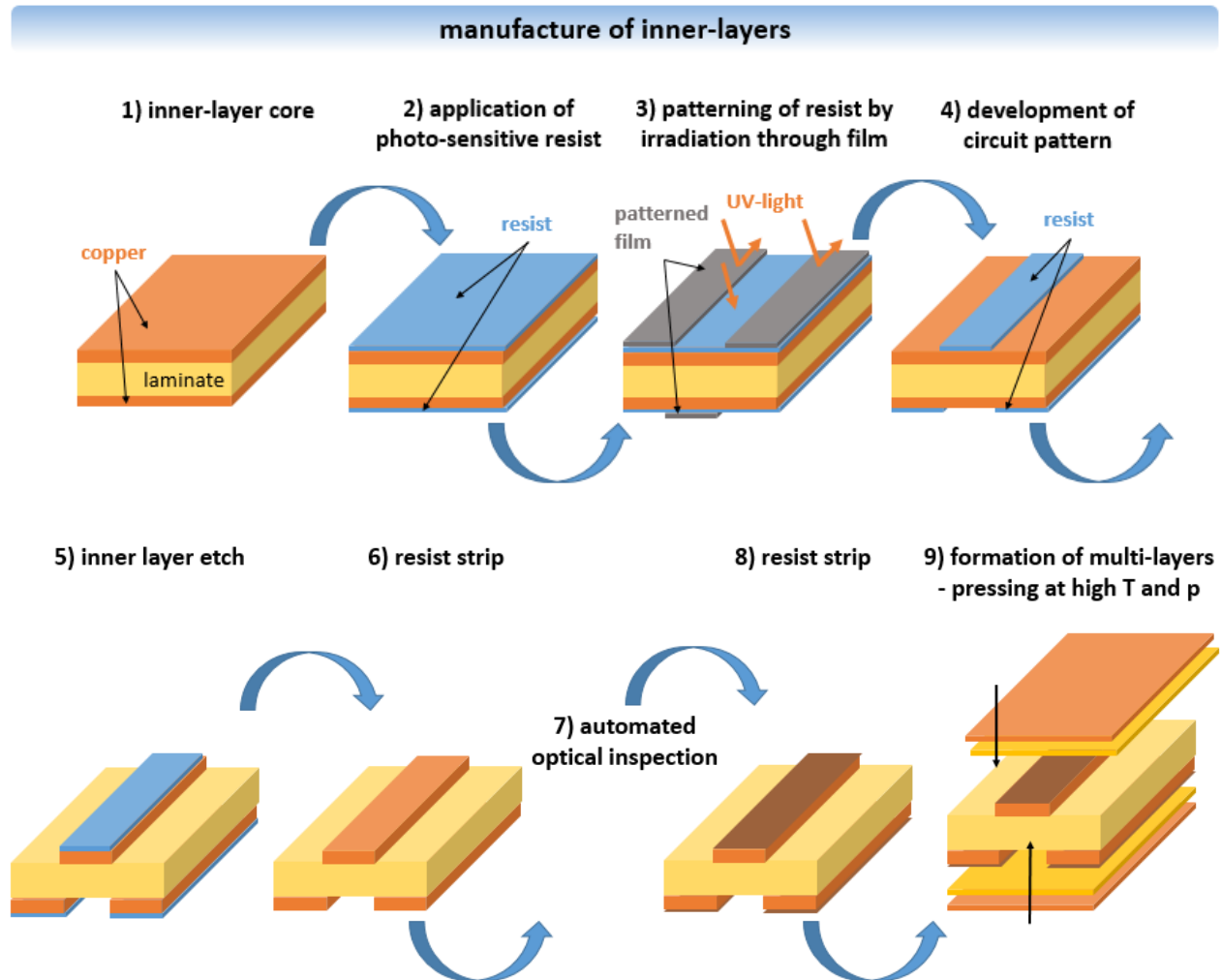


Figure 19: Manufacture of PCBs - inner-layer core

Next, holes are drilled through a stack of panels according to the board design (primary drill). They are prepared a few mils larger than required in the end to allow for copper plating. Raised edges and metal burrs, which originate from the drilling process, are removed in a mechanically abrasive process (deburring). Furthermore, thin coatings of resin are formed at the inner layer connections (inside of the holes) as a consequence of the frictional heat and motion of the drill bits. In order to improve connectivity, this excess resin is removed chemically in the desmear process. In the next step, the metallic base for electroplating is applied by chemical deposition of a thin copper layer on all exposed surfaces of the panel, including the drilled holes. Then, the panel is coated completely (also holes) with the photo-sensitive resist, which was already applied on the inner-layer cores. The resist is developed as described for the inner-layer cores, creating the circuit

pattern by irradiation with UV-light through a patterned film and subsequent removal of the non-polymerized areas via chemical solution. All drilled holes, which are exposed, will be plated through. In the following electroplating process, copper (~ 1 mm) is deposited onto the exposed metal surfaces on the panel. In order to maintain the copper traces, hole pads and walls during the outer-layer etch, all exposed copper surfaces are covered with tin in another plating process. In the first step of the "strip-etch-strip" process (SES), the resist is removed from the panel. While the tin plating is not affected, holes, which were covered by the resist, are now open and will remain non-plated. In the etch process (2nd step of SES), all copper is removed from the panel, except areas covered by tin. Finally, the tin is stripped chemically in the last step of SES, revealing pads, traces and plated through holes of copper on the laminate surface according to the circuit pattern. [106,111]

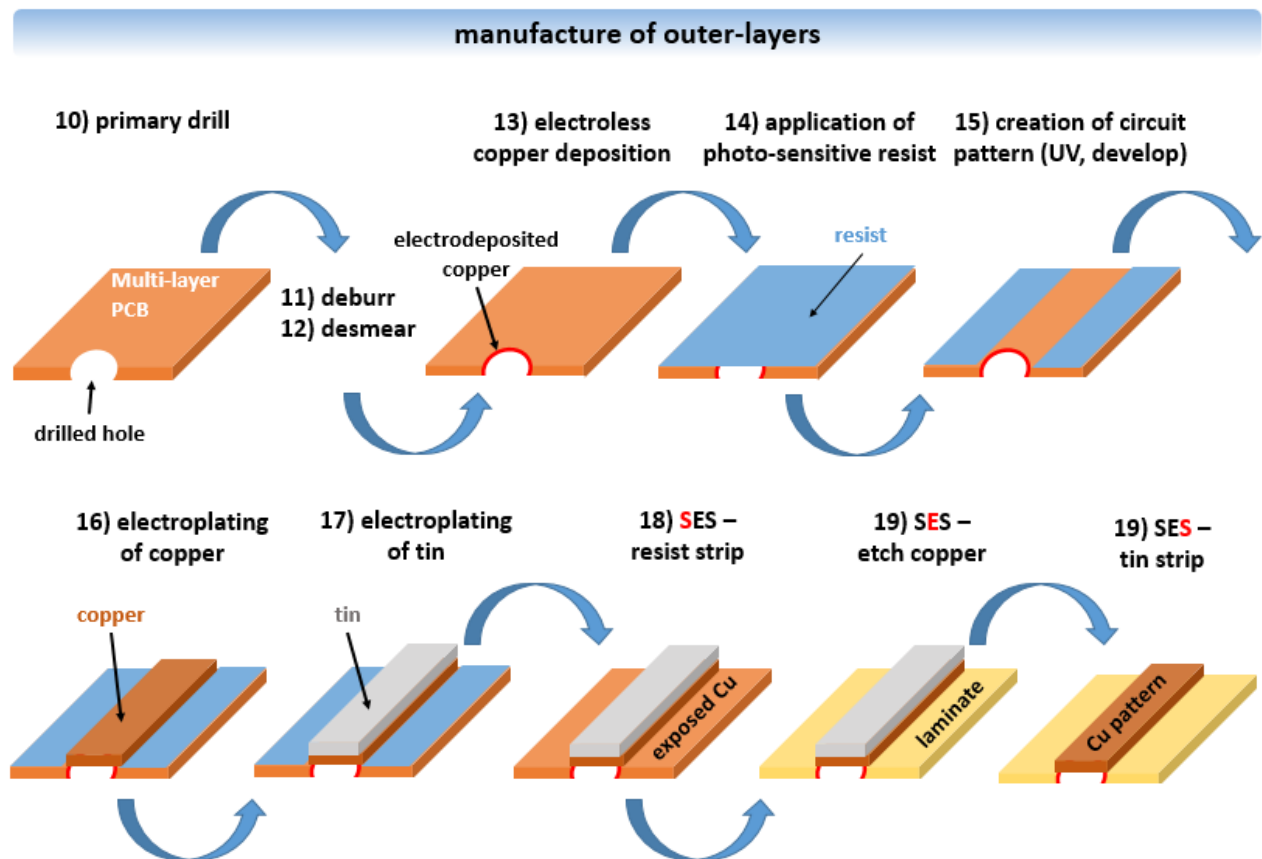


Figure 20: Manufacture of PCBs - outer-layers

The exposed copper features are cleaned from contaminations and superficial oxidation products by scrubbing with pumice, in order to improve adhesion to the solder mask. This photo-sensitive epoxy based ink is coated all over the panel and dried to the touch but not fully cured. Next, it is exposed to light through a film tool and developed, exposing pads and holes as defined by the circuit pattern (similar to patterning process). Then, curing is completed by baking in the oven or by the use of infrared heat sources. The solder mask is used to restrict areas, which will be covered with solder and protects the panel from contamination handling damage and shorts during assembly and installation. Information such as component placement, part name or number, date code and logo are silk screened onto one or both sides of the panel. After curing the ink by baking, the hot air solder leveling process (HASL) is started. The panel is coated with flux to promote coating of copper during dipping into a bath of molten solder. The solder covers all exposed metal surfaces. Excess solder is removed from holes and the pad surfaces are smoothed by high pressure hot air blasting. [106,111]

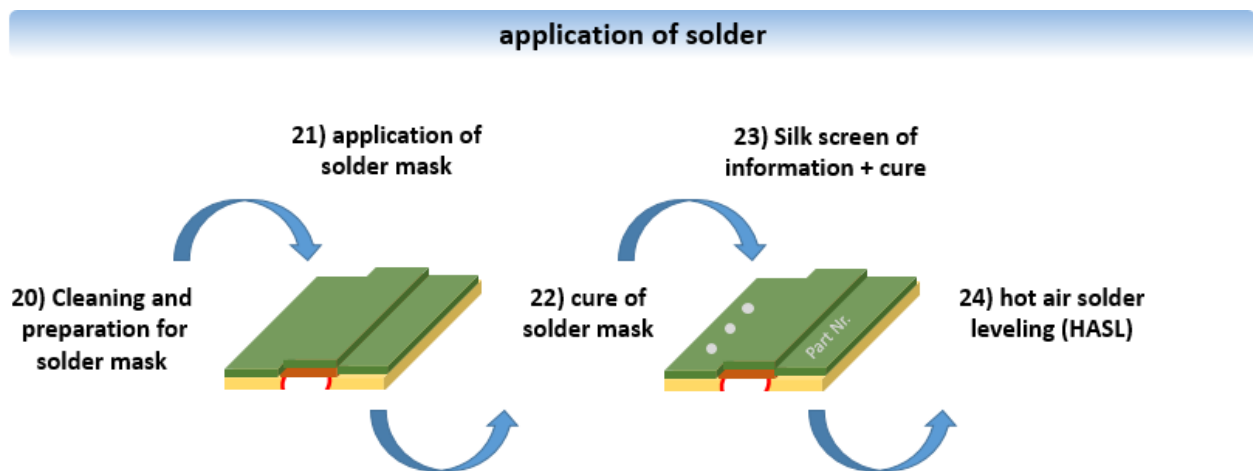


Figure 21: Manufacture of PCBs: application of solder

The produced PCB is then cut to size and checked for fabrication requirements such as cleanliness, sharp edges, burrs, etc. Moreover, an electrical performance test is done to detect opens or shorts, which are repaired if possible. Finally, there is another visual inspection of the product before packaging and distribution. [106,111]

4. Strategies and approaches

As described in chapter 2 (scope of the thesis), the designed PSA tape is applied temporarily in the production of PCBs. In order to ensure reliable fixation of the microelectronic components, high initial tack and adhesive strength are required during the application. In addition, easy and clean removability after exposure to high temperatures and pressures (200 °C, 20 bar) is required to prevent delamination in subsequent processing steps. These contradictory demands are combined in one PSA by selection of a suitable basic adhesive system and the incorporation of a release function, allowing for debonding on demand. Firstly, a suitable adhesive system is selected. From the wide range of PSA basic materials, acrylate and epoxy based adhesives are chosen because the diversity of available monomers enables precise adjustment of the adhesive properties. Moreover, polyacrylics and epoxy adhesives are thermally stable and provide a high resistance against aging and chemicals. Although polysiloxane adhesives perfectly fit the requirement of thermal stability (resistant up to 250 °C), they are excluded at the request of the company partner. In general, debonding on demand can be achieved by a variety of mechanisms, which can be initiated by changes in temperature, exposure to UV or VIS irradiation as well as by electronic or magnetic effects (see also chapter 1, Introduction).

In this thesis, acrylic and epoxy based (co)polymers are synthesized as the basic adhesive material. The monomer composition is varied in order to adjust the adhesive properties (hard and soft monomers) and the thermal stability of the adhesive (aromatic compounds). Moreover, photo-responsive moieties such as vinyl or acryl groups are introduced to the side chains to enable UV-induced crosslinking of the adhesive polymers. Another approach utilized with *acrylic* PSAs, is the formation of semi-interpenetrating networks (semi-IPN). Therefore, the acrylic PSA is blended with multifunctional acrylic monomers and a photoinitiator, building semi-IPN with the base polymer upon UV-induced polymerization. The chemical composition of the synthesized adhesive polymers is examined by infrared (IR) and nuclear magnetic resonance (NMR) spectroscopy, while the thermal properties are investigated by thermogravimetric analysis (TGA) and differential scanning calorimetry (DSC). Moreover, gel permeation chromatography (GPC) is performed to determine the molecular weight distribution of the adhesive polymers.

Adhesive tapes are prepared by coating a solution of the adhesive formulations onto a PET carrier, which can be either untreated, corona activated or modified by an organosilane coupling agent. The PSA layers, which vary in the structure of the basic adhesive polymer, the structure and concentration of the multifunctional monomers and

-Strategies and approaches-

the photoinitiator concentration, are characterized by IR-spectroscopy, displaying their reaction kinetics and the debonding efficiency during UV-irradiation. Moreover, the T_g of the adhesive formulations is determined by DSC measurements prior to and after UV-induced crosslinking and the thermal stability is investigated by TGA. The performance of the PSA tapes is followed by peel tests prior to and after photo-triggered debonding. Furthermore, the removability from different substrates after exposure to temperatures ranging from room temperature up to 240 °C was evaluated by the use of optical light microscopy in dependence of the adhesive formulation, the carrier pretreatment and other processing parameters as well as the surface quality of the substrate.

5. Experimental part

5.1. Chemicals and materials

The **acrylic monomers** 2-ethylhexyl acrylate (2-EHA; 98 %), methyl acrylate (MA; 99 %), butyl acrylate (BA; ≥ 99 %), acrylic acid (AA; 99 %), 1-vinyl-2-pyrrolidone (VP; ≥ 99 %), ethylene glycol phenyl ether acrylate (EGPEA; 75-125 ppm HQ, 0,120 ppm MEHQ), vinyl methacrylate (VMA; 98%) and isobornyl acrylate (IBA; technical grade, 200 ppm MEHQ) as well as the **epoxy monomers** glycidyl methacrylate (GMA; $\geq 97.0\%$), 2-ethylhexyl glycidyl ether (2-EHGE; 98 %) and glycidyl isopropyl ether (GIPE; 98 %) were purchased from Sigma Aldrich (United States).

Azobisisobutyronitril (AIBN; 98 %) was obtained from Acros Organics (United States). Boron trifluoride ethylamine (BF₃-ethylamine; ARADUR® HT 973) was supplied by Huntsman Advanced Materials (United States). Butylated hydroxytoluene (BHT; ≥ 99 %), tetramethylammonium bromide (TMAB; 98 %) and hydroquinone (HQ; reagent plus, $\geq 99.5\%$) were obtained from Sigma Aldrich (United States). Sodium hydroxide (≥ 99 %) and sodium sulfate (≥ 99 %, water free) were purchased by Carl Roth. The **photoinitiators** 2-dimethylamino-2-(4-methyl-benzyl)-1-(4-morpholin-4-yl-phenyl)-butan-1-one (Irgacure 379), bis(2,4,6-trimethylbenzoyl)-phenylphosphineoxide (Irgacure 819) and ethyl (2,4,6-trimethylbenzoyl) phenylphosphinate (Lucirin TPO-L /Irgacure TPO-L) were kindly provided by BASF (Germany).

Ethyl acetate (EtAc; 99 %), ethanol (EtOH; 96 %) and *d*-chloroform (CDCl₃; <0.01 % H₂O) were obtained from VWR International (United States). Methanol (MeOH; ≥ 99.5 %) and toluene (≥ 99.5 %) were supplied by Carl Roth GmbH & Co KG (Germany). 2-butanone (MEK; ≥ 99 %), acetic acid (AcOH; 99.7 %) and tetrahydrofuran (THF; anhydrous ≥ 99.9 %, 250 ppm BHT) were purchased from Sigma Aldrich (United States).

The **multifunctional crosslinking agents** trimethylolpropane triacrylate (TMPTA; 600 ppm MEHQ), di(trimethylolpropane) tetraacrylate (DTMPTA; 1000 ppm MEHQ), pentaerythritol tetraacrylate (PETA; 350 ppm MEHQ) and dipentaerythritol penta/hexaacrylate (DPEPHA; ≤ 650 ppm MEHQ) were obtained from Sigma Aldrich (United States). Ethoxylated (3) trimethylolpropane triacrylate (SR 454), ethoxylated (10) bisphenol dimethacrylate (SR 480), propoxylated (3) trimethylolpropane triacrylate (SR 492) and ethoxylated (4) pentaerythritol tetraacrylate (SR 494) were kindly provided by Arkema (France).

The **organosilanes** 3-methacryloxypropyl trimethoxysilane (3-MAPTMS; > 98 %) and 3-acryloxypropyl trimethoxysilane (3-APTMS; 95 %) were purchased from Wacker Chemie (Germany) and ABCR (Germany), respectively. Bis(acylphosphane)oxide-4-

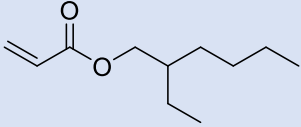
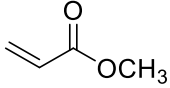
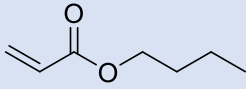
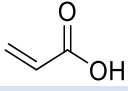
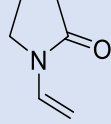
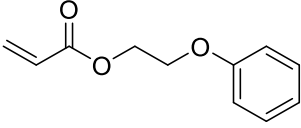
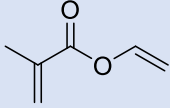
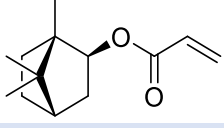
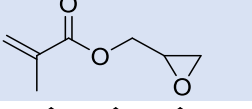
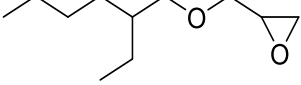
-Experimental part-

(trimethoxysilyl)butyl-3-[bis(2,4,6-trimethylbenzoyl)phosphinoyl]-2-methyl-propionate (TMESI² BAPO) was kindly provided by ETH Zürich, where it was synthesized according to Ref [19].

Sulfuric acid (H₂SO₄, 96 %) was purchased from Carl Roth, sodium persulfate (NaPS; ≥ 99.9 %) from Sigma Aldrich.

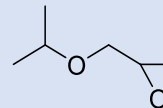
All chemicals were used without further purification.

Table 3: List of chemicals and the corresponding chemical structures

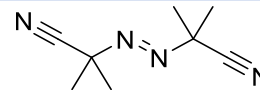
Name	chemical structure
2-ethylhexyl acrylate (2-EHA)	
methyl acrylate (MA)	
butyl acrylate (BA)	
acrylic acid (AA)	
1-vinyl-2-pyrrolidone (VP)	
ethylene glycol phenyl ether acrylate (EGPEA)	
vinyl methacrylate (VMA)	
isobornyl acrylate (IBA)	
glycidyl methacrylate (GMA)	
2-ethylhexyl glycidyl ether (2-EHGE)	

-Experimental part-

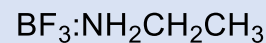
glycidyl isopropyl ether
(GIPE)



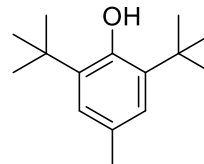
azobisisobutyronitril
(AIBN)



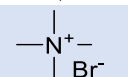
BF₃-ethylamine
(HT 973)



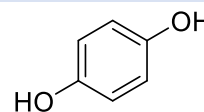
butylhydroxy toluene
(BHT)



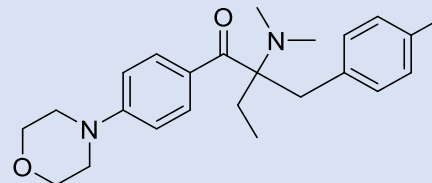
tetramethylammonium bromide **(TMAB)**



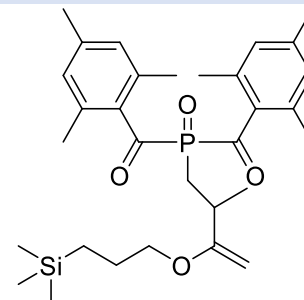
hydroquinone
(HQ)



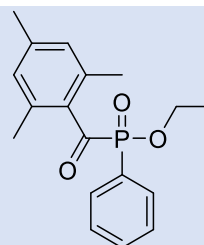
2-dimethylamino-2-(4-methyl-benzyl)-1-(4-morpholin-4-yl-phenyl)-butan-1-one
(Irgacure 379)



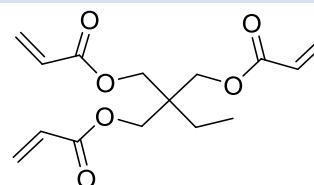
bis(2,4,6-trimethylbenzoyl)-
phenylphosphineoxide
(Irgacure 819)



ethyl (2,4,6-trimethylbenzoyl)-
phenylphosphinate
(Irgacure TPO-L)

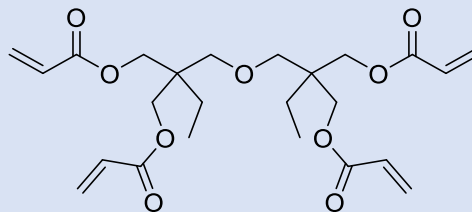


trimethylolpropane triacrylate
(TMPTA)

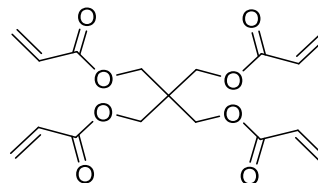


-Experimental part-

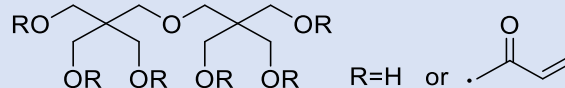
di(trimethylolpropane) tetraacrylate
(DTMPA)



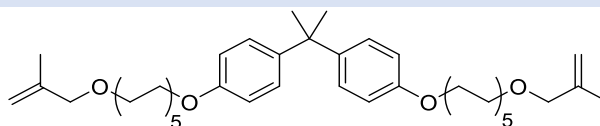
pentaerythritol tetraacrylate
(PETA)



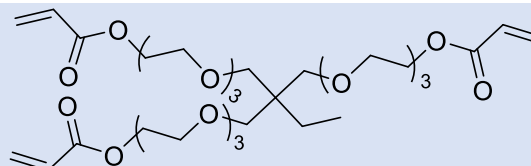
dipentaerythritol penta/hexaacrylate
(DPEPHA)



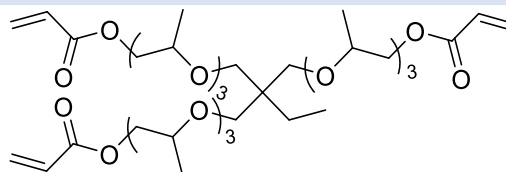
ethoxylated (10) bisphenol dimethacrylate
(SR 480)



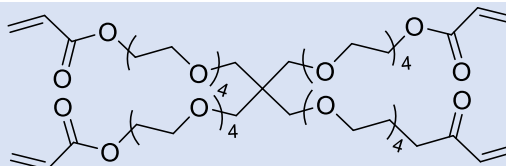
ethoxylated (3) trimethylolpropane triacrylate
(SR 454)



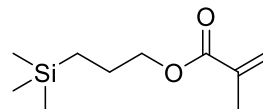
propoxylated (3) trimethylolpropane triacrylate
(SR 492)



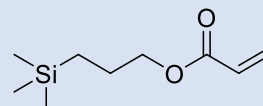
ethoxylated (4) pentaerythritol tetraacrylate
(SR 494)



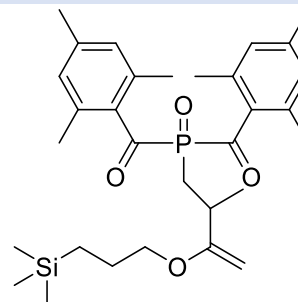
3-methacryloxypropyl trimethoxysilane
(3-MAPTMS)



3-acryloxypropyl trimethoxysilane
(3-APTMS)



bis(acylphosphane)oxide-4-(trimethoxysilyl)butyl-3-[bis(2,4,6-trimethylbenzoyl)phosphinoyl]-2-methylpropionate
(TMESI² BAPO)



Carrier and liner materials

Two types of polyethylene terephthalate (PET) films were applied as carrier material in PSA tape preparation. A 180 µm thick PET foil was purchased by AGFA (Belgium), while Coveme (Italy) provided a 50 µm thick PET foil, which was chemically etched with trifluoroacetic acid on one side.

A siliconized PET foil of 50 µm was used as liner.

Substrates

Tarnish protected copper, BondFilm® treated copper and cured FR 4 materials (hereinafter referred to as "cured epoxy" or "prepreg") were kindly provided by the company partner (AT&S) and applied as substrates during adhesion experiments. In order to reveal the pristine copper surface the tarnish protection layer (chromium-zinc coating) was removed by dipping tarnish protected copper substrates into an aqueous solution of H₂SO₄ (50 g/L) and NaPS (50 g/L) for 40 seconds at 35 °C. Subsequently, the substrates were washed with deionized water and dried in a nitrogen gas flow. Structured PCBs were used to test BondFilm® and epoxy surfaces simultaneously.

5.2.Machines and devices

Atomic force microscopy (AFM)

A Nanosurf easy Scan atomic force microscope (Nanosurf, Switzerland) operating in "tapping mode" was applied to investigate the topography of different substrates. The AFM was equipped with standard silicon cantilevers from Budgetsensors with a radius of curvature <10 nm, a 48 N/m spring constant and a 190 kHz resonance frequency. The average roughness (Sa) and root mean square roughness (Sq) was calculated using the Gwyddion software (v 2.44, v 2.51).

Attenuated total reflection Fourier transformed infrared spectroscopy (ATR-FT-IR)

A Bruker Vertex 70 FT-IR-spectrometer (Bruker, United States; software OPUS®) equipped with a Platinum attenuated total reflection unit (ATR) was employed to investigate the chemical composition of the synthesized adhesive polymers. 16 scans were accumulated with a resolution of 4 cm⁻¹.

Corona treatment

A corona treatment system TG3001 Ahlbrandt (Germany) was applied to activate the carrier. The power output P [W] and treatment speed v [m/min] were adjusted individually and are given for the respective experiments. The respective corona dose [$\text{W}\cdot\text{min}/\text{m}^2$] is calculated according to equation (1)

$$\text{Corona dose} = \frac{P}{v * b} \quad (1)$$

where P is the applied power output, v is the treatment speed which was set to 1.8 m/min and b is the width of the table (0.4 m).

Contact angle measurements

The static water contact angles of different substrates were determined at temperatures of 20-23 °C at a relative humidity of 50-80 % using a Krüss DSA 100 Drop Shape Analysis System (Krüss, Germany). A 2 μL droplet of ultrapure water was deposited on the surfaces and the water contact angle was calculated by taking the arithmetic average of 5-10 droplets, applying the Young & Laplace equation and the software Drop Shape Analysis.

Film Application/Coating

Quadrupole film applicators by Erichson, Model 360 with 1 cm or 10 cm length were used to coat adhesive formulations onto PET carriers.

Differential scanning calorimetry (DSC)

The glass transition temperatures (T_g) of the adhesive polymers and formulations were determined by means of DSC, applying a DSC 204 F1 Phoenix 240-12-0215-L by Netzsch (Germany; software: Netzsch Proteus), a Perkin Elmer DSC 4000 (Perkin Elmer, United States; software: Pyris) or a Mettler Toledo DSC 1 STARe System (Mettler Toledo, United States; STARe software).

Fourier transformed infrared spectroscopy (FT-IR)

The UV-cure kinetics of the different adhesive formulations were investigated by a Perkin Elmer Spectrum One FT-IR-spectrometer (Perkin Elmer; United States; software OPUS®). 16 scans were accumulated with a resolution of 4 cm⁻¹.

Gel permeation chromatography (GPC)

Gel permeation chromatography (GPC) was performed on a Merck Hitachi system (Germany; Software MultiDetector Software, V 3.2 by PL) with a combined refractive index–viscosity detector by Viscotec (Viscotec 200, Germany) in order to determine the number and weight average molecular weight (M_n , M_w) and the polydispersity PDI (M_w/M_n) of the synthesized acrylic copolymers. The measurements were carried out on separation columns by Agilent Technologies, GPC 50 (pre-column: 1x PSS SDV, 8x50 mm, particle size 5 μm; analysis column: 2xPSS SDV, Analytical Linear M, 8x300 mm, particle size 5 μm) and THF was employed as eluent. Polystyrene standards supplied by Polymer Standard Service were used for calibration.

Nuclear magnetic resonance spectroscopy (NMR)

Information about the chemical structure of the synthesized adhesive polymers was provided by ¹H-NMR spectra recorded with a Varian 400 MR spectrometer (Varian, United States; software VNMR) operating at 399.72 MHz. The spectra were evaluated by the use of the software ACD/NMR Processor (academic version).

Optical light microscopy

An Olympus BX 51 microscope equipped with an Olympus U-TVO 5XC3 camera (Olympus, Japan; software Stream Essentials) was applied to investigate substrates surfaces with regard to adhesive residues.

Surface Tack Measurement

The surface tack of PSA tapes was determined using a MTS 831 Polymer Testing System by MTS (United States; software Test Suite), where the adhesive tapes were pressed onto tarnish protected substrates with 25 N for 90 seconds and subsequently detracted at constant pull-off speed of 300 mm/min.

Radiometer

An EIT UV Power Puck II, S/N 18052 (EIT, United States) was employed for the determination of all applied UV-exposure doses.

Spin coater

In order to investigate the UV-cure kinetics adhesive formulations (150 mg/mL in 2-butanone) were spin cast onto CaF₂ discs with a Spincoater 4000 by electronic microsystems LTD (UK) applying a speed of 4000 rpm and a ramp of 5000 rpm.

Tensile testing machine

The adhesive forces of the PSA tapes were determined via peel strength tests on a Zwick Z010 AroundLine material testing machine (Zwick Roell, Germany; software TestXpert II) equipped with a 500 N load cell and a 1 kN clamp. Therefore, the tapes were laminated onto tarnish protected copper substrates and peeled off with 300 mm/min in a 90 ° angle.

Thermogravimetric analysis (TGA)

The thermal stability of the synthesized adhesive polymers and adhesive formulations was investigated by means of TGA applying a Mettler Toledo (United States) STARe System, TGA/DSC 1 with a STARe System, GC 200 gas controller. The samples were heated to 600 °C under nitrogen atmosphere (10-20 mL/min) at a rate of 5 °C/min and the mass loss was determined using the STARe software.

UV-light curing systems

An *Omnicure S1000* by Lumen Dynamics (Excelitas Canada Inc., Canada) was used to irradiate the samples in UV-cure kinetic measurements with an intensity of 4.18 mJ/cm² and wavelengths in the range of 250-470 nm.

A *Light Hammer 6* by Fusion UV Systems, Inc. (Heraeus, Germany) was employed to pre-crosslink the PSA tapes and to trigger their UV release. The irradiation doses and rate of transportation (conveyor belt LC6E) were adjusted individually.

UV-VIS Spectroscopy

A Cary 50 spectrophotometer by Agilent Technologies (US) was employed to record the UV-VIS spectra of the PET carriers in the range of 200-800 nm at a scan rate of 600 nm/min. (Software: Scan, Version 3)

X-ray photoelectron spectrometry (XPS)

A K- α -X-ray photoelectron spectrometer by Thermo Scientific (United States; software Thermo Avantage processing (v.5932)) equipped with an Al-K- α source ($h\nu = 1486.6$ eV) and a hemispherical analyzer was applied to study the modification of PET carriers. 400 μm spots were investigated with an energy step size of 0.1 eV and a pass energy of 10 eV. Hydrogen was omitted in the calculation of the surface composition and the C1 s line at a binding energy of 284.8 eV (hydrocarbons or hydrocarbon groups) has been used to calibrate the binding energy scale for XPS measurements.

5.3.Synthesis of adhesive polymers

Acrylic copolymers

Ethyl acetate (EtAc), the respective monomers (see Table 4) and AIBN were added to a three necked flask. The reaction solution was purched with nitrogen for 30 minutes under mechanical stirring and was subsequently heated to 80 °C in order to initiate the free radical polymerization. After 4 hours the acrylic copolymers were isolated and purified by precipitation into cold methanol (MeOH). The polymers were dried at 50 °C under reduced pressure (100 mbar). [112,113]

Table 4 shows the mixing ratios of all synthesized acrylic copolymers. The composition of **acryl_1** was based on Ref [114], comprising 2-ethylhexyl acrylate (2-EHA), methyl acrylate (MA), butyl acrylate (BA), acrylic acid (AA) and 1-vinyl-2-pyrrolidone (VP). In order to vary the properties of the adhesive, the composition of acryl_2 - acryl_6 was altered: MA was replaced completely by ethylene glycol phenyl ether acrylate (EGPEA) in **acryl_2**, while equal amounts of MA and EGPEA were used in **acryl_3**. **Acryl_4** was synthesized using vinyl methacrylate (VMA) instead of MA. Isobornyl acrylate (IBA) was added in the synthesis of **acryl_5**, whereas acrylic acid was removed from the copolymer composition in **acryl_6**. Figure 22 shows the copolymerization reaction of acryl_1 as a representative example.

The yields of polymerization amounted to 94.4 % for acryl_1, to 27.1 % for acryl_2, to 53.2 % for acryl_3, to 25.2 % for acryl_4, to 86.1 % for acryl_5 and to 86.6% for acryl_6.

¹H-NMR of **acryl_1** (δ , 400 MHz, 20°C, CDCl₃, ppm): 4.01 and 3.94 (m, CH₂OCOR^{7a, 9a}), 3.62 (s, CH₃^{3a}), 2.29 (s, CH₂^{1, 3, 5, 5a, 7, 9}), 1.91 (s, CH₂^{5b}and CH^{9b}), 1.57 (m, CH₂^{7b, 9c}), 1.34-1.26 (m, CH₂^{7c, 9e, 9f, 9g} and CH¹⁻¹⁰), 0.93-0.86 (m, CH₃^{7d, 9d, 9h}).

¹H-NMR of **acryl_5** (δ , 400 MHz, 20°C, CDCl₃, ppm): 4.64 (s, CH^{11a}), 4.03 and 3.96 (m, CH₂OCOR^{7a, 9a}), 3.64 (s, CH₃^{3a}), 2.29 (s, CH₂^{1, 3, 5, 5a, 7, 9}), 1.92 (s, CH₂^{5b, 11b} and CH^{9b}), 1.73-1.58 (m, CH₂^{7b, 9c, 11b, 11d, 11e}, CH^{11c}), 1.38-1.28 (m, CH₂^{7c, 9f, 9g, 11d, 11e} and CH¹⁻¹⁰), 1.15-1.07 (m, CH₂^{9e}) and 0.95-0.83 (m, CH₃^{7d, 9d, 9h, 11f, 11g, 11h}).

¹H-NMR of **acryl_6** (δ , 400 MHz, 20°C, CDCl₃, ppm): 4.02 and 3.95 (m, CH₂OCOR^{5a, 7a}), 3.63 (s, CH₃^{1a}), 2.28 (s, CH₂^{1, 3, 3a, 5, 7}), 1.91 (s, CH₂^{3b}and CH^{7b}), 1.62 and 1.56 (m, CH₂^{5b, 7c}), 1.35-1.27 (m, CH₂^{5c, 7e, 7f, 7g} and CH¹⁻⁸), 0.95-0.86 (m, CH₃^{5d, 7d, 7h}).

FT-IR of **acryl_1** (cm⁻¹): 2958, 2930, 2873 and 2861 (CH), 1731 (C=O), 1645 (C=C), 1450, 1380 and 1336 (HCH), 1242 and 1159 (HCH/C-O-C), 1117, 1062 and 1034 (C-O-C), 961, 907, 829 and 768 (C=CH).

-Experimental part-

FT-IR of **acryl_4** (cm^{-1}): 2959, 2931, 2874 and 2862 (CH), 1734 (C=O), 1647 (C=C), 1460 and 1386 (HCH), 1229 and 1161 (HCH/C-O-C), 1132 and 1030 (C-O-C), 974, 874, 762 and 698 (C=CH).

FT-IR of **acryl_5** (cm^{-1}): 2957, 2931 and 2874 (CH), 1730 (C=O), 1645 (C=C), 1453 and 1380 (HCH), 1235 and 1159 (HCH/C-O-C), 1117 and 1051 (C-O-C), 968, 839 and 768 (C=CH).

FT-IR of **acryl_6** (cm^{-1}): 2957, 2930, 2913 and 2862 (CH), 1732 (C=O), 1698 (C=C), 1451 and 1380 (HCH), 1236 and 1160 (HCH/C-O-C), 1118, 1064 and 1034 (C-O-C), 963, 906, 829 and 768 (C=CH), 725 ($(\text{CH}_2)_{n>3}$).

The corresponding FT-IR- and ^1H NMR spectra are provided in chapter 6.1.1 (see Figure 28 and Figure 29) and in the appendix (Figure_A 1, Figure_A 3).

Table 4: Composition of the synthesized acrylic copolymers

	2-EHA [wt%]	MA [wt%]	BA [wt%]	AA [wt%]	VP [wt%]	EGPEA [wt%]	VMA [wt%]	IBA [wt%]	AIBN [wt%]
acryl_1	54.98	20.05	18.04	5.44	1.49	0.00	0.00	0.00	0.19
acryl_2	54.98	0.00	18.04	5.44	1.49	20.05	0.00	0.00	0.19
acryl_3	54.98	10.02	18.04	5.44	1.49	10.02	0.00	0.00	0.19
acryl_4	54.98	0.00	18.04	5.44	1.49	0.00	20.05	0.00	0.19
acryl_5	41.24	15.41	15.40	5.58	1.64	0.00	0.00	20.74	0.19
acryl_6	54.98	22.77	20.76	0.00	1.49	0.00	0.00	0.00	0.19

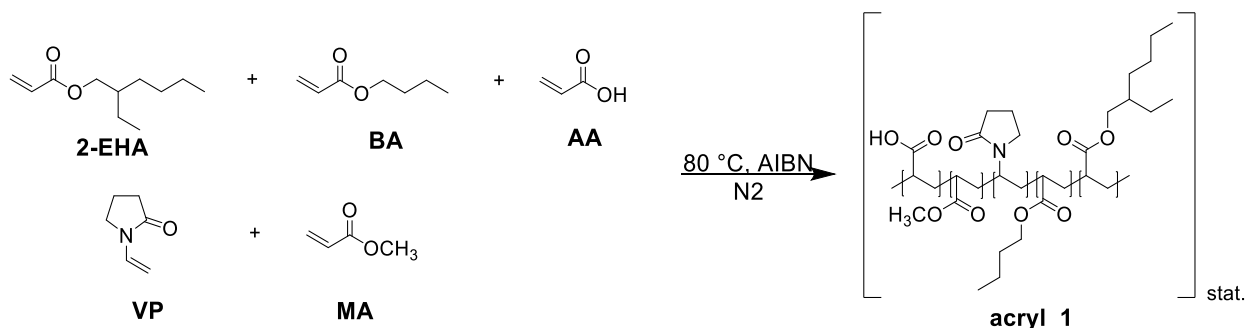


Figure 22: Copolymerization reaction of acryl_1

-Experimental part-

Another variation was the side chain functionalization of acryl_1. Acrylic pendant groups were attached to the copolymer via ring opening reaction of glycidyl methacrylate (GMA) with the AA side chains of the copolymer (see Figure 23) [115]. Firstly, acryl_1 was synthesized and purified as described above. The copolymer was dissolved in 2-butanone and 10 wt% GMA, 1 wt% tetramethylammonium bromide (TMAB) and 0.2 wt% hydroquinone (HQ) were added. The reaction solution was purched with nitrogen for 30 minutes under mechanical stirring and was subsequently heated to 80 °C. After 20 hours of reaction time the solid product (**acryl_1_scf**) was dissolved in 2-butanone and extracted three times with NaOH (5 % in water) to remove HQ. The organic phase (fraction 1) was isolated and the NaOH phase, which still contained some undissolved polymer, was extracted several times with toluene (fraction 2). The filtered polymer was rejected and fraction 1 and 2 were dried with Na₂SO₄ at 40 °C under vacuum (100 mbar). The overall yield of polymerization was 18.5 %, whereas the ratio of fraction 1 amounted to 7.3 % and fraction 2 made up 11.2 %.

FT-IR of **acryl_1_scf** (cm⁻¹): 3389 (OH), 2962, 2931, 2874 and 2861 (CH), 1736 (C=O), 1664 (C=C), 1574 (C=O), 1459, 1413 and 1366 (HCH), 1262 and 1165 (CHC/C-O-C), 1135-987, 974 and 844 (C-O-C, C=CH).

The corresponding FT-IR spectrum is provided in the appendix (Figure_A 1).

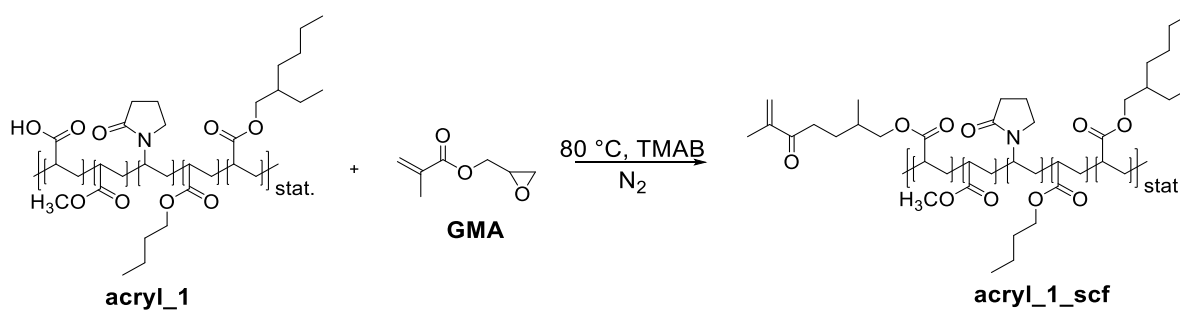


Figure 23: Side chain functionalization of acryl_1

Polyether based polymers

Epoxy acrylic monomers (see Table 5) and 1 wt% BF₃-ethylamine were added to a flask. [116] The bulk reaction was performed under mechanical stirring at temperatures of 70-95 °C (reflux). [117,118] Reaction times varied from 15 minutes to several hours, depending on the polymer composition. After cooling to room temperature (rt) the product was precipitated in cold EtOH [119] and dried at 50 °C. Polyether_2 and polyether_3 were synthesized under light exclusion to prevent undesired UV-induced polymerization of the acrylic moieties. In addition, butylated hydroxy toluene (BHT) was applied in the synthesis of polyether_2 as radical scavenger.

The composition of the different polyether polymers is listed in Table 5. **Polyether_1** was a homopolymer of GMA, while **polyether_2** and **polyether_3** were copolymers of GMA, 2-ethylhexyl glycidyl ether (2-EHGE) and glycidyl isopropyl ether (GIPE). The corresponding reactions are shown in Figure 24.

The yield of polymerization amounted to < 5% for polyether_1 and _3, while the yield of polyether_2 could not be determined.

FT-IR of **polyether_1** (cm⁻¹): 3425 (OH), 2939 (CH), 1710 (C=O), 1641 (C=C), 1458 and 1366 (HCH), 1248 and 1171 (CHC/C-O-C), 1129 and 1045 (C-O-C), 945, 861 and 819 (C=CH), 766 and 659 ((-CH₂-)_{n>3}).

FT-IR of **polyether_2** (cm⁻¹): 3479 (OH), 3053, 2960, 2930, 2874 and 2863 (CH), 1723 (C=O), 1640 (C=C), 1460, 1381 and 1318 (HCH), 1297, 1254 and 1161 (CHC/C-O-C), 1133, 1104 and 1019 (C-O-C), 942, 911 and 847 (C=CH).

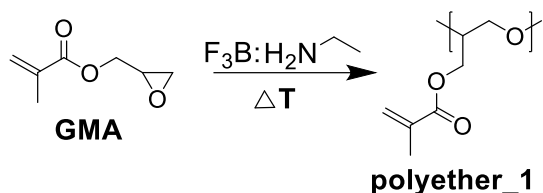
FT-IR of **polyether_3** (cm⁻¹): 3517 (OH), 2961, 2930 and 2876 (CH), 1721 (C=O), 1638 (C=C), 1455, 1379 and 1318 (HCH), 1296, 1252 and 1156 (CHC/C-O-C), 1131, 1081 and 1015 (C-O-C), 984, 940, 910, 844 and 816 (C=CH), 762 and 656 ((-CH₂-)_{n>3}).

The corresponding FT-IR spectra are provided Figure 34 and see Figure_A 4 in the appendix.

Table 5: Composition of the synthesized polyether adhesives

	GMA [wt%]	2-EHGE [wt%]	GIPE [wt%]	BF₃-H₂NCH₂CH₃ [wt%]
polyether_1	100	0	0	1
polyether_2	25	55	20	1
polyether_3	50	30	20	1

Synthesis of polyether_1



Synthesis of polyether_2 and polyether_3

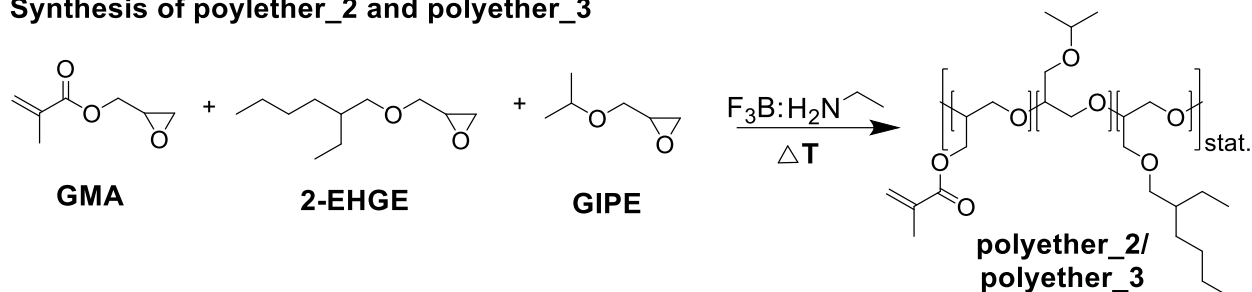


Figure 24: Polymerization reactions of polyether_1, polyether_2 and polyether_3

5.4. Physico-chemical characterization of the synthesized polymers

All measurements were performed as described in chapter 5.2.

Spectroscopic methods

ATR-FT-IR- and 1H NMR spectroscopy were carried out to investigate the chemical composition and to gain information about the chemical structure of the synthesized adhesive polymers.

GPC

GPC was performed to determine the average molecular weight (M_n , M_w) and the polydispersity $PDI(M_w/M_n)$ of the synthesized polymers. THF was used as eluent. The oven temperature was set to 30 °C and the flow rate was 0.5 mL/min. Polystyrene standards supplied by Polymer Standard Service were used for calibration.

TGA

The thermal stability of the synthesized adhesive polymers was investigated by thermogravimetric analyses (TGA). The copolymers were heated from 25 °C to 600 °C at a heating rate of 5 °C/min and the respective degradation onset and end temperatures T_{ON} and T_{END} were determined graphically as the intersections of the tangents with the horizontal lines before and after the degradation step.

DSC

The glass transition temperatures (T_g) of the adhesive polymers and formulations were determined by means of DSC. A nitrogen flow of 20 mL min⁻¹ was employed and the adhesive was heated from -80 °C to +70 °C at a heating rate of 20 K/min. The T_g was taken as the midpoint of the heat flow curve of the second scan. In addition, the results were compared to the theoretical T_g calculated by the use of the Fox-equation (2)

$$\frac{1}{T_g} = \sum \left(\frac{w_x}{T_{g_x}} \right) \quad (2)$$

where T_g is the glass transition temperature of the copolymer, w_x is the weight percentage of the monomer x and T_{g_x} is the glass transition temperature of the homopolymer of monomer x . [62,120]

Table_A 1 lists the glass transition temperatures of the homopolymers which were used for the calculation of the theoretical T_g .

5.5.Preparation of UV-curable PSA tapes

Adhesives and adhesive formulations

The synthesized polymers were used as basic adhesive in PSA tapes. The polymers were dissolved in 2-butanone and mixed with various concentrations of different multifunctional acrylic monomers and the photoinitiator Lucirin TPO-L. The adhesive formulations were stirred for 15 min at rt with a magnetic stirrer. The compositions of all applied adhesives are listed in Table 6.

-Experimental part-

Table 6: Composition of the applied adhesive formulations

	polymer	type of multifunctional monomer	weight fraction of multifunctional monomer [wt%] ¹	weight fraction of Lucirin TPO-L [wt%] ¹
adhesive 1	acryl_1	DPEPHA	10	1
adhesive 2	acryl_1	DPEPHA	10	5
adhesive 3	acryl_1	DPEPHA	15	0.75
adhesive 4	acryl_1	DPEPHA	20	0.5
adhesive 5	acryl_1	DPEPHA	20	0.75
adhesive 6	acryl_1	DPEPHA	20	1
adhesive 7	acryl_1	DPEPHA	20	5
adhesive 8	acryl_1	DPEPHA	50	1
adhesive 9	acryl_1	DPEPHA	50	5
adhesive 10	acryl_1	DTMPTA	10	1
adhesive 11	acryl_1	DTMPTA	10	5
adhesive 12	acryl_1	DTMPTA	20	0.5
adhesive 13	acryl_1	DTMPTA	20	0.75
adhesive 14	acryl_1	DTMPTA	20	1
adhesive 15	acryl_1	DTMPTA	50	1
adhesive 16	acryl_1	PETA	10	1
adhesive 17	acryl_1	PETA	10	5
adhesive 18	acryl_1	PETA	20	1
adhesive 19	acryl_1	SR 454	10	1
adhesive 20	acryl_1	SR 454	10	5
adhesive 21	acryl_1	SR 480	50	5
adhesive 22	acryl_1	SR 492	10	1
adhesive 23	acryl_1	SR 492	10	5
adhesive 24	acryl_1	SR 494	10	1
adhesive 25	acryl_1	SR 494	10	5
adhesive 26	acryl_1	SR 494	20	1
adhesive 27	acryl_1	SR 494	50	1
adhesive 28	acryl_1	TMPTA	10	1
adhesive 29	acryl_1	TMPTA	10	5
adhesive 30	acryl_5	DPEPHA	10	1
adhesive 31	acryl_5	DPEPHA	20	1
adhesive 32	acryl_5	DTMPTA	10	1
adhesive 33	acryl_5	DTMPTA	20	1
adhesive 34	acryl_6	DPEPHA	10	1
adhesive 35	acryl_6	DPEPHA	20	1
adhesive 36	acryl_6	DTMPTA	10	1
adhesive 37	acryl_6	DTMPTA	20	1

¹ based on 100 wt% copolymer

Two variations of tape preparation were established:

Tape preparation - *method I*

The adhesive formulations were coated onto unmodified, corona treated or modified PET carriers with a quadruple film applicator by Erichsen (Model 360) applying wet film thicknesses in the range of 30-120 μm (see Figure 46, step I). The prepared adhesive layers were dried at 50 °C for 30 min and pre-crosslinked under nitrogen atmosphere via UV-irradiation employing a Light Hammer 6 by Fusion UV Systems, Inc. (Heraeus, Germany) with a minimum irradiation dose of 80 mJ/cm^2 .

Tape preparation - *method II*

The adhesive formulations were coated onto siliconized PET liners using a quadruple film applicator by Erichsen (Model 360) applying wet film thicknesses of 90 μm (see Figure 46, step I). The prepared adhesive layers were dried at 50 °C for 30 min and transferred to unmodified, corona treated or modified carriers via lamination on a hot base (175-150 °C, see Figure 46, step II). The tapes were pre-crosslinked through the carrier by UV-irradiation employing a Light Hammer 6 by Fusion UV Systems, Inc. (Heraeus, Germany) with a minimum irradiation dose of 80 mJ/cm^2 .

As can be derived from Table 6, the composition of the applied adhesives varied in structure of the basic adhesive copolymer and multifunctional acrylate, as well as in concentration of the multifunctional acrylate and the photoinitiator. The dose for UV-crosslinking was adjusted to the individual adhesive composition to ensure proper network formation. Moreover, experiments without pre-crosslinking and variations of the pre-crosslinking dose were performed for tapes prepared according to *method I*.

Modification of the PET carrier by attachment of organosilanes

2 wt% of 3-MAPTMS, 3-APTMS or TMESI² BAPO were dissolved in EtOH, which had been acidified with AcOH to pH values between 4 and 5. Chemically etched PET carriers were exposed to corona discharge of 1100 W using a Corona Treatment System TG3001 by Ahlbrandt (Germany). The corresponding corona dose was determined to be 1528 $\text{W min}/\text{m}^2$ according to equation (1). The surface activated carriers were immersed into the organosilane solutions for 2 h at rt and subsequently thermally treated at 110 °C overnight. The resulting modified carriers were washed with EtOH and dried at rt.

5.6.Characterization of the PSA tapes

Characterization of the adhesive layer

UV-cure kinetic measurements

The UV-cure kinetics of the multifunctional acrylic monomers was investigated for selected adhesives (see Table 11) by means of FT-IR spectroscopy. The adhesive formulations (150 mg/mL in 2-butanone) were spin-cast onto CaF₂ discs with a Spincoater 4000 from electronic microsystems LTD (UK) at a speed of 4000 rpm and a ramp of 5000 rpm. The coated discs were dried at 50 °C for 15 min and irradiated stepwise under N₂ employing an Omnicure S1000 by Lumen Dynamics (Excelitas Canada Inc., Canada). The intensity amounted to 4.2 mJ/cm² with wavelengths ranging from 250-470 nm. Exposure dose and intensity were determined using a Power Puck II S/N 18052 by EIT Inc. (EIT, United States).

A Spectrum One FT-IR Spectrometer by Perkin Elmer Instruments (United States) was applied to monitor the consumption of the C=C double bonds during UV-induced crosslinking by following the decrease of the characteristic C=C peak at 985 cm⁻¹ [23] with increasing exposure time and UV-dose. The absorbance at 2960 cm⁻¹ was used as an internal standard and the conversion of the C=C double bonds was calculated according to equation (3)

$$Conversion = \left(1 - \frac{[A]_{C=Cx}/[A]_{ISx}}{[A]_{C=C0}/[A]_{IS0}} \right) * 100 \quad (3)$$

where $[A]_{C=Cx}$ is the peak intensity of C=C double bonds at an exposure time x , $[A]_{C=C0}$ is the peak intensity of C=C double bonds prior to UV-irradiation, $[A]_{ISx}$ is the peak intensity of the internal standard at an exposure time x and $[A]_{IS0}$ is the peak intensity of the internal standard prior to UV-irradiation.

Determination of the glass transition temperature (T_g)

The T_g of selected polymer networks (adhesives 2, 6, 8, 11, 15, 16, 19, 22, 25, 27 and 28; see Table 6, chapter 5.5) was determined by DSC analysis, employing a Mettler Toledo DSC 1 STARe System (Mettler Toledo, United States). The adhesive formulations were weight into aluminum crucibles and the solvent was evaporated at 90 °C overnight. They were irradiated under nitrogen atmosphere with a Light Hammer 6 by Fusion UV Systems, Inc. (Heraeus, Germany) applying individual UV-irradiation doses based on the findings of the UV-cure kinetics. The samples were heated from -60 °C to 100 °C at a

rate of 40 °C/min and a nitrogen flow of 50 mL/min. The T_g was taken as the midpoint of the cooling curve. Additionally, adhesive 6 was investigated in an extended temperature range up to 300°C. In order to examine the influence of the pre-crosslinking step on the T_g of the adhesive, adhesive 6 was irradiated with an UV-dose of 80 mJ/cm² before TGA analysis.

Investigation of the thermal stability of the polymer networks

The thermal stability of selected polymer networks (adhesives 1, 2, 6, 8, 10, 11, 14-16, 19, 22 and 24-28; see Table 6, chapter 5.5) was investigated by TGA measurements which were carried out on a Mettler Toledo (United States) STARe System, TGA/DSC 1 with a STARe System, GC 200 gas controller. The adhesive formulations were weight into aluminum oxide crucibles and the solvent was evaporated at 90 °C overnight. The samples were heated to 600 °C under nitrogen atmosphere (50 mL/min) at a rate of 5 °C/min and the weight loss was determined using the STARe software. The degradation onset and end temperatures T_{ON} and T_{END} were determined graphically as the intersections of the tangents with the horizontal lines before and after the degradation step. In addition, the point of maximum degradation T_{MID} was derived from the first derivative of the temperature-weight loss curves.

Characterization of the modified carriers

XPS analysis of unmodified and functionalized PET carriers was performed with a K-Alpha photoelectron spectrometer (Thermo Scientific, United States) equipped with an Al-K α X-ray source ($h\nu = 1486.6$ eV) and a hemispherical analyzer. The energy step size was 0.1 eV and the pass energy amounted to 10 eV, whilst a spot size of 400 μm was used.

The wetting properties of the carriers prior to and after surface modification were determined by *contact angle measurements* using a DSA 100 Drop Shape Analysis System (Krüss, Germany). A 2 μL droplet of ultrapure water was deposited on unmodified, corona treated or modified PET films at 20-23 °C and a relative humidity of 50-80 %. The respective water contact angles were calculated by taking the arithmetic average of 5-10 droplets, applying the Young & Laplace equation and the software Drop Shape Analysis.

Determination of the adhesive strength

The adhesion strength of PSA tapes prepared by *method I and method II* was explored by means of peel strength tests on a Zwick Z010 AroundLine material testing machine. The tapes were laminated onto tarnish protected copper substrates (Cr-Zn coated, 15 x 2 cm) and peeled off with 300 mm/min in a 90 ° angle. [6] The peel strength was measured, prior to and after UV-irradiation with a Light Hammer 6 by Fusion UV Systems, Inc. (Heraeus, Germany) applying an irradiation dose of 1080 mJ/cm². Moreover, the adhesion strength after pre-crosslinking with a UV-dose of 80 mJ/cm² was recorded. The average adhesion strength was calculated from the plateau of the respective force-displacement curves of at least three samples.

Determination of the surface tack

The surface tack of adhesive tapes prepared by *method I* was determined by a variation of the compression-tensile test combination described in Ref [121]. Adhesive tapes with a diameter of 5 cm were prepared and fixed to the die of a MTS 831 Polymer Testing System by MTS (United States). Initially the samples were pressed vertically onto tarnish protected copper substrates (Cr-Zn coated, 10 x 10 cm) applying a constant force of 25 N. After a holding time of 90 s, the die was detracted vertically at a constant pull-off speed of 300 mm/min. The surface tack was taken as the maximum force recorded during detracted. An average over 3 samples was determined for pre-crosslinked PSA tapes, while only single measurements were done for the corresponding released tapes (UV-cured with 1080 mJ/cm²). Figure 25 shows the experimental set up.



Figure 25: Experimental Set-up of surface tack measurements

Application of the PSA tapes – Adhesion experiments

The PSA tapes were laminated onto different substrates (5 x 1.5 cm), including tarnish protected copper substrates, pristine copper and BondFilm® treated copper as well as cured epoxy and structured PCBs. Subsequently, the tapes were irradiated through the carrier with a Light Hammer 6 by Fusion UV Systems, Inc. (Heraeus, Germany) applying individual UV-doses, depending on the adhesive composition. The removability of the tapes was investigated after adhesion at rt or after storage for 1h at elevated temperatures (140 °C - 240 °C) by peeling them off manually. The revealed substrate surfaces were investigated with regard to adhesive residues by means of optical light microscopy using an Olympus BX 51 microscope (Olympus, Japan) equipped with an Olympus U-TVO 5XC3 camera.

5.7.Characterization of the substrates and carrier materials

The different **substrates** (tarnish protected copper, pristine copper, BondFilm® treated copper, epoxy) were investigated with regard to their topography employing a Nanosurf easy scan atomic force microscope (Nanosurf, Switzerland) operating in “tapping mode”. The AFM was equipped with standard silicon cantilevers from Budgetsensors with a radius of curvature <10 nm, a 48 N/m spring constant and a 190 kHz resonance frequency. The average roughness (Sa) and root mean square roughness (Sq) were calculated from an average of 3 spots of 20 µm² (protected copper, epoxy, BondFilm®) or 50 µm² (pristine copper) using the Gwyddion software (v2.03).

The removal of the anti-tarnish layer from tarnish protected copper substrates was proven by X-ray photoelectron spectroscopy (XPS). The measurements were carried out with a K-Alpha photoelectron spectrometer (Thermo Scientific, United States), which was equipped with an Al-K α X-ray source ($h\nu = 1486.6$ eV) and a hemispherical analyzer. The energy step size was 0.1 eV and the pass energy amounted to 10 eV, whilst a spot size of 400 µm was used.

The wetting properties of the substrates were determined by contact angle measurements using a DSA 100 Drop Shape Analysis System (Krüss, Germany). A 2 µl droplet of ultrapure water was deposited on tarnish protected copper, pristine copper, BondFilm® treated copper and cured epoxy at 20-23 °C and a relative humidity of 50-80 %. The respective water contact angles were calculated from an average of 5-10 droplets, applying the Young & Laplace equation and the software Drop Shape Analysis.

-Experimental part-

The absorption spectrum of the **PET carriers** was investigated by UV-VIS spectroscopy in the range of 200-800 nm. The measurements were performed on a Cary 50 UV-VIS spectrophotometer by Agilent Technologies (US) at a scan rate of 600 nm/min. Information about the chemical composition and the wetting properties of the etched PET carrier before and after corona treatment were obtained from XPS and contact angle measurements, which were performed for the characterization of the modified carriers (see chapter 5.6).

6. Results and discussion

The aim of this work was to develop a removable pressure sensitive adhesive tape (PSA-tape), which is used for chip embedding in the production of printed circuit boards (see chapter 2 for details). Consequently, the requirements included high initial tack and reliable fixation of the components, high thermal stability (≥ 200 °C) as well as easy and clean peel from metallic and epoxy-based surfaces in the end of the application.

The performance of PSAs is highly influenced by the right balance of adhesion and cohesion. Both parameters are determined by the chemical composition and structure of the basic adhesive polymers. The tack and shear resistance (cohesion) of an adhesive depend on its fluidity and therefore the internal mobility and flexibility of the polymer main and side chains. This is reflected by the glass transition temperature (T_g). High tack and hence a high degree of mobility are associated with low T_g values. As it depends on the choice of the monomers, the T_g constitutes a key parameter for the adjustment of the adhesive properties. [6,10,20,22,23] From the broad spectrum of basic adhesive materials, **acrylic PSAs** were selected due to the inherent tack of polyacrylics and the wide range of monomers ((meth)acrylic esters and vinyl components) offering precise adjustment of the material properties. [20] Acrylic copolymers were synthesized in a free radical polymerization and applied as the basic adhesive material in PSA tapes. They were mixed with a photoinitiator and multifunctional acrylic monomers in order to form semi-interpenetrating networks (semi-IPN) upon UV-irradiation. This network formation did not only increase the heat resistance, but also constituted the basis of the UV-release mechanism, which ensured clean and controlled peel. [24,25] The principle and effects of IPN formation are explained in more detail in chapter 6.2.

Besides acrylic copolymers, **polyethers** are referred to as suitable adhesives for PSAs [9,34,87]. Polyethers are synthesized from epoxy monomers via ring opening polymerization [116]. As their properties are affected by the chemical structure [60,117,122], the huge variety of epoxy monomers allows for the adjustment to individual requirements. [123] While the C-O-C linkages in the backbone comprise high chemical and thermal stability [117,123–125], clean peel was supported by UV-induced crosslinking of pendant acrylic groups. [24,25]

The following chapter deals with the syntheses and characterization of acrylic copolymers and polyethers, which were applied as basic adhesive polymers in PSA tape preparation. The composition of the adhesives was altered in order to modify their properties including thermal stability, tack and removability.

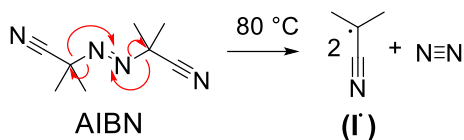
6.1.Synthesis and characterization of the adhesive copolymers

6.1.1. Acrylic Copolymers

Synthesis and purification

Acrylic copolymers were synthesized in a free radical polymerization in EtAc at 80 °C. The reaction was started by isobutyronitrile radicals, which were generated by the thermally induced homolytical cleavage of AIBN (see Figure 26, I). The general mechanism for the polymerization of acrylic monomers is illustrated in Figure 26, II. In order to prevent oxygen inhibition and an associated low degree of polymerization the syntheses were performed under nitrogen atmosphere. [65,126] Since high thermal stability and clean peel were the main demands on the PSA tape, the composition of the basic adhesive polymer was varied in order to modify its adhesive properties and to introduce reactive sites for crosslinking in the side chains.

I: Activation of AIBN



II: Polymerization of acrylic monomers

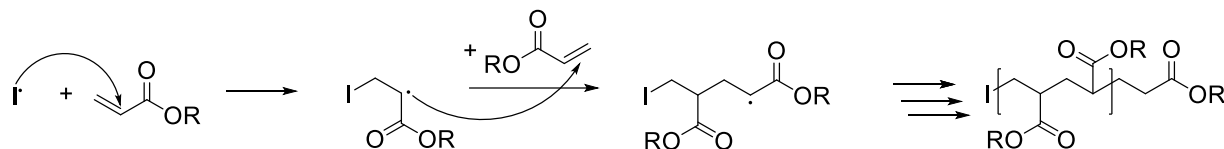


Figure 26: Free radical polymerization of acrylic monomers

As already mentioned above, the T_g is a crucial parameter for governing the adhesive properties of PSAs. The wide range of acrylic components is classified into soft, hard and polar/functional monomers. Soft monomers are characterized by a low T_g as well as long side-chains and determine the tack and peel adhesion of the polymer. Important examples are 2-ethyl hexyl acrylate (2-EHA), *n*-butyl acrylate (BA) and *iso*-octyl acrylate. In addition, hard monomers such as methyl acrylate (MA), methyl methacrylate or vinyl acetate comprise a high T_g and short side chains. They increase the internal strength, the peel force and the stiffness of the polymer. A combination of both, soft (50-98 %) and hard monomers (10-35 %), is essential to achieve a balance between tack and cohesion.

In addition, polar or functional monomers as AA may be incorporated to an extent of 10-30 %. While polar monomers increase the cohesion within the PSA and enhance Van der Waals interactions with polar substrates, functional monomers introduce active sites for crosslinking or grafting. [6,9,10,22]

The composition of **acryl_1** (see Table 4) was based on Ref [114]. The soft monomers 3-EHA and BA made up about 73 wt% of the mixture to ensure a low T_g and high initial tack. The remaining 27 wt% were composed of MA, AA and *N*-vinyl pyrrolidone (VP), which belong to the class of hard and functional monomers and therefore provide inner strength and cohesion within the PSA. Acryl_1 was precipitated in cold MeOH and left for sedimentation in the fridge overnight. The white product was tacky and highly viscous and turned to a colorless solid after the evaporation of the solvent. The reaction yield was determined to 94.4 %.

In order to increase the thermal stability of the copolymer, MA was replaced by EGPEA for the synthesis of **acryl_2**. It was decided to exchange MA as it is not essential for the tack, but makes up a portion of the reaction mixture (20.05 wt%), which is high enough to reveal the effect of the new monomer. EGPEA promised improved thermal stability due to resonance stabilization of the aromatic ring system [21] and the stable ether linkages. [124,125] However, within a few minutes at reaction temperature an elastic yellowish gel was formed, which was neither tacky nor soluble. Since a polymer solution was required for purification (precipitation), attempts to dissolve acryl_2 were performed in different solvents under stirring and heating. Though acryl_2 swelled in 2-butanone, it could not be dissolved completely. According to literature, the solid rubbery form can be related to the incorporation of EGPEA [127], while the insolubility was explained by π -stacking of aromatic polymer side chains. In addition, a narrowing of the bandgap is described for π -stacking systems, which is a possible explanation for the yellowish color. [128] Finally, the polymer was dried and the reaction yield was determined to 27.1 %. The comparatively low polymerization yield was interpreted as a consequence of the limited mobility of the reactive species (radicals, monomers), resulting from steric hindrance and π -stacking of the aromatic side chains of EGPEA.

The composition of **acryl_3** contained only 10.02 % EGPEA to overcome the problems of acryl_2. Precipitation of the product gave a hazy white solution in MeOH, which was left for sedimentation in the fridge overnight. The sediment was dried revealing a tacky colorless polymer. Centrifugation of the supernatant did not lead to separation of significant amounts of product throughout the first trials, so the remaining hazy solution was rejected. The reaction yield amounted to 53.2 %. Considering the fact that the supernatant was hazy after precipitation, it is recommended to apply higher amounts of

MeOH in future experiments to ensure efficient precipitation and thus to prevent material losses during the purification process.

Acryl_4 provided reactive sites for crosslinking, which were introduced by replacing MA with vinyl methacrylate (VMA) in the polymer composition. Since the vinyl group is far less reactive than the methacrylic moiety [129], an acrylic copolymer with pendant vinyl groups is generated. These functional side groups offer reactive moieties, which participate in the UV-induced crosslinking reaction. This means that the side chains of the adhesive base polymer can crosslink with each other and with the multifunctional monomers, which were added to the adhesive formulations to build semi-IPN during the photo-release. Thus, a highly efficient UV-triggered release [25,83,88] was expected. In addition, crosslinking improves the thermal stability of polymers [23,24,130]. A white and tacky polymer was isolated by precipitation, which turned colorless after drying. The reaction yield was determined to 25.2 %. As already observed for acryl_3, it was not possible to isolate all the product by centrifugation. Thus, increased amounts of precipitant (MeOH) are proposed for future experiments to increase the yields of polymerization.

Another approach to improve the thermal stability of the adhesive was to add ~20 wt% isobornyl acrylate (IBA) to the polymer composition (**acryl_5**). [131,132] A colorless and tacky polymer was precipitated and left for sedimentation in the fridge overnight. After evaporation of the solvent, the reaction yield amounted to 86.1 %.

It is stated in literature, that AA moieties can slowly migrate to the interface, where they intensify the interactions with the substrate, especially with metallic surfaces. The increased interactions may cause cohesive rather than adhesive failure of the PSA [9,22,62], which is related to adhesive residues. In order to provide clean peel after application, AA was removed from the polymer composition of **acryl_6**. A colorless and tacky polymer was precipitated and sedimented in the fridge overnight. After evaporation of the solvent, the reaction yield was determined to 86.6 %.

The synthesis of **acryl_1_scf** constituted another approach to generate reactive sites in the polymer side chains, which contribute to the crosslinking reaction. As already explained for acryl_4, this renders possible an improvement of the thermal stability and the release function. An acrylic pendant group was attached to the main chain of acryl_1 via the reaction of the AA carbonyl group and the epoxy moiety of glycidyl methacrylate (GMA). [115] Acryl_1 and GMA (molar excess) were dissolved in 2-butanone. TMAB was added to initiate the ring opening reaction between AA and GMA yielding acryl_1_scf. The proposed reaction mechanism is depicted in Figure 27. HQ was applied to inhibit the thermally induced radical polymerization across the acrylic groups in GMA [133,134]. Acrylic radicals are scavenged by HQ via hydrogen abstraction and formation of the

resonance stabilized quinone [135], which in turn can further react with chain radicals resulting in a species of low reactivity. [136] After a reaction time of 20 h a brown solid polymer was formed, which was not fully soluble in 2-butanone. HQ was removed by extraction with a NaOH solution [137] and the brown organic phase (fraction 1) was isolated. The remainder was extracted with toluene and filtered from the undissolved polymer, which was rejected. Fraction 1 and 2 (filtrate) were dried with Na₂SO₄, the solvent was evaporated and the products were finally dried at 40 °C under vacuum. While fraction 1 yielded a colorless viscous and tacky polymer, fraction 2 gave a brown porous and non-tacky solid. The overall yield of polymerization was determined to 18.5 %, whereas the ratio of fraction 1 amounted to 7.3 % and fraction 2 made up 11.2 %.

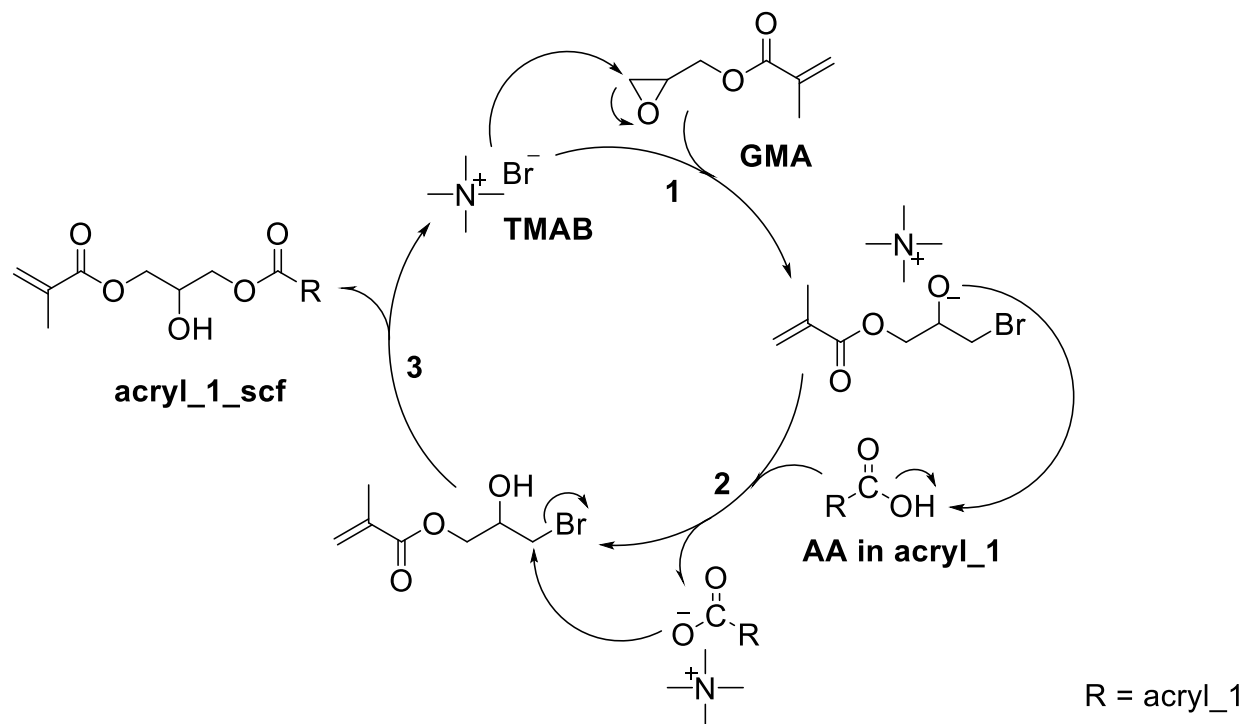


Figure 27: Proposed reaction mechanism for the side chain functionalization of acryl₁: (1) TMAB induced ring opening reaction of the epoxy moiety in GMA, (2) generation of carboxylate group and (3) displacement of Br⁻ by nucleophilic attack and regeneration of TMAB. [138]

For the preparation of PSA tapes, the synthesized acrylic copolymers were dissolved in volatile solvents to facilitate coating onto polyethylene terephthalate (PET) carriers. [20] Acryl_1, acryl_3, acryl_5 and acryl_6 showed satisfying solubility in 2-butanone, whereas acryl_2, acryl_4 and acryl_1_scf were not soluble in any of the applied solvents (2-butanone, toluene, acetone, EtAc and DCM).

Characterization of the acrylic copolymers

The chemical composition of the synthesized acrylic copolymers was investigated by means of FT-IR- and $^1\text{H-NMR}$ spectroscopy.

The FT-IR-spectrum of acryl_1 (see Figure 28) displayed typical bands for polyacrylics, including the hydrocarbon stretch vibrations at $3000\text{-}2800\text{ cm}^{-1}$ ($\text{CH}_3\text{-}$ and $\text{-CH}_2\text{-}$), the carbonyl stretch vibration at 1735 cm^{-1} (C=O) and the C-O-C stretch vibration at 1160 cm^{-1} . [113] The characteristic broad peak of the carboxylic acids group in AA ($3300\text{-}2500\text{ cm}^{-1}$) was missing due to the comparatively low portion of AA. The small band at 1645 cm^{-1} and some signals in the fingerprint region ($961, 907, 829, 768\text{ cm}^{-1}$) suggested that some unreacted monomers remained trapped in the copolymer after purification. [139,140]

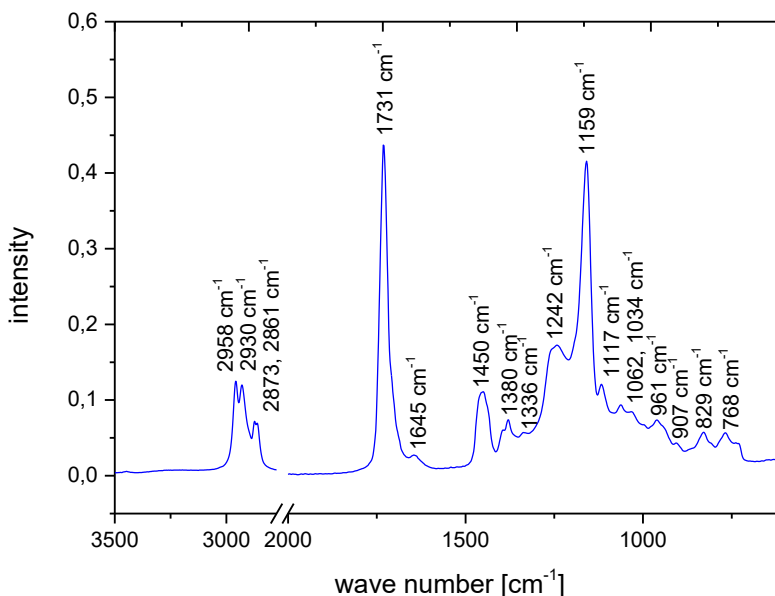


Figure 28: FT-IR-spectrum of acryl_1

Furthermore, **FT-IR-spectroscopy** was applied to evaluate the modification of the acrylic copolymers. Therefore, the spectra of acryl_4, acryl_5, acryl_6 and acryl_1_scf (see appendix Figure_A 1) were compared to the spectrum of acryl_1. Distinct signals at 1647, 974 and 874 cm^{-1} were revealed for acryl_4, which were assigned to C=C double bonds of the vinyl pendant group. The spectrum of acryl_1_scf exhibited some changes in the fingerprint region, which were attributed to the attachment of GMA, and a broad signal at 3389 cm^{-1} , which was attributed to the hydroxyl group, formed during the ring opening reaction of the epoxy functionality. Furthermore, a prominent peak at 1574 cm^{-1} was detected, which was related to carboxylic acid salts. Based on these findings, it was suggested that the side chain modification of acryl_1 was not successful and the carboxylic acid of AA had built the corresponding sodium salt during purification with NaOH. In contrast, the incorporation of IBA in acryl_5 did not change the spectrum significantly but rather lead to overlapping signals of the already existing hydrocarbon side chains. The removal of AA from the polymerization mixture (acryl_6) could not be shown by FT-IR-spectroscopy as the characteristic broad peak of the carboxylic acid in AA (3300-2500 cm^{-1}) was already missing in acryl_1. [139,140] An overview of the FT-IR-peaks and the corresponding assignment are provided by Table_A 2 in the appendix.

Since the incorporation of IBA in acryl_5 was not proven by FT-IR-spectroscopy, **$^1\text{H-NMR}$ spectroscopy** was applied to investigate acryl_1 and acryl_5 in more detail. Moreover, the ^1H -spectrum of acryl_6 was recorded. Peak assignment and interpretation of all spectra are summarized in Table 7. An assignment of the peaks to the respective copolymer structures is depicted in Figure 29 (acryl_1) and Figure_A 2 and Figure_A 3 in the appendix (acryl_5 and acryl_6).

The results reveal that the incorporation of IBA (acryl_5) gave rise to the peaks at 4.64 ppm, 1.73 ppm and 0.83 ppm. In contrast, the removal of AA from the polymerization mixture (acryl_6) could not be displayed as the OH-resonance of the carboxylic acid (~ 12 ppm) [141] was also missing in the spectrum of acryl_1.

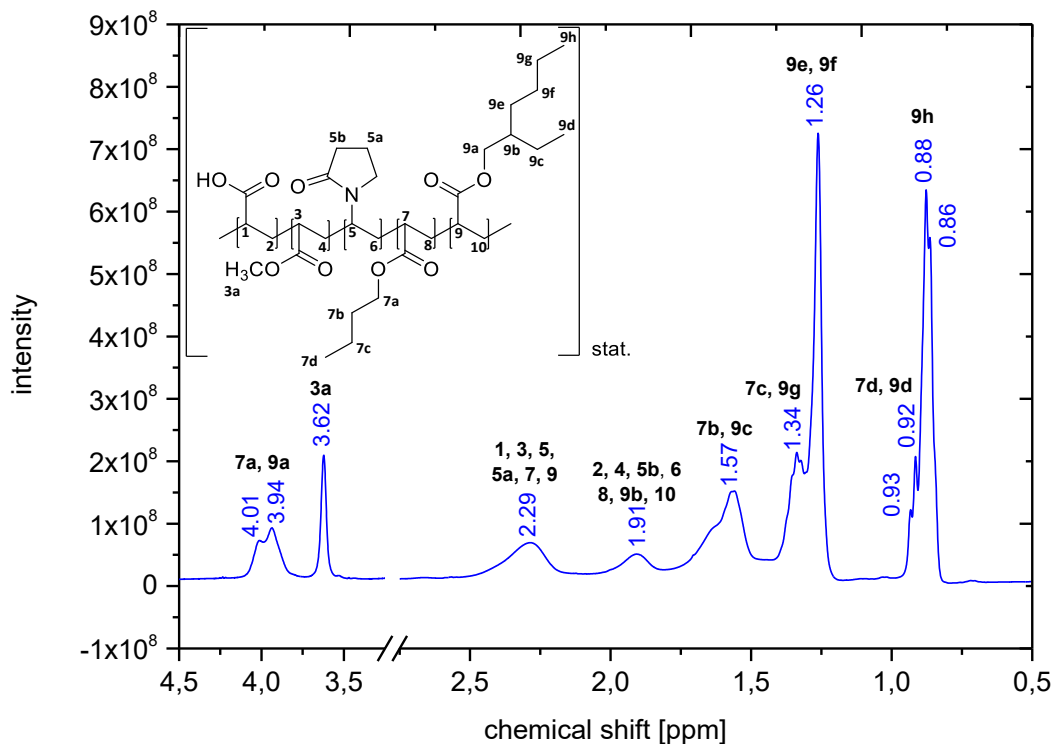


Figure 29: $^1\text{H-NMR}$ spectrum of *acryl_1*

Table 7: Results of $^1\text{H-NMR}$ spectroscopy of *acryl_1*, *acryl_5* and *acryl_6*: peak assignment [113,133,142]

assignment	multiplicity	Chemical shift [ppm]			interpretation
		<i>acryl_1</i>	<i>acryl_5</i>	<i>acryl_6</i>	
CH	s		4.64		CH in IBA
CH₂COCOR	m	4.01	4.03	4.02	CH ₂ COCOR in BA and 2-EHA
		3.94	3.96	3.95	
CH₃	s	3.62	3.64	3.63	CH ₃ of MA
CH₂	s	2.29	2.29	2.28	unsubstituted CH ₂ of main chain
	s	1.91	1.92	1.91	substituted CH ₂ of main chain and VP
CH₂ and CH					CH of 2-EHA
	s/m	1.57	1.73-1.58	1.62-1.56	CH ₂ of BA and 2-EHA
	m	1.34-1.26	1.38-1.28	1.35-1.27	
CH₂	m		1.15-1.07		CH ₂ of BA and 2-EHA
CH₃	m	0.93-0.86	0.95-0.83	0.93-0.86	CH ₃ of BA, 2-EHA and IBA

The molecular weight distribution of acryl_1, acryl_5 and acryl_6 was determined by **GPC**. In contrast, the analysis of acryl_2, acryl_4 and acryl_1_scf was not possible due to insufficient solubility of these polymers. Moreover, acryl_3 was not characterized by GPC because of the comparatively low amounts of synthesized material. The corresponding values of the number and weight average molecular weight (M_n , M_w) and PDI are summarized in Table 8. The broad poly dispersity indices (PDI) were the result of the random and uncontrolled nature of free radical polymerization reactions. A broad PDI is stated to be beneficial for the performance of PSAs: Short polymer chains enable good adhesion and wetting of the substrate due to high mobility, while long polymer chains contribute to the development of the cohesive strength within the adhesive layer. [143] The particularly high PDI of acryl_5 was seen as a consequence of the incorporation of the bulky IBA, which sterically hindered polymerization propagation. This assumption is supported by the comparatively low values for M_n and M_w , indicating that chain growth was hindered to a certain extent.

Table 8: Molecular weight distributions of acryl_1, acryl_5 and acryl_6 including M_n , M_w and PDI

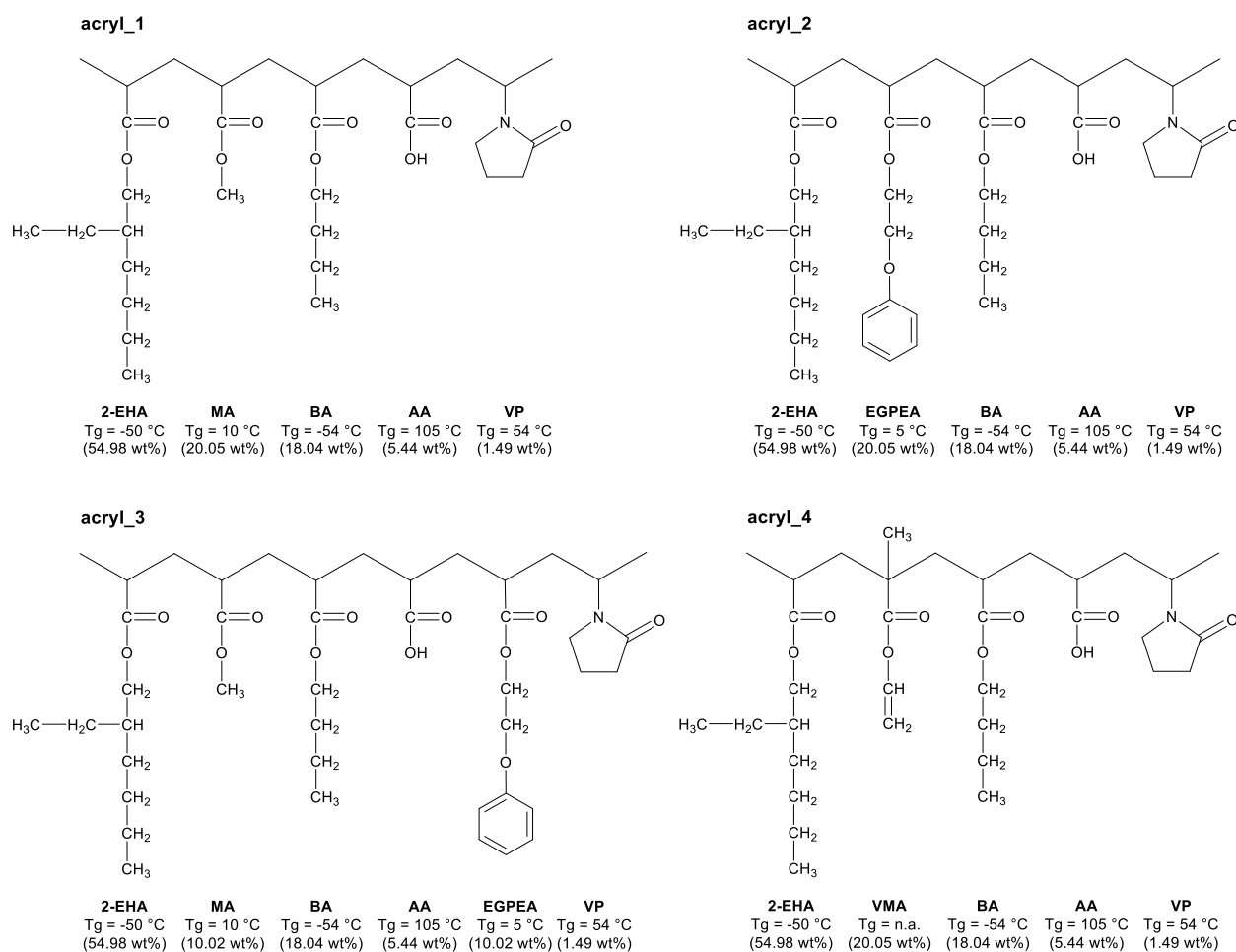
Copolymer	M_n [g/mol]	M_w [g/mol]	PDI
acryl_1	124,400	511,600	4.11
acryl_5	59,800	170,900	9.62
acryl_6	575,800	816,400	4.78

The **glass transition temperature (T_g)** of a polymer is as a measure for its adhesive and cohesive properties. Typically, PSAs exhibit T_g s in the range of -15 °C to -5 °C, whereas this value ranges from -75 °C to -25 °C for common acrylic PSAs. Since the choice of monomers governs the T_g of a polymer, the compositions of the random acrylic copolymers acryl_1-6 are illustrated schematically in Figure 30. [10,20]

The T_g s of the adhesives were obtained from DSC measurements and compared to the theoretical values, calculated using the Fox equation (2). Since there is no information about T_g of VMA available in literature, the theoretical T_g of acryl_4 could not be estimated. Taking into account that DSC measurements provide a repeatability of 2.5 °C and a reproducibility of 4.0 °C for the determination of the T_g [144], a good agreement of the experimental and theoretical data was observed (see Table 9). The T_g of acryl_1 was determined to -32 °C, while the calculated value amounted to -34 °C. As predicted by the Fox equation, the T_g s of acryl_2 and acryl_3 did not significantly differ from the

-Results and discussion, Synthesis and characterization of the adhesive copolymers-

corresponding value of acryl_1 because the homopolymers of the exchanged monomers (MA, EGPEA) comprised similar T_g s (see Table_A 1). In contrast, the incorporation of IBA increased the T_g considerably (acryl_5). Although AA made up only about 5.5 wt% of the polymer composition, its removal decreased the T_g of acryl_6 to -38 °C. The high impact of this monomer is based on the comparatively high T_g of poly(AA) (105 °C). Based on the findings of FT-IR-spectroscopy, acryl_1_scf had been rejected and was not investigated by DSC analysis.



-Results and discussion, Synthesis and characterization of the adhesive copolymers-

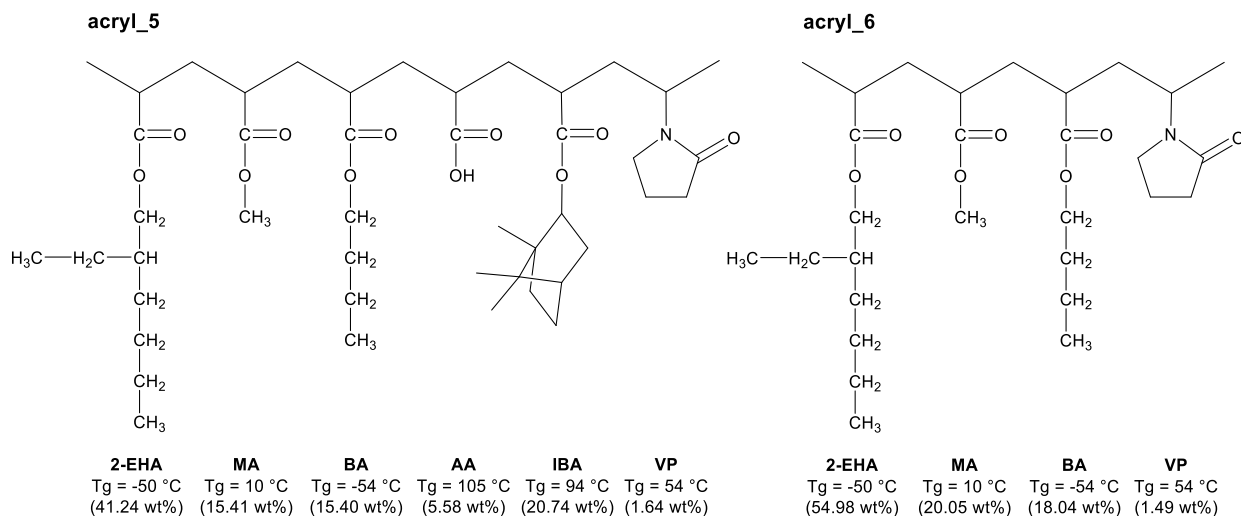


Figure 30: Schematic illustration of the composition of acryl_1-6

Table 9: Experimentally determined and calculated T_g s of the synthesized acrylic copolymers

Copolymer	T_g by DSC [°C]	T_g calculated [°C]
acryl_1	-32	-34
acryl_2	-30	-35
acryl_3	-39	-34.5
acryl_4	-35	n.a.*
acryl_5	-12	-14
acryl_6	-38	-38.5

*... no prediction possible because no information about T_g of VMA available in literature

The **thermal stability and degradation** of the synthesized copolymers was studied by TGA analysis. Figure 31 displays the determination of the degradation onset and end temperature (T_{ON} and T_{END}) at the representative example of acryl_1. T_{ON} and T_{END} were defined as the intersections of the tangent with the horizontal lines before and after the degradation step. [145] The first weight loss stage ends at about 100 °C and was assigned to the evaporation of 2-butanone, which was used to transfer the polymers into the crucibles. According to TGA experiments, acryl_1 began to degrade at 370 °C. The incorporation of EGPEA in acryl_2 and acryl_3 as well as the removal of AA in acryl_6 slightly decreased T_{ON} of the copolymers (see Table 10). The effect of VMA was even more pronounced, reducing T_{ON} of acryl_4 to 333°C. Moreover, the results revealed that the addition of IBA did not lead to the desired improvement of the thermal stability.

The thermogram of acryl_5 displays two degradation steps at $T_{ON,1} = 270$ °C and $T_{ON,2} = 343$ °C (see Figure 32). A multistep decomposition of poly(IBA) was also observed by Ozlem et al. who detected the first degradation products around 250 °C. The loss of the isobornyl ring occurred at 340 °C via cleavage of the *o*-isobornyl bond. [132] Although T_{ON} varied according to the chemical composition, all the acrylic copolymers were degraded almost completely (> 90 %) at temperatures > 415 °C (T_{END}). Acryl_1_scf was not investigated by TGA analysis since the findings of FT-IR-spectroscopy already revealed that the side chain modification of acryl_1 was not successful and the carboxylic acid of AA had built the corresponding sodium salt during purification with NaOH.

Table 10: Degradation onset temperatures T_{ON} of the synthesized acrylic copolymers

Copolymer	T_{ON} [°C]	T_{END} [°C]
acryl_1	370	406
acryl_2	356	412
acryl_3	361	413
acryl_4	333	410
acryl_5	270; 343	412
acryl_6	360	411

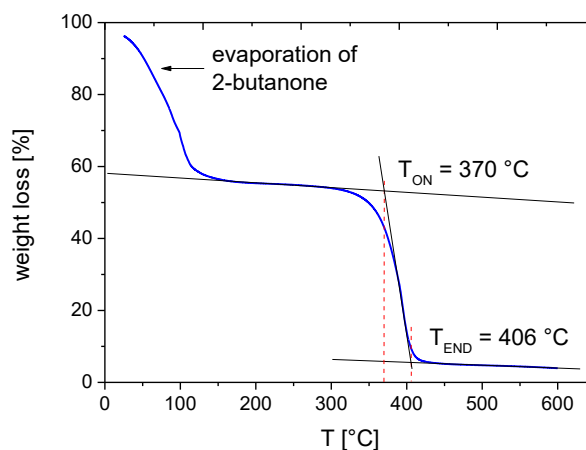


Figure 31: Determination of the degradation onset and end temperature from the weight loss curves (TGA) as the intersections of the tangent with the horizontal lines before and after the degradation step

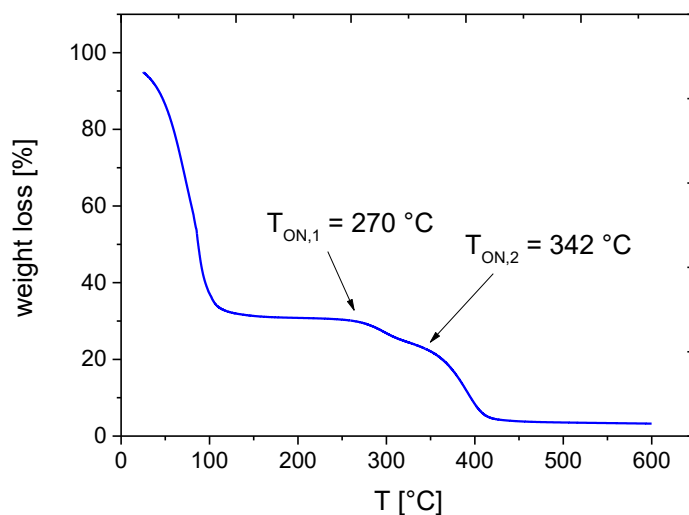


Figure 32: TGA thermogram of acryl_5 showing a 2-step degradation

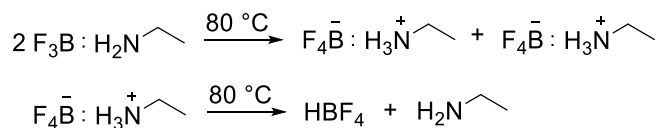
6.1.2. Polyethers

Synthesis and purification

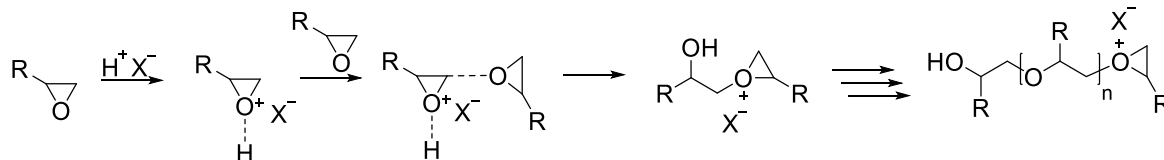
Polyether based adhesives were synthesized in a cationic ring opening reaction of mono-epoxy monomers at 70-90 °C employing boron trifluoride ethylamine ($\text{BF}_3 \cdot \text{H}_2\text{NCH}_2\text{CH}_3$) as a catalyst. [116] During thermal activation of $\text{BF}_3 \cdot \text{NH}_2\text{CH}_2\text{CH}_3$, the complex breaks down and is converted to tetrafluoroboric acid (HBF_4), which finally initiates the ring opening reaction by complexing with epoxy groups (see Figure 33). [146] Propagation proceeds via two competing chain growth mechanisms: Activated chain ends (ACE) form cyclic tertiary onium ions, while activated monomers (AM) proceed via linear secondary onium ions, which are less reactive. [117]

The composition of the polyether adhesives was varied, in order to adjust the adhesive properties and the T_g . [60] Applying the same principle as for acrylic copolymers, branched monomers were introduced to increase the tack and to decrease the T_g of the adhesive. Acrylic side groups were incorporated and UV-crosslinked in the triggered release mechanism. The associated network formation further improves the thermal stability and supports the residue-free removability by increasing the cohesion and the T_g of the PSA. [23,26,130] The respective compositions of the polyether adhesives are summarized in Table 5.

I: Activation of boron trifluoride ethylen diamine



II: Cationic ring opening polymerization activated chain end (ACE)



activated monomer (AM)

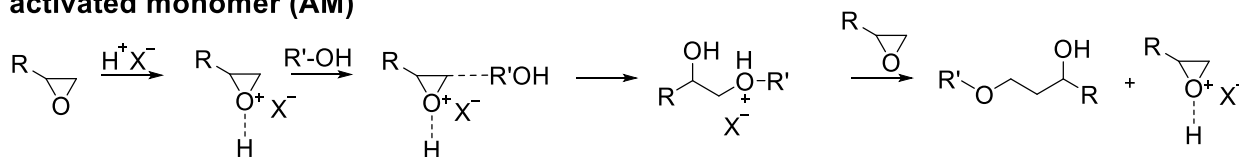


Figure 33: Mechanism for cationic ring opening by the use of boron trifluoride ethylamine complexes ($\text{BF}_3 \cdot \text{NH}_2\text{CH}_2\text{CH}_3$) including two competing chain growth mechanisms: activated chain end (ACE) and activated monomer (AM) [117,146,147]

Polyether_1 was synthesized by homopolymerization of GMA, resulting in a polyether backbone with pendant acrylic groups. The acrylic moieties served as crosslinking sites for the UV-induced release mechanism, where adhesion is decreased and cohesion is increased by network formation. [24] Since no polymerization was observed at 70 °C, the reaction temperature was continuously increased in steps of 5 °C every 15 minutes. At a temperature of 90 °C, vitrification occurred rapidly and the reaction was quenched by cooling to room temperature (rt). The glassy yellowish polymer was dissolved in 2-butanone and precipitated in cold EtOH. A white non-tacky precipitate was isolated and dried at 50 °C, revealing a yellowish slightly tacky polymer and a reaction yield of 3.3 %. Material was lost by the rejection of the hazy supernatant, which was not further purified because of the experiences gained during isolation of the acrylic copolymers. Moreover, it has to be considered that vitrification restricts the molecular mobility of the reactive species and therefore the kinetic chain length. [148] A possible solution to this problem may be the reactivation of the reaction by heating above T_g . [123]

Based on the same considerations as for the acrylic copolymers, the tack of **polyether_2** was modified by the addition of the branched epoxy monomers 2-EHGE (55 wt%) and GIPE (20 wt%). In order to prevent premature polymerization of the acrylic groups in GMA, the reaction was protected from light and BHT was added as a radical scavenger [149]. In contrast to the synthesis of polyether_1, no solid polymer was obtained even after a reaction time of 2.5 h at 80 °C and another 3.5 h at 90 °C. The color of the reaction mass had changed from colorless to orange. As the liquid was removed, a polymeric film at the wall of the flask was observed. However, attempts to isolate this product by scratching and dissolution failed and polyether_2 was rejected.

To overcome the problems during isolation, the mixing ratios were adjusted to 50 wt% GMA, 30 wt% 2-EHGE and 20 wt% GIPE in **polyether_3**. The reaction was done under protection from light to prevent premature polymerization of the acrylic groups. A yellowish non-tacky gel was obtained after a reaction time of 1 h at 80 ° and another 3.5 h at 90 °C. Though toluene turned out to be the most effective among various solvents, the product could not be dissolved completely. Precipitation in cold EtOH gave a white solid, which turned yellow upon drying. The reaction yield was neglectible due to the numerous dissolution attempts and material losses during purification.

As already mentioned for the acrylic copolymers, adhesive solutions were required during tape preparation. Therefore, polyether_1 and polyether_3 were dissolved in 2-butanone, whereof only polyether_3 gave an applicable solution.

Characterization of the synthesized polyether based copolymers

The synthesized polyethers were characterized by **FTIR-spectroscopy**. The spectrum of polyether_1 (see Figure 34) was taken as a representative example, showing typical bands for both the polyether backbone and the acrylic side chain of GMA. The spectra of polyether_2 and polyether_3 are provided in the appendix (Figure_A 4). The broad peak at 3425 cm^{-1} was assigned to the hydroxyl group, which arose due to the ring opening of the epoxy ring [123], while the $\text{C}=\text{O}$ stretch vibration at 1710 cm^{-1} was related to the acrylic pendant group. [113] The signal at 1641 cm^{-1} and some peaks in the finger print region ($945, 861, 819, 766\text{ cm}^{-1}$) [139,140] evidenced that there were still unreacted acrylic groups left, which were available for UV-crosslinking. Moreover, the vibrations at 2939 cm^{-1} (CH_3 - and $-\text{CH}_2$ -) and $1171\text{-}1045\text{ cm}^{-1}$ were not only characteristic for the polyether main chain [123] but also observed for the acrylic copolymers (see chapter 6.1.1). A detailed list of peak assignments is provided in Table_A 3 in the appendix.

The FT-IR-spectra of the polyether adhesives and acryl_1 were compared and the respective peaks at $\sim 1640\text{ cm}^{-1}$ were integrated. The normalized peak heights (2960 cm^{-1} was taken as an internal standard) revealed that the amount acrylic $\text{C}=\text{C}$ double bonds left in the polyethers exceeded the unreacted acrylic groups in acryl_1. The highest ratio of $\text{C}=\text{C}$ was left in Polyether_2. This was related to the use of BHT, which effectively prevented the thermally induced polymerization of the acrylic groups in GMA.

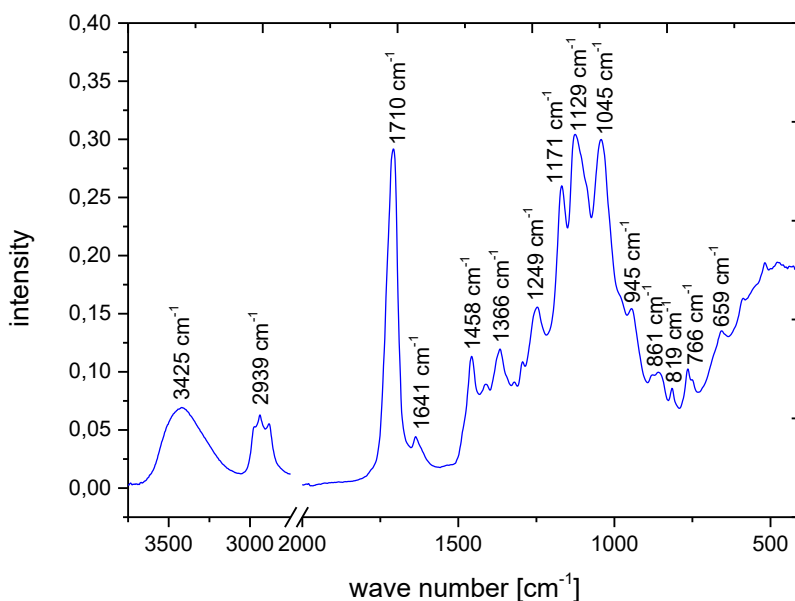


Figure 34: FT-IR-spectrum of polyether_1

TGA measurements of polyether_1 revealed a degradation onset temperature of T_{ON} of 336 °C and an endpoint of degradation of T_{END} at 412 °C, which were similar to the results obtained for the acrylic copolymers. The corresponding thermogram is provided in the appendix (Figure_A 5).

The prepared polyether adhesives were not further characterized as the syntheses did not yield high amounts of material.

6.1.3. Conclusion about the synthesis of adhesive copolymers

Acrylic copolymers were synthesized as basic adhesive materials for UV-curable PSA tapes. The properties of the polymers were modified by variation of the chemical compositions. In order to increase the thermal stability of the adhesives, monomers comprising aromatic side chains [21] or isobornyl groups [131,132] were added to the composition of acryl_2, acryl_3 and acryl_5. Reactive sites for UV-crosslinking were introduced to the structure of acryl_4 and acryl_1_scf, while AA was removed from the composition of acryl_6 to reduce the interactions with polar substrates. [9,22,62]

Moreover, polyether adhesives were synthesized from mono-functional epoxy monomers. The polyether backbone provided thermal stability, while clean peel was supported by the UV-crosslinking of pendant acrylic groups. Branched monomers were added in different amounts to adjust the tack of the adhesives. However, only the synthesis of acryl_1, acryl_3, acryl_5, acryl_6 and polyether_3 resulted in tacky and soluble adhesives. Satisfying yields of polymerization (> 85 %) were achieved for acryl_1, acryl_5 and acryl_6. The yield of acryl_3 was > 50 % while < 30 % were obtained by the syntheses of the remaining acrylic polymers. In contrast, the polyether synthesis was less successful: The yields of polyether_1 and polyether_3 were very low and the synthesis of polyether_2 was rejected as the product could not be isolated.

Typical FT-IR-signals were detected for both, the acrylic copolymers and the polyethers. Furthermore, the results revealed a successful incorporation of the vinyl side chains in acryl_4. In contrast, the side chain functionalization (scf) did not lead to the desired product as the signal at 1547 cm^{-1} suggested the formation of sodium salts with the carboxylic acid moiety. [139,140] $^1\text{H-NMR}$ of acryl_5 proved the incorporation of IBA, while the removal of AA in acryl_6 could not be confirmed. According to GPC measurements, acryl_1, acryl_5 and acryl_6 were characterized by broad PDIs, which offer good adhesion properties (short chains) and the required cohesion (long chains). [143] Moreover, it was found that the isobornyl groups in acryl_5 limited chain growth by steric hindrance. The T_g s of the acrylic copolymers ranged from -40 to $-30\text{ }^\circ\text{C}$ and the degradation onset temperatures T_{ON} were determined to 370 - $330\text{ }^\circ\text{C}$. Although the incorporation of IBA increased the T_g as expected to $-12\text{ }^\circ\text{C}$, it led to a decrease of the thermal stability. The thermogram obtained by TGA measurements showed a two-step degradation, with the first step starting at $270\text{ }^\circ\text{C}$. Against our expectations, the polyethers did not show superior thermal stability over the acrylic copolymers.

6.2.Design of photo-curable PSA tapes

The adhesive system

The synthesized adhesive polymers were employed in the preparation of photo-curable PSA tapes. To facilitate coating the polymers were dissolved in volatile solvents. [20] Applicable adhesive solutions of acryl_1, acryl_3, acryl_5, acryl_6 and polyether_3 were obtained by dissolution in 2-butanone.

One of the major requirements of the PSA tape was easy and clean peel from different substrates, including pristine copper, tarnish-protected copper, BondFilm® treated copper and epoxy-based surfaces. Residue-free removability was provided by a photo-triggered release mechanism, which reduced the adhesion and increased the cohesion of the PSA on demand as a consequence of crosslinking and chain entanglement. [20,22,26,27] Therefore, the acrylic moieties in the side chains of polyether_3 were exploited to build inter- and intramolecular linkages between the polymer chains upon UV-irradiation.

In contrast, the UV-release mechanism of the acrylic PSAs was based on the formation of semi-interpenetrating networks (semi-IPN). The acrylic copolymer solutions were mixed with a photoinitiator and selected multifunctional acrylic monomers, which polymerized in a free radical reaction upon UV-exposure. As a result, semi-IPN were formed with the base polymer (see Figure 35). [150] This network formation led to an increase of the thermomechanical stability as well as the heat and creep resistance. [22,151] Another consequence of crosslinking was the restriction of the chain mobility, which was related to reduced adhesion as well as increased cohesion and T_g values. [20,21,23–25] Thus, a photo-triggered release function was realized, which enabled easy and clean peel of the PSA tape in the end of its application.

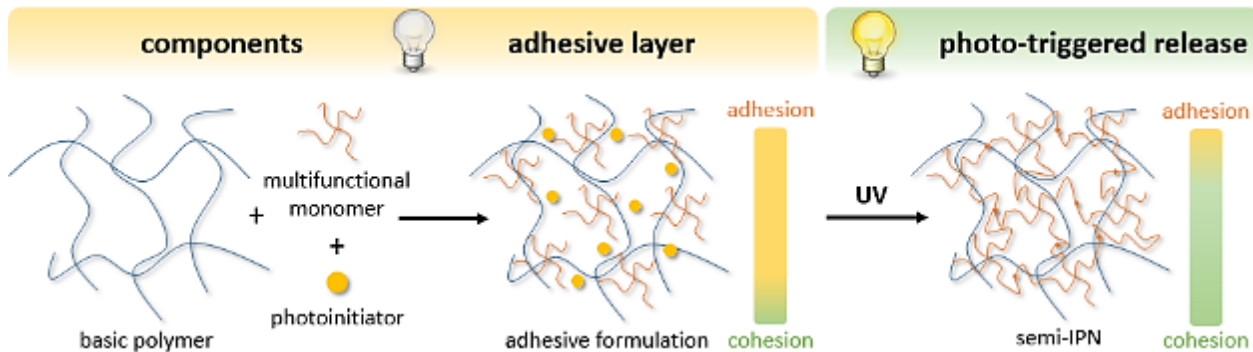


Figure 35: Photo-triggered release mechanism of acrylic PSAs

Lucirin TPO-L was utilized as photoinitiator for the UV-release mechanism in the acrylic PSAs. Since it is a liquid, Lucirin TPO-L offers good miscibility and easy incorporation into the adhesive formulation. The absorption maximum is in the UV/VIS spectral region, ranging from 350-420 nm. As a representative of type I photoinitiators, Lucirin TPO-L is cleaved and forms two radicals upon irradiation. The scission of the C-P bond generates benzoyl- and phosphinoyl-radicals (see Figure 36), which are both highly reactive. [100,152]

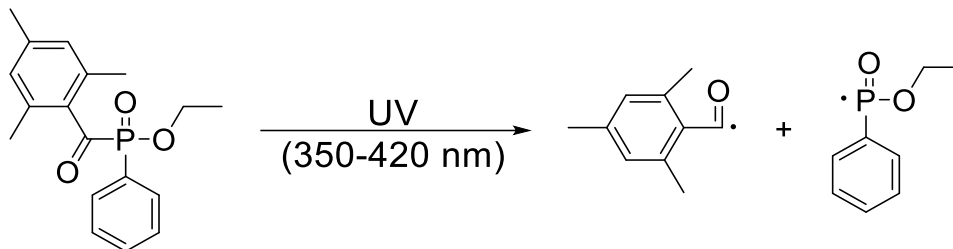


Figure 36: Scission of Lucirin TPO-L and generation of benzoyl- and phosphinoyl-radicals

Screening experiments

In a screening experiment, the curing efficiency of Lucirin TPO-L was compared to Irgacure 379 and Irgacure 819. The structures of these **photoinitiators** are shown in Figure 37. Adhesive formulations containing acryl_1, 10 wt% DTMPA and 1, 5 or 10 wt% of the respective photoinitiator (PI) were prepared and coated onto PET carriers. Adhesion experiments on pristine copper surfaces revealed that Irgacure 379 did not efficiently trigger the release upon UV-irradiation. Better results were obtained for Lucirin TPO-L and Irgacure 819, which reduced the tack of the tape significantly and enabled residue-free removability. Finally, Lucirin TPO-L was preferred due to its superior miscibility (liquid) and slightly better performance.

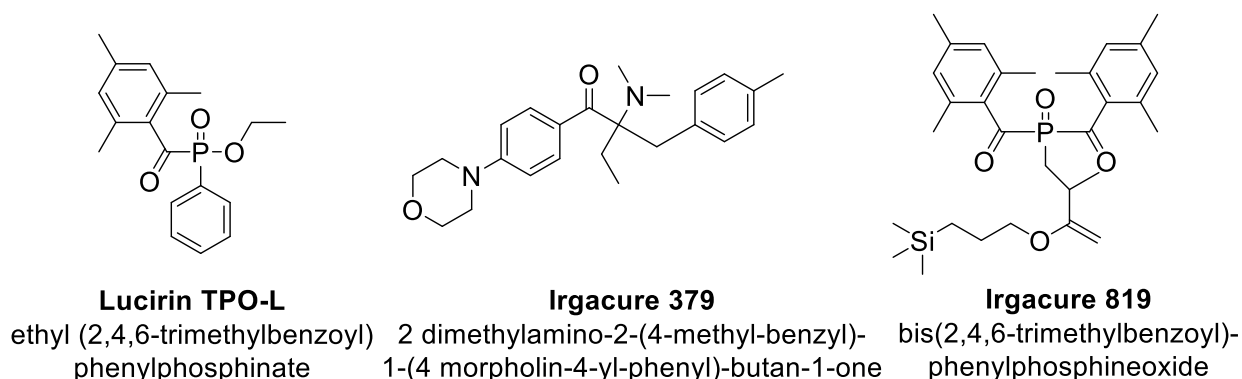


Figure 37: Structures of the photoinitiators Lucirin TPO-L, Irgacure 379 and Irgacure 819

Experiments with **tapes based on polyether_3** revealed bad adhesion properties and thus insufficient fixation of the substrates. In contrast, the acrylic PSAs provided satisfying initial tack. Due to these findings and the low reaction yields (~3 %), polyether adhesives were rejected and the focus was set on acrylic based adhesives.

All acrylic PSA tapes tested comprised efficient release after UV-irradiation. Screening experiments at rt showed noticeably decreased tacks and clean peel after UV-irradiation. Drawbacks of tapes based on **acryl_3**, 10 wt% DTMPTA and 1 or 5 wt% Lucirin TPO-L included prolonged drying of the adhesive layer during tape preparation and low yield of polymerization (53.2 %) compared to acryl_1 (94.4 %), acryl_5 (86.1 %) and acryl_6 (86.6 %). Moreover, the incorporation of aromatic side chains did not improve the thermal stability as desired (see TGA measurements in chapter 6.1.1). For these reasons, acryl_3 was not further investigated in this work.

To conclude, screening experiments led to the rejection of acryl_3 and epoxy_3 as basic adhesive materials, while acryl_1, acryl_5 and acryl_6 were found suitable adhesives for the production of PSA tapes. In order to provide easy and clean peel in the end of the application, solutions of the copolymers (2-butanone) were mixed with Lucirin TPO-L and selected multifunctional acrylates, which form semi-IPN upon UV-irradiation. In this work, the focus was set on adhesive formulations based on acryl_1, since acryl_5 and acryl_6 based adhesives were investigated in more detail in "Synthese und Anwendung von UV-sensiblen Haftklebstoffen auf Acrylatbasis" by Nikolaus Heindl (bachelor thesis).

6.2.1. Characterization of the adhesive layer

UV-cure kinetics

As explained above, the release mechanism of the developed PSA tapes was achieved by photo-triggered crosslinking of multifunctional acrylic monomers and the related formation of semi-IPNs with the base polymer. For this purpose, the synthesized acrylic copolymers (acryl_1, acryl_5 or acryl_6) were blended with Lucirin TPO-L (PI) and selected multifunctional acrylates. The UV-induced conversion of the acrylic C=C double bonds was investigated by means of FT-IR-spectroscopy as a function of type and concentration of the acrylic monomer. The decrease of the characteristic absorption at 985 cm^{-1} (C=C) [139,140] was monitored upon prolonged UV-exposure (see Figure 39a). Furthermore, the impact of the base polymer structure and the photoinitiator concentration was explored.

Network formation requires at least bifunctional monomers. In order to achieve high network densities [148] and consequently a significant reduction of the adhesive strength [24,25], tri- and tetra-functional acrylates as well as a penta/hexa-functional acrylates were utilized as crosslinking agents (see Figure 38). The influence of the monomer structure on C=C double bond conversion and the reaction rate was evaluated with regard to functionality, spacer chain length and pendant groups other than acrylic moieties. [148,151,153] As demonstrated in Figure 39b, the polymerization rates (R_p) were estimated from the initial linear portion of the irradiation time-conversion plots applying the direct proportional relationship of $slope = R_p/[M_0]$. [154,155]

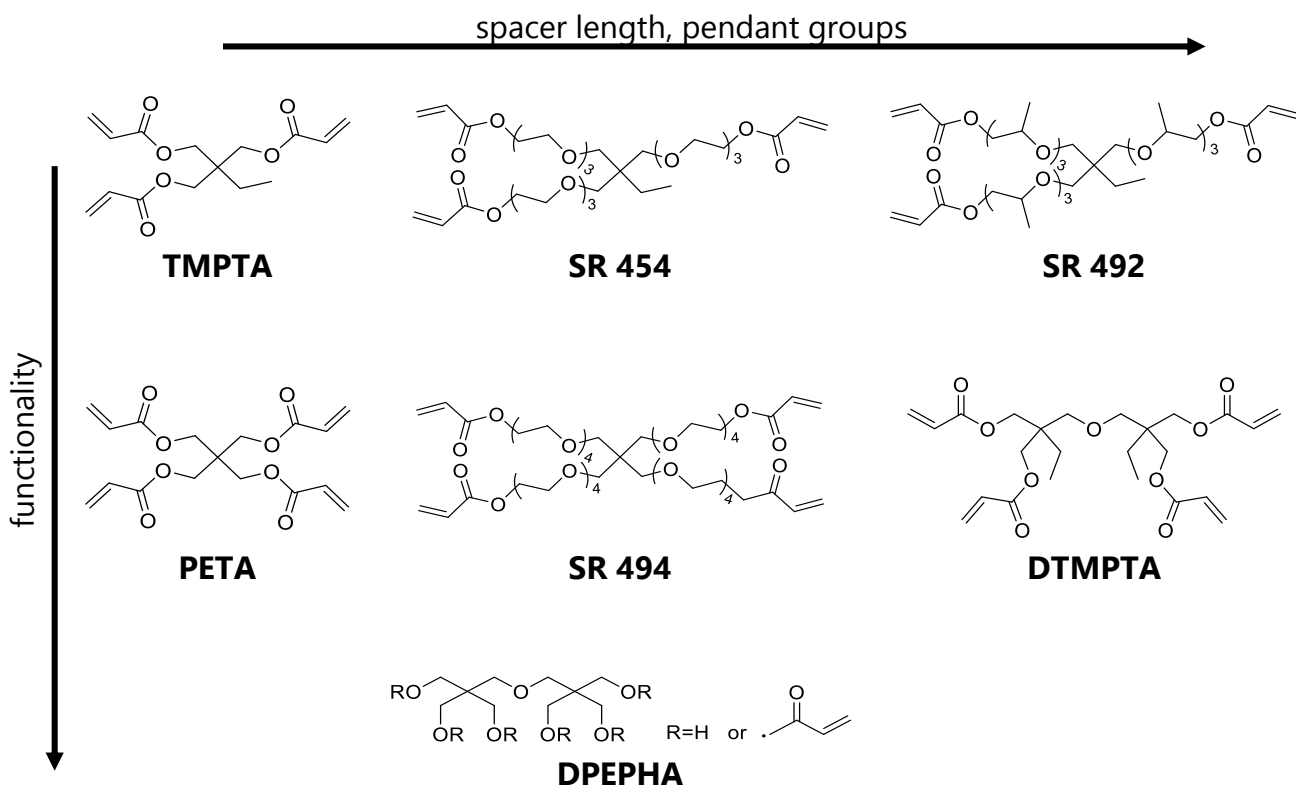


Figure 38: Structures of multi-functional acrylic monomers used for the preparation of adhesive films

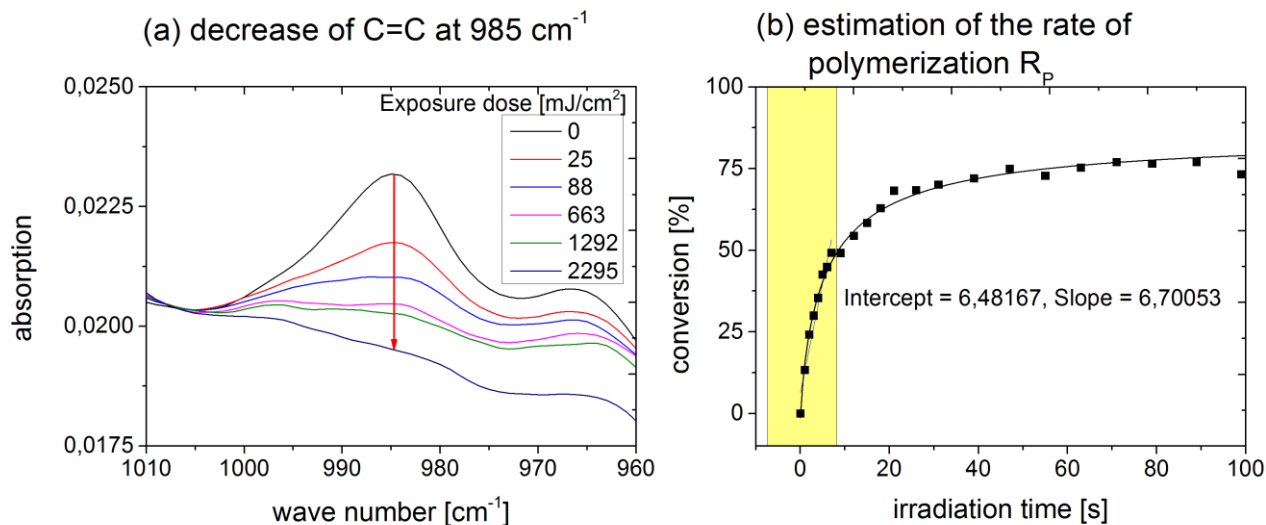


Figure 39: (a) FT-IR spectrum of adhesive 1 (acryl_1, 10 wt% DPEPHA, 1 wt% Lucirin TPO-L) as a function of irradiation dose. Decrease of the peak at 985 cm⁻¹ related to the C=C double bond of the acrylic moieties. (b) Estimation of the polymerization rate by determination of the slope of the initial portion of the irradiation time-conversion plot at the representative example of adhesive 1.

The steep slopes at the initial part of the irradiation time-conversion plots revealed an immediate onset of auto-acceleration, followed by a flat section, where translational diffusion becomes limited and segmental diffusion was more pronounced. Finally, the curves reached a plateau indicating the endpoint of polymerization and the level of maximum conversion.

The influence of the **base polymer structure** on C=C double bond conversion and polymerization rate was investigated at the example of adhesive layers containing 10 wt% DPEPHA and 1 wt% Lucirin TPO-L (adhesive 1; see Figure 40a). The reduction of the final conversion of acryl_5 from 84 % (acryl_1) to 74 % was related to the bulky IBA side chains, which sterically hindered the diffusion of the reactive species. This was confirmed by the low reaction rate for the system based on acryl_5. In contrast, the removal of the AA side chains in acryl_6 led to increased conversion (~100 %) and a higher reaction rate as a consequence of the missing inter- and intramolecular interactions within the bulk. [9] The nearly complete conversion of DPEPHA and acryl_6 require significantly higher irradiation doses compared to systems with other base polymers (see Table 11).

In further experiments, the number of initiating radicals was increased by increasing the **PI content** from 1 to 5 wt% at a given monomer concentration of 10 wt% DPEPHA, DTMPTA or SR 494. It is well known that for photo-induced radical reactions, in a simplified

relationship, the initiation rate (R_i) is directly proportional to the concentration of the initiating species $[PI]$, the quantum yield of the photoinitiation (ϕ), the intensity of the incident light (I_0) and the molar extinction coefficient of the initiator (ϵ): $R_i = 2 \phi I_0 \epsilon [PI]$. [156,157] Thus, high PI contents are associated with high conversion and fast reactions [100]. The results showed, distinctly increased monomer conversions for all systems containing 5 wt% PI, enabling nearly full consumption of the respective acrylic monomers upon prolonged UV-exposure. This was clearly demonstrated at the example of the DPEPHA system, where the final conversion was enhanced from 84 % to ~ 100 % by the increase of the PI concentration (see Figure 40b). In addition, the polymerization rates were accelerated considerably, while the irradiation doses for maximum conversion were reduced (see Table 11 and Figure_A 6a-b).

In a third series of measurements, the influence of the **monomer concentration** on the kinetic parameters was studied. The monomer content in adhesive systems based on acryl_1 and DPEPHA, DTMPTA or SR 494 was varied from 10 to 50 wt% at a constant PI concentration of 1 wt% (adhesives 1, 6, 8, 10, 14, 15, 24, 26 and 27; see Table 6, chapter 5.5). As indicated by the respective slopes in Figure 40c, Figure_A 6c and Figure_A 6d, the reaction rates of the DPEPHA and DTMPTA systems were not changed significantly by increasing monomer contents. Different results were found for SR 494 adhesives, where higher amounts of monomer (20 and 50 wt%) accelerated the polymerization. In general, the reactions started at the same speed (independent on the monomer concentration), but systems containing higher amounts of monomer required increased irradiation doses for maximum conversion (see Table 11). The prolonged cure time and higher irradiation doses were explained by the constant level of PI applied throughout the series, where the same amount of initiating radicals was used to crosslink increased amounts of material. The final conversions decreased with increasing monomer concentration. However, it has to be considered, that the final conversion is a relative value, which refers to the individual adhesive formulation. When regarding to the absolute amount of C=C double bonds, even more moles were consumed at higher monomer concentrations. Upon this extended polymerization, diffusion processes became a limiting factor, which did not allow for complete conversion in the 20 and 50 wt% systems.

Besides these aspects, also the **monomer structure**, including functionality, spacer chain length and pendant groups other than the acrylic moieties, affects the cure kinetics. Highly functional monomers are associated with high crosslinking densities and high reaction rates due to the large number of reactive sites. As polymerization proceeds, the formation of dense networks restricts the mobility of reactive species (monomers, radicals) and thus the conversion extent. [148] Moreover, (even small) pendant groups other than acrylic moieties may block the crosslinking reaction by hindrance of the free rotation of

the C=C double bonds. As a consequence, conversion decreases and the reaction is slowed down. [148,153] It is stated in literature, that long and flexible spacers enable high final conversion based on their high segmental diffusion. While the initial stages of polymerization are dominated by translational diffusion (diffusion of the monomer molecules), the final reaction stages are governed by the mobility of unreacted monomer segments (C=C moieties). Though diffusion of long chains may be suppressed by entanglement, vitrification does not occur and segmental diffusion allows for high final conversion. However, this process is rather slow, causing low reaction rates for long spacers. [148,153] Inconsistent results concerning the influence of the spacer length on the reaction rate were found in literature. Increasing as well as decreasing rates with increasing repeating units of the spacer chain are documented for di(meth)acrylic monomers. [148] Other references clearly state that the rate of polymerization (R_p) can be accelerated by the use of short spacers, owed to their high mobility, low entanglement and higher relative concentration of C=C double bonds. Since small monomers show a rapid onset of gelation, the final conversion is reduced by diffusion limitation. [151]

In this work, the impact of the monomer structure on final conversion and reaction rates was investigated in a series of adhesive formulations based on acryl_1, containing 1 wt% Lucirin TPO-L and 10 wt% of the respective monomer (adhesives 1, 10, 16, 19, 22, 24 and 28, see Table 6, chapter 5.5). The results showed **final conversions** in the range of 85 % for adhesives containing TMPTA, PETA and DPEPHA, while even higher conversions (> 95 %) were achieved by SR 454, SR 492, SR 494 and DTMPTA (see Table 11). As expected, the highly functional DPEPHA showed comparatively low conversion. In spite of its low degree of functionality, TMPTA exhibited low conversions. This was related to steric hindrance within the monomer structure, where every branch acted as a pendant group, which potentially blocked polymerization. On the contrary, high conversions were observed for the remaining tri-functional monomers (SR 454 and SR 492) since they comprised low functionality and long chained spacers, which offer increased segmental diffusion (see Figure 40d). Enhanced mobility by long spacers also allowed a nearly complete consumption of C=C double bonds in the SR 494 adhesive system. This PSA exhibited superior conversion to all tri-functional acrylates in spite of its higher degree of functionality. Figure 40e illustrates a comparison of all applied tetra-functional monomers. Similar to TMPTA, PETA was sterically hindered by its branches, leading to reduced conversion. This effect was less pronounced for DTMPTA and SR 494, where the acrylic groups were connected by longer chains. Concerning DTMPTA, the ethyl pendant groups seemed not to hinder the polymerization reaction markedly.

Against the expectations based on literature research [148], the lowest **rates of polymerization** were found for the penta/hexa-functional acrylate, while the tri-functional monomers SR 454 and SR 492 polymerized most rapidly (see Table 11). The impact of the spacer length was evaluated within the series of tri- and tetra-functional monomers. The reaction rates of the tri-functional monomers increased with the number of repeating units, whereas no clear trend was revealed for the tetra-functional acrylates. The lower reaction rate of DTMPTA may originate from steric hindrance by the ethyl groups, which were suggested to have more impact on the reaction rate than on conversion.

Furthermore, the evaluation of the **irradiation dose required for maximum conversion** indicated, that the rapid onset of polymerization of the tri-functional monomers (TMPTA, SR 454, SR 492) and PETA (see slopes in Table 11) was followed by prolonged crosslinking of these adhesives in the decelerated state of the reaction (near plateau).

-Results and discussion, Design of photo-curable PSA tapes-

Table 11: Summary of all data drawn from the reaction kinetics, including final monomer conversion, reaction rates (slope of the initial linear portion in the irradiation time-conversion curves) and the UV-irradiation dose required for the maximum monomer conversion.

type of multifunctional monomer and acrylic copolymer	weight ratio monomer + PI	reaction rate (slope = R_p/M_0) [s^{-1}]	conversion [%]	UV-dose for maximum conversion [mJ/cm^2]
acryl_1 DPEPHA	10 + 1	6.7	84	1041
acryl_1 DPEPHA	10 + 5	25.3	~100	309
acryl_1 DPEPHA	20 + 1	4.5	74	1292
acryl_1 DPEPHA	50 + 1	6.7	56	1547
acryl_1 DTMPA	10 + 1	9.4	95	1630
acryl_1 DTMPA	10 + 5	13.5	96	88
acryl_1 DTMPA	20 + 1	9.6	79	326
acryl_1 DTMPA	50 + 1	6.6	61	878
acryl_1 PETA	10 + 1	16.8	87	4736
acryl_1 SR 454	10 + 1	24.0	97	2876
acryl_1 SR 492	10 + 1	22.2	~100	3637
acryl_1 SR 494	10 + 1	16.4	~100	255
acryl_1 SR 494	10 + 5	86.6	~100	13
acryl_1 SR 494	20 + 1	29.1	93	4544
acryl_1 SR 494	50 + 1	27.8	85	7365
acryl_1 TMPTA	10 + 1	18.0	85	3039
acryl_5 DPEPHA	10 + 1	1.3	74	2475
acryl_6 DPEPHA	10 + 1	14.5	~100	4761

-Results and discussion, Design of photo-curable PSA tapes-

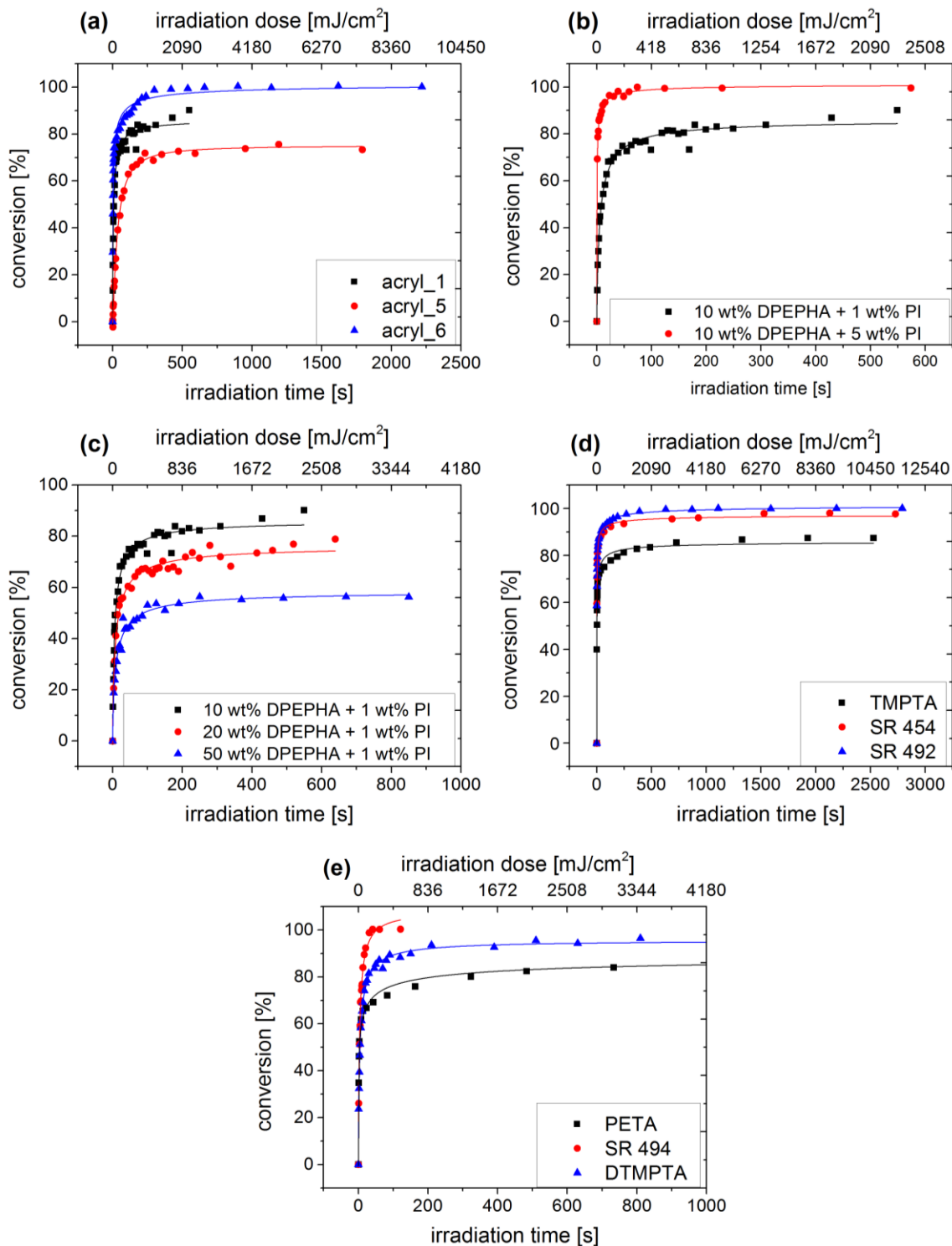


Figure 40: Conversion of C=C double bonds in adhesive layers based on (a) 10 wt% DPEPHA and 1 wt% Lucirin TPO-L as a function of the structure of the basic adhesive polymer, (b) acryl_1 containing as a function of the photoinitiator concentration at a constant DPEPHA concentration of 10 wt%, (c) acryl_1 as a function of the monomer concentration at a photoinitiator concentration of 1 wt%, (d) acryl_1 containing 10 wt% TMPTA, SR 454 or SR 492 and 1 wt% Lucirin TPO-L monitoring the impact of the monomer structure within the series of tri-functional acrylates, (e) acryl_1 containing 10 wt% PETA, SR 494 or DTMPTA and 1 wt% Lucirin TPO-L monitoring the impact of the monomer structure within the series of tetra-functional acrylates.

***T_g* of the UV-cured adhesives**

The photo-triggered release mechanism was characterized by DSC measurements. Upon UV-exposure, semi-IPN were generated by crosslinking of the multifunctional monomers in the adhesive formulation. This network formation was associated with a reduction of adhesion and an increase of cohesion, which were reflected by changes in the *T_g*. [21,22,24,25] Thus, selected adhesive formulations based on acryl_1 (see chapter 5.6) were crosslinked, applying the UV-doses for maximum conversion determined in the corresponding UV-cure kinetic experiments. The samples were heated from -60 °C to 100 °C and the *T_g* was determined from the respective cooling curves. The influence of the monomer structure and concentration as well as the PI content on the formation of the semi-IPN was investigated. Highly functional monomers (DPEPHA) were expected to achieve higher network densities and thus higher *T_g*s [23,65], due to the large number of reactive sites in the molecule. [148]. Long spacers, as present in SR 454, SR 492, SR 494, typically reduce the crosslinking density. [22,148] Based on the increased amounts of initiating radicals, which start more polymer chains simultaneously, high PI contents are associated with fast reactions and high conversion [100] as well as with high crosslinking densities. [158] Furthermore, it is stated in literature that the crosslinking density of hydrogels increases with the monomer concentration. [159]

As illustrated in Figure 41 at the example of a series of DPEPHA adhesives the baseline of the cooling curves continued to decrease after reaching the glass transition region. Hence, the determination of the distinct *T_g*s was not possible, but the onset temperature of the respective glass transitions (*T_{gON}*) was determined employing the tangent method as well as the second derivative of the heat flow curves. Both evaluation methods revealed similar *T_{gON}* of about 60 °C for all adhesive formulations, independent on the type and amount of multi-functional acrylate or the PI concentration. As illustrated in Figure_A 7a, adhesives comprising high levels of initiating radicals (5 wt% PI) exhibited *T_{gON}* values in the same range as formulations with low PI content (50 wt% monomer + 1 wt% PI). Furthermore, the monomer structure did not affect the onset of the glass transition (see Figure_A 7b). From the series of DPEPHA adhesives in Figure 41 it was derived that variations of the monomer concentration at a constant PI level (20 vs 50 wt% DPEPHA + 1 wt% Lucirin TPO-L) did not have a significant impact on *T_{gON}* of the PSA formulation.

However, DSC measurements proved a change of the *T_g* for all adhesive formulations upon UV-irradiation and thus the efficiency of the photo-release mechanism. While the initial tack of the PSA was governed by the linear structure of acryl_1 (*T_g* = -32°C), the semi-IPN dominated the adhesive properties after UV-crosslinking (*T_{gON}* = 60 °C). [22]

In further experiments, the impact of the UV-dose on network formation was displayed using adhesive 6 (20 wt% DPEPHA + 1 wt% PI). One sample was fully cured, according to UV-cure kinetics (irradiation dose of 1400 mJ/cm²), while another sample was only pre-crosslinked applying an UV-dose of 80 mJ/cm². Again, similar onsets of the glass transition were observed (~60 °C). These results indicated that the semi-IPN had already formed to a high extent after exposure to comparatively low irradiation doses. This conclusion was supported by the findings of UV-cure kinetics, which showed that more than 50 % of DPEPHA in adhesive 6 were consumed after applying ~ 80 mJ/cm² (see Figure 40c).

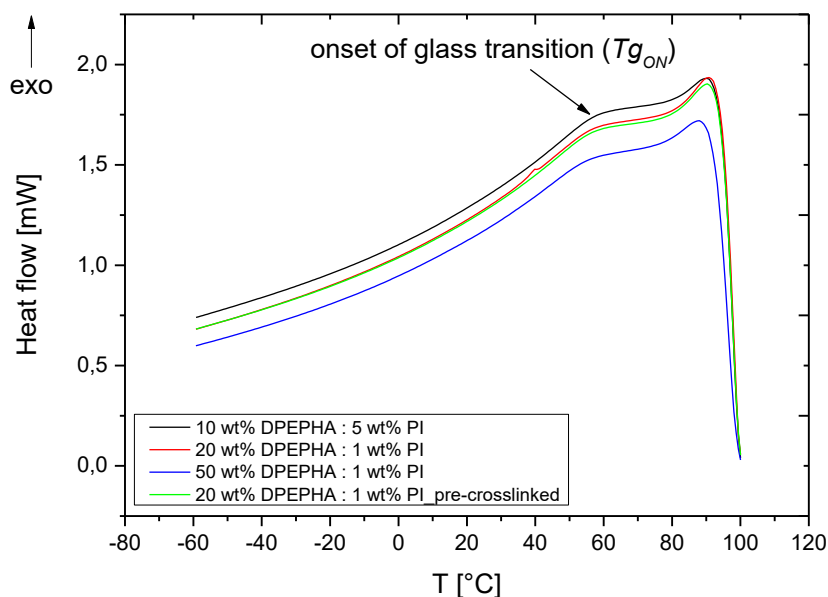


Figure 41: DSC measurements of DPEPHA adhesives (cooling curves)

Since the decline of the base line (Tg_{ON}) set in almost immediately after cooling had been started, adhesive 6 was investigated in an extended temperature range up to 300°C. Transient oscillation effects were excluded because the base line began to decrease at almost the same temperature as in previous experiments (see Figure 42). The slightly higher value of the sample heated to 300 °C ($Tg_{ON} = 76$ °C) originated from thermally induced crosslinking of the remaining C=C double bonds, which had not been consumed during UV-irradiation (conversion after UV = 74 %, see kinetic measurements). This additional crosslinking reaction was indicated by a significant peak in the range of 135-260 °C, which was only observed during the first heating cycle (see Figure 42b, black curve).

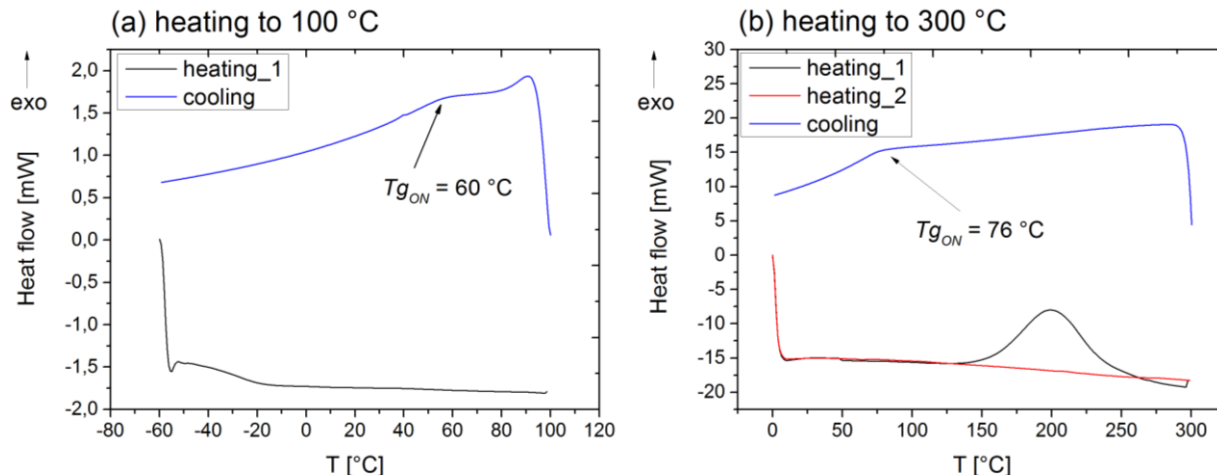


Figure 42: Heat flow of adhesive 6 (20 wt% DPEPHA + 1 wt% PI) heated to (a) 100 °C and (b) 300 °C

Thermal stability of the UV-cured adhesives

One of the most important issues in this work was to ensure high thermal stability of the PSA tape. The heat resistance of a PSA can be improved by the adjustment of the chemical composition of the basic copolymer (see chapter 6.1.1) on the one hand, and by network formation on the other hand. In the present work, semi-IPN, which are formed upon UV-crosslinking of multifunctional acrylic monomers, contributed to the UV-release mechanism as well as the thermal stability of the PSAs. [21–25,151] The improvement of the thermal stability of the PSA by network formation was explored by means of TGA measurements as a function of monomer structure and concentration as well as PI content. The use of highly functional monomers with short spacers and the application of low PI or high monomer concentrations, respectively, are usually associated with high crosslinking densities [22,100,148,159], which in turn improve the heat resistance of PSAs. [24] Selected adhesive formulations based on acryl_1 (see Table 12) were UV-crosslinked according to the findings in photo-cure kinetics and heated to 600 °C under nitrogen. The corresponding thermograms were used to determine the onset and end point of degradation T_{ON} and T_{END} as the intersections of the tangent with the horizontal lines before and after the degradation step (see Figure 43). [145] In addition, the point(s) of maximum degradation T_{MID} was derived from the peak(s) in the first derivative of the temperature-weight loss curve.

Similar degradation onset temperatures in the range of $T_{ON} = 370\text{-}378\text{ }^{\circ}\text{C}$ were determined for all adhesive formulations, independent of the type and concentration of the multifunctional acrylate and the PI content (see Table 12). The lowest value for T_{ON} was associated with increased PI concentrations (5 wt%) in all the investigated series (DPEPHA, DTMPTA and SR 494). Usually, high levels of PI provide a multitude of radicals, which initiate numerous growth centers. The resulting polymers exhibit broad molecular weight distributions and are comparatively soft. [100] As a consequence, these adhesives were more prone to thermal degradation than the high molecular weight polymers obtained with lower PI contents. Against the expectations based on literature research [100], T_{ON} was reduced by very high monomer contents (50 wt%). UV-cure kinetics of the respective adhesives revealed incomplete conversion of the multifunctional acrylates. It was suggested, that the remaining monomers degraded before network degradation started or that they may act as plasticizers and were thus responsible for the slight reduction of T_{ON} . On the contrary, T_{END} was increased because the high monomer concentrations supported the formation of highly crosslinked networks [159]. Additionally, the reduced amount of initiating radicals per 1 mol monomer (high monomer at constant PI concentration) favored the formation of high molecular weight polymers [100]. Though degradation started at similar temperatures for both, adhesives with high PI and high monomer concentrations, the higher network density and the increased molecular weight of PSAs containing 50 wt% of the respective monomer led to a retardation of the thermal degradation (higher T_{END}). [23]

Furthermore, the monomer structure influenced T_{END} . Adhesives based on DPEPHA, DTMPTA, PETA and TMPTA (short spacers) exhibited higher values for T_{END} than monomers comprising long spacers. The shoulders at $T = 430\text{-}485\text{ }^{\circ}\text{C}$ in the respective weight loss spectra indicated a two-step degradation, which shifted T_{END} to higher temperatures (see Figure 43a and Table 12). [160] This was even more clearly shown by the first derivative of the corresponding thermograms, which revealed two peaks $T_{MID,1}$ at $405\text{-}410\text{ }^{\circ}\text{C}$ and $T_{MID,2}$ at $460\text{-}465\text{ }^{\circ}\text{C}$ (see Figure 43b). On the contrary, adhesives based on SR 494, SR 454 and SR 492 (long spacers) degraded in a single step. Thus, complete decomposition was retarded by the use of short chained monomers (higher T_{END}), which were associated with higher crosslinking densities. [22,148].

The series of DPEPHA and DTMPTA adhesives revealed that the second degradation step became more important at high monomer concentrations. As shown in Figure 43c and Figure_A 8a, the shoulders in the weight loss curves increased distinctly for adhesives containing 50 wt% (adhesives 8 and 15; see Table 6, chapter 5.5). Thus, T_{END} was shifted to higher temperatures and $T_{MID,2}$ increased at the expense of $T_{MID,1}$ (see Figure 43d and Figure_A 8b). This was again related to high network densities and high molecular weights,

which were enhanced by the increased amount of crosslinkable material. [23,100,159] The impact of the monomer concentration was even observed for adhesives based on SR 494. As described above, these PSAs degraded in a single step at low monomer concentrations, but as the crosslinking density increased as a consequence of high monomer contents, a small shoulder developed in the weight loss curves and the corresponding first derivation (see Figure_A 8c and d).

The improvement of the thermal stability by the formation of semi-IPN is demonstrated in Figure 43e, by a comparison of the basic adhesive copolymer and a representative adhesive mixture (adhesive 6; 20 wt% DPEPHA + 1 wt% PI). Although T_{ON} of acryl_1 (370 °C) was similar to the respective values of the adhesive formulations (370-378 °C), an improvement of the thermal stability was obtained since T_{MID} and T_{END} were shifted to higher temperatures (see Figure 43e and Table 12). Thus, an extended temperature range was required for the complete decomposition of the cured PSAs, meaning that the formation of the semi-IPNs at least retarded full degradation of the adhesives. However, it is well known that the degradation in the early stages is important for the overall thermal stability. [145]

-Results and discussion, Design of photo-curable PSA tapes-

Table 12: Results of TGA measurements of the cured PSAs, including the onset (T_{ON}) and endpoint (T_{END}) of degradation as well as the point of maximum degradation rate (T_{MID})

type of multifunctional monomer	mixing ratio monomer + PI [wt%]	T_{ON} [°C]	T_{END}^* [°C]	$T_{MID,1}$ [°C]	$T_{MID,2}$ [°C]
DPEPHA	10 + 1	378	480	410	462
DPEPHA	10 + 5	370	481	405	460
DPEPHA	20 + 1	374	485	407	465
DPEPHA	50 + 1	372	485	406	466
DTMPTA	10 + 1	377	483	408	464
DTMPTA	10 + 5	371	473	406	450
DTMPTA	20 + 1	376	476	407	461
DTMPTA	50 + 1	372	483	407	465
SR 494	10 + 1	377	438	410	
SR 494	10 + 5	370	433	408	
SR 494	20 + 1	376	438	408	
SR 494	50 + 1	374	444	407	
PETA	10 + 1	373	480	408	460
SR 454	10 + 1	377	434	409	
SR 492	10 + 1	375	432	407	
TMPTA	10 + 1	377	479	408	460

*In case of DPEPHA, DTMPTA, PETA and TMPTA, T_{END} was determined as the intersection of the tangent at the slope of the shoulder in the weight loss curve with the horizontal lines after the degradation step (see Figure 43f).

-Results and discussion, Design of photo-curable PSA tapes-

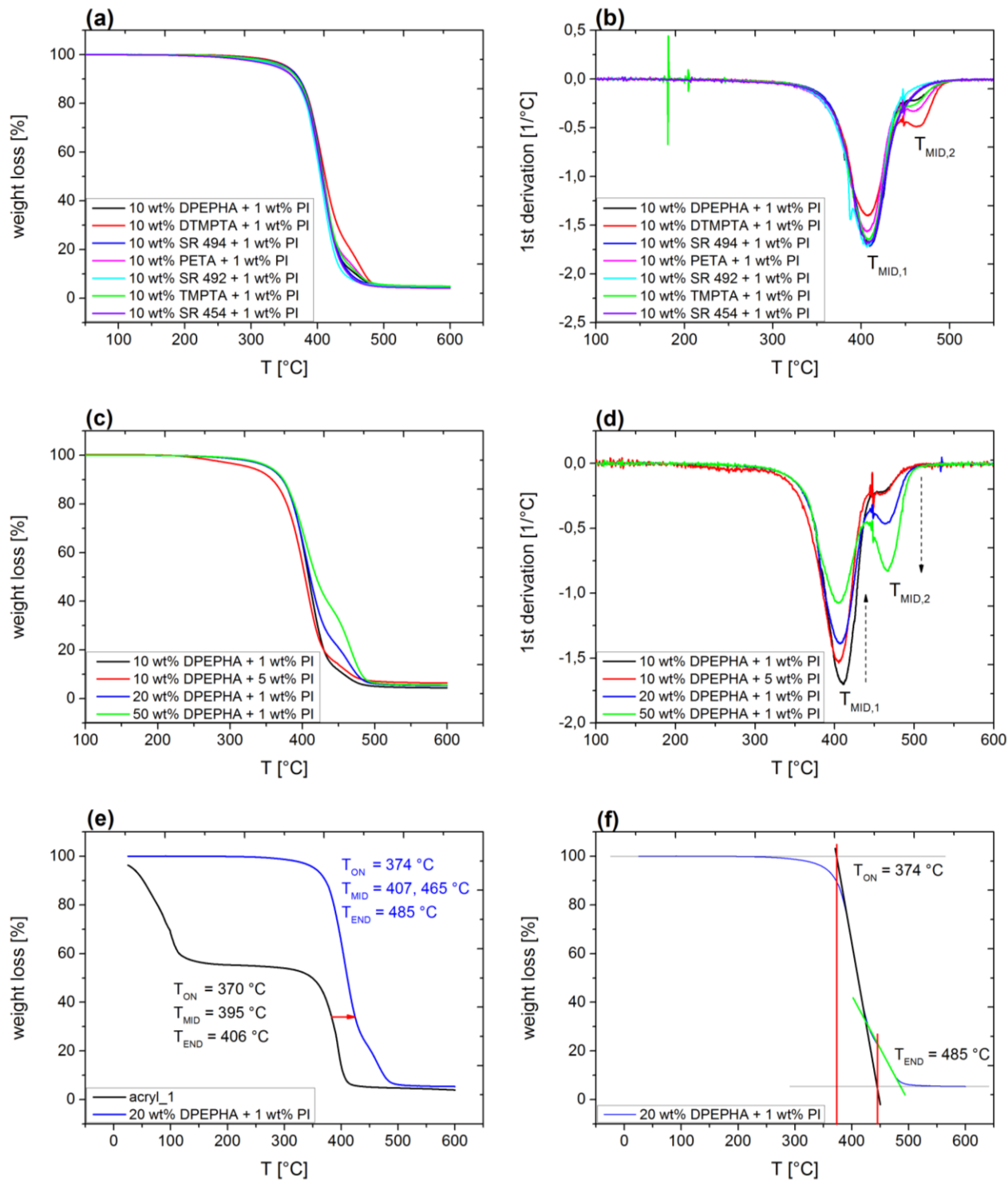


Figure 43: (a) Thermograms of adhesive formulations as a function of the monomer structure. (b) First derivatives of the temperature-weight-loss curves of adhesive formulations containing 10 wt% of different multifunctional monomers. (c) Thermograms of DPEPHA adhesives as a function of monomer and PI content. (d) First derivatives of the temperature-weight-loss curves of the DPEPHA adhesives. (e) Comparison of the thermograms of acryl_1 and adhesive 6 (20 wt% DPEPHA, 1 wt% Lucirin TPO-L) to demonstrate the improved thermal stability of the cured adhesive formulations. (f) Determination of the degradation onset and end point as the intersections of the tangents and the horizontal lines before and after the degradation steps

Adhesion strength of the PSA tapes

The efficiency of the photo-triggered release was characterized by means of peel strength tests prior to and after UV-irradiation. However, these tests were only performed for the most promising PSA formulation and are thus discussed in chapter 6.1.3.

6.2.2. Basic steps of tape preparation

PSA tapes, in their simplest form, are mono-webs, consisting of a flexible carrier, which is coated with an adhesive layer. Further varieties may involve the application of adhesion promoters or release coatings between the adhesive and the backing material, and a release liner, which protects the PSA film. [6,7,9] Still, coating is the common procedure in the manufacturing of classical pressure sensitive products (PSPs). The coating method depends on the physical state of the adhesive, the carrier material and the end use of the produced PSP. Typical techniques are roll-coating, slot-die coating, extrusion, calendaring as well as blade, cast and spray-coating. [6,9] The adhesive is either directly coated onto the carrier or it is applied onto a release liner and subsequently transferred to the face stock material. [6,12] In this work, the adhesive formulations, consisting of a basic adhesive copolymer, multifunctional monomers and a PI, were prepared as solutions in 2-butanone to facilitate handling and film formation. A quadrupole film applicator (doctor blade/knife) was used for **coating** since this constitutes a simple and rapid method for film formation. Moreover, it offers an easy change of the PSA and the layer thickness. While adhesives are usually coated as liquids, the corresponding PSPs are applied in the solid state. [6] The solvent has to be removed completely from the adhesive layer [9], in order to provide good release properties of the PSP. [20] This was demonstrated at the example of tapes based on acryl_1, 10 wt% of DTMPTA and 10 wt% Lucirin TPO-L, which were adhered to pristine copper. The samples were irradiated on the bottom half and peeled off manually. A comparison of the irradiated and the covered parts of the substrates (see Figure 44a) shows that adhesive residues were reduced due to adequate drying of the adhesive layer before application. In addition, the presence of the solvent seemed to inhibit the UV-crosslinking reaction of the multifunctional acrylates since the non-dried adhesive layer remained tacky after irradiation. A possible explanation for the impaired photo-reactivity of the non-dried adhesive layers may be the photolysis of 2-butanone, resulting in methyl and propionyl radicals [161], which may react with the activated multifunctional acrylates and hence terminate the crosslinking reaction. In a small series of experiments, the **drying** conditions were optimized to 30 minutes at 50 °C. As a result, the removability

of the tape was improved significantly (less adhesive residues; see Figure 44b) and the UV-release was no longer compromised.

Another important factor in the production of PSA tapes is the **carrier material** and its **pre-treatment**. Besides paper, cloth and metal foils, polymer films are used as backing material. These include PP, HDPE, LDPE, PET, PC and PVC as well as polystyrene, cellulose acetate and cellophane. [1,9,114] In order to achieve good coating, the carrier is usually pre-treated by physical or chemical methods, including flame or laser treatment, UV-radiation, corona discharge, plasma treatment or chemical etching. The chemical and morphological modification of the carrier (oxidation, crosslinking, chain scission, ablation, roughening) increases its surface polarity and thus allows for improved wetting and coupling of the adhesive. [9] Here, PET was selected from the wide range of suitable carrier materials, since it constitutes a well-established material for the preparation of PSA tapes in both, science [22,24,151] and industry [162–164]. An untreated and a chemically etched PET foil were investigated with regard to their wetting properties and their influence on tape removability. Tapes based on adhesive 25 (acryl_1, 10 wt% SR 494 and 5 wt% Lucirin TPO-L) were prepared and applied onto pristine copper substrates at rt. After UV-irradiation they were peeled off manually. Superior wetting and leveling of the adhesive formulation was observed on the etched carrier. This was related to the increased roughness, originating from chemical etching, which allowed for enhanced adhesive penetration and good anchorage of the PSA. [20,62] As a result, the amount of adhesive residues on the substrate was significantly reduced by the use of the etched PET carrier. This is clearly shown by the microscopy images in Figure 44c and d.

Since photo-curing was done through the backside of the carrier (applied tape), UV-transparency of the PET foils was required to ensure an efficient release. The absorption spectra of the carriers were investigated in the range of 200-800 nm by UV-VIS spectroscopy. Figure_A 9 shows that both carriers were transparent to UV-VIS and thus did not interfere with the activation of the PI (Lucirin TPO-L) at wavelengths of 350-420 nm. Based on the comparable UV-transparency and its superior wetting properties, the etched PET foil was used as carrier material exclusively.

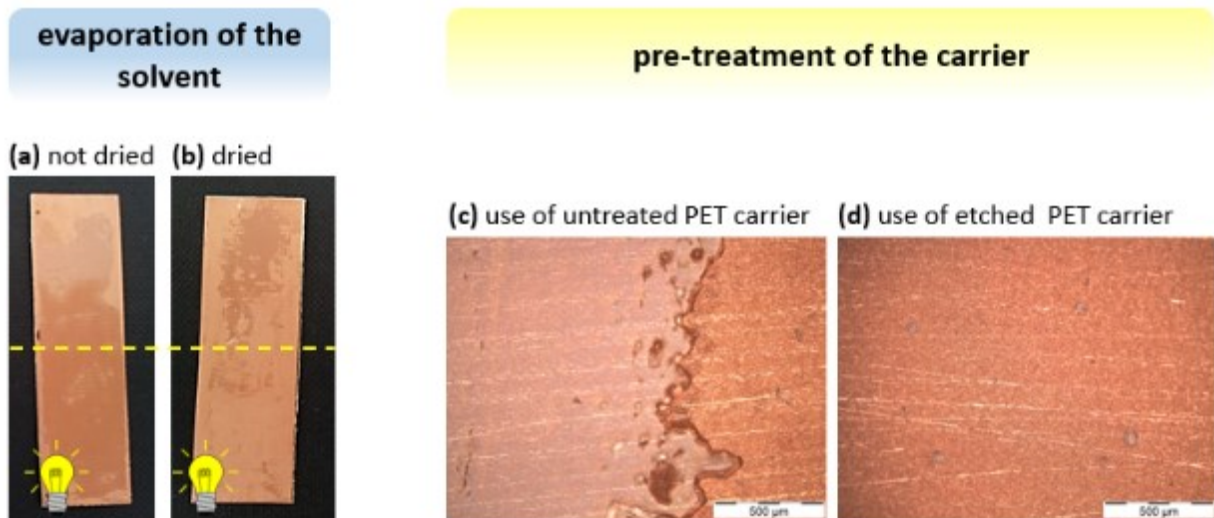


Figure 44: Left: Improvement of the removability and the UV-release mechanism by evaporation of the solvent. (a) Substrate after removal of tape prepared without drying step. (b) Substrate after removal of tape with dried adhesive layer. Right: Improvement of the removability by the use of chemically etched PET carrier. (c) Substrate after removal of tape prepared on non-treated PET (released part). (d) Substrate after removal of tape prepared on chemically etched PET (released part).

In addition to chemical etching, **corona treatment** was applied to further improve the interactions of the carrier with the PSA. Corona discharge is stated the most common method for surface treatment of carrier materials. [9] The PET surfaces are oxidized in a free radical mechanism, forming functional groups such as C-OH, C=O, COOH, C-O-C, epoxy, ester and hydroperoxide. [66–68] In addition, the surface is roughened by ablation. [9,68] Thus, the polarity and roughness of the carrier is increased and good wetting and coupling of the adhesive layer is provided. [20,62] The efficiency of the surface activation was proven by X-ray photoelectron spectroscopy (XPS), which revealed an increased oxygen content on the carrier surface after corona treatment with 1528 W min/m^2 (see Table 13). Moreover, corona treated carriers showed decreased contact angles with water and thus improved wetting by polar liquids as required for coating with the adhesive formulations. According to equation (1) the corona dose depends on the applied power output, the treatment speed v and the width of the table b . The optimum corona dose was determined by variation of the power output at fixed v and b (1.8 m/min, 0.4 m). As shown in Table 14, the water contact angle was reduced significantly by the application of a corona dose of 1528 W min/m^2 , while additional treatment only led to minor decrease. Thus, a dose of 1528 W min/m^2 was chosen as a standard for the treatment of the applied PET carriers.

-Results and discussion, Design of photo-curable PSA tapes-

Table 13: Surface composition of untreated and corona treated PET carriers determined by XPS measurements.

	surface composition [at%]		
	C	O	Si #
untreated PET	48.2	37.1	14.7
corona treated PET	45.5	40.8	13.8

#silicon signal due to silica particles in PET (non-migratory additive for better handling) [165,166]

Table 14: Water contact angles of the PET carriers as a function of the applied corona dose and corresponding power out.

power output [W]	corona dose [W min/m ²] *	water contact angle [°]
0	0	58.6 ± 2.8
1100	1528	27.2 ± 5.9
3300	4583	18.8 ± 1.9

*calculated by equation (1), see chapter 5.2.

Beside the chemical composition of the adhesive layer (PI content, structure, concentration and functionality of the crosslinking monomers), the degree of crosslinking and the T_g have a distinctive influence on the tack of PSA tapes. Therefore, the adhesion performance of the photo-curable PSA tapes can be controlled by the applied UV-irradiation dose. [22] In order to fulfill the requirements of high initial tack and clean removability, the applied tapes were crosslinked via UV-irradiation in the end of the application. Initially, high tack was ensured by low molecular weights of the non-crosslinked adhesive formulation, while easy and clean peel was achieved by photo-crosslinking of the multifunctional monomers. The formation of semi-IPNs was related to increased molecular weights and consequently, to increased cohesion and reduced adhesion. [9,21,22,24–26] In the uncured state, the low molecular weight components allow for deep penetration into the microstructure of the substrate (see Figure 45a, I). This provides good adhesion via mechanical interlocking [20]. During UV-irradiation, the PSA is crosslinked and molecular mobility becomes limited. As a consequence, the cured adhesive cannot deform sufficiently to escape from the morphological cavities during peel. Finally, shearing over the sharp edges of the microstructure of the substrate leads to adhesive residues (see Figure 45a, II). To prevent this, the adhesive layer was **pre-crosslinked** before tape application. The precise balance of adhesion and cohesion by adjustment of UV-irradiation dose (see chapter 6.3.3), allowed for sufficiently high initial tack and a certain extent of crosslinking [22,26], which limited the access to deep sites in the surface morphology of the substrates (see Figure 45b, I). In addition, the reduced contact area between the substrate and the PSA supported clean removability. [20,21] This enabled applications even on substrates with high surface area such as BondFilm® treated copper (see chapter 6.3.1, Figure 49a).

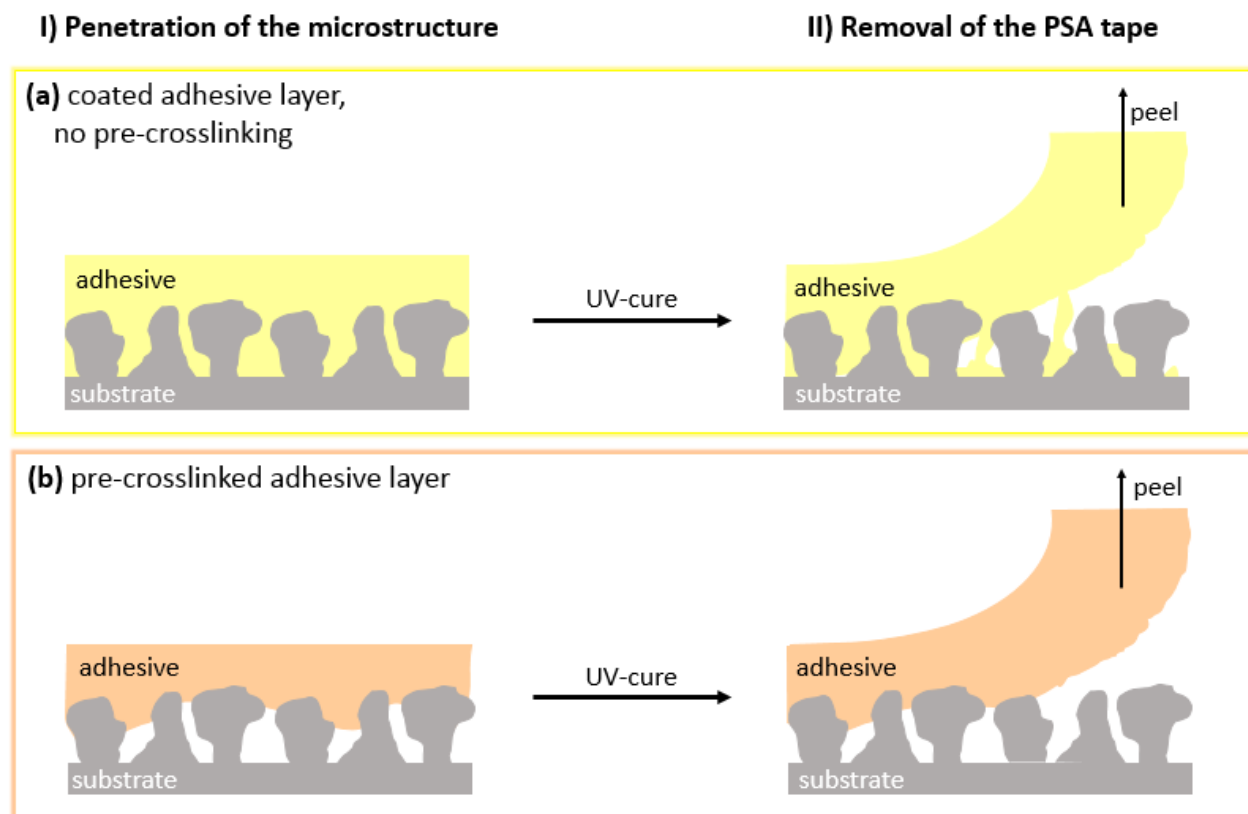


Figure 45: Differences in the extent of adhesive penetration of the substrate microstructure by (a) the uncured and (b) the pre-crosslinked PSA tape and the consequences during peel.

According to literature, the adhesive layer can be applied either by direct coating of the carrier or by coating of a release liner and subsequent transfer to the carrier. [6,12] Consequently, **two preparation methods** were developed.

Method I. The adhesive formulation was coated directly onto the carrier (see Figure 46, step I). The prepared PSA layer was dried at 50 °C for at least 30 minutes and pre-crosslinked with 80 mJ/cm² under nitrogen to prevent oxygen inhibition of the UV-induced network formation. [100,152]

Method II. The adhesive was coated onto siliconized release liners (see Figure 46, step I). The prepared PSA layer was dried and subsequently transferred to the carrier via lamination on a hot base (175-150 °C, see Figure 46, step II). The transfer of the adhesive layer was based on preferred wetting of the etched carrier surface and easy separation from the siliconized liner. In addition, the high temperatures of the base decreased the viscosity of the PSA. This supported the adhesive penetration into the microstructure of

the carrier and consequently, the adhesion to the same [20,60]. Pre-crosslinking was done through the backside of the carrier, usually applying a UV-dose of 80 mJ/cm². Oxygen inhibition was prevented by the liner, which still covered the adhesive layer and thus limited the access of O₂.

The basic steps of both methods are summarized as workflow charts in Figure 47. Due to its superior wetting properties and its enhanced anchorage of the adhesive, the etched PET carrier was used exclusively. Optionally, the carrier was corona treated. While the wet film thickness was varied from 30 to 120 μm in *method I*, this parameter was fixed to 90 μm in *method II*.

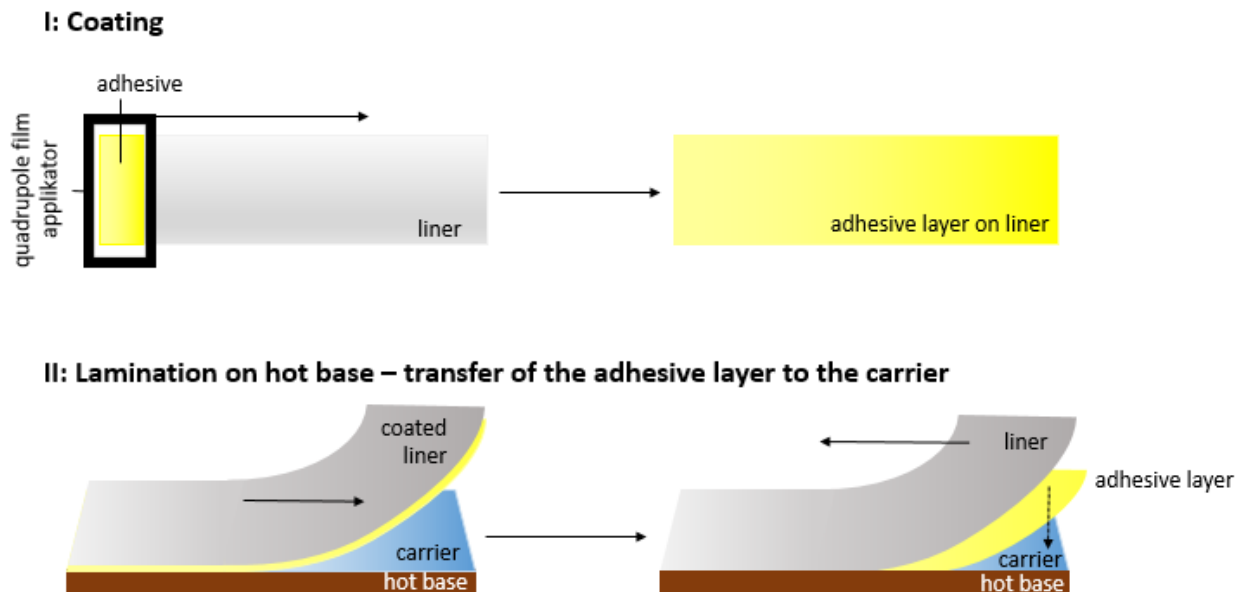


Figure 46: Preparation of PSA tapes. Step I: coating of the adhesive onto the carrier (method I) or onto the liner (method II), Step II: transfer of the adhesive layer via lamination on a hot base

6.2.3. Conclusion about the impact of the chemical composition and summary of the basic steps in PSA development

The basic adhesive system was selected by screening experiments. Blends of acryl_1 with multifunctional acrylates and Lucirin TPO-L provided photo-curable PSAs, which reduced their adhesive strength on demand due to formation of semi-IPNs. The related increase of cohesion enabled easy peel and clean removability.

It is well known, that the adhesion performance is strongly dependent on the chemical composition of a PSA. [22] The influence of the basic copolymer, the type of multifunctional acrylate as well as the monomer and PI concentration on the photo-triggered release was investigated by **FT-IR-spectroscopy**. Kinetic measurements revealed high final conversions and reaction rates for PSAs based on acryl_6 (reduced interactions within the bulk) and systems with increased levels of PI (5 wt%). Moreover, it was found that the final conversion was reduced by bulky groups in the copolymer (IBA in acryl_5) and high monomer contents (50 wt%). Concerning the chemical structure of the monomer, high conversions were associated with low functional long chained monomers, which comprised low steric hindrance (SR 454, SR 492, SR 494). In contrast, no clear trend was found for the influence on the reaction rate. The irradiation dose for maximum conversion decreased upon a high level of initiating radicals as present in systems with 5 wt% PI and low monomer contents. **DSC** experiments displayed an increase of the T_g of the adhesives upon UV-exposure. While the initial tack of the PSA was governed by the linear structure of acryl_1 ($T_g = -32^\circ\text{C}$ for acryl_1), the semi-IPN dominated the adhesive properties after UV-crosslinking ($T_{gON} = 60^\circ\text{C}$). The impact of the chemical composition of the individual adhesive formulations could not be investigated in detail, since the continuously decreasing baseline did not allow for the determination of the distinct T_g s. In addition, it was shown that the semi-IPN had already been formed to a high extent after exposure to comparatively low irradiation doses (80 mJ/cm^2). According to **TGA** measurements, the formation of semi-IPN slightly improved the thermal stability of the PSAs. The cured adhesives comprised similar T_{ON} and increased T_{END} , compared to the basic copolymer (acryl_1). Hence, complete decomposition was retarded by the formation of semi-IPN. It was observed, that T_{ON} was rather independent on the chemical composition, while T_{END} shifted to higher temperatures for highly crosslinked systems (high monomer contents, short spacers).

The adhesive formulation, the **carrier material and treatment** as well as the **process parameter** play an important role. It was shown that chemically etched PET carriers provided superior wetting and leveling of the adhesive. The etched surface allowed for good anchorage of the adhesive layer and consequently improved removability.

In addition, corona treatment further improved these properties. The adhesive layers were coated onto the carriers with a quadrupole film applicator since it represents a common, simple and rapid method. The subsequent evaporation of the solvent turned out to be essential for clean removability and an efficient UV-release. In order to prevent excessive penetration of the substrate, which is often related to cohesive failure, the PSA layers were pre-crosslinked. The corresponding UV-irradiation dose has to be adjusted individually, depending on the chemical composition and film thickness of the adhesive layers, to ensure sufficient initial tack. Finally, two preparation methods were developed (see Figure 47). While the adhesive is directly coated onto the carrier in *method I*, it is applied to a release liner and subsequently transferred to the carrier in *method II*.

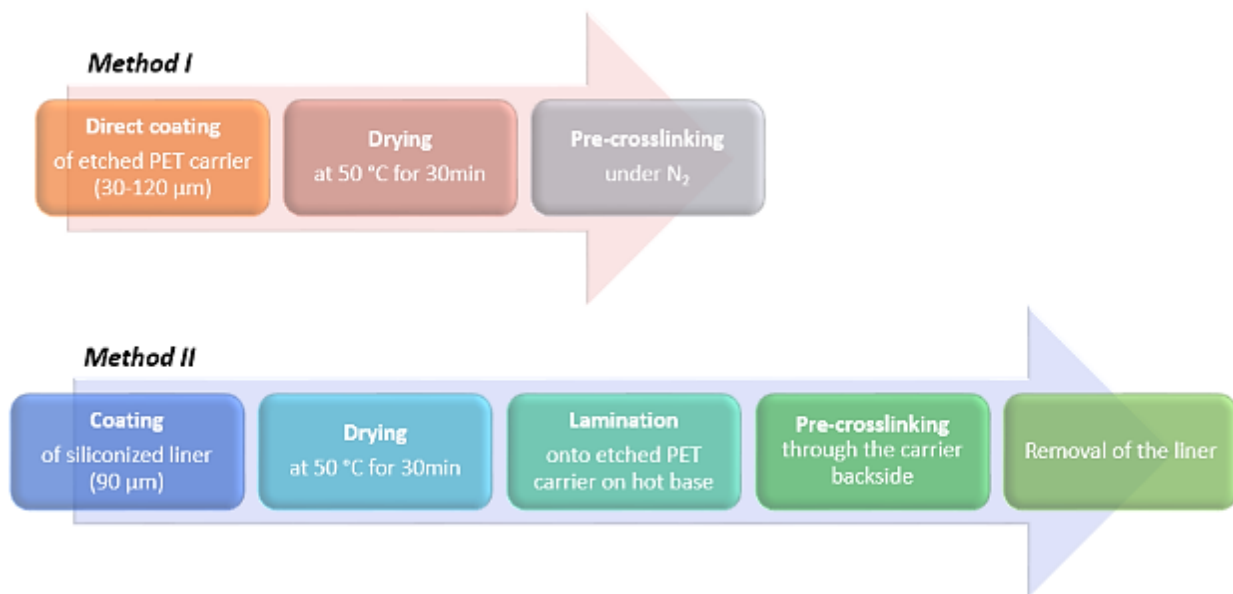


Figure 47: Workflow of the two tape preparation methods

6.3. Performance of the designed PSA tapes

In this chapter, factors, which affect adhesive performance and tape removability, are discussed. The effect of the chemical composition of the PSAs and the influence of various process parameters were investigated at the example of tapes prepared by *method I*. In order to provide good comparability, as few parameters as possible were altered within one experiment. Moreover, the impact of the surface quality of the substrates and the preparation method are displayed. The removability of the PSA tapes was evaluated using optical light microscopy. Clean peel was assigned with "✓", some or thin layers of residues with "∼" and many residues with "✗".

6.3.1. Impact of the surface quality of the joint substrate

In this work, removable PSA tapes for the embedding process of microelectronic chips and components into printed circuit boards (PCBs) were designed. During embedding, the tapes are applied temporarily onto metal and polymer surfaces, such as BondFilm® treated copper and cured epoxy prepregs, which are typically used for the production of PCBs. Thus, adhesion to and removability from these substrates as well as the performance on tarnish protected copper and pristine were investigated.

It is stated in literature, that the surface quality of the substrate constitutes an important factor influencing bonding and debonding because the polarity (surface energy) and porosity (roughness) of the adhered surface govern its wettability. Good wetting is a basic requirement for adhesion, which is achieved if the PSA comprises similar or lower surface tension than the substrate. After wetting, the adhesive penetrates the microstructural cavities (pores, capillaries and undercuts) of the surface, where it physically and chemically interacts with the substrate. Therefore, the development of an adhesive joint depends on the surface roughness and chemical composition of the substrate, the cold flow and viscosity of the adhesive as well as on application time and temperature. [1,20,21,60,62] Clean removability of the PSA tape requires (a) adequate cohesion to prevent fracture of the adhesive layer and (b) good anchorage of the PSA to the carrier. [20,62] Adhesion to the carrier must exceed the interactions with the substrate and can be enhanced by carrier pre-treatment, including corona discharge and priming. In addition, the reduction of the PSA-substrate contact area also supports residue-free peel. [9,20,21]

Since the **chemical composition** and the roughness of the adherent are important for the interpretation and understanding of the adhesion performance of the tape, these aspects are discussed for the applied substrates hereinafter. As described in chapter 3.5.2,

multilayer PCBs are composites of copper foil and epoxy prepregs, which are arranged in alternating layers on both sides of an inner core material. [167] Typically, the copper foils are pretreated to ensure reliable adhesion to the epoxy layers. While etching technologies and the black oxide treatment rely on mechanical adhesion only, oxide replacement technologies additionally offer a certain extent of chemical adhesion. [107,108] Here, **BondFilm® treated copper** substrates were applied. In this oxygen replacement technique the copper surface is roughened with an etchant of H_2SO_4 and peroxide to enable good mechanical interlocking with cured epoxy prepregs, which is seen as the main adhesion mechanism in PCBs. In addition, an organometallic layer containing benzotriazole derivatives provides some extent of chemical adhesion. The coupling effect of the azole compounds is based on covalent bonds to copper (benzodiazolato Cu(I) or bis(benzotriazolato) Cu(II)) and its participation in the ring opening polymerization of the epoxy resin. [107–110] The chemical composition of the BondFilm® treated copper surfaces was analyzed by XPS measurements, revealing high concentrations of carbon (60.2 at%), oxygen (15.1 at%) and nitrogen (16.2 at%), which was attributed to the organometallic layer (benzotriazole derivative), as well as copper (6.3 at%, underlying material) and some amounts of sulfur (1.1 at%) silicon (0.6 at%) and chlorine (0.6 at%), which originate from the etching and pretreatment process (see Table 16).

During PCB processing the single layers are patterned by etching of the laminated copper sheets, revealing the underlying **epoxy** material (FR 4, prepreg). Thus, the tapes performance was also tested on cured epoxy surfaces. Prepregs are glass fiber webs, which are impregnated with epoxy resin and pre-cured to B-stage. [167,168] According to XPS measurements, the chemical composition of the epoxy surfaces was dominated by C (63.6 at%) and O (29.4 at%). In addition, lower amounts of Si (4.3 at%), Cl (0.7 at%) and Br (0.9 at%) were detected. While Si originated from the incorporated glass fibers, the Cl and Br signals were attributed to halogenated flame retardant compounds. [169–171] Furthermore, some amounts of Cr and S were found. Adhesion experiments considering prepreg substrates were performed on structured PCBs, comprising both BondFilm® and epoxy surfaces.

Moreover, **tarnish protected and pristine copper** were applied as substrate materials in adhesion experiments. Due to their high reactivity, copper or copper alloy substrates are usually protected from tarnishing and oxidation during storage by chromium-zinc coatings, which are deposited electrolytically from alkaline solutions (NaOH, pH = 12-14). This is important because tarnished and oxidized surfaces may cause problems in the manufacture of PCBs, such as insufficient bond strength to epoxy prepregs during lamination or inhomogeneous etching of the copper foil. The surface composition of the tarnish protected copper substrates was investigated via XPS measurements. The results

were in good accordance with literature, showing high contents of Zn (20.7 at%) and O (44.6 at%) as well as C (31.3 at%), Cr (2.5 at%) and Cu (1.1 at%) on the substrate surfaces (see Table 16). [172,173] Pristine copper was revealed by rinsing tarnish protected substrates in an aqueous solution of sulfuric acid (H_2SO_4) and sodium persulfate (NaPS) for 40 sec at 35 °C. The absence of Zn and Cr as well as the high content of Cu on the deprotected substrates indicated the removal of the anti-tarnish coating (see Table 16). Metallic copper is stated to readily stain and tarnish during rt storage or high temperature processing. [172,173] Thus, it was important to apply these substrates right after rinsing and avoid long storage before applying the PSA tapes.

The **topography** of the substrates was investigated by means of atomic force microscopy (AFM). To quantify surface roughness, Sa (average roughness) and Sq (root mean square roughness) were determined from an average of 3 spots. The results are summarized in Table 15. Although BondFilm® treatment includes a roughening process, the respective substrates exhibited the lowest roughness of all investigated surfaces, while the highest Sa and Sq values belonged to cured epoxy. However, a comparison of the 3D-images in Figure 48 revealed fine superordinate structures on BondFilm® treated copper, which significantly enlarge the surface area. In contrast, the epoxy surfaces did not show any additional structures. Tarnish protected and pristine copper showed slightly higher Sa and Sq than BondFilm® substrates. Tarnish protected surfaces also carried some superordinate structures, which were removed in the deprotection process, revealing pristine copper. Nevertheless, this did not lead to significant changes of the surface roughness.

Table 15: Average roughness and root mean square roughness (Sq) of tarnish protected copper, pristine copper, BondFilm® treated copper and cured epoxy substrates

	Sa [nm]	Sq [nm]
tarnish protected copper	154 ± 26	193 ± 31
pristine copper	148 ± 10	189 ± 15
BondFilm® treated copper	88 ± 5	112 ± 6
cured epoxy	554 ± 92	684 ± 109

In addition, the different substrates were characterized by contact angle measurements with water. The water contact angle was reduced significantly from $72.9^\circ \pm 8.8^\circ$ to $21.2^\circ \pm 1.4^\circ$ after removing the tarnish protecting layer from the copper substrates. Since tarnish protected and pristine copper showed similar surface roughness (see Table 15), this was attributed to a change in surface composition and polarity as well as to the presence of the superordinate structures on tarnish protected copper. Moreover, the distinct increase of the water contact angle by BondFilm® treatment ($132.6^\circ \pm 1.3^\circ$) was seen as a result of the high amount of superordinate structures on the surfaces of the substrates and the applied adhesion promoting layer (benzotriazoles). In addition, the cured epoxy showed rather high hydrophobicity (water contact angle = $107.5^\circ \pm 4.5^\circ$), which was again attributed to the chemical composition of this surface.

To sum up, BondFilm® treated copper was seen as the most challenging substrate for the desired application. Although its adhesion promoting layer and its high surface area were necessary for substrate fixation during PCB processing, these factors were expected to be detrimental for clean peel in the end of the application of the tape. In contrast, the cured epoxy surfaces did not exhibit superordinate structures (lower surface area) and were therefore supposed to allow for residue-free removability. Concerning tarnish protected copper and pristine copper, some impairment of clean peel was suggested. While tarnish protected copper carried some superordinate structures, which enhance mechanical interlocking, the metallic copper surfaces were more prone to interactions with the polar acrylic acid units of the PSA. [56,174,175]

-Results and discussion, Performance of the designed PSA tapes-

Table 16: Chemical composition of tarnish protected copper, pristine copper, BondFilm® treated copper and cured epoxy surfaces

	chemical composition [at%]									
	Zn	Cu	C	O	Cr	Si	S	N	Cl	Br
tarnish protected copper	20.7 ± 1.4	1.1 ± 0.1	31.3 ± 1.0	44.6 ± 0.4	2.5 ± 0.15	-	-	-	-	-
pristine copper	-	37.7 ± 0.6	30.1 ± 0.2	32.2 ± 0.4	-	-	-	-	-	-
BondFilm® treated copper	-	6.3 ± 0.1	60.2 ± 0.7	15.1 ± 0.3	-	0.6 ± 0.2	1.1 ± 0.2	16.2 ± 0.3	0.6 ± 0.1	-
cured epoxy	-	-	65.3 ± 1.7	28.1 ± 1.4	≤ 0.5	4.3 ± 0.05	≤ 0.6	≤ 0.9	0.6 ± 0.1	0.9 ± 0.05

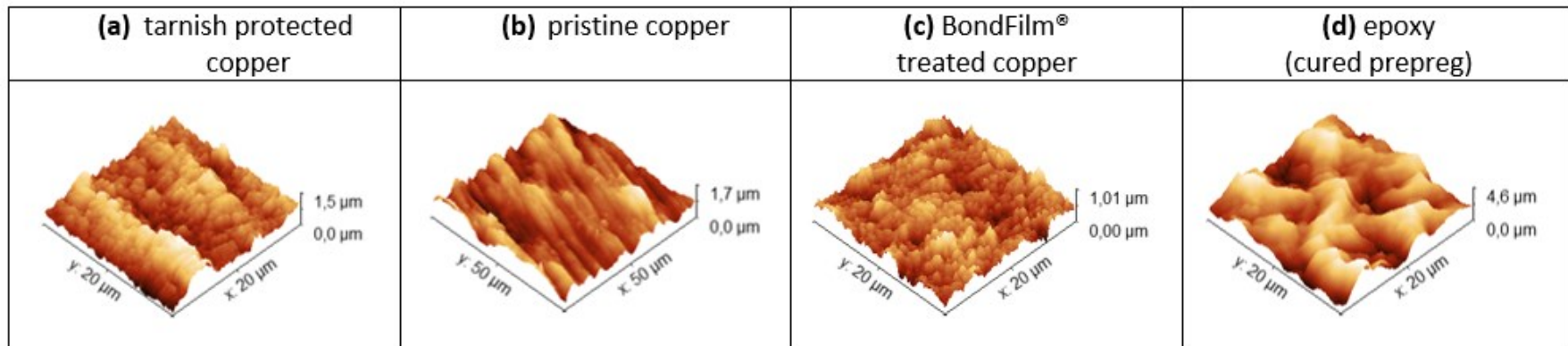


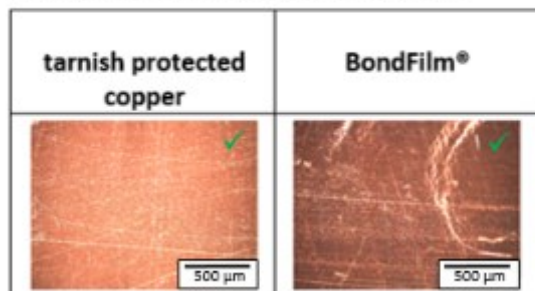
Figure 48: 3D images of tarnish protected copper, pristine copper, BondFilm® treated copper and cured epoxy, displaying the roughness of the substrates

Due to the importance of BondFilm® or structured BondFilm® surfaces in the present application, most adhesion experiments were done on these substrates in order to adapt the performance of the tape to the challenging requirements during application and peel.

The impact of the surface quality of the substrates was demonstrated by adhesion experiments on BondFilm® and tarnish protected copper. *Method I* tapes based on formulations containing acryl_1, 10 wt% SR 494 and 5 wt% Lucirin TPO-L were applied at rt and removed manually after UV-curing (7750 mJ/cm²). As already mentioned in chapter 6.2.2, the application on and clean removability from surfaces comprising high surface area such as BondFilm® substrates was realized by the introduction of a pre-crosslinking step. The PSA layer was crosslinked to a certain extent in order to prevent penetration into deep sites of the microstructure and residues, which may result from insufficient deformability during peel.

The results showed clean peel of pre-crosslinked PSA tapes from both, tarnish protected copper and BondFilm® substrates (see Figure 49a). Further experiments revealed that residue-free peel from tarnish protected copper did not necessarily require pre-crosslinking, whereas similar performance on BondFilm® substrates was exclusively achieved by application of this additional step (Figure 49b). This was attributed to the high surface area and the organometallic layer on BondFilm® treated copper, which promote adhesion but prevent clean peel.

(a) performance of pre-crosslinked PSAs on substrates with different surface quality



(b) necessity of pre-crosslinking on BondFilm® substrates

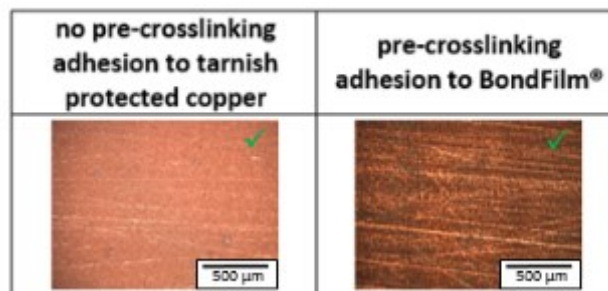


Figure 49: Effect of pre-crosslinking on the removability of the tapes in dependence of the surface quality of the substrates

Since the adhesion performance is influenced by the crosslinking state of the adhesive layer, it is also important to consider the impact of the preparation method. As a consequence of the different irradiation procedures of *method I* and *method II*, different crosslinking gradients develop throughout the adhesive layer surfaces. This aspect is discussed in detail in chapter 6.3.4.

6.3.2. Influence of the adhesive composition

Adhesion performance and removability of PSA tapes depend on the proper balance of adhesion and cohesion [10,20], which in turn are a function of T_g , crosslinking density and molecular weight [27,34,174]. It was already proven by UV-cure kinetics, that network formation was greatly affected by the chemical composition of the adhesive layer (see chapter 6.2.1). Thus, the impact of the basic adhesive copolymer, the amount and type of multifunctional acrylate as well as the PI-content on *adhesion performance*, including tack, peel and removability, is evaluated in the following.

In advance of these experiments, it has to be mentioned, that UV-irradiation doses, which were applied to trigger the release mechanism of the tapes, do not necessarily correlate with the irradiation dose for maximum conversion determined in UV-cure kinetics. This difference arises from different thicknesses of the adhesive layers prepared for kinetic measurements (spin casting) and for adhesion experiments (quadruple film applicator). Furthermore, it has to be considered that not only the overall UV-dose, but also the applied intensity influences the conversion of UV-curable adhesive systems [175]. As a consequence, the use of different UV-curing systems for kinetic measurements and tape irradiation during adhesion experiments did not allow for a direct resumption of the UV-doses determined in kinetic measurements. Thus, the irradiation doses, were adjusted empirically to the individual adhesive composition to ensure proper adhesion performance.

Effect of the chemical composition of the basic adhesive copolymer

Three different basic adhesive polymers - acryl_1, acryl_5 and acryl_6 - were applied in the production of PSA tapes containing 10 or 20 wt% DPEPHA or DTMPTA and 1 wt% Lucirin TPO-L (adhesives 1, 6, 10, 14 and 23-37). The tapes were prepared according to *method I* without further treatment of the etched PET carriers. The applied wet film thicknesses amounted to 90 μm . In order to investigate the impact of the polymer composition on adhesion performance and removability, the tapes were applied onto BondFilm® treated copper substrates. While DPEPHA based tapes were irradiated with 1000 mJ/cm^2 , a UV-dose of 7750 mJ/cm^2 was applied to cure the DTMPTA tapes.

Although tapes based on acryl_5 exhibited lower tack during application, they showed poor removability from the substrates. Some amounts of whitish and hazy residues were left even after adhesion at rt and were further increased as the application temperature was increased to 160 °C (see Figure 50). In contrast, PSAs based on acryl_1 and acryl_6 were more strongly fixed to the substrates and caused less residues after peel. Although none of the tapes was removed cleanly after storage for 1h at 160 °C, residues were significantly reduced for tapes based on acryl_1 or acryl_6 and 20 wt% DTMPTA. Against our expectations (see chapter 6.1.1), the removal of AA in acryl_6 did not improve the removability of the tapes. The absence of the intended effect was attributed to the comparatively low portion of AA (5.5 wt%) in the adhesive copolymer (acryl_1). Consequently, it was suggested, that the BondFilm® surface, which favors adhesion, was the dominating factor here. Residues remained on the substrates due to the high surface area and the adhesion promoting layer, which enforced the interactions with the PSA. This was even more pronounced at elevated temperatures, which decreases the viscosity of the PSA (softening), and thus favors penetration of the adhesive into deep sites of the substrates microstructure. The low initial tack of acryl_5 based tapes was associated with the increased T_g of this copolymer [176] (see chapter 6.1.1) and the high extent of adhesive residues after peel was attributed to an ineffective release mechanism. It was already shown by UV-cure kinetics, that the photo-crosslinking of multifunctional acrylates was restricted by the incorporated IBA group (see chapter 6.2.1). Due to the low crosslinking degree, cohesion within the adhesive was not sufficiently high to provide clean peel.

-Results and discussion, Performance of the designed PSA tapes-

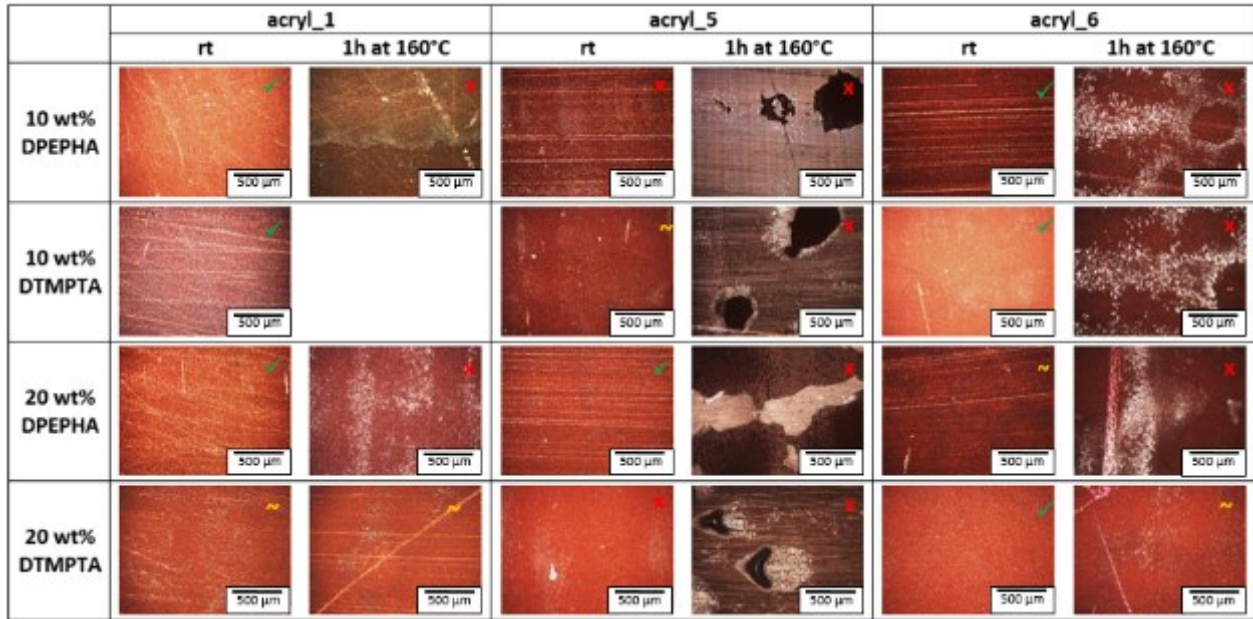


Figure 50: BondFilm® substrates after removal of tapes containing 10 or 20 wt% DPEPHA or DTMPTA and 1 wt% Lucirin TPO-L as a function of the basic adhesive copolymer

Influence of the chemical structure of the multifunctional acrylic monomer

PSA tapes based on acryl_1 were prepared by *method I* on etched PET carries, which had not been further treated. Adhesive formulations containing 10 wt% of the respective multifunctional acrylates and 5 wt% Lucirin TPO-L (adhesives 2, 11, 17, 20, 23, 25 and 29) were applied with a wet film thickness of 90 μm . The tapes were adhered to BondFilm® treated copper substrates and peeled off manually after adhesion at rt or 1h at elevated temperatures. In contrast to the standard settings for *method I*, the UV-doses for pre-crosslinking were adjusted to 1550 mJ/cm^2 or 295 mJ/cm^2 (PETA, SR 454, TMPTA) in these experiments. The photo release was triggered with 7750 mJ/cm^2 in the end of the application.

As illustrated in Figure 51, good results were obtained by the use of DPEPHA, DTMPTA, SR 494 or PETA as multifunctional acrylate. While PSAs containing TMPTA, SR 454 and SR 492 caused massive amounts of whitish and hazy residues after application at 140 °C throughout wide parts of the substrates, only thin layers of DPEPHA, SR 494 and PETA adhesives remained on the substrates and the PSA based on DTMPTA did not leave any residue at all. However, as the application temperature was further increased to 150 °C, massive residues of DTMPTA and PETA adhesives were found on the respective BondFilm® surfaces. In addition, the layer thickness of residues left by DPEPHA-based PSAs increased significantly upon 160 °C.

It was proposed, that residues developed due to softening of the adhesive and subsequent penetration into the surface morphology of the BondFilm® substrates (see also chapter 6.2.2). Since viscosity is a function of temperature [65], the cured PSAs penetrated more deeply into the highly structured BondFilm® surfaces the higher the application temperature was [60,177]. Thus, the contact area was increased and the resulting mechanical and chemical interactions with the substrate were more intense than those with the carriers. Consequently, the locus of failure was continuously shifted towards the adhesive-carrier interface. Finally, the PSAs failed adhesively throughout wide parts of the adhesive joint (see Figure 51) due to insufficient deformability of the cured adhesive, which was required during peel to escape from the microstructural cavities. Alternatively, in this stage cohesive failure at a weak boundary layer on the PET carrier surface has to be considered. Since this occurs so close to the interface, it is often interpreted as interfacial fracture. [68,177] Moreover, the results revealed a direct correlation of the monomer functionality and the maximum application temperature. In general, highly functional monomers build networks with high crosslinking densities [148] and high molecular weights, which are in turn related to high viscosities [65,178] and increased T_g [21,23–25] As a consequence, semi-IPN of the tetra- and penta/hexa functional monomers (SR 494,

-Results and discussion, Performance of the designed PSA tapes-

PETA, DTMPTA or DPEPHA) comprised higher resistance to softening and penetration into the microstructure of the highly structured BindFilm® substrates than the trifunctional TMPTA, SR 454 and SR 492.

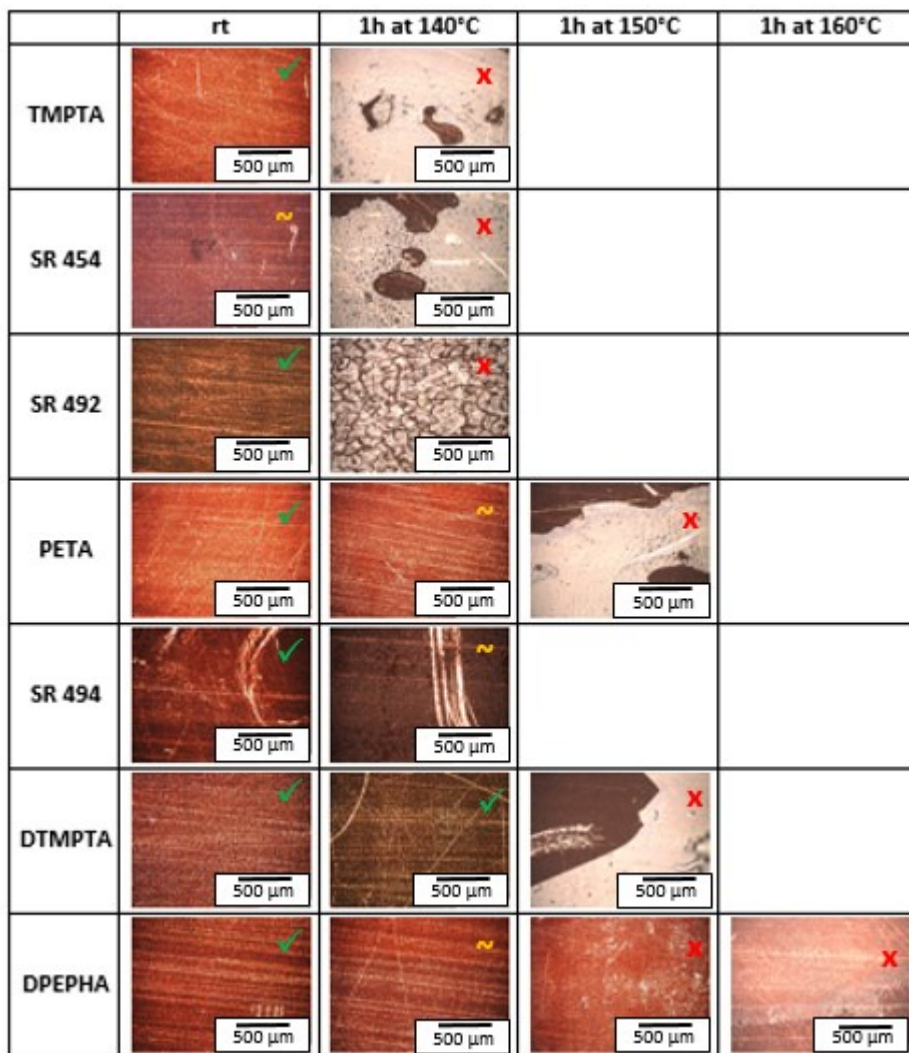


Figure 51: BondFilm® substrates after removal of tapes based on acryl_1, 10 wt% of multifunctional acrylate and 5 wt% Lucirin TPO-L as a function of the monomer structure

Besides the multifunctional acrylic monomers used so far, also an **aromatic** compound was tested as suitable crosslinking agent in order to improve the thermal stability of the polymer networks (IPN). [21] PSA tapes based on adhesive 21 (acryl_1, 50 wt% of SR 480 and 5 wt% Lucirin TPO-L) were prepared according to *method I*. The adhesive formulation was coated onto etched PET carriers applying a wet film thickness of 90 μm . The tapes were pre-crosslinked with a UV-dose of 1550 mJ/cm^2 and finally cured upon UV exposure with 7750 mJ/cm^2 . First tests on BondFilm® substrates revealed that the use of the aromatic crosslinker did not improve the removability of the tape. First tests on BondFilm® substrates revealed that the use of the aromatic crosslinker did not improve the removability of the tape. This was explained by the fact that the main cause of adhesive residues was the reduction of the viscosity of the adhesive upon high temperatures, which is related to penetration into the microstructure of the substrate and consequently to shearing over sharp edges during peel (see chapter 6.2.2, Figure 45). The di-functional SR 480 did not provide sufficiently high crosslinking densities for clean peel. The correlated low cohesion within the adhesive caused residues after application at rt (see Figure_A 10) and even more residues after storage at 150 °C.

Influence of the monomer concentration

The effect of the monomer content was investigated at the example of tapes based on acryl_1, which were prepared according to *method I*. Etched PET carriers were coated with 90 μm (wet film) of adhesive formulations containing 10 wt% of PETA, SR 494, DTMPTA or DPEPHA and 5 wt% Lucirin TPO-L (adhesives 2, 11, 17 and 25) and PSAs containing 20 wt% of these monomers and 1 wt% Lucirin TPO-L (adhesives 6, 14, 18 and 26). In addition, tapes based on adhesive 7 and 9 (20/50 wt% DPEPHA, 5 wt% PI) were prepared. The tapes were pre-crosslinked with UV-doses of 1550 mJ/cm^2 or 295 mJ/cm^2 (PETA), adhered to BondFilm® treated copper substrates, irradiated with 7750 mJ/cm^2 , stored at 160 °C for 1h and peeled off manually.

The microscopy images in Figure 52 revealed that increased concentrations of multifunctional acrylate enabled improved removability after application at elevated temperatures. The layer thickness of adhesive residues was reduced significantly by the use of increased monomer contents, independent on the type of multifunctional acrylate. Especially PSAs containing 20-50 wt% DTMPTA or DPEPHA enabled (almost) clean peel. This was related to enhanced network formation and thus highly efficient release properties [21,24,25], which had already been indicated in UV-cure kinetics (see chapter 6.2.1) by increased C=C double bond conversion of adhesive systems comprising high monomer levels. Although clean peel was achieved in some cases,

-Results and discussion, Performance of the designed PSA tapes-

this was often accompanied by low tack of the corresponding tapes and consequently, insufficient fixation of the substrates. Kim et al. found, that a low percentage of the required UV-dose can already reduce peel strength significantly due to migration of the crosslinkers to the air-polymer surface. [112] Thus, it was found that the implementation of both, satisfying adhesion and residue-free removability, did not only require the adjustment of the chemical composition, especially of the PI-content (see below), but also an optimization of the process parameters, including UV-dose, film thickness and carrier treatment (see chapter 6.3.3).

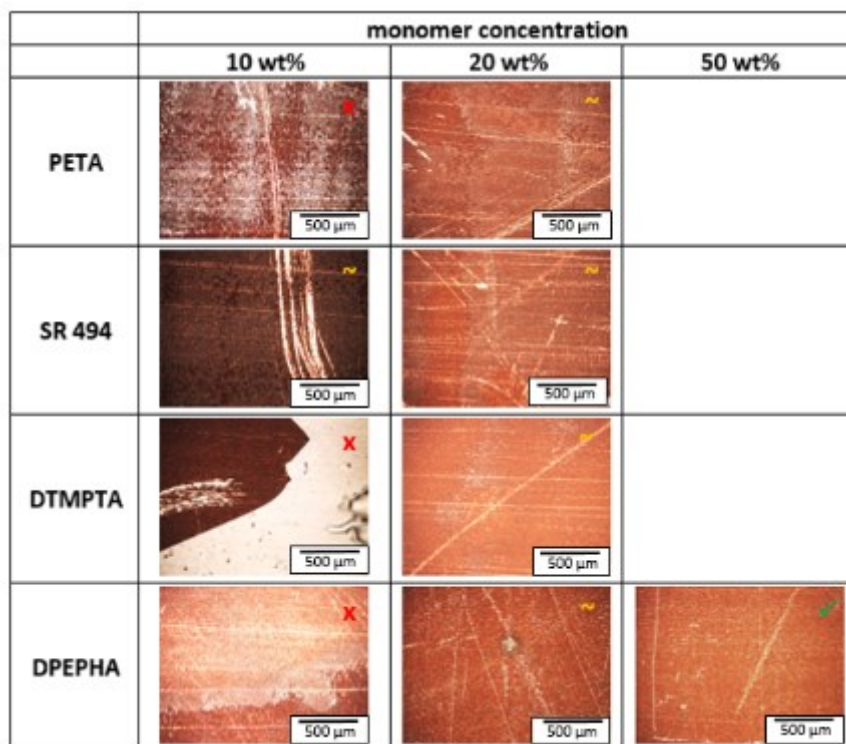


Figure 52: BondFilm® substrates after removal of tapes based on acryl_1, PETA, SR 494, DTMPTA or DPEPHA as a function of the monomer concentration

Influence of the photo initiator concentration

Besides the monomer structure and content, the PI concentration has a significant influence on network formation and UV-curing of the PSA. The removability from (structured) BondFilm® substrates was investigated at rt and 160 °C as a function of PI content (0.5-5 wt%) by the application of tapes based on acryl_1 and 20 wt% of DTMPTA or DPEPHA. Adhesives 4-7 and 12-14 were coated onto etched PET carriers according to *method I*, applying wet film thicknesses of 30 or 90 µm. Pre-crosslinking and UV-doses for curing were adjusted individually for each tape, depending on its wet film thickness and chemical composition (see Table_A 4 in the appendix).

In general, all tapes comprised satisfying tack throughout the application and fixed the substrates as desired. The only exception was the DPEPHA-based tape containing 5 wt% Lucirin TPO-L, which did not offer sufficient adhesive strength after irradiation. It is stated in literature, that the tack of UV-curable PSAs already decreases significantly at low percentage of the required UV-dose. [112] Here, the increased amounts of PI even accelerated network formation (see chapter 6.2.1, UV-cure kinetics) and thus debonding. Although the tape did not adhere properly to the BondFilm® substrate, adhesive residues (whitish and hazy) were left even after adhesion at rt (see Figure 53). The fact that the residues formed granulates instead of thin layers indicated that the applied UV-dose was too high leading to an over-cure of the PSA and hence to an embrittlement of the adhesive layer. [179] In contrast, the adhesive systems containing lower amounts of PI were removed cleanly after adhesion at rt. Application at 160 °C revealed that systems comprising too low amounts of PI (0.5 wt%) did not fully cure and consequently did not comprise sufficient cohesion for clean peel. Better results were achieved with adhesives containing 0.75 or 1 wt% Lucirin TPO-L, which only left thin layers of residues on the substrate surfaces. Considering the cured epoxy parts of the structured substrates, clean removability was observed after application at rt as well as after 160 °C. However, some residues remained at the epoxy-BondFilm® edge after storage at elevated temperatures. This was also explained by penetration of the softened PSA into these edges leading to mechanical adhesion and subsequent cohesive failure upon peel.

Based on these results, it was decided to focus on PSAs with 0.75-1 wt% PI. The already low amounts of residues were completely eliminated by precise adjustment of the process parameters, including UV-dose, layer thickness and carrier treatment (see chapter 6.3.3). Moreover, lower amounts of PI are more cost efficient. Thus, an adequate adjustment of the process parameters was not performed for 5 wt% systems.

-Results and discussion, Performance of the designed PSA tapes-

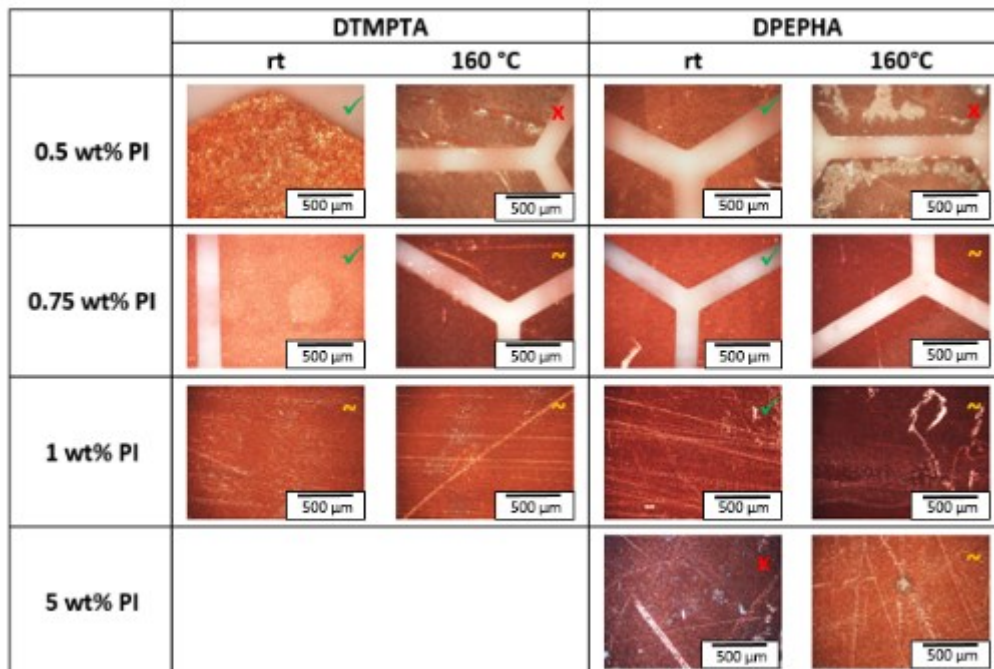


Figure 53: (Structured) BondFilm® substrates after removal of tapes based on acryl_1, 20 wt% DTMPTA or DPEPHA as a function of the PI concentration

Besides the nature of the substrate (morphology and composition) and the chemical composition of the adhesive layer, the film thickness of the adhesive, carrier pre-treatment and the applied UV-dose during pre-crosslinking and photo-release, affect the adhesive performance and removability of PSA tapes. The impact of these process parameters is discussed in the following chapter.

6.3.3. Impact of process parameters

Effect of the adhesive film thickness

It is stated in literature that tack, peel and shear resistance depend on the thickness of the applied PSA layer or the coating weight, respectively. [9,20,180] Below thicknesses of 2500 μm , which are typical for commercial PSAs, tack and peel increase with the film thickness. In contrast, Kaelble detected only a minor effect on the peel force for PSA layers $\geq 50 \mu\text{m}$ (nonlinear dependence). [180] Coating weights are usually kept in a range where its impact on tack, peel and shear is minimal. [9] The adjustment of the adhesive layer thickness enables the control of the adhesive character of PSA products (permanent/removable). In general, lower coating weights are applied to ensure removability of the PSPs. However, proper contact build up with the substrate (adhesive flow) requires a critical coating weight, which depends on the nature and characteristics of substrate and carrier. [20]

The effect of adhesive layer thickness was investigated at the example of tapes based on adhesive 6 (acryl_1, 20 wt% DPEPHA and 1 wt% Lucirin TPO-L). The adhesive layer was applied onto etched PET carriers according to *method I* with wet film thicknesses of 30, 60 or 90 μm . After evaporation of the solvent, the resulting adhesive layers amounted to about 15, 30 and 45 μm , which is in the typical range for PSA tapes. [6] The tapes were pre-crosslinked with a UV-dose of 200 mJ/cm^2 , adhered to BondFilm® substrates and additionally UV-cured with an exposure dose of 200 mJ/cm^2 . They were evaluated empirically with regard to their initial tack and peel strength. All tapes fixed the substrates properly, independent of the layer thickness, and were removed cleanly after adhesion at rt. Although the adhesive layer thickness was within the range of decisive impact on the adhesive properties, no significant difference in peel strength was noticed during peel.

Based on these results, a standard wet film thickness of 30 μm was defined for *method I*. On the contrary, 90 μm were applied in *method II* because a thicker, more compact PSA layer proved to be advantageous during adhesive transfer via hot lamination.

Corona treatment of the carriers

As already mentioned in chapter 6.2.2, corona treatment was applied in addition to chemical etching in order to further improve the interactions of the carrier with the PSA. In particular, enhanced interactions at the adhesive-carrier interface were required at elevated temperatures. As described in chapter 6.3.2 (*Influence of the chemical structure of the multifunctional acrylic monomer*), the locus of failure was continuously shifted towards the carrier surface, resulting in increasingly thick layers of adhesive residues on

BondFilm® substrates. On the one hand, this was attributed to deep penetration of the microstructure of the substrate by the softened PSA and to comparatively weak anchorage to the carrier on the other hand. Moreover, the presence of a weak boundary layer, which may arise from manufacture or chemical etching (carrier pretreatment by supplier) [165], was considered. This layer of low molecular weight oxidized material was reported to influence adhesion in dependence on its solubility in the adhesive matrix. In case of insolubility, a negative effect on adhesion performance was observed. [68]

To overcome these problems, the carrier was corona treated. During discharge polar functional groups, including C-OH, C=O, COOH, C-O-C, epoxy, ester and hydroperoxide, were generated on the PET foil [66–68], and the surface was roughened by ablation. [9,68] The increased polarity and porosity did not only improve wetting but also supported anchorage of the adhesive layer. [20,62,69] Furthermore, it was suggested that the weak boundary layer – if present - was reduced or even removed during corona-induced surface degradation. [56,70] In case of over-treatment, excessive degradation may lead to a replacement of this superficial low molecular weight oxidized material. Thus, the removal of the original weak boundary layer may be followed by the development of a new one. [56] The efficiency of surface activation was proven by XPS spectroscopy and contact angle measurements with water (see chapter 6.2.2 for details). In a screening experiment, the optimum corona dose was determined to 1528 W min/m².

Concerning tape preparation, it is important to consider hydrophobic recovery. As described in the Theoretical background (chapter 3.2.4), the activation of plasma or corona treated polymer surfaces decreases with time due to a thermodynamic effect. A rearrangement of the polymer chains (conformational movement, rotation), which is based on dipol-dipol interactions of the superficial polar groups with air, minimizes the surface free energy by orientation of the covalently attached functional groups towards the bulk. [69–71] It was shown that hydrophobic recovery proceeds rapidly during the first week [70] or even within hours [72] after corona treatment. Thus, coating of the PSAs was done immediately after corona treatment of the carrier to provide maximum interaction with the activated PET surface.

The influence of corona treatment on adhesion performance was investigated by the use of tapes based on adhesive 3 (acryl_1, 15 wt% DPEPHA and 0.75 wt% Lucirin TPO-L). According to *method I*, the adhesive formulation was coated onto chemically etched PET carriers, which were (i) not further treated or (ii) corona activated (1528 W min/m²), applying a wet film thickness of 30 µm. The tapes were pre-crosslinked with 80 mJ/cm², applied to structured BondFilm® substrates and photo-cured with a dose of 1000 mJ/cm².

-Results and discussion, Performance of the designed PSA tapes-

The samples were subjected to elevated temperatures (140-170 °C) for 1h and removed manually.

The results showed that corona treatment of the carriers significantly improved the removability of the tapes at elevated temperatures. While clean peel from BondFilm® substrates was limited to 140 °C so far, corona activation of the carrier enabled application temperatures of 160 °C. As illustrated in Figure 54, non-treated tapes caused many residues on BondFilm® substrates after application at 160 °C. In contrast, corona activated tapes were peeled cleanly under the same conditions. This was attributed to an improved anchorage of the PSA to the carrier, which was based on enhanced mechanical interlocking and interactions with the polar functional groups at the carrier surface. However, experiments at 170 °C revealed the upper limit of corona treated tapes. As already observed in chapter 6.3.2, the tapes were cleanly removed from the cured epoxy parts of the structured substrates. Moreover, the residues at the borders between BondFilm® treated copper and epoxy material were reduced by corona treatment of the PET film and the related fixation of the PSA to the carrier.

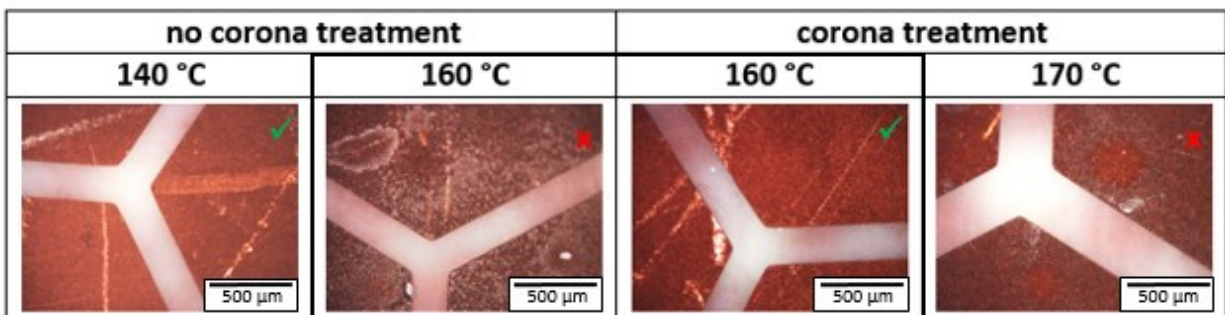


Figure 54: Structured BondFilm® substrates after removal of tapes based on acryl_1, 15 wt% DPEPHA and 0.75 wt% Lucirin as a function of carrier pre-treatment with corona discharge

Adjustment of the irradiation dose for the pre-crosslinking step and the UV-triggered release

The adhesive performance of photo-curable tapes strongly depends on the chemical composition of the PSA (structure and amount of multifunctional acrylic monomer and PI, T_g of the basic adhesive copolymer). Another powerful parameter in the adaption of tack and peel is the applied UV-dose. [22] In particular, precise adjustment of this parameter is required in the pre-crosslinking step to provide high initial tack in combination with a

certain extent of crosslinking, which limits penetration into the microstructures of the substrates and thus supports clean peel (see also 6.2.2). For the adaption of the pre-crosslinking doses, it was taken into account that already a low percentage of the required UV-dose distinctly affects the tack of photo-curable adhesives. Kim et al. found, that this is related to migration of the crosslinking agent to the air-polymer surface [112]. In order to provide high tack, systems, which required a pre-crosslinking dose $< 80 \text{ mJ/cm}^2$ (limited by lamp parameters), were rejected. These included PSAs with high reaction rates such as adhesives based on PETA, TMPTA, SR 454 or SR 492 or systems containing 5wt% Lucirin TPO-L (compare Table 11 in chapter 6.2.1). In contrast, formulations based on DPEPHA and DTMPTA exhibited lower reaction rates and moderate UV-doses for maximum conversion. Thus, the irradiation parameters were more easily adjusted for these systems. Moreover, the photo-curing step was optimized in order to provide the right balance between adhesion and cohesion, which is crucial for clean removability. [7,10,20] Adhesive residues may arise in both over- and under-cured systems (see Figure 55). While excessive UV-irradiation leads to embrittlement of the PSA (over-cured), too low UV-doses do not provide sufficiently high crosslinking densities (under-cure). The adhesive remains soft and fails cohesively during peel. [6,179] The kinetic measurements in chapter 6.2.1 showed, that the reaction rate and the UV-dose required for maximum conversion strongly depend on the chemical composition of the adhesive formulation. Consequently, the applied irradiation doses for pre-crosslinking and the photo-triggered release had to be adjusted individually. However, it was not possible to directly resume the UV-doses determined in the cure kinetics to the initiation of the release of the tapes, because different UV-curing systems were used providing different lamp parameters (intensity! [175]). Finally, a pre-crosslinking dose of 80 mJ/cm^2 was set as standard. DPEPHA adhesives were released applying 1000 mJ/cm^2 , while 7750 mJ/cm^2 were applied for DTMPTA adhesives.

Figure 55 illustrates the importance of precise UV-irradiation adjustment. Adhesive 6 (acryl_1, 20 wt% DPEPHA and 1 wt% Lucirin TPO-L) was coated onto chemically etched, corona treated PET carriers with a wet film thickness of $30 \mu\text{m}$ according to *method I*. The tapes were pre-crosslinked with 80 mJ/cm^2 , applied onto structured BondFilm® substrates and cured with 500 mJ/cm^2 (under-cure) and 1000 mJ/cm^2 (optimized cure), respectively. After storage for 1 hour at $160 \text{ }^\circ\text{C}$, the tapes were peeled off manually. While optimal cure enabled clean removability all over the substrates, incomplete network formation of the under-cured PSA caused a layer of adhesive residues on the BondFilm® parts. This cohesive failure was related to a reduction of the viscosity of the adhesive upon high temperatures [6], which facilitated penetration into the microstructure of the

BondFilm® surface. On the contrary, too high irradiation doses lead to embrittlement of the PSA layer. [179] Especially formulations with increased PI concentrations (5 wt%) were prone to over-cure due to their high reaction rates and conversions (see Table 11). This was demonstrated at the example of a tape based on adhesive 7 (acryl_1 and 20 wt% DPEPHA containing 5 wt% Lucirin TPO-L). The adhesive was coated onto an etched PET carrier with 90 µm wet film thickness. The PSA layer was pre-crosslinked with 1550 mJ/cm², applied onto structured BondFilm® and irradiated with 7750 mJ/cm². Although the tape did not comprise sufficient tack to fix the substrate, the brittle PSA left granulates of adhesive residues on the BondFilm® parts of the surface.

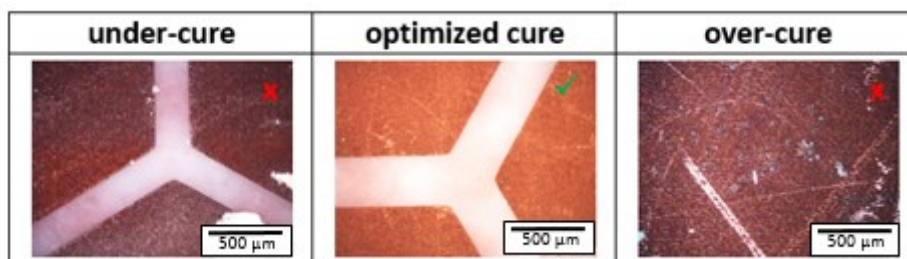


Figure 55: BondFilm® substrates after peel of under-cured, optimally cured and over-cured PSAs

Besides the applied UV-dose, also the tape preparation method and the corresponding workflow influenced the adhesion performance. As described in more detail in chapter 6.3.4, tapes prepared by *method I* comprised lower surface tack than those prepared by *method II*. This is based on the different approaches of pre-crosslinking and the resulting crosslinking gradients, which were formed throughout the adhesive layers. Moreover, it turned out to be essential to fully crosslink the adhesive *before* high temperatures were applied, in order to prevent penetration of the PSA into deep sites of the microstructure of the substrates and thus the development of adhesive residues, which may occur as a consequence of insufficient deformability during peel (see chapter 6.2.2 for details). Nevertheless, fixation of the substrate was still provided at optimized UV-irradiation. It was suggested, that this was possible due to a kind of key-lock effect between the substrate and the cured adhesive. During wetting the latter builds a perfect counterpart to the topography of the substrate, which gets “frozen” upon UV-crosslinking. Mechanical interlocking fixes the substrate until the tape is peeled off. However, the right extent of penetration is crucial to provide residue-free peel as well as proper fixation and can be controlled by adjustment of the individual pre-crosslinking and UV-doses for curing.

6.3.4. Influence of the preparation method

As already mentioned in chapter 6.2.2 two preparation methods were developed. The main difference concerned coating and pre-crosslinking. While the adhesive layer was applied directly onto the carrier in *method I*, it was first coated to a release liner and subsequently transferred to the carrier in *method II* (hot lamination). During pre-crosslinking, *method I* tapes were irradiated on top of the adhesive layer, whereas *method II* tapes were pre-crosslinked through the backside of the carrier. Since the maximum level of irradiation is obtained on top of the exposed side of a tape, crosslinking gradients developed throughout the adhesive layers. [9] Due to the differences in tape preparation, maximum crosslinking was obtained at the *top* of *method I* tapes, and at the *carrier-adhesive interface* of *method II* tapes. As a result, tapes prepared by *method II* comprised higher surface tacks than those prepared by *method I*.

The impact of the preparation method on adhesion performance and removability from pristine and tarnish protected copper as well as from BondFilm® substrates was investigated using tapes based on adhesive 6 (acryl_1, 20 wt% DPEPHA and 1 wt% Lucirin TPO-L). The PSA was applied onto etched PET carriers according to *method I* (30 µm) and *method II* (90 µm), respectively. The carriers were corona treated before coating to fix the PSA more tightly to the carrier and thus enable clean peel. All tapes showed satisfying tack and were pre-crosslinked with a UV-dose of 80 mJ/cm² and UV-cured with 1000 mJ/cm².

Method II tapes showed clean peel from tarnish protected copper substrates after application at 220 °C, whereas *method I* tapes already left some residues after 160 °C (data not shown). Similar results were obtained from adhesion experiments on pristine copper, where *method II* tapes were removed without leaving residues after storage at 200 °C, but *method I* tapes only allowed for clean peel up to 180 °C. In contrast, *method II* was not advantageous when peeling from BondFilm® surfaces. Here, best results were achieved with tapes prepared according to *method I*, which were removed cleanly after application at 160 °C. The divergent trends on the BondFilm® treated surfaces and the copper substrates (tarnish protected and pristine copper) point out the distinctive impact of the substrate nature, including surface topography and chemical composition (see also chapter 6.3.1). The superordinate structures on BondFilm® substrates offer high surface area for mechanical interlocking with the PSA, while the organometallic layer enhances chemical adhesion. Since the on top irradiation of *method I* tapes limits penetration into deep layers of the microstructure of the substrates and restricts contact with the pro-adhesion coated surface, *method I* tapes show superior performance over *method II* tapes. In contrast, tarnish protected copper and pristine copper exhibit less structured surfaces, enabling clean peel of *method II* tapes, which comprise a lower crosslinking

density on top of the adhesive layer. The slight difference of the maximum application temperature on the copper substrates evolves from the metallic character of pristine copper, which makes this substrate more prone to polar interactions with the PSA. However, the reason for the superior performance of *method II* tapes on tarnish protected and pristine copper is not yet clear. Based on the combination of the comparatively low surface roughness, the low extent of superordinate structures on these substrates and the on-top pre-crosslinking, we expected at least similar results or even less residues by *method I* tapes. Though further research is required to find an explanation for the observed results, this was not part of the present work, where the main focus was set to the removability from BondFilm® substrates.

Another thing to mention is that, pristine copper substrates partially oxidized during storage at elevated temperatures though they were covered by PSA tapes. This was attributed to inhomogeneous coating, which caused defects and irregular cure throughout the PSA layer of *method I* tapes on the one hand, and led to discontinuous transfer of the adhesive during hot lamination in *method II* tapes on the other hand. As a consequence, the substrates were not fixed throughout the whole area and sites on pristine copper substrates, which were not covered by the PSA due to defects or partial lift off (inhomogeneous cure), were oxidized rapidly during storage at temperatures ≥ 160 °C by the enclosed O₂. Adhesive residues were exclusively found at the edges of the oxidized areas, while the remaining substrate was free from residues (see Figure 56). This was attributed to a local increase of the surface roughness due to the formation of (porous) copper oxide [181,182], which made the affected areas prone to mechanical interlocking with the PSA.

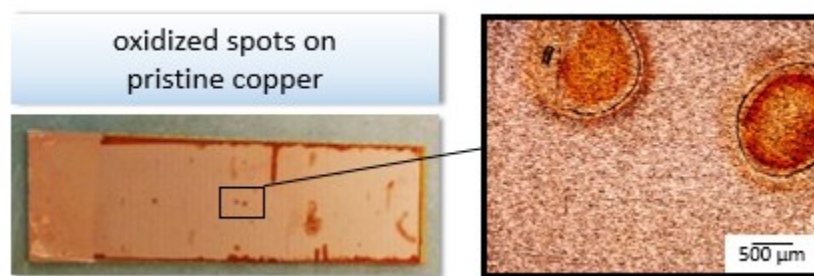


Figure 56: Pristine copper substrates after storage at 180 °C comprising oxidized spots with adhesive residues

6.3.5. Conclusion about the adhesion performance

Firstly, the impact of the surface quality of the substrate on adhesion performance and removability of the PSA tapes was discussed. While proper adhesion during application is governed by wetting and thus by the polarity (chemical composition) and porosity (roughness) of the adhered *substrate* surface, clean removability requires adequate adhesion and anchorage to the *carrier*. [20,62] The applied substrates (BondFilm® treated copper, cured epoxy, tarnish protected copper and pristine copper) were characterized by XPS, AFM and contact angle measurements. The lowest surface roughness was detected for BondFilm® treated copper ($S_a = 88 \pm 5$ nm, $S_q = 112 \pm 6$ nm). However, the corresponding 3-D images revealed high portions of superordinate structures on these surfaces, generating a high surface area. In combination with the organometallic adhesion promoting layer, high mechanical and chemical interactions with the PSA were expected, preventing clean removability. The high contact angles (133°) with water were seen as a result of the highly structured surface and the chemical composition of BondFilm® substrates, which was dominated by C (60 at%), O (15 at%) and N (16 at%) due to the presence of the adhesion promoting layer (benzotriazole derivatives). Moreover, some impairment of residue-free peel was assumed for tarnish protected and pristine copper. The superordinate structures on the first and the metallic character of the second, made these substrates prone to interactions with the PSA. Since the surface roughness of the copper substrates was comparatively low ($S_a = 154 \pm 26$ nm, $S_q = 193 \pm 31$ nm and $S_a = 148 \pm 10$ nm, $S_q = 189 \pm 15$ nm), the moderate contact angle (73°) of tarnish protected copper was mainly seen as a result of the superordinate structures, while the low contact angle (21°) of pristine copper originated from the metallic character of this substrate. Besides, the removal of the anti-tarnish coating was proven by XPS measurements, displaying the elimination of Zn (21 at%) and Cr (2.5 at%) as well as the significant increase of Cu from 1 at% to 38 at%. Despite the high surface roughness of cured epoxy ($S_a = 554 \pm 92$ nm, $S_q = 684 \pm 109$ nm), the lack of superordinate structures on these substrates promised clean removability of the PSA tapes. The high contact angle of the prepregs (107°) was attributed to the surface chemistry, which was mainly based on C (64 at%) and O (29 at%).

The influence of the chemical composition of the PSA on tack and removability was investigated with respect to the **structure of the copolymer**, the type and amount of multifunctional acrylic monomer as well as the photoinitiator concentration. Adhesion experiments on BondFilm® treated copper revealed that PSAs based on acryl_1 and acryl_6 exhibited better tack and removability than formulations based on acryl_5. This was related to the higher T_g and the bulky IBA units, which sterically restrict the UV-crosslinking reaction. Further experiments showed a direct correlation of **monomer**

functionality and maximum application temperature. While formulations containing the di- and tri-functional monomers SR 480, TMPTA, SR 454 and SR 492 caused massive residues after application at 140 °C, only thin layers of residues were left on BondFilm® treated copper by the tetra- and penta/hexa functional PETA, SR 494, DTMPTA and DPEPHA. This was explained by higher crosslinking densities, T_g and viscosity of these adhesives, which prevent excessive penetration of the substrate morphology and too intense interactions of the PSA with the adhesion promoting layer. However, as the application temperature was further increased, the locus of failure was shifted towards the adhesive-carrier interface. Adhesive residues were reduced significantly by increased **monomer concentrations** (20-50 w%), independent of the type of multifunctional acrylate. Best results were achieved with the highly functional DTMPTA and DPEPHA due to the development of highly crosslinked semi-IPN. Nevertheless, clean peel was often accompanied by low tack. Variations of the **PI concentration** were performed in the range of 0.5-5 wt%. The optimum PI content was determined to 0.75-1 wt%, offering clean removability at rt and only thin layers of white and hazy residues at 160 °C. In contrast, high PI contents (5 wt%) quickly lead to an over-cure of the PSA, resulting in granulate residues on the substrate surface, while too low amounts of PI (0.5 wt%) did not fully cure the multifunctional monomers.

In addition, the impact of process parameters, including layer thickness, corona treatment of the carrier and the applied UV-dose during pre-crosslinking and release, were displayed. According to literature, tack, peel and shear depend on the **layer thickness** and the coating weight. [9,20,180] Although the wet film thickness was varied in the range of 30-90 μm , the adhesive properties did not change markedly. On the contrary, **corona treatment** of the carrier had big influence on the adhesion performance: The discharge treatment oxidized and roughened the carrier surface, which enabled improved interaction and anchorage of the PSA layer. [20,62,69] As a consequence the prepared tapes were removed cleanly from BondFilm® substrates after application at 160 °C. Another essential parameter was the **applied UV-dose** during pre-crosslinking and release. The individual and precise adjustment to the respective adhesive system allowed for a good balance of tack and peel and avoided under- or over-cure of the PSA. Formulations comprising too high reaction rates (5 wt% PI, tri-functional monomers and PETA) were rejected due to the limits of the available lamp parameters. In contrast, the adhesive properties of systems based on DTMPTA and DPEPHA were easily tunable due to their moderate reaction rates. Last but not least, the **preparation method** influenced the adhesion performance too. Differences in the preparation process caused different crosslinking gradients throughout the PSA layer. [9] As a result, *method I* tapes exhibited lower tack and limited penetration to the microstructure of the substrates than *method II*

tapes. Adhesion experiments revealed divergent trends on BondFilm® treated and copper substrates (tarnish protected and pristine copper), depending on the topography and chemistry of the substrates. While the reason for the superior performance of *method II* tapes on tarnish protected and pristine copper surfaces (220 °C, 200 °C without residues) is not yet clear, the advantage of *method I* tapes on BondFilm® treated copper was explained by the limited interactions with the high surface area and the adhesion promoting layer.

After all, residue-free removability from the different substrates were as expected (see above and 6.3.1): The most challenging surface for clean peel was BondFilm® treated copper. Due to its high level of superordinate structures and the adhesion promoting layer, it was prone to residues after tape removal, especially after application at elevated temperatures, where the viscosity of the PSA was reduced facilitating penetration into the substrates microstructure. In contrast, all tapes were cleanly peeled from the epoxy parts of the structured substrates. The removability from tarnish protected and pristine copper was poor due to mechanical and chemical interactions of the PSA with these substrates.

To sum up, the reduction of the viscosity of the adhesive and the related penetration into the substrates microstructure is seen as the main cause for adhesive residues after high temperature applications. In contrast, thermal decomposition of the adhesives was excluded due to the findings in TGA measurements (see chapter 6.2.1) and the fact that the observed residues were whitish and hazy rather than yellowish, orange or brownish. Consequently, high crosslinking densities and high T_g were required to provide residue-free peel. Unfortunately, this was contradictory to the requirements for high initial tack (low T_g). As a consequence, a compromise between these properties was required, which was approached by a precise adjustment of the pre-crosslinking dose (see chapter 6.3.3). For further experiments it was decided to focus on adhesive systems based on acryl_1 containing 20 wt% DPEPHA and 0.75-1 wt% Lucirin-TPO-L. Moreover, corona treatment was advantageous to support the anchorage of the PSA to the carrier. The standard UV-dose for pre-crosslinking was determined to 80 mJ/cm², while the corresponding value for an efficient UV-release amounted to 1000 mJ/cm².

Table 17 summarizes the best performance for the tested adhesive systems as a function of monomer type.

-Results and discussion, Performance of the designed PSA tapes-

Table 17: Maximum application temperature of the tested adhesives systems based on acryl_1 as a function of monomer type

Type of monomer	Adhesive Composition Monomer + PI concentration [wt%]	Process Parameters: Wet film thickness, corona treatment, preparation method	Substrate	Max. application temperature*
TMPTA	10 + 1/ 10 + 5	90 µm no corona <i>method I</i>	protected Cu BondFilm® cured epoxy	rt
SR 454	10 + 1/ 10 + 5	90 µm no corona <i>method I</i>	protected Cu BondFilm® cured epoxy	rt
SR 492	10 + 1/ 10 + 5/ 10 + 10	90 µm no corona <i>method I</i>	protected Cu BondFilm® cured epoxy	rt
PETA	10 + 1/ 10 + 5	90 µm no corona <i>method I</i>	protected Cu cured epoxy ® cured epoxy	rt
SR 494	10 + 1	120 µm no corona <i>method I</i>	protected Cu	160 °C
DTMPTA	20 + 1	30 µm corona <i>method I</i>	BondFilm®	160 °C
	20 + 1	90 µm no corona <i>method II</i>	protected Cu	240 °C
DPEPHA	20 + 1	30 µm no corona <i>method I</i>	pristine Cu	180 °C
	20 + 1	30 µm corona <i>method I</i>	BondFilm®	160 °C

*with clean removability

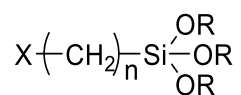
-Results and discussion, Improvement of the removability by the use of adhesion promoters-

6.1.Improvement of the removability by the use of adhesion promoters

Previous adhesion experiments showed that the surface quality of the substrate had a significant influence on the adhesion performance of the PSA tapes (see chapter 6.3). Especially BondFilm® substrates, which comprise a high surface area and an adhesion promoting layer, turned out to be challenging surfaces, since the main cause of adhesive residues after application at elevated temperatures was found to be the reduction of the viscosity of the PSA and the consequent penetration into the microstructure of the adherents. During peel, cohesive failure occurred within the bulk or close to the adhesive-substrate interface, depending on the PSA formulation and the resulting network density. Best results were achieved using systems based on acryl_1, 20 wt% DPEPHA or DTMPTA and 0.75-1 wt% Lucirin TPO-L. However, clean removability after temperature storage at 160 °C was limited to tapes with corona treated carriers. The discharge treatment roughened the PET surface and generated oxidized species, which enhanced interactions with the PSA layer and improved anchorage between the adhesive and the carrier. Thus, it was revealed that carrier treatment and anchorage to the same is another important factor influencing residue-free peel.

Based on the improvement with corona treatment, adhesion promoters were applied to the PET films in order to *covalently* attach the PSA to the carriers and consequently to provide clean peel after temperature treatment > 160 °C. The use of adhesion promoters is a common technique in tape manufacturing, which offers covalent anchorage of the adhesive to the carrier. [9] Such coupling agents are capable to undergo chemical reactions with the substrate on the one hand, and with the (polymeric) adhesive on the other hand. [1,9,183] As a result, a chemical bridge is formed between the two materials, which enhances or improves the initial bond strength by improved substrate wetting or secondary bonding via Van der Waals or dipole-dipole interactions, hydrogen bonding or acid-base reactions. [53] Adhesion promoters are mainly applied with plastic film carriers, including PET, polyamide and PTFE, which are comparatively difficult to adhere. The chemical nature of the adhesion promoter depends on the carrier as well as on the adhesive. [9] Some examples are ABS, isocyanates and (organo)silane derivatives. Typically, adhesion promoters are solvent-born, water-born or applied as solid state products. [9]

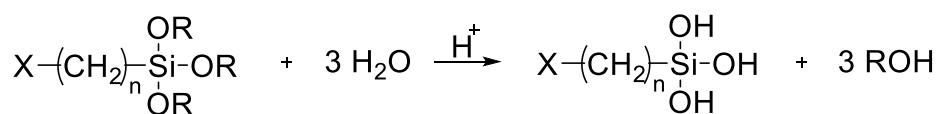
Organosilane coupling agents represent the most important group of technical adhesion promoters. [1,21,53,184] They are bifunctional molecules with the general formula



-Results and discussion, Improvement of the removability by the use of adhesion promoters-

where RO is a hydrolysable group, such as methoxy or ethoxy groups, X is an organofunctional group, including amino, hydroxy, vinyl, (meth)acryl, mercapto or epoxy functionalities, and R' is a spacer between the organofunctional group and the silicon atom. Adhesion promotion of organosilane coupling agents is based on a series of reactions: Firstly, the RO -moieties are hydrolyzed stepwise in the presence of water, building the corresponding silanols (Figure 57, I). Subsequently, these labile intermediates adsorb to superficial OH -groups at the substrate via hydrogen bonding. In the following condensation reaction, the silanols are covalently coupled to the substrate surface under elimination of water, resulting in siloxane bonds (Figure 57, II). Simultaneously, there is a competitive reaction with adjacent silanols, which generates a polysiloxane network at the surface. The retained organofunctional groups are orientated away from the surface and are available for interactions and reactions with the adhesive. [1,21,60,184,185] Upon coating, the adhesive diffuses into the adhesion promoting layer, which can be seen as a diffuse interphase between substrate and adhesive, where physical and chemical interactions take place. [21,53] If the siloxane and the adhesive are highly compatible, they can copolymerize, while partial compatibility or weak interactions lead to the formation of IPNs (phases cure separately) or pseudo-IPN (siloxane network penetrated by adhesive). [184] Effective layer thicknesses of silane coupling agents amount to more than hundreds of Angstrom [21], which corresponds to a multilayer structure. [184,185]

Step I: Hydrolysis



Step II: Adsorption and Condensation

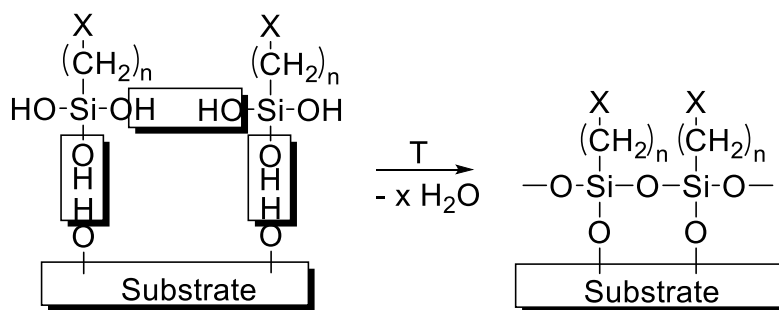


Figure 57: Mechanism of attaching silane coupling agents to substrate surfaces: hydrolysis (I) and condensation reaction (II) of organosilanes [184]

-Results and discussion, Improvement of the removability by the use of adhesion promoters-

Typically, organosilane adhesion promoters are applied from aqueous or water-alcohol solution. [183,184] The hydrolysis and condensation reactions are influenced by many factors, including pH, the type and concentration of the applied silane and the presence of catalyst (mineral acids, AcOH, NH₃, KOH, KF, HF, Ti-/V-alkoxides or oxides). [60,186,187] First of all, the **presence of water** is essential to start hydrolysis of the silane compounds. [1,186] Another important factor is the **pH value** of the solution. At neutral conditions hydrolysis proceeds at lowest rates. Changes by 1 unit of pH - in either acid or base direction - accelerates the reaction significantly (10-fold). In contrast, condensation shows its minimum rate at pH = 2.5-4. [187,188] Hence, acid conditions are associated with fast hydrolysis and slow condensation rates [188,189] as well as with a low extent of self-condensation. On the contrary, base catalyzed systems show high self-condensation (gelation!) since condensation starts as soon as silanol groups are available. [186,189] Moreover, the pH value affects the amount of adsorbed silane molecules and their orientation at the surface. [184,186] The stability and reactivity of the adhesion promoter is greatly affected by the **silane structure**. The effect of the spacer length on hydrolysis and condensation is a consequence of its impact on the bond strength of the alkoxy group to the silicon atom. [1,60] Furthermore, the nature of the organofunctional group (neutral/cationic/anionic) plays an important role. [185] In general, long, branched and bulky groups decelerate hydrolysis and condensation. [187] Thus, small alkoxy groups, such as methoxy or ethoxy moieties, are preferred to enable fast hydrolysis rates. [188] In turn, bulky moieties can be applied to control hydrolysis and condensation reactions by steric stabilization of the labile silanol intermediates. [184] The silane structure also influences the quality of the coating. While short alkyl chains preferably build randomly orientated and disorganized films, the increased intermolecular interactions of long alkyl chains in the adsorbed molecules lead to well-ordered silane layers. [189]

A standard procedure for the application of adhesion promoters onto surfaces includes (i) dipping the cleaned substrates into a silane solution, (ii) removing the excess material by washing and (iii) drying the silane film at 100-110 °C. [183,186] The drying conditions (temperature and duration) govern the number of siloxane bonds with the surface and with adjacent silanols and consequently the structure of the adhesion promoting film. [184] As hydrolysis and condensation follow the Arrhenius equation, increased temperatures have an accelerating effect on the reaction rates. [190] Reaction temperatures of 50-70 °C significantly enhance hydrolysis and condensation, while even higher temperatures do not further push the reaction. [191] Also, the silane concentration has big impact on the condensation rate as well as on the nature of the adhesion promoting layer. Typically, the dipping solution contains 0.1-3 wt% of the respective silane component. [183,186] Increasing amounts of silane were found to

-Results and discussion, Improvement of the removability by the use of adhesion promoters-

accelerate condensation profoundly. [188,189] In general, high silane contents [189] and unpolar solvents [53] increase the film thickness of the deposited coupling agent. However, *Walker* stated that the silane content should be below 4wt% to prevent extensively thick and non-uniform layers, which develop upon pre-condensation in solution and the associated formation and physio-sorption of silane oligomers. [189,192]

6.1.1. Modification of the PET carrier – application of adhesion promoters

In this work, 3-methacryloxypropyl trimethoxysilane (3-MAPTMS), 3-acryloxypropyl trimethoxysilane (3-APTMS) and bis(acylphosphane)oxide-4-(trimethoxysilyl)butyl-3-[bis(2,4,6-trimethylbenzoyl)phosphinoyl]-2-methyl-propionate (TMESI² BAPO) were applied as coupling agents to strengthen the adhesive-carrier interface. These organosilanes were covalently attached to the PET surface via the methoxy groups (hydrolyzable groups) and provided either unsaturated C=C moieties or photoactive groups (organofunctional group) for reactions with the coated PSA.

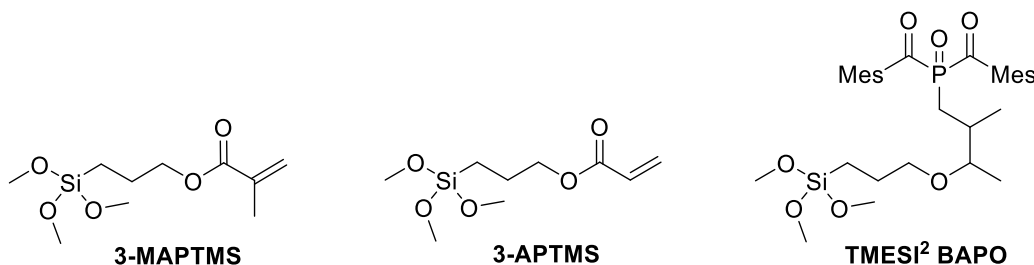


Figure 58: Chemical structures of the organosilanes used for surface modification of the PET carriers

Since the neat PET surface does not contain any reactive functionalities for coupling with the organosilanes, the carrier surface was oxidized by corona discharge (1528 Wmin/m²). As already explained in chapter 6.3.3, corona treatment of PET follows a free-radical mechanism that leads to the formation of oxidized functional groups such as C-OH, C=O, COOH, C-O-C, epoxy, ester and hydroperoxide. [66–68] In particular, the generated superficial hydroxyl groups participate in the subsequent immobilization of the organosilane compounds, which is achieved via condensation reaction with the silanol moieties. [189]

Due to hydrophobic recovery (see 6.3.3) [69–72], the PET carriers were modified immediately after corona treatment. For surface modification, 2wt% of the respective organosilanes were dissolved in EtOH (96 %), which had been acidified to pH 4-5 by the

-Results and discussion, Improvement of the removability by the use of adhesion promoters-

addition of AcOH. [189,193,194] Hydrolysis was induced by traces of water in the solvent and accelerated by acidic conditions. [183,185,188] The activated PET carriers were immersed into the silane solutions for 2h at rt (Figure 59, step I) and subsequently cured at 110 °C overnight (Figure 59, step II). [183,193,194] Thus, adsorption, physical immobilization (H-bonds of silanols and superficial OH-/COOH groups) and oligomer formation took place in step I [60,184], while the thermal treatment in step II completed condensation and led to covalent attachment of the respective silanols to the carrier via siloxane linkages. Since the applied adhesion promoters carried three hydrolyzable groups per molecule, crosslinked oligolayers were built on the carrier surface by reactions between neighboring silanol molecules. [186]

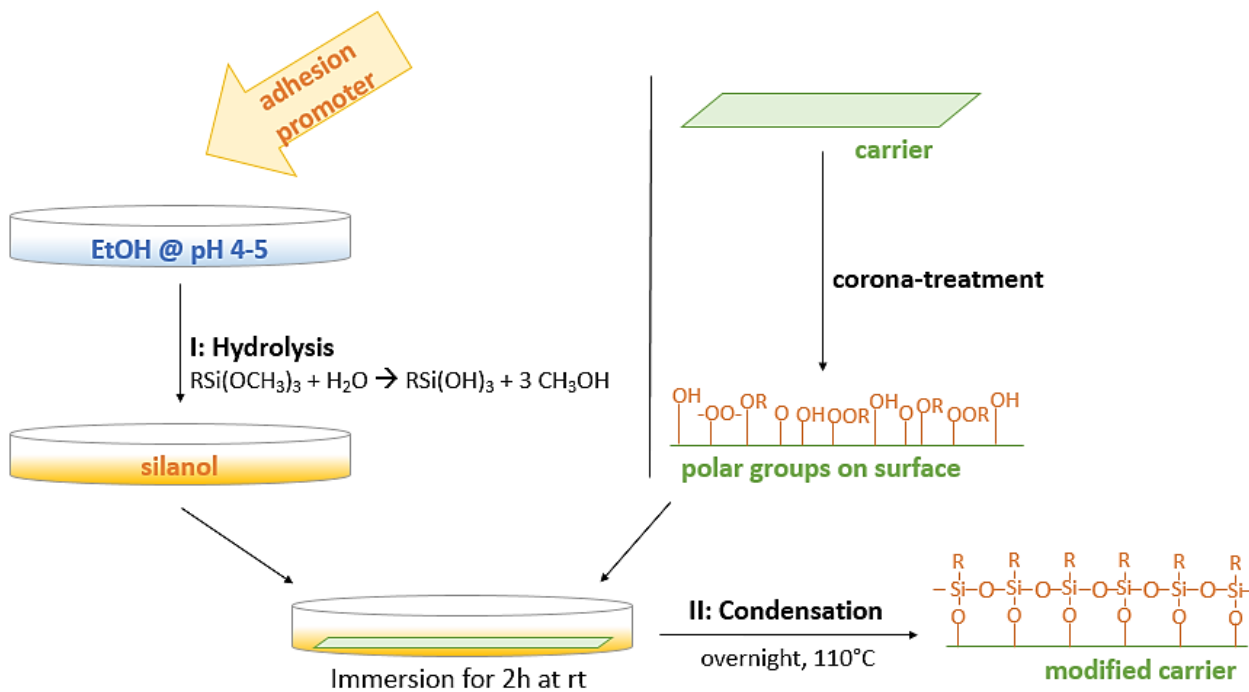


Figure 59: Attachment of adhesion promoters to the carrier surface – surface modification procedure

Although increased temperatures (50-70 °C) would enhance hydrolysis and condensation [191], the immersion bath was not heated to allow for slow but uniform adsorption to the surface. Moreover, a low pH value and moderate silane concentration were chosen to prevent pre-condensation and thus too thick and non-uniform layers. Consequently, the solutions were prepared freshly and applied directly after preparation. [60,184,189,192] Finally, the excess silane (not covalently bond) was removed by washing with EtOH and the modified carriers were dried at rt.

-Results and discussion, Improvement of the removability by the use of adhesion promoters-

Characterization of the modified carriers

The successful application of the different adhesion promoters was proven by XPS and contact angle measurements prior to and after surface modification of the PET carrier. The deconvoluted XPS high resolution C1s, Si2p and P2p spectra of an unmodified but etched carrier, a corona treated carrier and the modified carriers are shown in Figure 60 and Figure_A 11 (see appendix). The hydrocarbon structures of the PET carrier (unmodified and corona treated) as well as the organic groups of the silanes gave rise to the peaks at 284.8 eV (C-C, hydrocarbon), 286.3 eV (C-O) and 288.9 eV (C=O) [195–197] in the **C 1s spectra** of all samples. In contrast, the peaks at 284.1 eV were assigned to CH₂-CH₂-Si-O [198] and were only observed after surface modification, which indicated the successful attachment of the organosilanes to the carrier surfaces. The high resolution **Si2p spectrum** of the unmodified, corona treated carrier was characterized by the peaks at 104.8 eV and 104.2 eV, respectively. These signals were attributed to inorganic SiO₂ particles or powder in the commercially used PET foils [199–202], which act as non-migratory additives for better web handling [165,166]. However, after the attachment of the silanes these signals shifted to 103.3 eV (SiO₂) [199,200,203,204] and a second peak arose at 102.4 eV (C-Si-O). The latter was assigned to organosilanes [200,203,205] and hence confirms the functionalization of the carrier. The layer thickness of the silanes was estimated to values below 10 nm based on the fact that the inorganic SiO₂ (filler; 103.3 eV) was still detected on the modified carriers and that XPS analysis is a highly surface sensitive technique, where signals typically originate within tens of angstroms below the solid surface. [54,206] In addition, the high resolution **P2p spectrum** of the TMESI² BAPO modified carrier revealed peaks at 131.8 eV (P-C) and 133.0 eV (P-O) which were related to the organic phosphorus groups (phosphine oxide units) in the BAPO moiety. [207,208] Peak assignments of the high resolution C1s, Si2p and P2p spectra is summarized in Table 18.

Although C, O and Si were already detected for unmodified but etched PET films, a distinct increase of the carbon content from ~45 at% to ~55-65 at% on the modified carriers indicated the attachment of the different organosilanes (see Table 19). The decrease of oxygen and silicon was also attributed to the application of the silane layers, which contained more C than O and Si and simultaneously shielded the respective signals originating from the PET film. In addition, about 4 at% of phosphorus were detected for TMESI² BAPO modified carriers.

-Results and discussion, Improvement of the removability by the use of adhesion promoters-

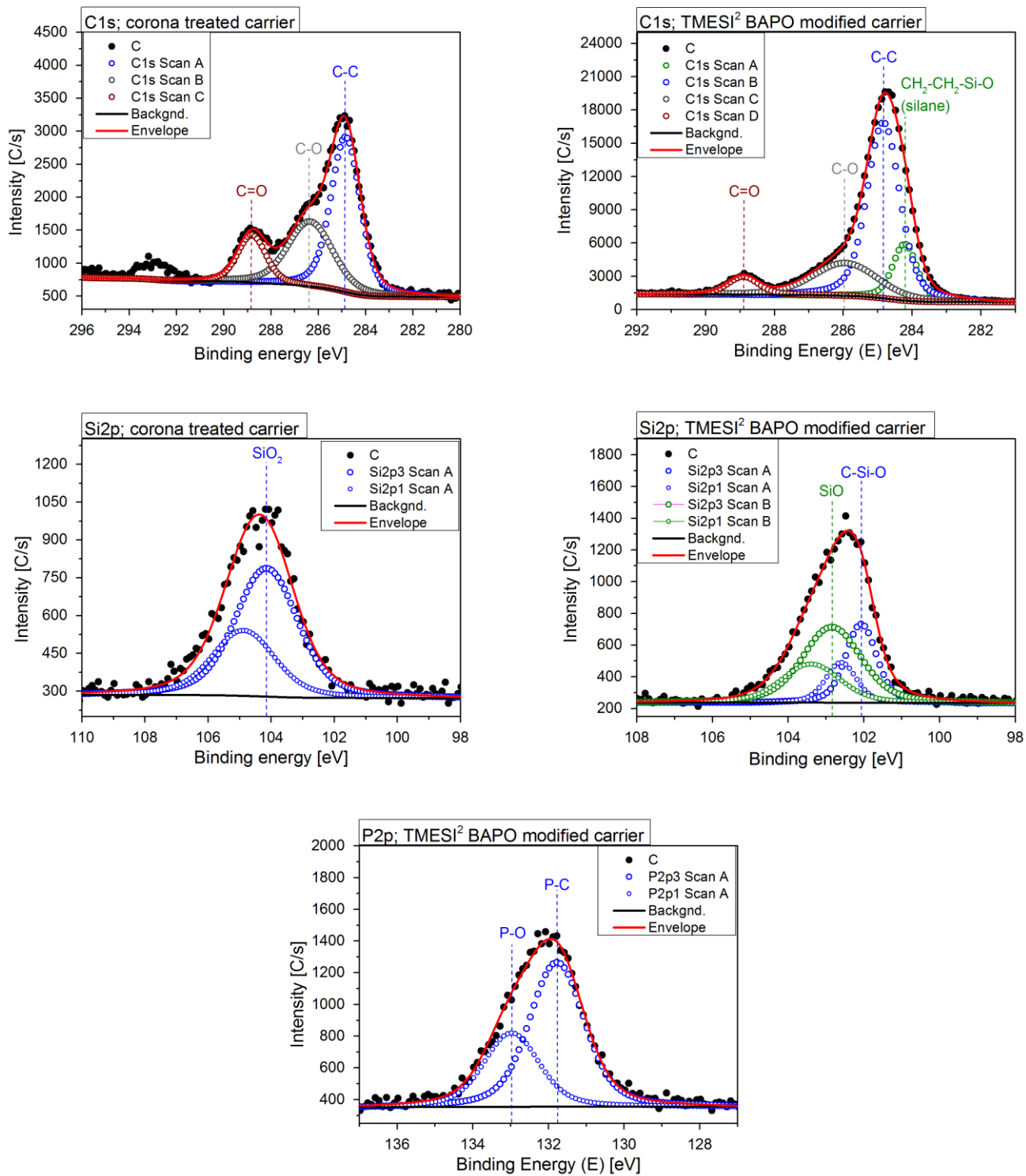


Figure 60: Deconvoluted XPS high resolution C1s, Si2p and P2p spectra of the corona treated and TMESI² BAPO modified PET carriers

-Results and discussion, Improvement of the removability by the use of adhesion promoters-

Table 18: Assigned peaks of the high resolution C1s, Si2p and P2p XPS spectra

	C1s [eV]	Si2p [eV]	P2p [eV]
CH₂-CH₂-Si-O	284.1		
C-C	284.8		
C-O	286.3		
C=O	288.9		
C-Si-O		102.4	
SiO₂ (inorg.)		103.3	
SiO₂ (inorg.)		104.2	
P-O			131.8

Table 19: Chemical composition [at%] of the unmodified but etched, the corona treated and the modified carriers

	relative concentration [at.-%]			
	C	O	Si	P
unmodified but etched carrier	48.2	37.1	14.7	-
Corona	45.5	40.8	13.8	-
3-MAPTMS	53.9	32.6	13.5	-
3-APTMS	62.7	28.8	8.8	-
TMESI² BAPO	66.9	23.9	5.1	4.1

In addition, contact angle measurements confirmed the modification of the PET carriers. The water contact angle decreased from 43 ° to 27 ° after corona treatment due to the establishment of polar groups on the carrier surface. After silanization, the water contact angles increased to 65-85 ° (see Table 20), depending on the respective adhesion promoter. This was attributed to the formation of hydrophobic siloxane layers and the apolar residues R reaching away from the carrier surface.

Table 20: Water contact angles of unmodified but etched, corona treated and carriers modified with 3-MAPTMS, 3-APTMS or TMESI² BAPO

sample	water contact angle [°]
unmodified but etched carrier	43.0 ± 1.6
corona treated carrier	27.2 ± 5.9
3-MAPTMS modified carrier	65.8 ± 3.7
3-APTMS modified carrier	77.5 ± 4.8
TMESI² BAPO modified carrier	84.6 ± 2.6

-Results and discussion, Improvement of the removability by the use of adhesion promoters-

6.1.2. Covalent attachment of the adhesive layer to the modified carriers

Adhesive layers based on acryl_1 and DPEPHA were applied onto the modified carriers according to *method I* and *method II* as described in chapter 6.2.2. DPEPHA adhesives were chosen due to their moderate reaction rate, which allows for good adjustment of the tack during pre-crosslinking, the high functionality of the multifunctional monomer and their superior performance in previous adhesion experiments. As shown schematically in Figure 61, covalent attachment of the PSA layers was achieved via UV-irradiation, initiating chemical reactions between the organofunctional groups of the immobilized adhesion promoters and the adhesive. More precisely, the unsaturated C=C moieties of 3-MAPTMS and 3-APTMS or the photo cleavable groups of TMESI2 BAPO, respectively, participated in the free radical crosslinking reaction of DPEPHA and were therefore covalently bound to the resulting semi-IPN.

As a consequence, improved adhesion strength at the PSA-carrier interface and thus clean peel from the substrates at application temperatures even higher than 160 °C was expected. Since immobilized silanes are stated to form open polymeric structures, which are easily to penetrate [60], it was suggested that interdiffusion of the adhesion promoting layer and the PSA further enhanced the interactions at the interface. [21,53]

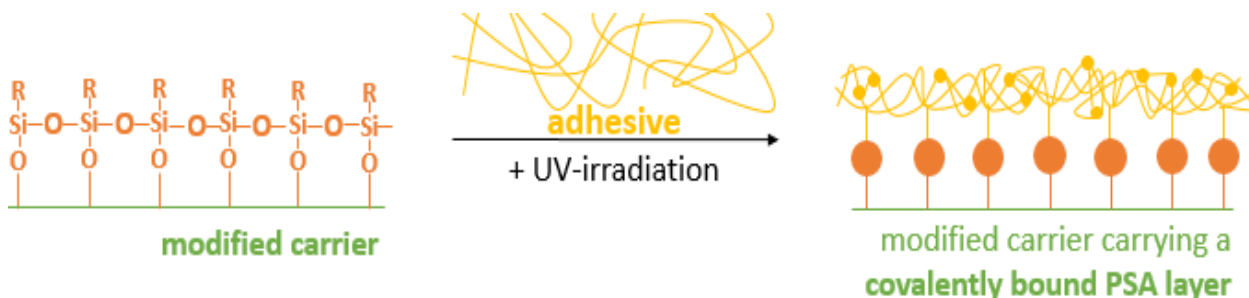


Figure 61: Scheme of covalent attachment of the adhesive layer to the modified PET carriers

6.1.3. Adhesion strength of the PSA tapes

Since reliable fixation during application and easy peel by debonding on demand were required, the photo-triggered release was characterized by means of peel strength tests prior to and after UV-irradiation. Adhesive layers comprising acryl_1, 20 wt% DPEPHA and 1 wt% Lucirin TPO-L (adhesive 6) were applied to unmodified and modified carriers either according to *method I* or *method II*. The tapes were adhered to tarnish protected copper (Cr-Zn coated) and peeled off at a constant speed of 300 mm/min and an angle of 90 °. [6]

-Results and discussion, Improvement of the removability by the use of adhesion promoters-

The peel speed of 300 mm/min was chosen according to common test methods of industrial manufacturers.

As already discussed in chapter 6.3.4, the initial tack of the PSA tapes was influenced significantly by the preparation method and the resulting crosslinking gradients, which developed during pre-crosslinking. In general, *method I* tapes were less tacky than those prepared by *method II*. This was also reflected by peel strength tests, where the peel strength of *method I* tapes was already below the calibration range ($< 1\text{N}$) after pre-crosslinking. The peel strength of *method II* tapes ranged from 1.5 to 2.5 N/cm - independent of the application of adhesion promoters - and were reduced significantly upon UV-irradiation ($< 0.50\text{ N/cm}$) as a result of IPN formation and the accompanied increase of cohesion and T_g ($-32\text{ }^\circ\text{C}$ to $57\text{ }^\circ\text{C}$). Although pre-crosslinking already increased the T_g of the PSA (see DSC measurements in chapter 6.2.1), the adhesive strength of *method II* tapes was not reduced markedly. This was explained by the crosslinking gradient, which arises from the preparation procedure, where the tapes were pre-crosslinked from the backside of the carrier.

Alternatively, the surface tack of *method I* tapes was measured by pressing them onto tarnish protected copper substrates (25 N, 90 s) and subsequent detrack at constant speed (300 mm/min). [121] However, the results showed high deviations within the series of one adhesion promoter and no distinct reduction of tack after UV-curing. The surface tacks ranged from 0.5 to 1 N/cm² for both, the pre-crosslinked and irradiated tapes (data not shown). Difficulties with the central and contactless application of the PSA tape (without touching the adhesive layer) to the die were seen as the predominant source for the high deviations.

6.1.4. Performance of tapes with modified carriers

So far, residue-free peel from BondFilm® substrates was limited to application temperatures of 160 °C, while clean removability from pristine and tarnish protected copper was possible after storage at temperatures of $\geq 200\text{ }^\circ\text{C}$. Since BondFilm® is the most challenging and most important surface for the desired application, it was important to go beyond this limitation. Therefore, corona treated PET carriers were modified with 3-MAPTMS, 3-APTMS or TEMSI² BAPO (see Figure 58), to covalently attach the adhesive layer to the carrier and hence to provide increased cohesion within the tape. Adhesive formulations containing acryl_1, 20 w% DPEPHA and 0.75-1 wt% Lucirin TPO-L (adhesives 5 and 6) were applied to the modified carriers according to *method I* (30 μm)

-Results and discussion, Improvement of the removability by the use of adhesion promoters-

and *method II* (90 μm). All tapes were pre-crosslinked with a UV-dose of 80 mJ/cm^2 and comprised satisfying tack. In order to investigate the adhesion performance and the removability of the tapes, they were applied onto BondFilm® substrates and UV-cured with 1000 mJ/cm^2 . In addition, the performance on pristine copper, tarnish protected copper was also investigated. The samples were stored for 1 hour at a selected temperature in the range of 160 -240 $^{\circ}\text{C}$, cooled to rt and peeled off manually. To demonstrate the effect of the adhesion promoters, the results were compared to the performance of tapes prepared on unmodified, corona treated carriers.

As depicted in Figure 62, the peel performance of *method I* tapes was improved by the use of modified carriers. Surface modification with TMESI² BAPO allowed for residue-free removability from **Bondfilm**® substrates after storage at 180 $^{\circ}\text{C}$, which is 20 $^{\circ}\text{C}$ above the maximum application temperature of the corresponding unmodified tapes. Moreover, modification with 3-APTMS enabled improved, but not completely clean peel after storage at 170 $^{\circ}\text{C}$. In contrast, this trend was not observed for *method II* tapes, which left residues after temperature storage (180 $^{\circ}\text{C}$), independent of the carrier modification. The divergent results for *method I* and *method II* tapes were attributed to the different approaches in pre-crosslinking. As already explained above (see chapter 6.3.4), *method I* tapes comprise higher crosslinking gradients at the surface of the adhesive layer than tapes prepared by *method II*. This prevents the PSA from excessive penetration into the substrate morphology and avoids residues, which result from insufficient deformability of the PSA during peel (see also chapter 6.2.2). Thus it was concluded, that the preparation method and the surface morphology are still the dominating factors here.

-Results and discussion, Improvement of the removability by the use of adhesion promoters-

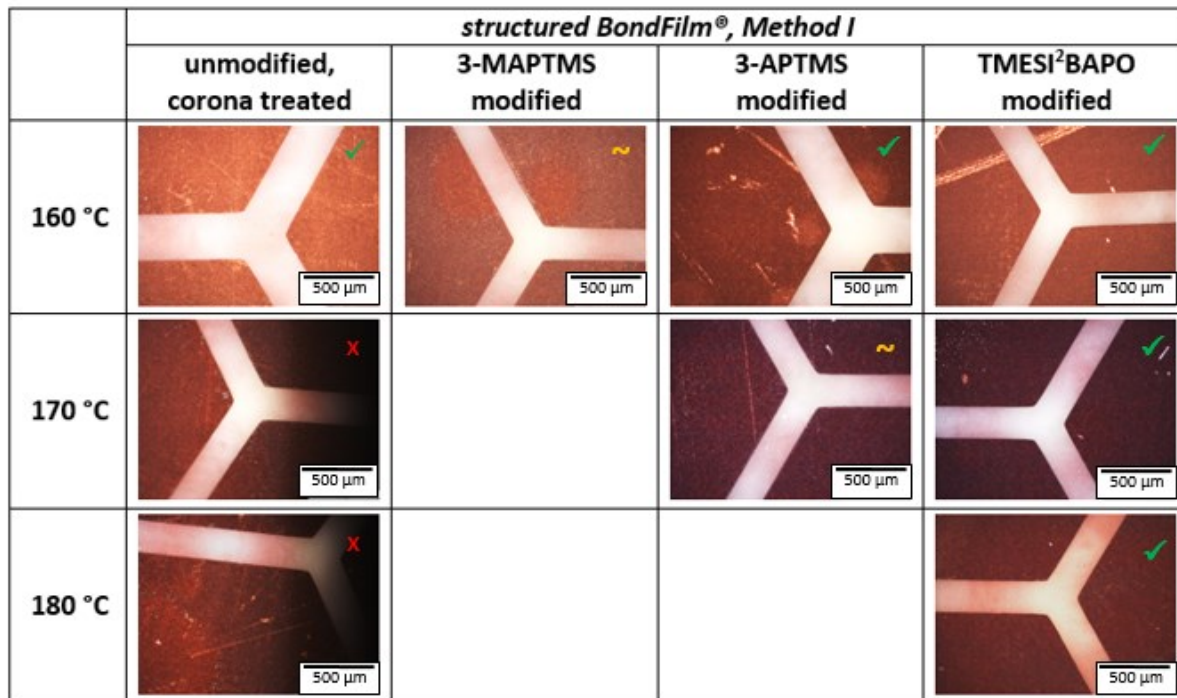


Figure 62: BondFilm® substrates after temperature storage and removal of PSA tapes as a function of carrier modification

The improved peel performance of TMESI² BAPO modified tapes within the series of *method I* tapes arises from efficient coupling of the PSA to the carrier and enhanced crosslinking throughout the adhesive layer. This was rendered possible by the UV-induced photolysis of BAPO, which results in up to four radicals (see Figure 63). [209] The highly reactive phosphinoyl radicals remain attached to the carrier, where they react with adjacent DPEPHA monomers, building covalent bonds between the adhesive and the carrier. Moreover, they contribute to the overall polymerization of the PSA layer, starting from the carrier-adhesive interface. On the contrary, the mesityl radicals are cleaved from the immobilized molecules and diffuse through the adhesive layer, where they initiate polymerization of DPEPHA monomers, although less effectively than the phosphinoyl radicals (also from Lucirin TPO-L). [205] Briefly spoken, the modification with TMESI² BAPO provided coupling sites for the covalent attachment of the adhesive layer and led to an increase of the total PI concentration. The combination of high amounts of growth centers with the highly functional monomer (penta/hexa acrylate) resulted in dense networks comprising increased cohesion within the PSA layer. Consequently, the resistance against peel forces and shearing over sharp edges of BondFilm® substrates during tape removal was improved.

-Results and discussion, Improvement of the removability by the use of adhesion promoters-

The reason for the superior performance of TMESI² BAPO over the other two adhesion promoters originates from differences in the reaction mechanisms. Attachment of the adhesive to 3-MAPTMS and 3-APTMS modified carriers occurs via the unsaturated (meth) acrylic moieties, which participate in the polymerization reaction of DPEPHA, induced by the photolysis of Lucirin TPO-L. Since 3-MAPTMS and 3-APTMS do not generate additional radicals during UV-irradiation, the PSA layer and the adhesive-carrier interface expected to be less densely crosslinked compared to TMESI² BAPO tapes. In addition, mechanical interactions can be considered, where the bulky groups of TMESI² BAPO may more effectively interdiffuse with the adhesive polymer network than the shorter and less branched segments of 3-MAPTMS and 3-APTMS. [53]

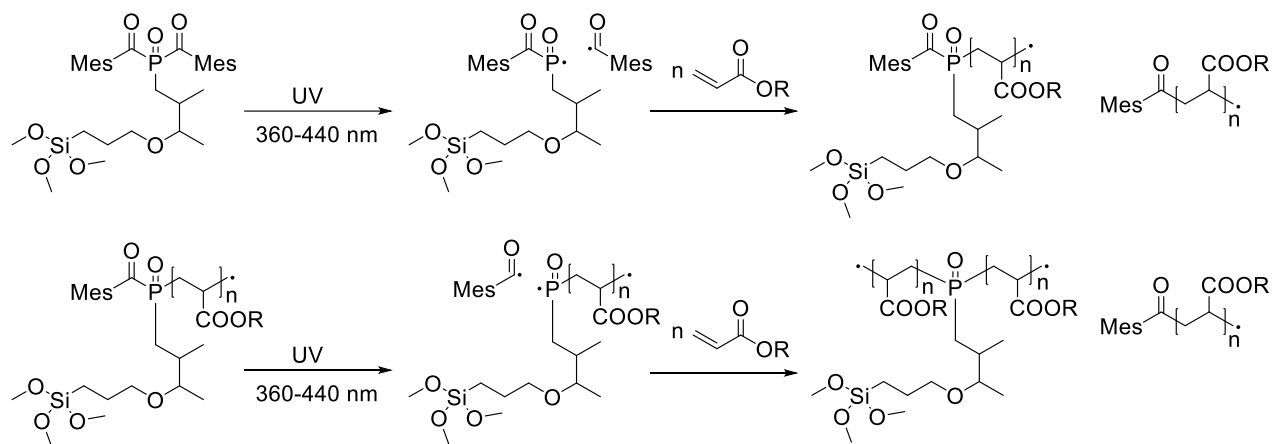


Figure 63: Schematic description of the photolysis of TMESI² BAPO and initiated polymerization of acrylic monomers [205]

Experiments on **tarnish protected copper** revealed that the use of TMESI² BAPO modified carriers in the preparation of *method II* tapes increased the maximum application temperature by 20 °C compared to unmodified (etched) carriers ($T_{\max} = 220^{\circ}\text{C}$). The irradiated part of the tape was removed without residues after storage at 240 °C. Again TMESI² BAPO performed better than 3-MAPTMS and 3-APTMS (see Figure 64), due to enhanced crosslinking at the adhesive-carrier interphase (tightly bound to carrier) and increased cohesion throughout the PSA layer (for details see above, experiments on BondFilm® substrates). However, no improvement was observed with modified *method I* tapes, for which the maximum application temperature on tarnish protected copper remained <160 °C.

As already mentioned in chapter 6.3.4, the reason for the superior performance of *method II* tapes on tarnish protected copper was not clarified and requires further

-Results and discussion, Improvement of the removability by the use of adhesion promoters-

research. However, no experiments with regard to the reproducibility or investigation of this effect were done, since the main focus was set to the removability from BondFilm® substrates anyway.

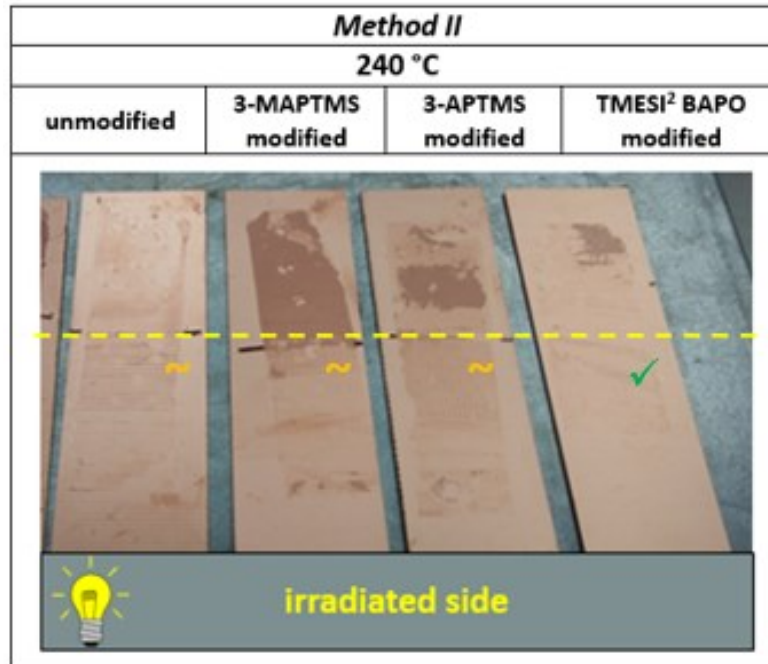


Figure 64: Tarnish protected copper substrates after temperature storage and removal of PSA tapes as a function of carrier modification

In contrast to the results of adhesion experiments on tarnish protected copper substrates, the use of adhesion promoters did not affect the removability from **pristine copper**. All the tapes prepared according to *method I* were removed without residues after application at up to 180 °C and all *method II* tapes were peeled cleanly after storage at 200 °C, irrespective of whether the carrier was modified or not. Still the surface quality was seen as the predominant factor, determining the peel performance. Again, the pristine copper substrates oxidized partially during temperature storage (see Figure 65). As already explained in chapter 6.3.4, this is a consequence of either low surface tack, based on irradiation on top of adhesion layer (*method I*), or of discontinuous adhesive layers, which may result from imperfect transfer during lamination (*method II*). The only residues found on these samples were located at the edges of the oxidized areas due to mechanical interlocking of the PSA with the rough and porous copper oxide areas [181,182]. However, these residues are not seen as representative, since ideal adhesion to the

-Results and discussion, Improvement of the removability by the use of adhesion promoters-

substrate would prevent oxidation of the substrate and consequently the development of adhesive residues.

Moreover, it was striking that all tapes were easily and (almost) cleanly removed from both, the irradiated and the non-irradiated part of pristine copper substrates. Since this was observed independently of preparation method, carrier modification and type of adhesion promoter, it was suggested that (further) crosslinking of DPEPHA and the related release of the PSA tape was initiated by a trigger different to UV-irradiation. Thermally induced polymerization was excluded, because the effect did not occur for similar tapes on other substrates. Due to the fact that this phenomenon was limited to pristine copper, a catalytic effect of copper ions, which are typically present on metallic copper exposed to air [210], on the radical polymerization of acrylic PSA formulation was considered. According to literature, Cu(I)-complexes and copper halides such as CuBr are used as catalysts in atom transfer radical polymerizations (ATRP) of vinyl, methacrylic and acrylic monomers. [211–213]

Besides the above mentioned reasons for surface oxidation of the pristine copper substrates (see chapter 6.3.4), also the copper ion induced polymerization may be considered. This additional and uncontrolled crosslinking of the PSA layer caused release beyond the desired extent, leading to complete loss of tack in some parts of the tape and to a lift off from the substrate. Thereby, parts of the copper surface were not covered by the PSA and were thus prone to oxidation in the hot air atmosphere during temperature storage.

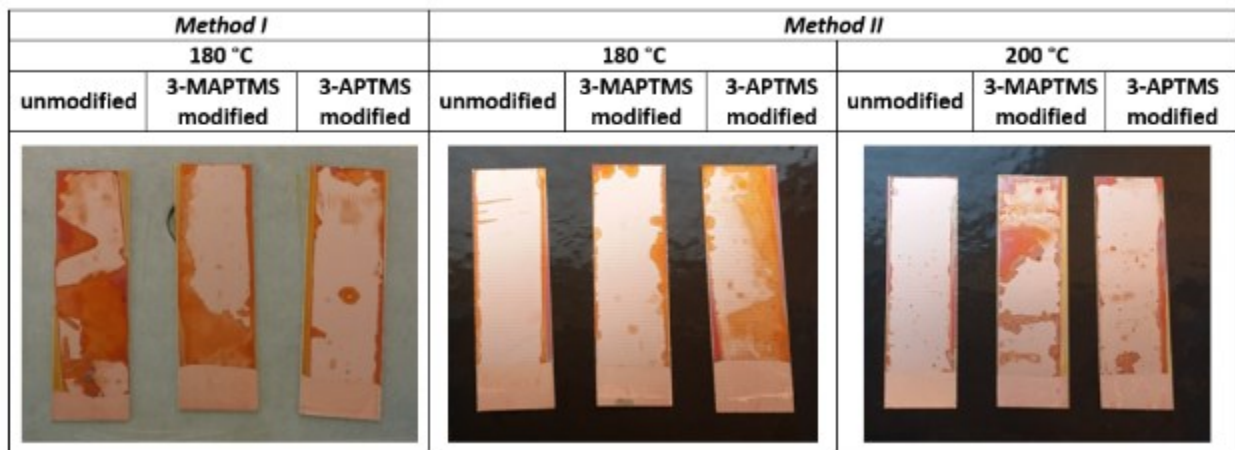


Figure 65: Pristine copper substrates after temperature storage and removal PSA tapes as a function of carrier modification

-Results and discussion, Improvement of the removability by the use of adhesion promoters-

6.1.5. Conclusion about the application of adhesion promoters and their impact on the removability of the tapes

Based on the improvement of removability achieved with corona treatment, the adhesive-carrier interface was further strengthened by the use of adhesion promoters. The PET carriers were modified with three different organosilanes (3-MAPTMS, 3-APTMS or TMESI² BAPO) in a two-step mechanism. Firstly, the silanes were hydrolyzed to the corresponding silanols, which adsorbed to the polar surface of the corona treated PET films. In the following drying step, the adhesion promoters were chemically attached to the carriers by condensation reactions of the silanols with superficial hydroxyl groups. Covalent attachment of the adhesive layer was achieved during UV-induced radical polymerization, involving the unsaturated C=C double bonds of 3-MAPTMS and 3-APTMS or the photo-cleavable group of TMESI² BAPO, respectively. In addition, interdiffusion of the cured adhesive and the siloxane layer contributed to adhesion at the PSA-carrier interface.

Successful application of the adhesion promoters was proven by XPS measurements, where characteristic binding energies of the organosilanes were detected on the silanized samples. These included signals at 284.1 eV in the C1s spectra and at 102.4 eV in the Si2p spectra, which are characteristic for CH₂-CH₂-Si-O and C-Si-O bonds, respectively. Additional signals at 131.8 eV (P-C) and 133.0 eV (P-O) in the P2p spectrum were found on TMESI² BAPO modified carriers, originating from the phosphine oxide moiety. Moreover, contact angle measurements showed a significant increase of the water contact angle from 43 ° to 65-85 ° after surface modification.

The modified carriers were used to prepare PSA tapes according to *method I* and *method II*. Based on previous results, the applied adhesive formulations consisted of acryl_1, 20 wt% DPEPHA and 0.75-1 wt% Lucirin TPO-L. The adhesive force of modified and unmodified tapes was determined in peel strength tests on tarnish protected copper at a speed of 300 mm/min and an angle of 90 °. While the results for *method I* tapes were below the detection limit (< 1N) due to on-top irradiation, the adhesive strength for *method II* tapes was in the range of 1.5-2.5 N/cm and was reduced significantly upon UV-irradiation (< 0.50 N/cm) as a result of IPN formation. Moreover, the prepared tapes were applied to BondFilm® substrates as well as to tarnish protected and pristine copper in order to investigate the impact of the adhesion promoters on the removability of the tapes after storage at high temperatures (160-240 °C). The results showed, that substrate morphology and preparation method were still the most influencing factors, determining peel performance. For the application on BondFilm® surfaces, *method I* tapes were still advantageous over those prepared by *method II*, because of the on-top UV-irradiation

-Results and discussion, Improvement of the removability by the use of adhesion promoters-

during pre-crosslinking and the associated limited penetration into the surface morphology. However, within the series of *method I* tapes, the application of TMESI² BAPO improved the removability from Bondfilm® and enabled clean peel after storage at 180 °C. The maximum application temperature was increased by 20 °C, compared to tapes based on unmodified, corona treated carriers. The effect of TMESI² BAPO was attributed to the generation of phosphinoyl and mesitoyl radicals by the photolysis of the BAPO moiety, which led to strong linkages at the adhesive-carrier interface and increased cohesion throughout the adhesive layer, based on enhanced crosslinking of DPEPHA.

Also, the general trend for the removal from tarnish protected copper and pristine copper did not change by the use of adhesion promoters. As already observed for unmodified tapes in chapter 6.3.4, tapes prepared by *method II* performed better on these substrates and the impact of the preparation method was less pronounced on pristine copper. the peel performance from pristine copper was not affected at all, the removability of *method II* tapes from tarnish protected copper was improved by carrier modification with TMESI² BAPO. The maximum application temperature was increased to 240 °C, which is 20 °C above the value for the corresponding unmodified, corona treated tapes.

7. Conclusion

A UV-curable pressure sensitive adhesive (PSA) tape for temporary application in the microelectronic industry was developed. The requirements included high thermal stability (up to 200 °C) and high initial tack as well as easy and clean peel in the end of the application. These contradictory demands are combined in one PSA by adjustment of adhesive composition and the incorporation of a UV-release function, allowing for debonding on demand.

Acrylic copolymers were synthesized in a free radical polymerization and used as basic adhesive materials. The chemical composition of the copolymers was varied in order to adjust the adhesive properties, to increase the thermal stability by the introduction of aromatic monomers or isobornyl acrylate and to introduce reactive sites for UV-crosslinking (vinyl side chain, side chain functionalization). Moreover, the polarity of the adhesive was reduced by removal of acrylic acid to prevent strong interactions with polar substrates such as metals. In addition, polyether adhesives were synthesized from mono-epoxy monomers, providing high thermal stability via the polyether backbone and acrylic sides chains for UV-reactivity. The main and side chain modifications of the synthesized adhesive polymers were proven by Fourier-transformed infrared spectroscopy (FT-IR) and nuclear magnetic resonance spectroscopy (NMR). The acrylic copolymers were characterized by glass transition temperatures (T_g s) in the range of -40 °C to -30 °C (differential scanning calorimetry, DSC), thermal stabilities up to 330-370 °C (thermogravimetric analysis, TGA) and broad poly dispersion indices (gel permeation chromatography, GPC), which offer good adhesion (short chains) and the necessary cohesion (long chains), which are required for the application as a PSA. Against our expectations, the polyethers did not show superior thermal stability over the acrylic copolymers, but decomposed at similar temperatures (336 °C).

The basic adhesive system was elaborated in screening experiments. Acrylic copolymers, were blended with multifunctional acrylates and the photoinitiator Lucirin TPO-L to give photo-curable PSAs, which reduce their adhesive strength due to the formation of semi-interpenetrating networks (IPNs). Moreover, crosslinking is related with an increase of cohesion, enabling easy peel and clean removability on demand. Network formation was proven by DSC measurements, showing an increase of the T_g value after UV-exposure. While the initial tack of the PSA was governed by the linear structure of the acrylic copolymers ($T_g = -32^\circ\text{C}$ for acryl_1), the semi-IPN dominated the adhesive properties after UV-crosslinking ($T_{gON} = 60^\circ\text{C}$). Furthermore, the thermal stability of the PSAs was slightly improved by UV-crosslinking. According to TGA measurements, the cured adhesives comprised similar T_{ON} as the basic acrylic copolymer (acryl_1), while T_{END} shifted to higher

-Conclusion-

temperatures for highly crosslinked systems (high monomer contents, short spacers). This means that the complete decomposition of the cured PSA was retarded by the formation of semi-IPNs.

Since the adhesion performance strongly depends on the chemical composition of the PSA, the influence of the basic acrylic copolymer, the structure and the concentration of the multifunctional acrylic monomers as well as the impact of the photoinitiator content on the photo-triggered release were investigated by FT-IR kinetic measurements. It was found that reduced interactions in the bulk of the basic adhesive polymer and high photoinitiator contents led to high final conversions of the C=C double bonds and high reaction rates. Moreover, multifunctional acrylic monomers with low functionality and long spacers increased the final conversion due to reduced steric hindrance, while bulky groups such as isobornyl side chains, reduced the final conversion.

PSA tapes were prepared by coating the adhesive formulations onto polyethylene terephthalate (PET) carriers. First experiments showed superior wetting and improved attachment of the adhesive on etched PET carriers. Furthermore, the evaporation of the solvent turned out to be essential to achieve clean removability and effective UV-release. In order to prevent excessive penetration of the substrates, which is often related to cohesive failure of the PSA, the adhesive layer was pre-crosslinked after coating. The applied irradiation dose for pre-crosslinking and UV-release were adjusted individually, depending on the adhesive formulation, to ensure sufficient tack and adhesive strength during use as well as efficient debonding in the end of the application. Finally, two methods for the preparation of PSA tapes were developed. With *method I* the adhesive formulation is directly coated onto the carrier, dried and pre-crosslinked. With *method II*, in contrast, the PSA is applied to a release liner, dried and subsequently transferred to the carrier via hot lamination. Pre-crosslinking is done through the release liner.

The performance and the removability of different PSA tapes were investigated in adhesion experiments, where the tapes were laminated onto the substrates and subsequently peeled off manually after adhesion at rt or storage at elevated temperatures (140 °C - 240 °C). The revealed substrate surfaces were evaluated with regard to adhesive residues by means of optical light microscopy. In course of these experiments, the impact of the nature of the substrate, the chemical composition of the PSA layer as well as the influence of carrier pre-treatment, the irradiation dose and the preparation method was examined. The results showed that BondFilm® treated copper was the most challenging substrate for clean peel due to the adhesion promoting layer and the high level of superordinate structures on its surface, which make it prone to mechanical and chemical interactions with the adhesive layer. These interactions were found to be the main cause

-Conclusion-

for adhesive residues, especially after application at high temperatures, where the viscosity of the adhesive is reduced and penetration of the substrate microstructure is enhanced. Concerning the chemical composition, higher tack and improved removability were observed for PSAs with low T_g and in the absence of bulky groups, which sterically restricted UV-crosslinking. Moreover, a direct correlation of the monomer functionality and the maximum application temperature was observed. Adhesive formulations containing highly functional monomers were associated with higher crosslinking densities and T_g values and consequently with a higher resistance against penetration of the substrate microstructure. In addition, adhesion experiments revealed that increased monomer contents of 20-50 wt% led to improved removability, independent on the structure of the multifunctional acrylate. The photoinitiator concentration was optimized to 0.75-1 wt%, preventing residues caused by over- and under-cure of the PSA layer. Another important factor concerning the cure of the PSA, is the adjustment of the irradiation dose applied during pre-crosslinking and UV-release. Further improvement of the removability was achieved by corona treatment of the carrier. Based on roughening and oxidation of the surface, the interactions and the bonding between the adhesive layer and the carrier were significantly increased. Last but not least, the performance and the removability of the tapes were influenced by the preparation method. Due to the different procedures, *method I* and *method II* tapes comprise different crosslinking gradients. Although the on top irradiation of *method I* tapes reduced the surface tack, it also limited penetration of the adhesive into the microstructure of the substrate and thus enabled superior performance on BondFilm® treated copper. In contrast, *method II* tapes were only cleanly removable from less challenging substrates (tarnish protected copper and pristine copper). Finally, residue-free peel from BondFilm® treated copper after application at 160 °C was realized by tapes based on acryl_1, 20 wt% of DPEPHA or DTMPTA and 1 wt% Lucirin TPO-L, prepared by *method I* on corona treated PET carriers.

The max. application temperature of the developed PSA tape was further increased by the application of adhesion promoters, which additionally strengthened the adhesive-carrier interface. Therefore, three different organosilanes were chemically attached to corona treated carriers in a two-step mechanism, encompassing the hydrolysis of methoxy groups and the condensation of the resulting silanols with superficial hydroxyl sites on the carriers. Subsequently, the coated PSA layers were covalently attached to the modified carriers during UV-irradiation, where either the unsaturated C=C moieties or the photoactive groups (bis(acylphosphane)oxide, BAPO) of the organosilanes were polymerized with the multifunctional acrylic monomer in a free radical mechanism. Surface modification was proven by XPS spectroscopy, where characteristic signals at 284.1 eV (CH₂-CH₂-Si-O), 102.4 eV (C-Si-O), 131.8 eV (P-C) and 133.0 eV (P-O) in the C1s, Si2p and P2p spectra indicated the presence of the respective organosilanes. In addition, the water contact

angle was increased from 43 ° to 65-85 ° after surface modification. The modified carriers were used to prepare PSA tapes containing 20 wt% of the penta/hexa functional acrylate and 0.75-1 wt% photoinitiator according to *method I* and *method II*. The adhesive strength of *method I* tapes was below the detection limit of 1 N due to on top irradiation. The adhesive strength of *method I* tapes in contrast, amounted to 1.5-2.5 N/cm and was reduced significantly to < 0.5 N/cm upon UV-irradiation. The impact of the adhesion promoters on clean removability was investigated in adhesion experiments at temperatures of 160-240 °C. The results showed that the substrate morphology and the preparation method were still the dominating factors determining peel performance. However, carrier modification with TMESI² BAPO (organosilane with photoactive groups) increased the maximum application temperature of *method I* tapes on BondFilm® treated copper to 180 °C. This was explained by the strengthening of the adhesive-carrier interface, resulting from the covalent attachment of the PSA, and increased cohesion throughout the adhesive layer, which is based on enhanced crosslinking of the highly functional acrylate by the mesityl radicals (photolysis of BAPO). In addition, a similar improvement was obtained for TMESI² BAPO modified *method II* tapes. Although clean removability was still limited to tarnish protected and pristine copper substrates, the maximum application temperature on tarnish protected copper was increased from 220 °C to 240 °C.

To sum up, the major achievements of this thesis are:

- The development of a PSA tape, which provides high thermal stability as well as clean removability on demand, which was realized by the UV-triggered formation of semi-IPN in acrylic adhesives, based on an acrylic copolymer, multifunctional acrylic crosslinkers and a photoinitiator.
- A detailed insight in the reaction kinetics of the developed adhesive system, with respect to the influence of to the structure of the basic copolymer, the type and concentration of the multifunctional crosslinker and the photoinitiator concentration.
- The elucidation of the impact of the nature of the substrate, the chemical composition of the adhesive and various processing parameters, including carrier pre-treatment, irradiation dose and preparation method, on the performance of the PAS tape.
- The identification of enhanced penetration of the substrate microstructure and the related intense mechanical and chemical interactions by the PSA as the main cause for residues at high temperature applications.
- The improvement of the maximum application temperature of the designed PSA tape by surface modification of the PET carrier with the TMESI² BAPO, which enables covalent attachment of the PSA layer and consequently strengthened adhesive-substrate interfaces.

8. Outlook

In this work, an acrylic based PSA tape comprising high thermal stability and residue-free removability on demand was developed. Therefore, an acrylic copolymer was blended with multifunctional acrylic monomers and a photoinitiator. Upon UV exposure, photo-induced crosslinking leads to the formation of semi-IPN, which is related with increased molecular weights, T_g s and cohesion as well as with the reduction of the adhesive strength.

Alternative approaches for the preparation of thermally stable and cleanly peelable PSAs, include the use of silicon acrylates, which resist high temperatures due to the siloxane backbone and provide UV-crosslinkable acrylic side chains for release on demand. [214] Moreover, the use of polymerizable photoinitiators [34], which are incorporated into the main chain of the adhesive polymer, is expected to improve residue-free removability of the PSA, since all compounds of the adhesive formulation are covalently connected (crosslinked) after UV-polymerization. In addition, alkyne compounds may be considered as crosslinking agents. Compared to the acrylic monomers (C=C) used in this work, the C≡C triple bond of alkynes is suggested to form networks of even higher crosslinking density and consequently to contribute to a more efficient release on demand.

Based on the work of Pang et al., who applied vinylated graphene-oxide to an acrylic PSA, the incorporation of modified nanoparticles represents an interesting approach to increase the thermal stability of adhesive systems. [24]

9. List of Figures

Figure 1: Process for embedding microelectronic components in a PCB by the use of a PSA tape.....	4
Figure 2: Classical adhesion theories.....	7
Figure 3: Classification of adhesive systems according to their chemical base, setting mechanism, application temperature and form of application	19
Figure 4: Reactions of one component polymerization adhesives [60].....	24
Figure 5: Curing reaction of polyaddition epoxy adhesives [60].....	25
Figure 6: Curing reactions of PUR polyaddition adhesives [60]	27
Figure 7: Curing reactions of phenol formaldehyde polycondensation adhesives [60] ...	28
Figure 8: Curing reactions of melamine-formaldehyde polycondensation adhesives [60]	29
Figure 9: Curing reactions of polycondensation silicone adhesives [60]	31
Figure 10: Curing reaction of polycondensation polyamide adhesives.....	32
Figure 11: Construction of single- and double sided tapes.....	42
Figure 12: Schematic reaction mechanisms of radical, cationic and anionic polymerization	46
Figure 13: Mechanism of free radical chain growth involving initiation, propagation and termination reactions as well as oxygen inhibition [99]	47
Figure 14: Mechanism of free radical addition involving initiation, propagation and termination reactions [99,100].....	48
Figure 15: Generation of free radicals according to type I and type II processes [100] ...	49
Figure 16: Formation of photo acid by heterolytic and homolytic cleavage of a triaryl sulfonium salt (PAG)	50
Figure 17: Reaction mechanism of cationic ring opening polymerization [100].....	51
Figure 18: Construction of single-sided, double-sided and multilayer PCBs	55
Figure 19: Manufacture of PCBs - inner-layer core	57
Figure 20: Manufacture of PCBs - outer-layers.....	58
Figure 21: Manufacture of PCBs: application of solder.....	59
Figure 22: Copolymerization reaction of acryl_1	72
Figure 23: Side chain functionalization of acryl_1.....	73
Figure 24: Polymerization reactions of polyether_1, polyether_2 and polyether_3.....	75
Figure 25: Experimental Set-up of surface tack measurements	81
Figure 26: Free radical polymerization of acrylic monomers.....	85
Figure 27: Proposed reaction mechanism for the side chain functionalization of acryl_1: (1) TMAB induced ring opening reaction of the epoxy moiety in GMA, (2) generation of	

-List of Figures-

carboxylate group and (3) displacement of Br ⁻ by nucleophilic attack and regeneration of TMAB. [138]	88
Figure 28: FT-IR-spectrum of acryl_1	89
Figure 29: ¹ H-NMR spectrum of acryl_1	91
Figure 30: Schematic illustration of the composition of acryl_1-6	94
Figure 31: Determination of the degradation onset and end temperature from the weight loss curves (TGA) as the intersections of the tangent with the horizontal lines before and after the degradation step	95
Figure 32: TGA thermogram of acryl_5 showing a 2-step degradation	95
Figure 33: Mechanism for cationic ring opening by the use of boron trifluoride ethylamine complexes (BF ₃ : NH ₂ CH ₂ CH ₃) including two competing chain growth mechanisms: activated chain end (ACE) and activated monomer(AM) [117,146,147]	96
Figure 34: FT-IR-spectrum of polyether_1	98
Figure 35: Photo-triggered release mechanism of acrylic PSAs	101
Figure 36: Scission of Lucirin TPO-L and generation of benzoyl- and phosphinyl-radicals	102
Figure 37: Structures of the photoinitiators Lucirin TPO-I, Irgacure 379 and Irgacure 819	102
Figure 38: Structures of multi-functional acrylic monomers used for the preparation of adhesive films	104
Figure 39: (a) FT-IR spectrum of adhesive 1 (acryl_1, 10 wt% DPEPHA, 1 wt% Lucirin TPO-L) as a function of irradiation dose. Decrease of the peak at 985 cm ⁻¹ related to the C=C double bond of the acrylic moieties. (b) Estimation of the polymerization rate by determination of the slope of the initial portion of the irradiation time-conversion plot at the representative example of adhesive 1	105
Figure 40: Conversion of C=C double bonds in adhesive layers based on (a) 10 wt% DPEPHA and 1 wt% Lucirin TPO-L as a function of the structure of the basic adhesive polymer, (b) acryl_1 containing as a function of the photoinitiator concentration at a constant DPEPHA concentration of 10 wt%, (c) acryl_1 as a function of the monomer concentration at a photoinitiator concentration of 1 wt%, (d) acryl_1 containing 10 wt% TMPTA, SR 454 or SR 492 and 1 wt% Lucirin TPO-L monitoring the impact of the monomer structure within the series of tri-functional acrylates, (e) acryl_1 containing 10 wt% PETA, SR 494 or DTMPTA and 1 wt% Lucirin TPO-L monitoring the impact of the monomer structure within the series of tetra-functional acrylates	110
Figure 41: DSC measurements of DPEPHA adhesives (cooling curves)	112
Figure 42: Heat flow of adhesive 6 (20 wt% DPEPHA + 1 wt% PI) heated to (a) 100 °C and (b) 300 °C	113

-List of Figures-

Figure 43: (a) Thermograms of adhesive formulations as a function of the monomer structure. (b) First derivatives of the temperature-weight-loss curves of adhesive formulations containing 10 wt% of different multifunctional monomers. (c) Thermograms of DPEPHA adhesives as a function of monomer and PI content. (d) First derivatives of the temperature-weight-loss curves of the DPEPHA adhesives. (e) Comparison of the thermograms of acryl_1 and adhesive 6 (20 wt% DPEPHA, 1 wt% Lucirin TPO-L) to demonstrate the improved thermal stability of the cured adhesive formulations. (f) Determination of the degradation onset and end point as the intersections of the tangents and the horizontal lines before and after the degradation steps..... 117

Figure 44: Left: Improvement of the removability and the UV-release mechanism by evaporation of the solvent. (a) Substrate after removal of tape prepared without drying step. (b) Substrate after removal of tape with dried adhesive layer. Right: Improvement of the removability by the use of chemically etched PET carrier. (c) Substrate after removal of tape prepared on non-treated PET (released part). (d) Substrate after removal of tape prepared on chemically etched PET (released part). 120

Figure 45: Differences in the extent of adhesive penetration of the substrate microstructure by (a) the uncured and (b) the pre-crosslinked PSA tape and the consequences during peel. 122

Figure 46: Preparation of PSA tapes. Step I: coating of the adhesive onto the carrier (method I) or onto the liner (method II), Step II: transfer of the adhesive layer via lamination on a hot base 123

Figure 47: Workflow of the two tape preparation methods 125

Figure 48: 3D images of tarnish protected copper, pristine copper, BondFilm® treated copper and cured epoxy, displaying the roughness of the substrates..... 130

Figure 49: Effect of pre-crosslinking on the removability of the tapes in dependence of the surface quality of the substrates..... 131

Figure 50: BondFilm® substrates after removal of tapes containing 10 or 20 wt% DPEPHA or DTMPTA and 1 wt% Lucirin TPO-L as a function of the basic adhesive copolymer.... 134

Figure 51: BondFilm® substrates after removal of tapes based on acryl_1, 10 wt% of multifunctional acrylate and 5 wt% Lucirin TPO-L as a function of the monomer structure 136

Figure 52: BondFilm® substrates after removal of tapes based on acryl_1, PETA, SR 494, DTMPTA or DPEPHA as a function of the monomer concentration..... 138

Figure 53: (Structured) BondFilm® substrates after removal of tapes based on acryl_1, 20 wt% DTMPTA or DPEPHA as a function of the PI concentration..... 140

Figure 54: Structured BondFilm® substrates after removal of tapes based on acryl_1, 15 wt% DPEPHA and 0.75 wt% Lucirin as a function of carrier pre-treatment with corona discharge 143

-List of Figures-

Figure 55: BondFilm® substrates after peel of under-cured, optimally cured and over-cured PSAs	145
Figure 56: Pristine copper substrates after storage at 180 °C comprising oxidized spots with adhesive residues.....	147
Figure 57: Mechanism of attaching silane coupling agents to substrate surfaces: hydrolysis (I) and condensation reaction (II) of organosilanes [184].....	153
Figure 58: Chemical structures of the organosilanes used for surface modification of the PET carriers.....	155
Figure 59: Attachment of adhesion promoters to the carrier surface – surface modification procedure.....	156
Figure 60: Deconvoluted XPS high resolution C1s, Si2p and P2p spectra of the corona treated and TMESI ² BAPO modified PET carriers.....	158
Figure 61: Scheme of covalent attachment of the adhesive layer to the modified PET carriers	160
Figure 62: BondFilm® substrates after temperature storage and removal of PSA tapes as a function of carrier modification.....	163
Figure 63: Schematic description of the photolysis of TMESI ² BAPO and initiated polymerization of acrylic monomers [205].....	164
Figure 64: Tarnish protected copper substrates after temperature storage and removal of PSA tapes as a function of carrier modification.....	165
Figure 65: Pristine copper substrates after temperature storage and removal PSA tapes as a function of carrier modification.....	166
Figure_A 1: ATR-FT-IR spectra of (a) acryl_4, (b) acryl_5, (c) acryl_6, and (d) acryl_1_scf.	199
Figure_A 2: ¹ H-NMR spectrum of acryl_5.....	200
Figure_A 3: ¹ H NMR spectrum of acryl_6.....	201
Figure_A 4: FT-IR spectra of (a) polyether_2 and (b) polyether_3.....	202
Figure_A 5: Weight loss curve of polyether_1 and determination of the degradation onset and end temperature	202
Figure_A 6: (a) Conversion of C=C double bonds in adhesive layers based on acryl_1 containing as a function of the photoinitiator concentration at a constant DTMPA concentration of 10 wt%. (b) Conversion of C=C double bonds in adhesive layers based on acryl_1 containing as a function of the photoinitiator concentration at a constant concentration of 10 wt% SR 494. (c) Conversion of C=C double bonds in adhesive layers based on acryl_1 as a function of the DTMPA concentration at a photoinitiator concentration of 1 wt%. (d) Conversion of C=C double bonds in adhesive layers based on	

-List of Figures-

acryl_1 as a function of the concentration of SR 494 at a photoinitiator concentration of 1 wt%.203

Figure_A 7: DSC measurements of different adhesive mixtures monitoring (a) the impact of the monomer : PI ratio and (b) the impact of the type of multifunctional acrylate.....204

Figure_A 8: (a) Thermograms of DTMPTA adhesives as a function of monomer and PI content. (b) First derivative of the temperature-weight-loss curves of the DTMPTA adhesives. (c) Thermograms of SR 494 adhesives as a function of monomer and PI content. (d) First derivative of the temperature-weight-loss curves of the SR 494 adhesives.205

Figure_A 9: Absorption spectra of the untreated and the chemically etched PET carrier206

Figure_A 10: BondFilm® substrates after removal of tapes based on acryl_1 and 50 wt% SR 480 and 5 wt% Lucirin TPO-L, which had been adhered at rt or stored at 150 °C.....206

Figure_A 11: Deconvoluted XPS high resolution C1s and Sip2 spectra of the unmodified, 3-MAPTMS and 3-APTMS modified carriers207

10. List of Tables

Table 1: Overview of intermolecular forces, the associated binding energies and operating distances [56,58–60]	6
Table 2: Differences between free radical and cationic photo-polymerization	52
Table 3: List of chemicals and the corresponding chemical structures	63
Table 4: Composition of the synthesized acrylic copolymers	72
Table 5: Composition of the synthesized polyether adhesives.....	74
Table 6: Composition of the applied adhesive formulations.....	77
Table 7: Results of ¹ H-NMR spectroscopy of acryl_1, acryl_5 and acryl_6: peak assignment [113,133,142]	91
Table 8: Molecular weight distributions of acryl_1, acryl_5 and acryl_6 including Mn, Mw and PDI.....	92
Table 9: Experimentally determined and calculated Tgs of the synthesized acrylic copolymers.....	94
Table 10: Degradation onset temperatures T _{ON} of the synthesized acrylic copolymers ...	95
Table 11: Summary of all data drawn from the reaction kinetics, including final monomer conversion, reaction rates (slope of the initial linear portion in the irradiation time-conversion curves) and the UV-irradiation dose required for the maximum monomer conversion.....	109
Table 12: Results of TGA measurements of the cured PSAs, including the onset (T _{ON}) and endpoint (T _{END}) of degradation as well as the point of maximum degradation rate (T _{MID})	116
Table 13: Surface composition of untreated and corona treated PET carriers determined by XPS measurements.	121
Table 14: Water contact angles of the PET carriers as a function of the applied corona dose and corresponding power out.....	121
Table 15: Average roughness and root mean square roughness (Sq) of tarnish protected copper, pristine copper, BondFilm® treated copper and cured epoxy substrates.....	128
Table 16: Chemical composition of tarnish protected copper, pristine copper, BondFilm® treated copper and cured epoxy surfaces.....	130
Table 17: Maximum application temperature of the tested adhesives systems based on acryl_1 as a function of monomer type	151
Table 18: Assigned peaks of the high resolution C1s, Si2p and P2p XPS spectra	159
Table 19: Chemical composition [at%] of the unmodified but etched, the corona treated and the modified carriers	159
Table 20: Water contact angles of unmodified but etched, corona treated and carriers modified with 3-MAPTMS, 3-APTMS or TMESI ² BAPO.....	159

-List of Tables-

Table_A 1: Glass transition temperatures of the acrylic compounds applied in the synthesis of the basic adhesive copolymers [120,127,132,178].....208

Table_A 2: List of FT-IR bands of acryl_1, acryl_4, acryl_5, acryl_6 and acryl_1_scf including peak assignment[139]..... 209

Table_A 3: List of FT-IR bands of polyether_1, polyether_2 and polyether_3 including peak assignment [139]210

Table_A 4: UV-doses for pre-crosslinking and photo triggered release applied in the experiments which displayed the impact of the PI concentration on PSA tape performance211

11. Literature

- [1] W. Brockmann, P. Ludwig Geiß, J. Kligen, S. Bernhard, Adhesive Bonding Materials, Applications and Technology, WILEY-VCH Verlag GmbH & Co KGaA, Weinheim, 2009.
- [2] Afera, PSA tape market data and trends: 2016 Freedonia Study, 2016. <https://www.afera.com/technical-centre/psa-tape-market-data-and-trends-2016-freedonia-study.html>.
- [3] MarketsandMarkets, Pressure Sensitive Adhesive Tapes Market by Resin type (Acrylic, Rubber, Silicone), Category (Commodity, Specialty), Backing Material (Polypropylene, Paper, PVC), Type, End-Use Industry, and Region - Global forecast to 2022, 2017. <https://www.giiresearch.com/report/mama569184-pressure-sensitive-adhesive-tapes-market-by-resin.html>.
- [4] M. Nerkar, Adhesive Tapes Market 2018: Industry Review, Research, Statistics, and Growth to 2022, 2018. <https://www.rednewswire.com/adhesive-tapes-market-2018-industry-review-research-statistics-and-growth-to-2022/>.
- [5] Z. Czech, A. Kowalczyk, J. Swiderska, Pressure-sensitive adhesives for medical applications, in: I. Akyar (Ed.), Wide Spectra Qual. Control, intech-open, 2011: pp. 309–332. doi:10.5772/67458.
- [6] G. Gierenz, W. Karmann, Adhesives and adhesive tapes, Wiley-VCH, 2001.
- [7] I. Benedek, M.M. Feldstein, Applications of Pressure-Sensitive Products, CRC Press Taylor & Francis Group, LLC, 2009.
- [8] A.S. Cantor, V.P. Menon, Pressure-Sensitive Adhesives, in: *Encycl. Polym. Sci. Technol.*, 2010: pp. 1–23.
- [9] I. Benedek, M.M. Feldstein, eds., Technology of pressure-sensitive adhesives and products, CRC Press Taylor & Francis Group, LLC, 2009.
- [10] Z. Czech, Synthesis and cross-linking of acrylic PSA systems, *J. Adhes. Sci. Technol.* 21 (2007) 625–635. doi:10.1163/156856107781192337.
- [11] C. Creton, Pressure-Sensitive Adhesives: An introductory Course, *Mrs Bull.* (2003) 434–439.
- [12] K.W. Kreckel, P.J. Hager, J.H. Rickert, Removable Adhesive Tape, US005516581A, 1996.
- [13] F. Von Trapp, ed., Wafer Dicing: A sticky Situation, *Int. Mag. Electron. Packag. Appl.* (2007) 38–43.
- [14] R. Puligadda, S. Pillalamarri, W. Hong, C. Brubaker, M. Wimplinger, S. Pragfrider, High-Performance Temporary Adhesives for Wafer Bonding Applications, in: *Mater. Res. Soc. Symp. Proc.*, 2007.
- [15] A. Hutchinson, Y. Liu, Y. Lu, Overview of disbonding technologies for adhesive bonded joints, *J. Adhes.* 93 (2017) 737–755. doi:10.1080/00218464.2016.1237876.

- [16] C. Kirsten, P. Christophlimek, R. Nonninger, H. Schirra, H. Schmidt, Lösbare Klebverbindungen, WO 00/73398 A1, 2000.
- [17] R.H. McCurdy, A.R. Hutchinson, P.H. Winfield, The mechanical performance of adhesive joints containing active disbonding agents, *Int. J. Adhes. Adhes.* 46 (2013) 100–113. doi:10.1016/j.ijadhadh.2013.06.001.
- [18] E. Inoue, T. Kasazaki, S. Kawahara, M. Yamamoto, K. Nagai, Adhesive tape for temporary attachment of green sheets for ceramic electronic devices and method for producing ceramic electronic devices, US 6,663,741 B1, 2003.
- [19] K. Suyama, H. Tachi, Photo-induced Decrosslinking in Pressure-sensitive Adhesives Composed of O -Acyloxime-based Photolabile Crosslinkers, *J. Photopolym. Sci. Technol.* 28 (2015) 45–48. doi:10.2494/photopolymer.28.45.
- [20] I. Benedek, *Pressure-Sensitive Adhesives and Applications*, 2nd ed., Marcel Dekker, Inc., New York, Basel, 2004.
- [21] A. V. Pocius, *Adhesion and Adhesives Technology - An Introduction*, 3rd ed., Carl Hanser Verlag, Munich, 2012. doi:10.3139/9783446431775.
- [22] H.-S. Joo, H.-S. Do, Y.-J. Park, H.-J. Kim, Adhesion performance of UV-cured acrylic pressure sensitive adhesives, *J. Adhes. Sci. Technol.* 20 (2006) 1573–1594. doi:10.1163/156856106778884271.
- [23] K. Bandzierz, L. Reuvekamp, J. Dryzek, W. Dierkes, A. Blume, D. Bielinski, Influence of network structure on glass transition temperature of elastomers, *Materials (Basel)*. 9 (2016). doi:10.3390/MA9070607.
- [24] B. Pang, C. Ryu, X. Jin, H. Kim, Preparation and properties of UV curable acrylic PSA by vinyl bonded graphene oxide, *Appl. Surf. Sci.* 285 (2013) 727–731. doi:10.1016/j.apsusc.2013.08.117.
- [25] N. Bhore, P. Mahanwar, Study of acrylic emulsion for ultraviolet curable pressure sensitive adhesives and its properties, *Pigment Resin Technol.* 40 (2011) 374–378. doi:10.1108/03699421111180518.
- [26] Z. Czech, M. Urbala, Application of novel unsaturated organosilane ethers in cationic UV-crosslinkable acrylic PSA systems, *Polimery*. 49 (2004) 837–840.
- [27] H.-H. Chu, C.-K. Wang, K.S. Chuang, C.-Y. Chang, Removable acrylic pressure-sensitive adhesives activated by UV-radiation, *J Polym Res.* 21 (2014). doi:10.1007/s10965-014-0472-x.
- [28] T. Ozawa, S. Ishiwata, Acrylate Copolymer/Ultraviolet Curable Oligomer Blends as Pressure-sensitive Adhesives, *J. Adhes.* 72 (2000) 1–16. doi:10.1080/00218460008029264.
- [29] I. Webster, The development of a pressure-sensitive adhesive for trauma-free removal, *Int. J. Adhes. Adhes.* 19 (1999).

- [30] J.M. Boyne, E.J. Millan, I. Webster, Peeling performance of a novel light switchable pressure-sensitive adhesive, *Int. J. Adhes. Adhes.* 21 (2001) 49–53.
- [31] K. Ebe, H. Seno, K. Horigome, UV curable pressure-sensitive adhesives for fabricating semiconductors. I. Development of easily peelable dicing tapes, *J. Appl. Polym. Sci.* 90 (2003) 436–441. doi:10.1002/app.12673.
- [32] C. Ryu, B. Pang, J. Han, H. Kim, Effect of Photo-crosslinking on Clean Debonding of Acrylic Pressure Sensitive Adhesives from Silicon Wafer, *J. Photopolym. Sci. Technol.* 25 (2012) 705–712.
- [33] C. Ryu, B. Pang, H. Kim, H. Kim, J. Park, S. Lee, K. Kim, Wettability and adhesion characteristics of photo-crosslinkable adhesives for thin silicon wafer, *Int. J. Adhes. Adhes.* 40 (2013) 197–201. doi:10.1016/j.ijadhadh.2012.08.005.
- [34] Z. Czech, H. Loclair, M. Wesolowska, Photoreactivity adjustment of acrylic PSA, *Rev. Adv. Mater. Sci.* 14 (2007) 141–150.
- [35] S.R. Trenor, T.E. Long, B.J. Love, Development of a light-deactivatable PSA via photodimerization, *J. Adhes.* 81 (2005) 213–229. doi:10.1080/00218460590922011.
- [36] S.M. June, T. Suga, W.H. Heath, Q. Lin, R. Puligadda, L. Yan, D. Dillard, T.E. Long, Photoactive Polyesters Containing o- Nitro Benzyl Ester Functionality for Photodeactivatable Adhesion, *J. Adhes.* 89 (2013) 548–558. doi:10.1080/00218464.2013.768112.
- [37] A.M. Schenzel, *Advanced Debonding on Demand Systems for Dental Adhesives*, Karlsruher Institut für technologie (KIT), 2017.
- [38] S. Radl, M. Kreimer, J. Manhart, T. Griesser, A. Moser, G. Pinter, G. Kalinka, W. Kern, S. Schlögl, Photocleavable epoxy based materials, *Polymer (Guildf)*. 69 (2015) 159–168. doi:10.1016/j.polymer.2015.05.055.
- [39] H. Akiyama, M. Yoshida, Photochemically reversible liquefaction and solidification of single compounds based on a sugar alcohol scaffold with multi azo-arms, *Adv. Mater.* 24 (2012) 2353–2356.
- [40] H. Akiyama, S. Kanazawa, Y. Okuyama, M. Yoshida, H. Kihara, H. Nagai, Y. Norikane, R. Azumi, Photochemically reversible liquefaction and solidification of multiazobenzene sugar-alcohol derivatives and application to reworkable adhesives, *ACS Appl. Mater. Interfaces*. 6 (2014) 7933–7941. doi:10.1021/am501227y.
- [41] H. Mutlu, C.M. Geiselhart, C. Barner-kowollik, Untapped potential for debonding on demand : the wonderful world of azo-compounds, *Mater. Horizons*. 5 (2018) 162–183. doi:10.1039/C7MH00920H.
- [42] S. Leijonmarck, A. Cornell, C.O. Danielsson, T. Åkermark, B.D. Brandner, G. Lindbergh, Electrolytically assisted debonding of adhesives: An experimental investigation, *Int. J. Adhes. Adhes.* 32 (2012) 39–45. doi:10.1016/j.ijadhadh.2011.09.003.
- [43] ElectRelease - electrically debonding adhesive, (n.d.). <http://www.eiclabs.com/ERtech.htm>

- (accessed August 24, 2018).
- [44] Q. Zhao, W. Zou, Y. Luo, T. Xie, Shape memory polymer network with thermally distinct elasticity and plasticity, *Sci. Adv.* 2 (2016) 1–8. doi:10.1126/sciadv.1501297.
- [45] J. Kolbe, T. Kowalik, M. Popp, M. Sebald, O. Schorsch, S. Heberer, M. Pridohl, G. Zimmermann, A. Hartwig, E. Born, Curable bonded assemblies capable of being dissociated, US 2004/0249037 A1, 2004.
- [46] M. Vogel, Kleben mit Magnetfeldern, *Phys. J.* 5 (2006) 16–17.
- [47] Nanotechnology Products and Applications, (n.d.). <https://www.nanowerk.com/products/product.php?id=5> (accessed August 27, 2018).
- [48] E. Sato, S. Iki, K. Yamanishi, H. Horibe, A. Matsumoto, Dismantlable adhesion properties of reactive acrylic copolymers resulting from cross-linking and gas evolution, *J. Adhes.* 93 (2016) 811–822. doi:10.1080/00218464.2016.1209114.
- [49] T. Inui, E. Sato, A. Matsumoto, Pressure-sensitive adhesion system using acrylate block copolymers in response to photoirradiation and postbaking as the dual external stimuli for on-demand dismantling, *ACS Appl. Mater. Interfaces.* 4 (2012) 2124–2132. doi:10.1021/am300103c.
- [50] T. Inui, K. Yamanishi, E. Sato, A. Matsumoto, Organotellurium-mediated living radical polymerization (TERP) of acrylates using ditelluride compounds and binary azo initiators for the synthesis of high-performance adhesive block copolymers for on-demand dismantlable adhesion, *Macromolecules.* 46 (2013) 8111–8120. doi:10.1021/ma401595w.
- [51] T. Inui, E. Sato, A. Matsumoto, High-molecular-weight polar acrylate block copolymers as high-performance dismantlable adhesive materials in response to photoirradiation and postbaking, *RSC Adv.* 4 (2014) 24719–24728. doi:10.1039/c4ra03745f.
- [52] K. Yamanishi, E. Sato, A. Matsumoto, Precise Synthesis of Acrylic Block Copolymers and Application to On-demand Dismantlable Adhesion Systems in Response to Photoirradiation and Postbaking, *J. Photopolym. Sci. Technol.* 26 (2013) 239–244. doi:10.2494/photopolymer.26.239.
- [53] A. Pizzi, K. Mittal, eds., *Handbook of Adhesive Technology, Revised and Expanded*, 2nd ed., Marcel Dekker, Inc., New York, Basel, 2003. doi:10.1201/9780203912225.
- [54] I. Skeist, ed., *Handbook of Adhesives*, 3rd ed., International Thomson Publishing, 1990. doi:10.1007/978-1-4613-0671-9.
- [55] P. Cognard, ed., *Handbook of Adhesives and Sealants: General Knowledge, Application of Adhesives, New Curing Techniques; Handbook of Adhesives and Sealants, Volume 2*, 1st ed., Elsevier, Amsterdam, Boston, Heidelberg, London, New York, Oxford, Paris, San Diego, San Francisco, Singapore, Sydney, Tokyo, 2006. <https://books.google.com/books?hl=fr&lr=&id=4UjQAEmjghUC&pgis=1>.
- [56] J. Friedrich, *Metal-Polymer Systems Interface Design and Chemical Bonding*, Wiley-VCH,

- Weinheim, 2018.
- [57] S. Ebnesajjad, A.H. Landrock, Introduction and adhesion theories, in: *Adhes. Technol. Handb.*, 3rd ed., Elsevier, 2014. doi:10.1016/B978-1-4377-4461-3.10001-X.
- [58] H. Mollet, A. Grubenmann, *Formulierungstechnik: Emulsionen, Suspensionen, feste Formen*, Wiley-VCH Verlag GmbH, Weinheim, New York, Chichester, Brisbane, Singapore, Toronto, 2000.
- [59] Kinloch A.J., *Adhesion and Adhesives-Science and Technology*, Springer-Science+Business Media, B.V., 1987.
- [60] G. Habenicht, *Kleben: Grundlagen, Technologien, Anwendungen*, 6th ed., Springer Verlag Berlin Heidelberg, Berlin, Heidelberg, 2009. doi:10.1007/978-3-540-85266-7.
- [61] I. Benedek, M. Feldstein, *Fundamentals of pressure sensitivity*, CRC Press, Taylor&Francis Group, LLC, 2009.
- [62] D.A. Dillard, A.V. Pocius, eds., *The Mechanics of Adhesion*, 1st ed., Elsevier Science B.V., 2002.
- [63] M.A. Butt, A. Chughtai, J. Ahmad, R. Ahmad, U. Majeed, I.H. Khan, Theory of Adhesion and its Practical Implications A Critical Review, *J. Fac. Eng. Technol.* (2007) 21–45. http://pu.edu.pk/images/journal/jfet/previous-pdf/JFET_03_2007_Theory_of_Adhesion_A_Critical_Review_f.pdf.
- [64] R. Lacombe, *Adhesion Measurement Methods: Theory and Practice*, 1st ed., CRC Taylor & Francis Group, 2005.
- [65] Z.W. Wicks, F.N. Jones, S.P. Pappas, D.A. Wicks, *Organic coatings science and technology*, 3rd ed., Wiley-Interscience a John Wiley & Sons, Inc., Publication, New Jersey, 2007.
- [66] J.M. Pochan, L.J. Gerenser, J.F. Elman, An e.s.c.a, study of the gas-phase derivatization of poly (ethylene terephthalate) treated by dry-air and dry- nitrogen corona discharge, *Polymer (Guildf)*. 27 (1986).
- [67] D. Briggs, S.M. P., *Practical Surface Analysis by Auger and X-Ray Photoelectron Spectroscopy*, John Wiley and Sons Ltd, Chichester, 1983. doi:10.1002/sia.740060611.
- [68] R. West, T.J. Barton, *Organosilicon chemistry-From Molecules to Materials*, VCH, Weinheim, New York, Basel, Cambridge, Tokyo, 1980. doi:10.1021/ed057p165.
- [69] E. Bormashenko, G. Chaniel, R. Grynyov, Towards understanding hydrophobic recovery of plasma treated polymers: Storing in high polarity liquids suppresses hydrophobic recovery, *Appl. Surf. Sci.* 273 (2013) 549–553. doi:10.1016/j.apsusc.2013.02.078.
- [70] S. Guimond, M.R. Wertheimer, Surface degradation and hydrophobic recovery of polyolefins treated by air corona and nitrogen atmospheric pressure glow discharge, *J. Appl. Polym. Sci.* 94 (2004) 1291–1303. doi:10.1002/app.21134.
- [71] E. Occhiello, M. Morra, G. Morini, F. Garbassi, P. Humphrey, Oxygen-plasma-treated

- polypropylene interfaces with air, water, and epoxy resins: Part I. Air and water, *J. Appl. Polym. Sci.* 42 (1991) 551–559. doi:10.1002/app.1991.070420228.
- [72] D. Angerbauer, *Oberflächenaktivierung und Funktionalisierung von Polyethylen*, Monatuniversität Leoben, 2011.
- [73] M. Harej, D. Dolenc, Autoxidation of Hydrazones. Some New Insights, *J. Org. Chem.* 72 (2007) 7214–7221. doi:10.1021/jo071091m.
- [74] A. V. Pocius, ed., *Adhesion and Adhesives Technology: An Introduction*, 3rd ed., Hanser Publications, Munich, Cincinnati, 2012.
- [75] S.R. Hartshorn, ed., *Structural Adhesives: Chemistry and Technology*, Plenum Press, New York, London, 1986. doi:10.1007/978-1-4684-7781-8.
- [76] M.. Wahab, ed., *The Mechanics of Adhesives in Composite and Metal Joints: Finite Element Analysis with ANSYS*, DEStech publications Inc., 2014.
- [77] S. Ebnesajjad, ed., *Adhesives Technology Handbook*, 2nd ed., William Andrew Inc., 2008.
- [78] Evonik, Adhesive systems, (n.d.). <https://adhesives-sealants.evonik.com/product/adhesives-sealants/en/adhesive-systems/pages/default.aspx>.
- [79] A guide to solvent based adhesives, (n.d.). <https://www.chemoxy.com/about-2/knowledge-hub/a-guide-to-solvent-based-adhesives/>.
- [80] S. Ebnesajjad, ed., *Handbook of Adhesives and Surface Preparation: Technology, Application and Manufacturing*, Elsevier, 2011.
- [81] J. Shields, ed., *Adhesives Handbook*, 3rd ed., Butterworth & Co (Publishers) Ltd., London, Boston, Durban, Singapore, Sydney, Toronto, Wellington, 1985.
- [82] R.W. Messler, ed., *Joining of Materials and Structures: From Pragmatic Process to Enabling Technology*, Elsevier, Butterworth, Heinemann, Amsterdam, Boston, Heidelberg, London, New York, Oxford, Paris, San Diego, San Francisco, Singapore, Sydney, Tokyo, 2004.
- [83] I. Benedek, *Pressure-Sensitive Formulation*, VSP BV, Utrecht, Boston, Tokyo, 2000.
- [84] R.J. Kirwan, ed., *Paper and Paperboard Packaging Technology*, Blackwell Publishing Ltd, 205AD.
- [85] I. Benedek, ed., *Pressure-Sensitive Design and Formulation, Application*, 2nd ed., CRC Press Taylor & Francis Group LLC, 2006.
- [86] M.R. Haddon, T.J. Smith, The chemistry and applications of UV-cured adhesives, *Int. J. Adhes. Adhes.* 11 (1991) 183–186.
- [87] A. Tiwari, H.K. Patra, X. Wang, *Advanced Material Interfaces*, Scrivener Publishing LLC, 2016.
- [88] I. Benedek, ed., *Developments in Pressure-Sensitive Products*, 2nd ed., CRC Press Taylor &

- Francis Group, LLC, 2005.
- [89] L.F.M. da Silva, A. Öchsner, D. Adams, Robert, eds., Handbook of Adhesion Technology, Springer Verlag Berlin Heidelberg, 2011. doi:10.1007/978-3-642-01169-6.
- [90] S.B. Lin, L.D. Durfee, R.A. Ekeland, J. McVie, G.K. Schallau, Recent advances in silicone pressure-sensitive adhesives, *J. Adhes. Sci.Technol.* 21 (2007) 605–623. doi:10.1163/156856107781192274.
- [91] A.K. Singh, D.S. Mehra, U.K. Niyogi, S. Sabharwal, R.K. Khandal, Polyurethane based pressure sensitive adhesives (PSAs) using electron beam irradiation for medical application, *J. Polym. Mater.* 28 (2011) 525–542.
- [92] R. Guradeep, Photochemistry, 5th ed., S.K. Rastogi for KRISHNA Prakashan Media (P) Ltd., 2008.
- [93] D.R. Arnold, N.C. Baird, J.C.D. Bolton, P.W.M. Jacobs, P. de Mayo, W.R. Ware, Photochemistry: An Introduction, Academic Press, Inc., London, 1974.
- [94] M. Persico, G. Granucci, Photochemistry: A Modern Theoretical Perspective, Springer International Publishing AG, 2018.
- [95] A. Albini, Photochemistry, Springer Verlag, Heidelberg, Berlin, New York, Dordrecht, London, 2016.
- [96] M. Charlier, M. Daniels, D. Elad, C. Fenselau, G.J. Fisher, W.W. Hauswirth, C. Helene, D.P. Hollis, H. e. Johns, T. Montenay-Garestier, G. Scholes, S.Y. Wang, Photochemistry and Photobiology of Nucleic Acids, Volume I, Academic Press, Inc., New York, San Francisco, London, 1976.
- [97] J.P. Fouassier, X. Allonas, D. Burget, Photopolymerization reactions under visible lights: principle, mechanisms and examples of applications, *Prog. Org. Coatings.* 47 (2003) 16–36. doi:10.1016/S0300-9440(03)00011-0.
- [98] A.B. Scranton, C.N. Bowman, R.W. Pfeiffer, eds., Photopolymerization: Fundamentals and Applications, American Chemical Society, 1997.
- [99] A. Ravve, ed., Light-Associated Reactions of Synthetic Polymers, Springer, 2006.
- [100] W.A. Green, Industrial Photoinitiators, CRC Press Taylor & Francis Group, Boca Raton, London, New York, 2010. doi:10.1201/9781439827468.
- [101] G. Kearney, The History of Printed Circuit Boards, (2016). <https://mint-tek.com/the-history-of-printed-circuit-boards-2/>.
- [102] A brief history of Printed Circuit Boards: Design and Manufacturing, (2018). <https://www.tempoautomation.com/blog/a-brief-history-of-printed-circuit-boards-design-and-manufacturing/>.
- [103] J. Brown, The history of printed circuit boards - Infographic, (n.d.). <https://www.pcb-solutions.com/pcb-market-monitor/the-history-of-pcb-infographic/>.

- [104] The history of circuit boards, (n.d.). <https://falconerelectronics.com/history-of-circuit-boards/>.
- [105] K. Gilleo, *The Circuit Centennial*, 2003.
- [106] How to Build a Printed Circuit, 2004. <https://www.4pcb.com/media/presentation-how-to-build-pcb.pdf>.
- [107] P. Brooks, H. Fuerhaupter, J. Hechler, B. Day, H. Yang, *High Performance Multilayer Bonding Systems*, 2002.
- [108] A. Zee, R. Massey, Use of non-etching adhesion promoters in advanced PCB applications, in: *Electron. Syst. Technol. Conf.*, 2010. doi:10.1109/ESTC.2010.5642930.
- [109] J.F. Ding, C.M. Chen, G. Xue, The Dynamic Mechanical Analysis of Epoxy Copper-Powder Composites Using Azole Compounds As Coupling Agents, *J. Appl. Polym. Sci.* 42 (1991) 1459–1464. doi:10.1002/app.1991.070420531.
- [110] G. Xue, P. Wu, Q. Dai, R. Cheng, The coupling mechanism of benzotriazole pre-treated copper metal and epoxy resin, *Die Angew. Makromol. Chemie.* 188 (1991) 51–61. doi:10.1002/apmc.1991.051880105.
- [111] Herstellung einer Multilayer Leiterplatte kurz und bündig erklärt, 2016. <http://www.flowcad.ch/cms/upload/downloads/PCBRoadshowHerstellungMultilayerLeiterplatte.pdf>.
- [112] P. Kim, S. Lee, J. Park, C. Park, H. Kim, Synthesis and characterization of thermally stable acrylic PSA using silicone urethane methacrylate with a semi-IPN structure, *J. Adhes. Sci. Technol.* 28 (2014) 15–30. doi:10.1080/01694243.2013.816835.
- [113] S.M. Taghizadeh, D. Ghasemi, Synthesis and Optimization of a Four-Component Acrylic-based Copolymer as Pressure Sensitive Adhesive, *Iran. Polym. J.* 19 (2010) 363–373.
- [114] B. Yuan, B. Wagner, *Acrylic based pressure sensitive adhesive formulation*, US 8,426,514 B2, 2013.
- [115] H.S. Do, J.H. Park, H.J. Kim, UV-curing behavior and adhesion performance of polymeric photoinitiators blended with hydrogenated rosin epoxy methacrylate for UV-crosslinkable acrylic pressure sensitive adhesives, *Eur. Polym. J.* 44 (2008) 381–388. doi:10.1016/j.eurpolymj.2008.07.046.
- [116] O. Hara, *Curing Agents for Epoxy Resin*, *Three Bond Tech. News.* (1990) 1–10.
- [117] P. Chabanne, L. Tighzert, J.-P. Pascault, Monoepoxy Polymerization Initiated by BF₃-Amine Complexes in Bulk. II. Influence of Water and By-Products on Polymer Formation, *J. Appl. Polym. Sci.* 53 (1994) 769–785.
- [118] M. Tackie, G.C. Martin, The polymerization mechanism and kinetics of DGEBA with BF₃-MEA, *J. Appl. Polym. Sci.* 48 (1993) 793–808. doi:10.1002/app.1993.070480505.
- [119] M.R. Buchmeiser, ed., *Polymeric Materials in Organic Synthesis and Catalysis*, Wiley-VCH

- Verlag Gm, Weinheim, 2004. doi:10.1002/anie.200385072.
- [120] K. Matyjaszewsk, Acrylic ester polymers, in: *Encycl. Polym. Sci. Technol.*, 4th ed., John Wiley & Sons, Inc., 2010. doi:10.1002/0471440264.
- [121] U.D. Cakmak, G. Grestenberger, Z. Major, A novel test method for quantifying surface tack of polypropylene compound surfaces, *Express Polym. Lett.* 5 (2011) 1009–1016. doi:10.3144/expresspolymlett.2011.98.
- [122] M. Debowska, L. Kurzeja, A. Baranowski, K. Hennek, K. Jerie, J. Rudzinska-Girulska, Influence of structure of a crosslinked epoxy resin on its proerties studied by poitron annihilation and other methods, *J. Radioanal. Nucl. Chem.* 210 (1996) 485–494.
- [123] M. González-González, J.C. Cabanelas, J. Baselga, Applications of FTIR on Epoxy Resins - Identification, Monitoring the Curing Process, Phase Separation and Water Uptake, in: T. Theophanides (Ed.), *Infrared Spectrosc. - Mater. Sci. Eng. Technol.*, InTech, 2012: pp. 261–284. doi:10.5772/2055.
- [124] S. Thomas, C. Sinturel, R. Thomas, *Micro and Nanostructured Epoxy/Rubber Blends*, WILEY-VCH Verlag GmbH & Co KGaA, Weinheim, 2014. doi:10.1002/9783527666874.
- [125] R. Klein, F.R. Wurm, Aliphatic polyethers: Classical polymers for the 21st century, *Macromol. Rapid Commun.* 36 (2015) 1147–1165. doi:10.1002/marc.201500013.
- [126] G. Moad, D.H. Solomon, *The chemistry of radical polymerization*, 2nd ed., Elsevier Ltd, Oxford, 2006.
- [127] P. Glöckner, T. Jung, S. Struck, K. Struder, *Radiation Curing: Coatings and Printing Inks*, Vincentz Network, Hannover, 2008.
- [128] T. Nakano, Synthesis, structure and function of π -stacked polymers, *Polym. J.* 42 (2010) 103–123. doi:10.1038/pj.2009.332.
- [129] T.Y. Lee, N. Cramer, C. Hoyle, J. Stansbury, C. Browman, (Meth)Acrylate Vinyl Ester Hybrid Polymerizations, *J Polym Sci A Polym Chem.* 47 (2009) 2509–2517. doi:10.1002/pola.23327.
- [130] A. Bhattacharya, J.W. Rawlins, P. Ray, eds., *Polymer Grafting and Crosslinking*, Wiley-Interscience a John Wiley & Sons, Inc., New Jersey, 2009. doi:10.1002/9780470414811.
- [131] E. Ihara, S. Honjyo, T. Itoh, K. Inoue, M. Nodono, Radical Copolymerization of Alkyl 2-Norbornene-2- carboxylate with Alkyl Acrylates : Facile Incorporation of Norbornane Framework into Poly (alkyl acrylate) s, *J. Polym. Sci. A Polym. Chem.* 45 (2007) 4597–4605. doi:10.1002/pola.
- [132] S. Ozlem, E. Aslan-Gürel, R.M. Rossi, J. Hacaloglu, Thermal degradation of poly(isobornyl acrylate) and its copolymer with poly(methyl methacrylate) via pyrolysis mass spectrometry, *J. Anal. Appl. Pyrolysis.* 100 (2013) 17–25. doi:10.1016/j.jaap.2012.10.024.
- [133] L. Valette, V. Massardier, J.P. Pascault, B. Magny, Synthesis and Photopolymerization of

- Acrylic Acrylate Copolymers, *J. Appl. Polym. Sci.* 86 (2002) 753–763. doi:10.1002/app.10975.
- [134] H. Becker, H. Vogel, The Role of Hydroquinone Monomethyl Ether in the Stabilization of Acrylic Acid, *Chem. Eng. Technol.* 29 (2006) 1227–1231. doi:10.1002/ceat.200500401.
- [135] E. Bendary, R.R. Francis, H.M.G. Ali, M.I. Sarwat, S. El Hady, Antioxidant and structure–activity relationships (SARs) of some phenolic and anilines compounds, *Ann. Agric. Sci.* 58 (2013) 173–181. doi:10.1016/j.aogas.2013.07.002.
- [136] M.S. Kharasch, F. Kawahara, W. Nudenberg, The mechanism of action of inhibitors in free radical initiated polymerizations at low temperatures, *J. Org. Chem.* 19 (1954) 1977–1990. doi:10.1021/jo01377a015.
- [137] S.R. Sandler, W. Karo, *Polymer Synthesis*, 2nd ed., Academic Press, Inc., San Diego, 1992.
- [138] G. Fogassy, C. Pinel, G. Gelbard, Solvent-free ring opening reaction of epoxides using quaternary ammonium salts as catalyst, *Catal. Commun.* 10 (2009) 557–560. doi:10.1016/j.catcom.2008.10.039.
- [139] G. Socrates, *Infrared Characteristic Group Frequencies*, 2nd ed., John Wiley & Sons, Inc., New York, Brisbane, Toronto, 1994.
- [140] M. Hesse, H. Meier, B. Zeeh, *Spektroskopische Methoden in der organischen Chemie*, 7th ed., George Thieme Verlag KG, Stuttgart, New York, 2005.
- [141] T. Kozluk, T. Sychaj, A. Hamielec, Compositional Analysis of Styrene-Acrylic Acid Copolymers by H-NMR, *Makromol. Chemie.* 188 (1987) 1951–1857.
- [142] D. Khandelwal, S. Hooda, A.S. Brar, R. Shankar, 1D and 2D NMR studies of isobornyl acrylate - Methyl methacrylate copolymers, *J. Mol. Struct.* 1004 (2011) 121–130. doi:10.1016/j.molstruc.2011.07.046.
- [143] P. Ghosh, *Adhesives and Coatings Technology*, Tata McGraw-Hill Publishing Company Limited, New Delhi, 2008.
- [144] G.W. Ehrenstein, G. Riedel, P. Trawiel, *Thermal Analysis of Plastics*, Carl, Munich, 2008. doi:10.1021/ed085p404.
- [145] A. Asif, L. Hu, W. Shi, Synthesis, rheological, and thermal properties of waterborne hyperbranched polyurethane acrylate dispersions for UV curable coatings, *Colloid Polym. Sci.* 287 (2009) 1041–1049. doi:10.1007/s00396-009-2062-8.
- [146] M. Ghaemy, M.H. Khandani, Study of Polymerization Mechanism and Kinetics of DGEBA with BF₃-amine Complexes Using FT-IR and Dynamic DSC, *Iran. Polym. J.* 6 (1997) 5–17.
- [147] I. Hamerton, *Recent Developments in Epoxy Resins*, 1996.
- [148] E. Andrzejewska, Photopolymerization kinetics of multifunctional monomers, *Prog. Polym. Sci.* 26 (2001) 605–665. doi:10.1016/S0079-6700(01)00004-1.

- [149] İ. Gülçin, Z. Huyut, M. Elmastaş, H.Y. Aboul-Enein, Radical scavenging and antioxidant activity of tannic acid, *Arab. J. Chem.* 3 (2010) 43–53. doi:10.1016/j.arabjc.2009.12.008.
- [150] P.M. Viakh, Y. Arao, eds., *Thermal degradation of polymer blends, composites and nanocomposites*, Springer Verlag, Cham, Heidelberg, New York, Dordrecht, London, 2015.
- [151] H.-S. Joo, Y.-J. Park, H.-S. Do, H.-J. Kim, S.-Y. Song, K.-Y. Choi, The curing performance of UV-curable semi-interpenetrating polymer network structured acrylic pressure-sensitive adhesives, *J. Adhes. Sci. Technol.* 21 (2007) 575–588. doi:10.1163/156856107781192346.
- [152] J.A. Schwarz, C.I. Contescu, K. Putyera, eds., *Dekker Encyclopedia of Nanoscience and Nanotechnology*, Marcel Dekker, Inc., New York, Basel, 2004.
- [153] E.J. Dietz, N.A. Peppas, Reaction kinetics and chemical changes during polymerization of multifunctional (meth)acrylates for the production of highly crosslinked polymers used in information storage systems, *Polymer (Guildf)*. 38 (1997) 3767–3781.
- [154] Y. Hua, F. Jiang, J. V. Crivello, Photosensitized onium-salt-induced cationic polymerization with hydroxymethylated polynuclear aromatic hydrocarbons, *Chem. Mater.* 14 (2002) 2369–2377. doi:10.1021/cm011703y.
- [155] J. V. Crivello, S.L. Shao, Synthesis and cationic photopolymerization of alkoxyallene monomers, *J. Polym. Sci. Part A Polym. Chem.* 37 (1998) 1199–1209. doi:10.1002/(SICI)1099-0518(19990415)37:8<1199::AID-POLA16>3.0.CO;2-L.
- [156] J.F. Fouassier, Jean-Pierre, Rabek, ed., *Radiation Curing in Polymer Science and Technology*, Elsevier Applied Science, London, New York, 1993.
- [157] T.M. Lovestead, A.K. O'Brien, C.N. Bowman, Models of multivinyl free radical photopolymerization kinetics, *J. Photochem. Photobiol. A Chem.* 159 (2003) 135–143. doi:10.1016/S1010-6030(03)00178-3.
- [158] R.C.B. Alonso, W.C. Brandt, E.J.C. Souza-Junior, R.M. Puppim-Rontani, M.A.C. Sinhoreti, Photoinitiator concentration and modulated photoactivation: influence on polymerization characteristics of experimental composites, *Appl. Adhes. Sci.* 2 (2014) 1–11. doi:10.1186/2196-4351-2-10.
- [159] H. Chavda, C. Patel, Effect of crosslinker concentration on characteristics of superporous hydrogel, *Int. J. Pharm. Investig.* 1 (2011) 17. doi:10.4103/2230-973X.76724.
- [160] J. Vandenberg, M. Peeters, T. Kretschmer, P. Wagner, T. Junkers, Cross-linked degradable poly(β -thioester) networks via amine-catalyzed thiol-ene click polymerization, *Polymer (Guildf)*. 55 (2014) 3525–3532. doi:10.1016/j.polymer.2014.05.043.
- [161] M.T.B. Romero, M.A. Blitz, D.E. Heard, M.J. Pilling, B. Price, P.W. Seakins, L. Wang, Photolysis of methylethyl, diethyl and methylvinyl ketones and their role in the atmospheric HOx budget, *Faraday Discuss.* 130 (2005) 73–88. doi:10.1039/b419160a.
- [162] Nitto, *Produktauswahl*, (n.d.).
<https://www.nitto.com/eu/de/products/spec/?PG=1&SF=0&SO=A&LS=tcm%3A72-4430->

- 1024&MS=#RESULT (accessed January 27, 2018).
- [163] 3M, Suchergebnis für "Hochtemperatur Polyester Klebeband," (n.d.). https://www.3mdeutschland.de/3M/de_DE/unternehmen-de/produkte/?N=5002385+8711017&Ntt=Hochtemperatur+Polyester+Klebeband&LC=de_DE&co=cc&gsaAction=scBR&rt=rs&type=cc (accessed January 27, 2018).
- [164] Tesa, Solution for the electronic industry 2017, 2017.
- [165] E.M. Mount III, Chemical Analysis of the Polyester/Metal Surface of a Delamination Failure, ANTECH 2006. (2006) 1022–1026.
- [166] Fink.D, ed., Transport Processes in Ion-Irradiated Polymers, SpringerVerlag, Berlin, Heidelberg, New York, 2004.
- [167] T. Garramone, Building a Printed Circuit, 2009.
- [168] N. Fujimaki, K. Koike, K. Takami, S. Ogata, H. Iinaga, Development of Printed Circuit Board Technology Embedding Active and Passive Devices for e-Function Module, OKI Tech. Rev. 77 (2010). <http://www.oki.com>.
- [169] S. Lu, I. Hamerton, The Chemistry of Halogen-Free Flame Retardant Polymers.Pdf, Prog. Polym. Sci. 27 (2002) 1661–1712. doi:10.1016/S0079-6700(02)00018-7.
- [170] T. Mariappan, C.A. Wilkie, Flame retardant epoxy resin for electrical and electronic applications, Fire Mater. 38 (2014) 588–598. doi:10.1002/fam.2199.
- [171] J.R. Marchetti, W.R. Thomas, Flame retardant B-staged epoxy resin prepregs and laminates made therefrom, 4,501,787, 1985.
- [172] C.-Y. Chao, L. Lin, Method for rinsing copper or copper base alloy foil after an anti-tarnish treatment, 5,356,527, 1994.
- [173] L. Lin, C.-Y. Chao, Chromium-Zinc Anti-Tarnish Coating on Copper Foil, 5,098,796, 1992. <https://patentimages.storage.googleapis.com/4a/ca/16/f2d849dfcadd1c/US5250662.pdf>
- [174] N.B. of Consultants&Engineers, The Complete Technology Book on Industrial Adhesives, Asia Pacific Business Press Inc., Delhi, 2008.
- [175] K.S. Anseth, L.M. Kline, T.A. Walker, K.J. Anderson, C.N. Bowman, Reaction Kinetics and Volume Relaxation during Polymerizations of Multiethylene Glycol Dimethacrylates, Macromolecules. 28 (1995) 2491–2499. doi:10.1021/ma00111a050.
- [176] Y. Fukamoto, E. Sato, H. Okamura, H. Horibe, A. Matsumoto, Control of adhesive strength of acrylate polymers containing 1-isobutoxyethyl and isobornyl esters in response to dual stimuli for dismantlable adhesion, Appl. Adhes. Sci. 5 (2017). doi:10.1186/s40563-017-0085-9.
- [177] L.-H. Lee, ed., Adhesion science and technology, Polym. Sci. Technol. Vol. 9A. 9 (1975). doi:10.1007/978-1-4615-8201-4.

- [178] J. Brandrup, E.H. Immergut, E.A. Grulke, eds., *Polymer Handbook*, John Wiley & Sons, Inc., New York, Chichester, Weinheim, Brisbane, Singapore, Toronto, 1999.
- [179] B. Purcell, Twenty Questions and Answer about UV curing and Related Concerns, (2009) 24–28. <https://www.nazdar.com/Portals/0/NewsItems/Articles/20QuestionsAboutUVCuring-BeaPurcell.pdf>.
- [180] D.H. Kaelble, Theory and Analysis of Peel Adhesion: Adhesive Thickness Effects, *J. Adhes.* 37 (1992) 205–214. doi:10.1080/00218469208031262.
- [181] Y. Wan, X. Wang, H. Sun, Y. Li, K. Zhang, Y. Wu, Corrosion Behavior of Copper at Elevated Temperature, *Int. J. Electrochem. Sci.* 7 (2012) 7902–7914.
- [182] S.-K. Lee, H.-C. Hsu, W.-H. Tuan, Oxidation Behavior of Copper at a Temperature below 300°C and the Methodology for Passivation, *Mater. Res.* 19 (2016) 51–56. doi:10.1590/1980-5373-MR-2015-0139.
- [183] Shin-Etsu Silicone, *Silane Coupling Agents*, 2014.
- [184] K.L. Mittal, ed., *Silanes and Other Coupling Agents*, 5th ed., CRC Press Taylor & Francis Group, Leiden, Boston, 2009. <http://booksandjournals.brillonline.com/content/books/9789047420019>.
- [185] E.P. Plueddemann, *Silane Coupling Agents*, Springer Science+Business Media, LLC, 1982. doi:10.1007/978-1-4899-0342-6.
- [186] R. Bel-Hassen, S. Boufi, M.-C. Brochier Salon, M. Abdelmouleh, N. Belgacem, Adsorption of silane onto cellulose fibers. II. The effect of pH on silane hydrolysis, condensation, and adsorption behavior, *J. Appl. Polym. Sci.* 108 (20AD) 1958–1968. doi:10.1002/app.27488.
- [187] C.J. Brinker, Hydrolysis and condensation of silicates: Effects on structure, *J. Non. Cryst. Solids.* 100 (1988) 31–50.
- [188] F.D. Osterholtz, E.R. Pohl, Kinetics of the hydrolysis and condensation of organofunctional alkoxy silanes: a review, *J. Adhes. Sci. Technol.* 6 (1992) 127–149. doi:10.1017/CBO9781107415324.004.
- [189] A.F. Scott, J.E. Gray-Munro, J.L. Shepherd, Influence of coating bath chemistry on the deposition of 3-mercaptopropyl trimethoxysilane films deposited on magnesium alloy, *J. Colloid Interface Sci.* 343 (2010) 474–483. doi:10.1016/j.jcis.2009.11.062.
- [190] K.W. Jang, S.H. Choi, S. Il Pyun, M.S. Jhon, The effects of the water content, acidity, temperature and alcohol content on the acidic sol-gel polymerization of tetraethoxysilane (TEOS) with Monte Carlo simulation, *Mol. Simul.* 27 (2001) 1–16. doi:10.1080/08927020108024516.
- [191] F. de Buyl, A. Kretschmer, Understanding hydrolysis and condensation kinetics of γ -glycidoxypropyltrimethoxysilane, *J. Adhes.* 84 (2008) 125–142. doi:10.1080/00218460801952809.

- [192] P. Walker, Organosilanes as adhesion promoters, *J. Adhes. Sci. Technol.* 5 (1991) 279–305. doi:10.1163/156856191X00585.
- [193] Gelest, *Silane Coupling Agents*, 3rd ed., n.d.
- [194] G.L. Witucki, A Silane Primer: Chemistry and Applications of Alkoxy Silanes, *J. Coatings Technol.* (1992). doi:10.1124/dmd.109.028449.
- [195] Y. Xia, R. Fang, Z. Xiao, L. Ruan, R. Yan, H. Huang, C. Liang, Y. Gan, J. Zhang, X. Tao, W. Zhang, Supercritical fluid assisted biotemplating synthesis of Si–O–C microspheres from microalgae for advanced Li-ion batteries, *RSC Adv.* 6 (2016) 69764–69772. doi:10.1039/C6RA13560A.
- [196] C. Sow, B. Riedl, P. Blanchet, Kinetic studies of UV-waterborne nanocomposite formulations with nanoalumina and nanosilica, *Prog. Org. Coatings.* 67 (2010) 188–194. doi:10.1016/j.porgcoat.2009.10.002.
- [197] S. Stankovich, D.A. Dikin, R.D. Piner, K.A. Kohlhaas, A. Kleinhammes, Y. Jia, Y. Wu, S.B.T. Nguyen, R.S. Ruoff, Synthesis of graphene-based nanosheets via chemical reduction of exfoliated graphite oxide, *Carbon N. Y.* 45 (2007) 1558–1565. doi:10.1016/j.carbon.2007.02.034.
- [198] Y.G. Ko, S.W. Karng, G.S. Lee, U.S. Choi, Smart glass substrate as colorimetric chemosensor for highly selective detection of silver ion, *Sensors Actuators, B Chem.* 177 (2013) 1107–1114. doi:10.1016/j.snb.2012.12.032.
- [199] I.M. Nagpure, S.S. Pitale, K.G. Tshabalala, V. Kumar, O.M. Ntwaeaborwa, J.J. Terblans, H.C. Swart, Luminescence response and CL degradation of combustion synthesized spherical SiO₂:Ce nanophosphor, *Mater. Res. Bull.* 46 (2011) 2359–2366. doi:10.1016/j.materresbull.2011.08.051.
- [200] Y. Liu, C. Wang, W. Li, L. Zhang, X. Yang, G. Cheng, Q. Zhang, Effect of energy density and feeding speed on micro-hole drilling in C/SiC composites by picosecond laser, *J. Mater. Process. Technol.* 214 (2014) 3131–3140. doi:10.1016/j.jmatprotec.2014.07.016.
- [201] W. Heiji, T. Hosoi, *Physics and Technology of Silicon Carbide Devices Fundamental aspects of silicon oxidation*, InTech, Rijeka, 2012. doi:10.5772/51514.
- [202] X. Peng, ed., *Nanowires-recent advances*, InTech, Rijeka, 2012. doi:10.5772/3367.
- [203] P.M. Dietrich, S. Glamsch, C. Ehlert, A. Lippitz, N. Kulak, W.E.S. Unger, Synchrotron-radiation XPS analysis of ultra-thin silane films: Specifying the organic silicon, *Appl. Surf. Sci.* 363 (2016) 406–411. doi:10.1016/j.apsusc.2015.12.052.
- [204] W. Yu, L. Deng, P. Yuan, D. Liu, W. Yuan, P. Liu, H. He, Z. Li, F. Chen, Surface silylation of natural mesoporous/macroporous diatomite for adsorption of benzene, *J. Colloid Interface Sci.* 448 (2015) 545–552. doi:10.1016/j.jcis.2015.02.067.
- [205] M. Sangermano, M. Periolatto, M. Castellino, J. Wang, K. Dietliker, J.L. Grützmacher, H. Grützmacher, A Simple Preparation of Photoactive Glass Surfaces Allowing Coatings via the

- "grafting-from" Method, ACS Appl. Mater. Interfaces. 8 (2016) 19764–19771. doi:10.1021/acsami.6b05822.
- [206] J.F. Moulder, W.F. Stickle, P.E. Sobol, K.D. Bomben, Handbook of X-ray Photoelectron Spectroscopy, Physical Electronics Division, Perkin-Elmer Corporation, Minnesota, United States, 1992.
- [207] F. Niu, L.-M. Tao, Y.-C. Deng, Q.-H. Wang, W.-G. Song, Phosphorus doped graphene nanosheets for room temperature NH₃ sensing, New J. Chem. 38 (2014) 2269. doi:10.1039/c4nj00162a.
- [208] Y. Li, S. Li, Y. Wang, J. Wang, H. Liu, X. Liu, L. Wang, X. Liu, W. Xue, N. Ma, Electrochemical synthesis of phosphorus-doped graphene quantum dots for free radical scavenging, Phys. Chem. Chem. Phys. 19 (2017) 11631–11638. doi:10.1039/C6CP06377B.
- [209] A. Huber, A. Kuschel, T. Ott, G. Santiso-quinones, D. Stein, J. Bräuer, R. Kissner, F. Krumeich, H. Schçnberg, J. Levalois-grützmacher, H. Grützmacher, Phosphorous-Functionalized Bis(acyl) phosphane Oxides for Surface Modification, Angew. Chem. Int. Ed. 51 (2012) 4648–4652. doi:10.1002/anie.201201026.
- [210] D.B. Yang, D. Wolf, Interfacial analyses of copper corrosion by acrylic and methacrylic acids using XPS, auger and grazing angle FTIR spectroscopy, Surf. Interface Anal. 23 (1995) 276–288. doi:10.1002/sia.740230503.
- [211] O.S. Taskin, B. Kiskan, Y. Yagci, An efficient, heterogeneous, reusable atom transfer radical polymerization catalyst, Polym. Int. 67 (2018) 55–60. doi:10.1002/pi.5485.
- [212] L. Frazer, Radical Departure: Polymerization Does More With Less, Environ. Health Perspect. 115 (2007) A 259-A 261.
- [213] B.P. Koiry, N.K. Singha, Copper mediated controlled radical copolymerization of styrene and 2-ethylhexyl acrylate and determination of their reactivity ratios, Front. Chem. 2 (2014) 1–8. doi:10.3389/fchem.2014.00091.
- [214] V.V. Krongauz, A.C. Trifunac, eds., Processes in Photoreactive Polymers, Chapman & Hall, 1995.

12. Curriculum Vitae

Personal Data

Name	Dipl.-Ing. Christine Bandl, BSc
Geburtsdatum	19.01.1990
Geburtsort	Leoben



Education

01/2015 - 09/2019	<i>Doctor's Degree (PhD)</i> Chemistry of Polymeric Materials, Montanuniversität Leoben Dissertation (PCCL): „Development of pressure sensitive adhesive tapes for temporary applications at high temperatures providing residue-free removability“
11/2014 – 03/2012	<i>Master's Degree</i> Technical Chemistry, Technical University of Graz and Karl-Franzens-Universität of Graz Diploma Thesis: „Investigation of olefin metathesis degradation as an alternative method for the exposure of rubber metal interfaces in tires“
09/2008 – 03/2012	<i>Bachelor's Degree</i> Chemistry, Technical University of Graz and Karl-Franzens-Universität of Graz Bachelor's Thesis: „Analyse von Schweißfülldrahtpulver“
09/2000 – 06/2008	<i>Secondary School</i> BG/BRG Leoben BG/BRG Kapfenberg

Professional Experience

01/2015 – 12/2017	Researcher at PCCL
since 01/2018	Researcher at Montanuniversität Leoben

13. Publications

Publications in peer-reviewed journals

"Simple and rapid method for restoring anti-adhesive organosilane coatings on metal substrates", C. Bandl, N. Krempl, W. Kern, W. Friesenbichler; Progress in Organic Coatings, 2019 – *submitted in 03/2019 (POC_2019_351), revised version under preparation*

"Externally triggered release mechanisms for debonding on demand adhesives and typical applications", C. Bandl, S. Schlögl, W. Kern; International Journal of Adhesion and Adhesives, 2019 – *submitted in in 03/2019*

Publications in non-reviewed journals

"Beschichtungen für Formen und Werkzeuge in der Kunststoff verarbeitenden Industrie", N. Krempl, W. Kern, C. Bandl, W. Friesenbichler, T. Gröger; KC aktuell, p. 22-23, Oktober 2018

"Beschichtungen mit beschränkter Haftung", N. Krempl, C. Bandl, T. Gröger, W. Kern, W. Friesenbichler; Chemiereport.at: Austrian life sciences, p. 49-52, 2018/8

Conference Paper

"Investigation of temporary binding pressure sensitive adhesives comprising external triggered release"; C. Bandl, S. Schlögl, S. Feldbacher, W. Kern; EURADH 2016: Adhesion '16, Book of Abstracts, p. 360 - 363

Oral Presentations

"Release Coatings for PCB production", C. Bandl, S. Feldbacher, S. Schlögl, W. Kern; PolyComp Annual Meeting 2016, Leoben, Austria

Poster

"Characterization of adhesives with triggered release", C. Bandl, S. Schlögl, S. Feldbacher, W. Kern; Polymer Processing Society, 2015, Graz, Austria

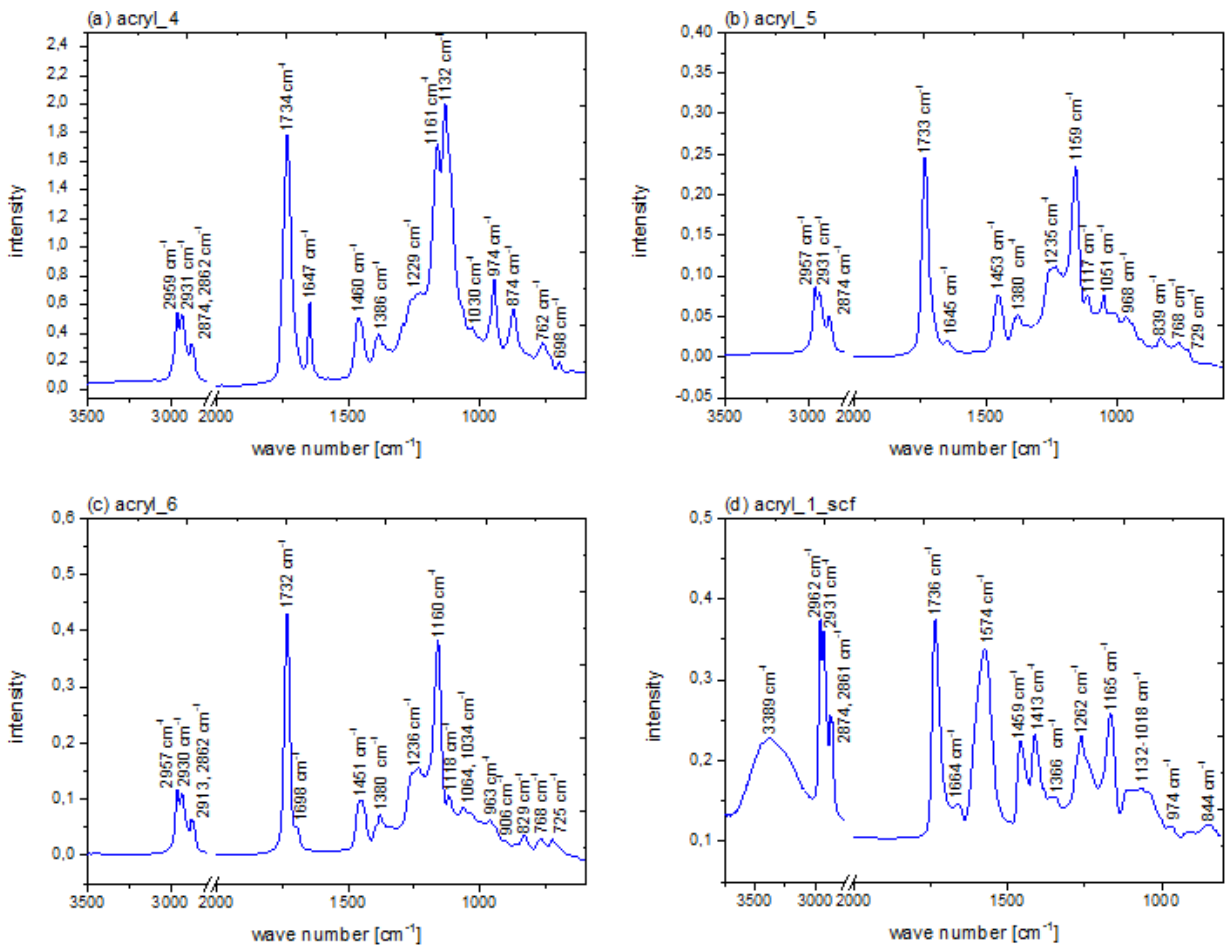
-Publications-

"Investigation of temporary binding pressure sensitive adhesives comprising external triggered release", C. Bandl, S. Schlögl, S. Feldbacher, W. Kern; EURADH 2016: Adhesion '16, Glasgow, UK

"Beschichtungen für Formen und Werkzeuge in der kunststoffverarbeitenden Industrie", N. Krempl, C. Bandl, W. Kern, W. Friesenbichler, G. Berger-Weber, T. Gröger; 2018, Leoben, Austria

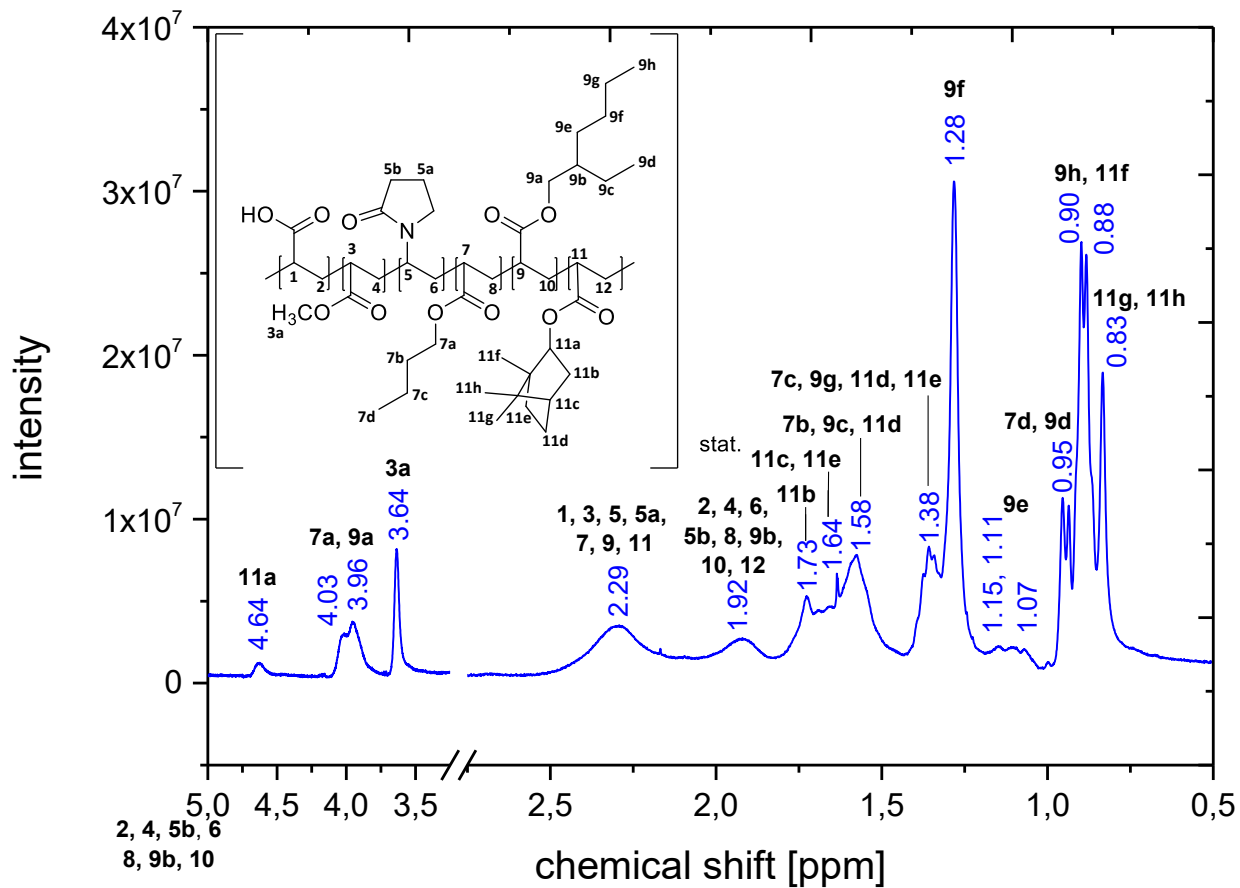
14. Appendix

Figure_A 1 shows the FT-IR-spectra of the synthesized acrylic copolymers acryl_1, acryl_4, acryl_5, acryl_6 and acryl_1_scf.

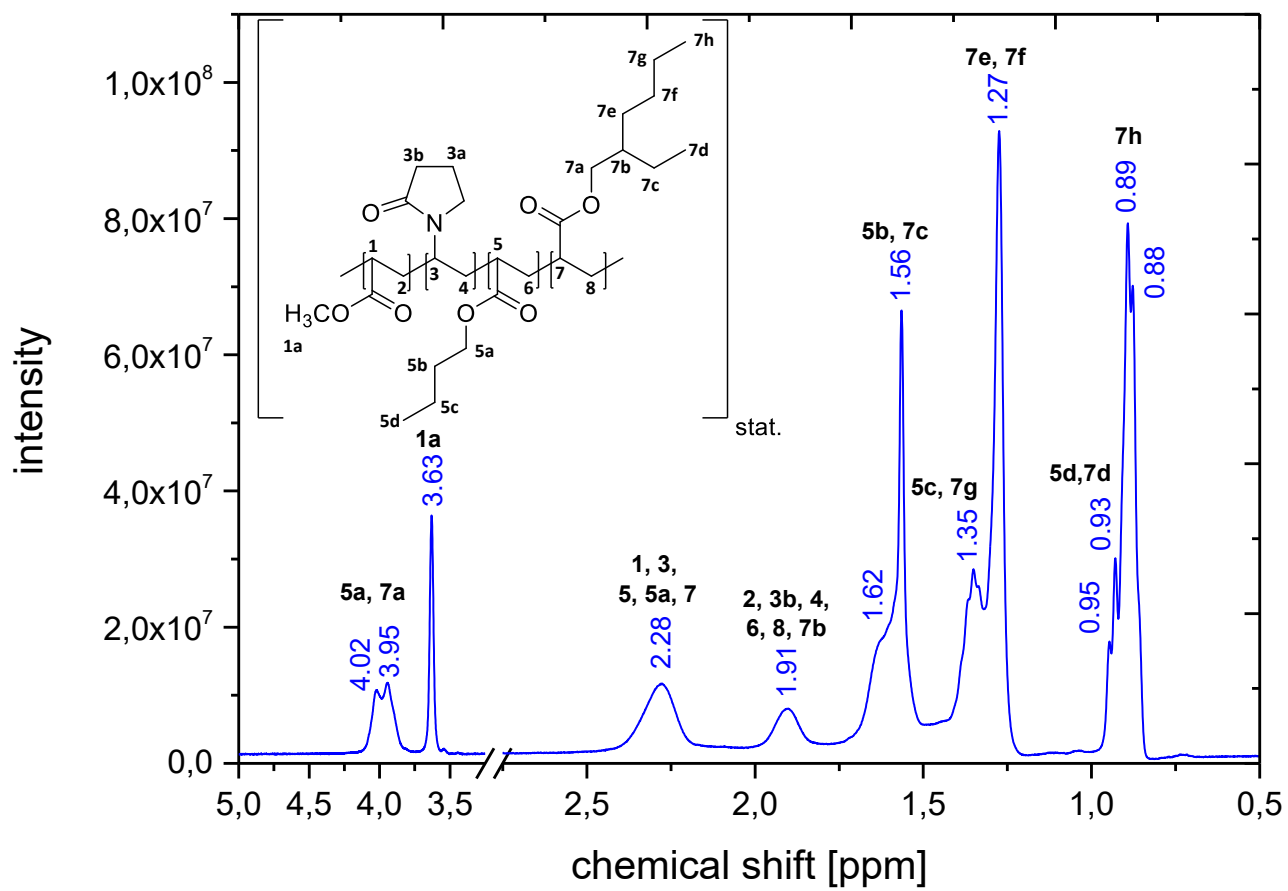


Figure_A 1: ATR-FT-IR spectra of (a) acryl_4, (b) acryl_5, (c) acryl_6, and (d) acryl_1_scf

Figure_A 2 and Figure_A 3 show the ¹H-NMR spectra of the synthesized copolymers acryl_5 and acryl_6.

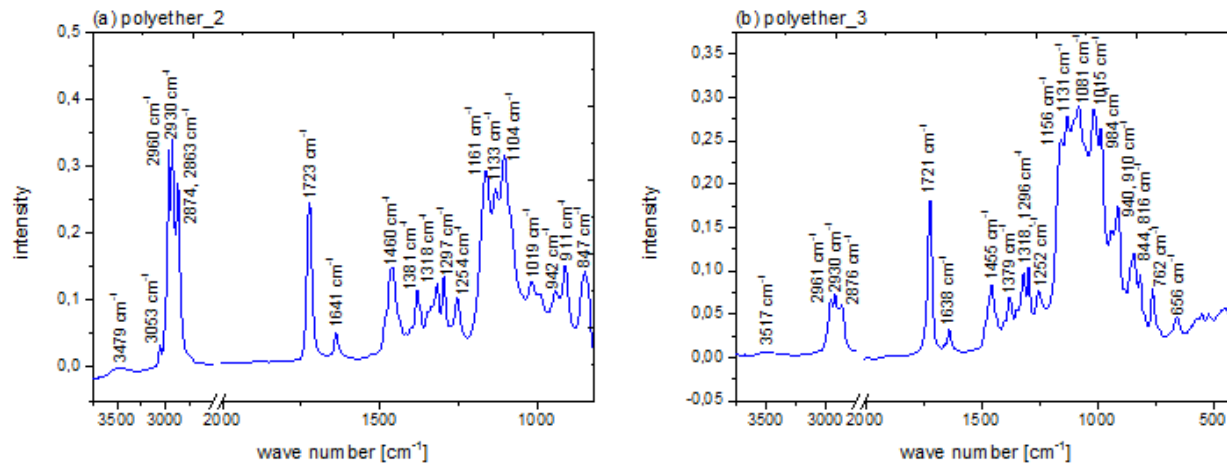


Figure_A 2: ¹H-NMR spectrum of acryl_5

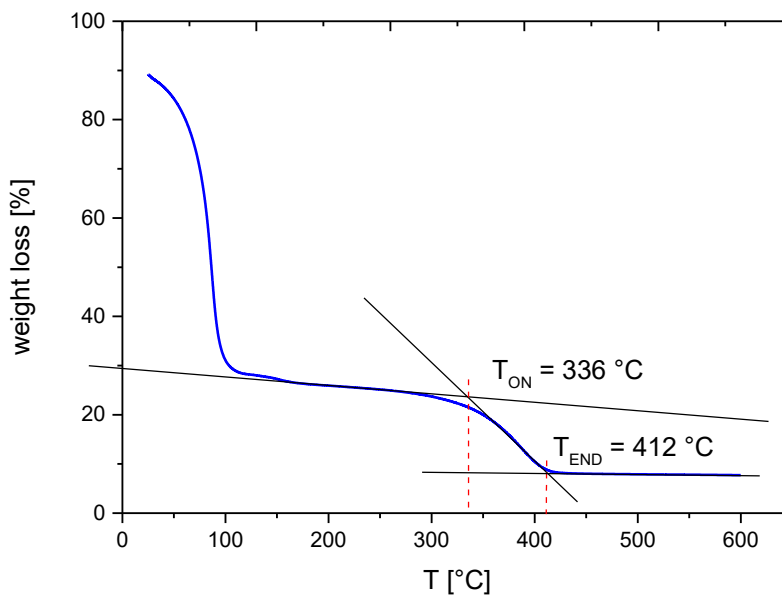


Figure_A 3: ¹H NMR spectrum of acryl_6

Figure_A 4 shows the FT-IR spectra of the synthesized polyether copolymers polyether_1, polyether_2 and polyether_3.

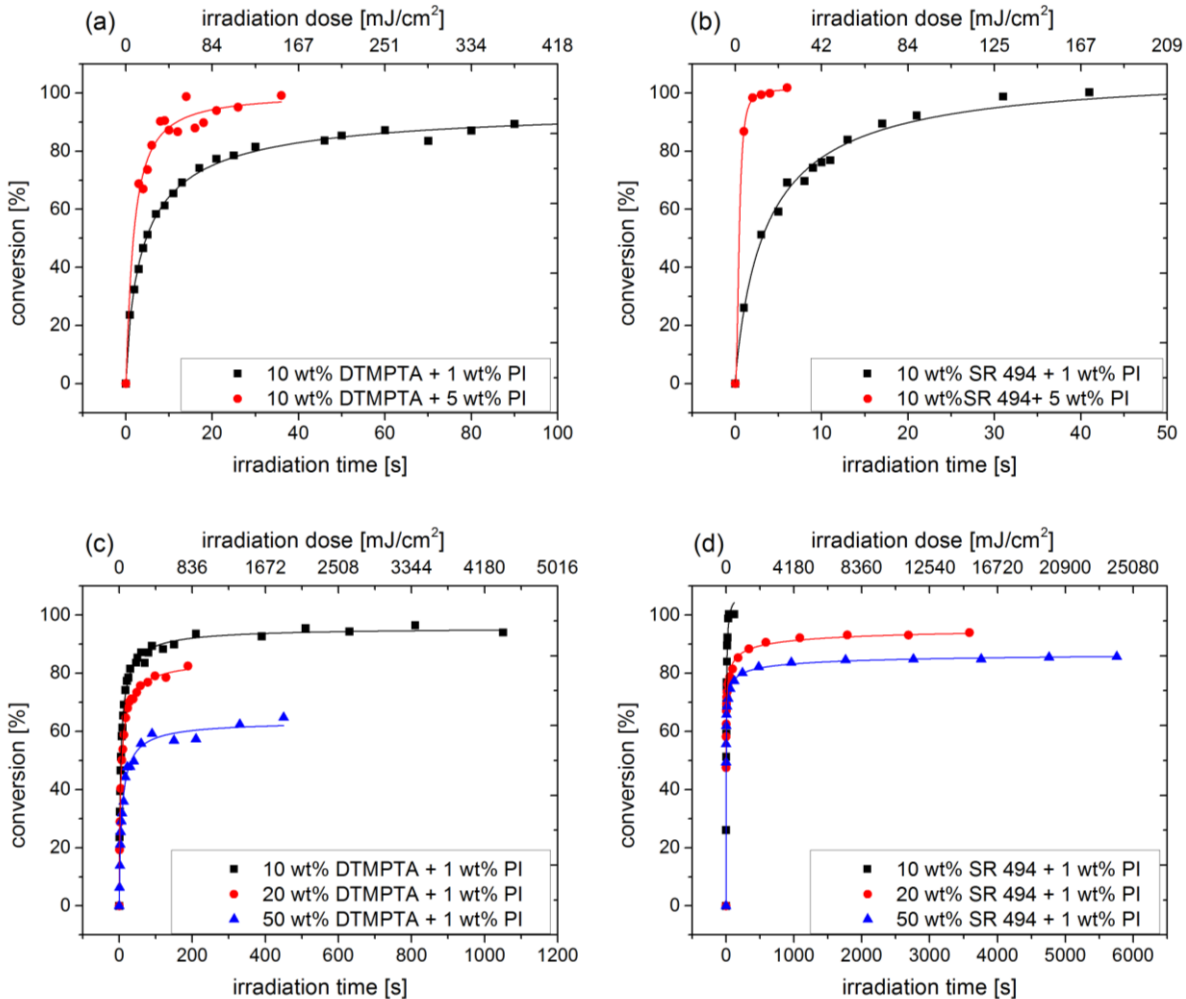


Figure_A 4: FT-IR spectra of (a) polyether_2 and (b) polyether_3



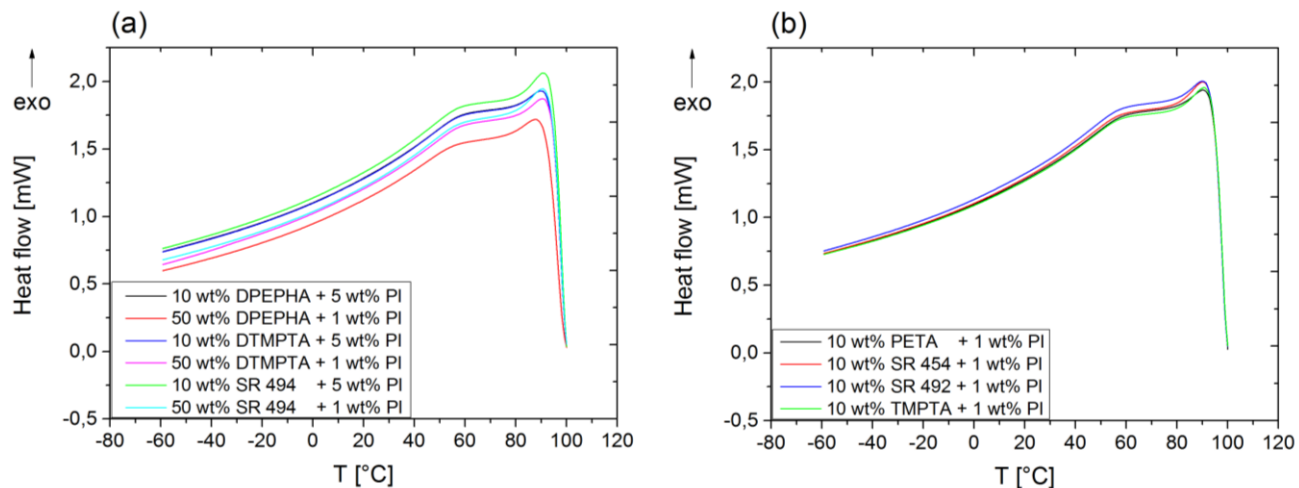
Figure_A 5: Weight loss curve of polyether_1 and determination of the degradation onset and end temperature

Figure_A 6 shows the effect of monomer and PI concentration on the C=C double bond conversion in adhesive layers based on acryl_1 and DTMPTA or SR 494, respectively.



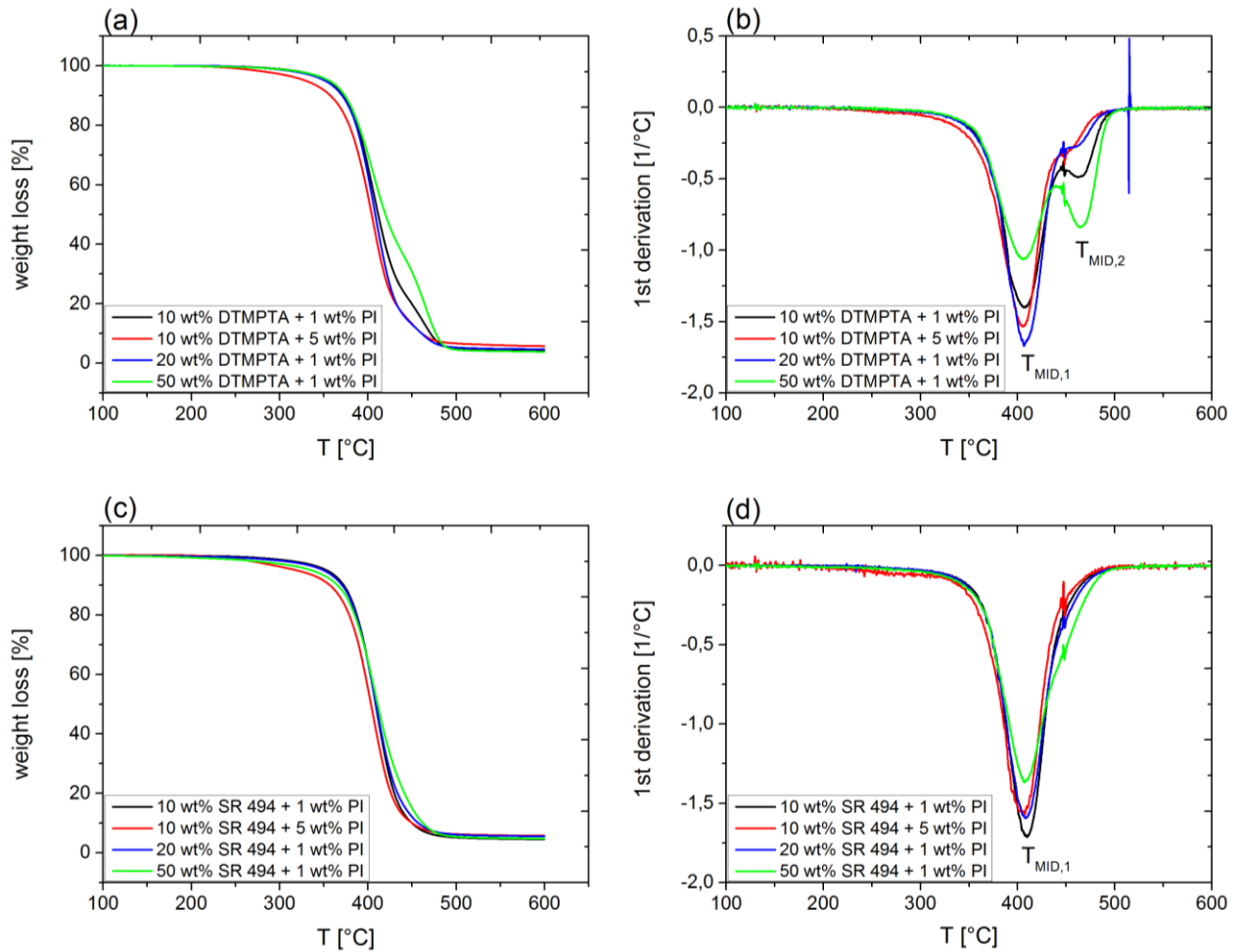
Figure_A 6: (a) Conversion of C=C double bonds in adhesive layers based on acryl_1 containing as a function of the photoinitiator concentration at a constant DTMPTA concentration of 10 wt%. (b) Conversion of C=C double bonds in adhesive layers based on acryl_1 containing as a function of the photoinitiator concentration at a constant concentration of 10 wt% SR 494. (c) Conversion of C=C double bonds in adhesive layers based on acryl_1 as a function of the DTMPTA concentration at a photoinitiator concentration of 1 wt%. (d) Conversion of C=C double bonds in adhesive layers based on acryl_1 as a function of the concentration of SR 494 at a photoinitiator concentration of 1 wt%.

Figure_A 7 displays the influence of the monomer type and content as well as the PI concentration on the T_g of the cured adhesive formulations.



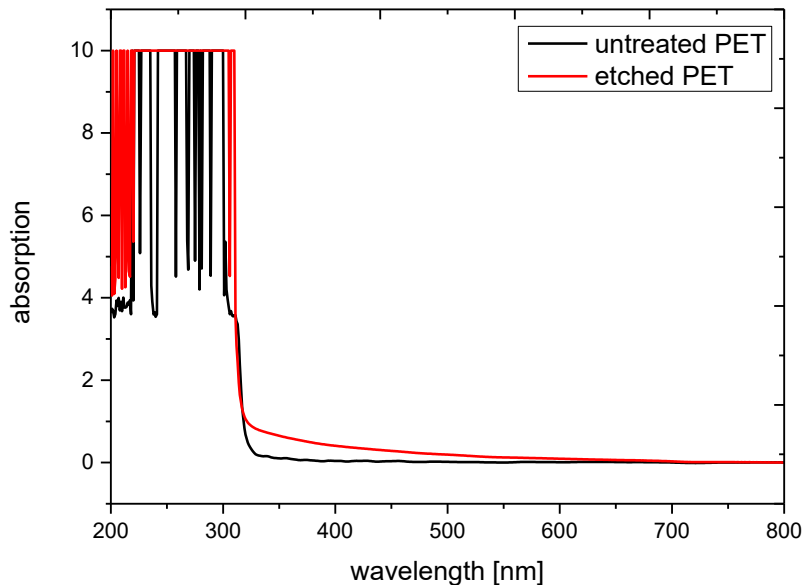
Figure_A 7: DSC measurements of different adhesive mixtures monitoring (a) the impact of the monomer : PI ratio and (b) the impact of the type of multifunctional acrylate

Figure_A 8 shows the thermograms and the corresponding first derivatives of the DTMPA and SR 494 adhesives, which were investigated by TGA measurements with regard to their thermal stability.



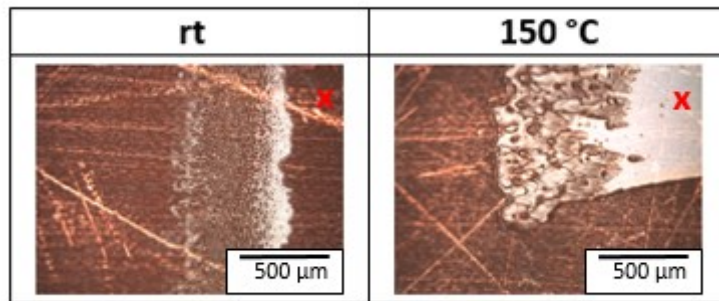
Figure_A 8: (a) Thermograms of DTMPA adhesives as a function of monomer and PI content. (b) First derivative of the temperature-weight-loss curves of the DTMPA adhesives. (c) Thermograms of SR 494 adhesives as a function of monomer and PI content. (d) First derivative of the temperature-weight-loss curves of the SR 494 adhesives.

Figure_A 9 shows the UV-VIS absorption spectra of the untreated and the chemically etched PET carriers.



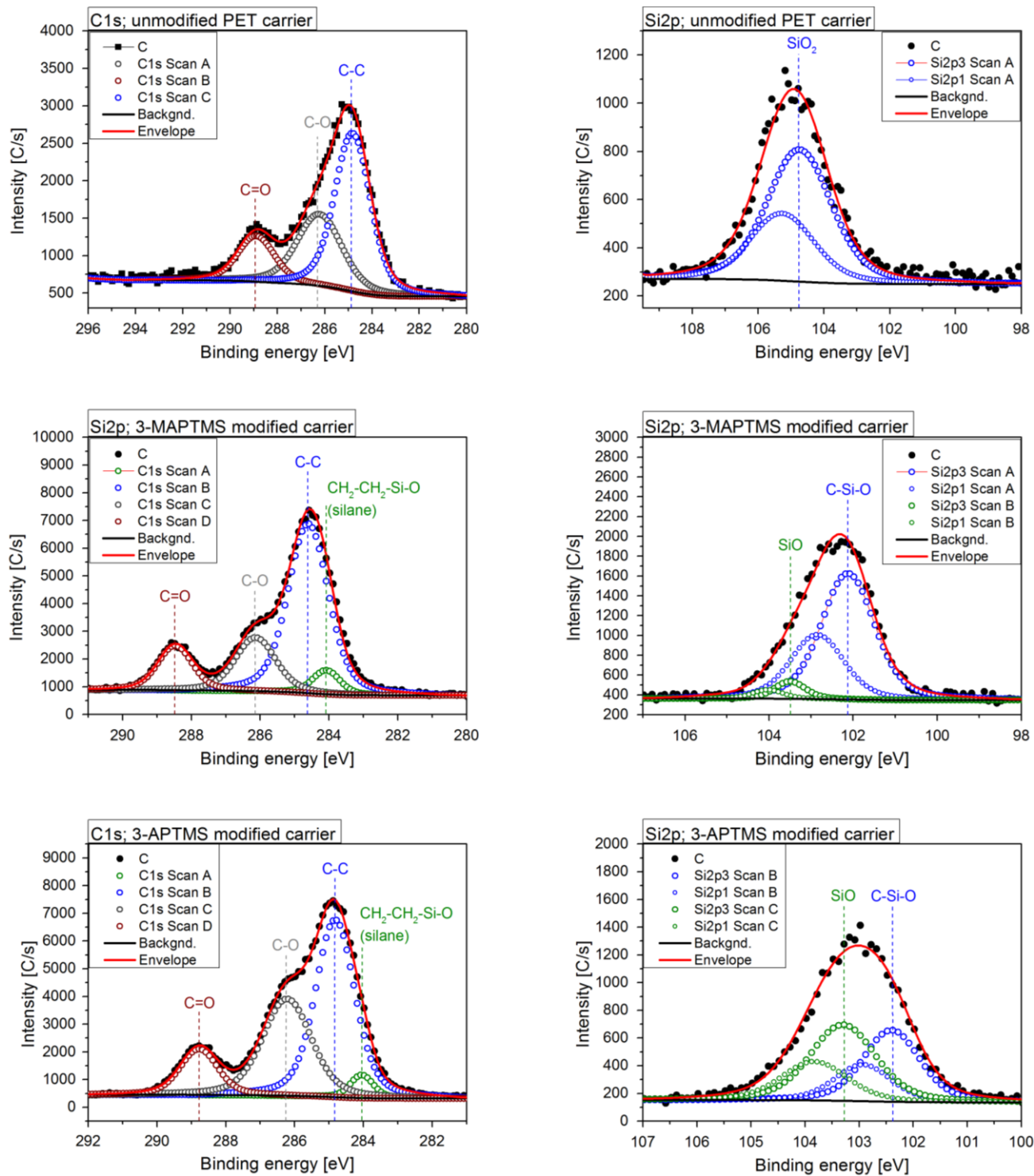
Figure_A 9: Absorption spectra of the untreated and the chemically etched PET carrier

Figure_A 10 illustrates the removalability of tapes containing aromatic multifunctional acrylates from BondFilm® substrates after adhesion at rt and storage at 150 °C.



Figure_A 10: BondFilm® substrates after removal of tapes based on acryl_1 and 50 wt% SR 480 and 5 wt% Lucirin TPO-L, which had been adhered at rt or stored at 150 °C

Figure_A 11 shows the deconvoluted XPS high resolution C1s and Sip2 spectra of the unmodified, the 3-MAPTMS and the 3-APTMS modified carriers.



Figure_A 11: Deconvoluted XPS high resolution C1s and Sip2 spectra of the unmodified, 3-MAPTMS and 3-APTMS modified carriers

Table_A 1 lists the glass transition temperatures of the acrylic monomers, which were used in the synthesis of acryl_1-acryl_6.

Table_A 1: Glass transition temperatures of the acrylic compounds applied in the synthesis of the basic adhesive copolymers [120,127,132,178]

Homopolymer	<i>T_g</i> [°C]
2-EHA	-50
MA	10
BA	-54
AA	105
VP	54
EGPEA	5
VMA	no information available
IBA	94

-Appendix-

Table_A 2 summarizes the results of the characterization of acryl_1, acryl_4, acryl_5 and acryl_6 by FT-IR-spectroscopy.

Table_A 2: List of FT-IR bands of acryl_1, acryl_4, acryl_5, acryl_6 and acryl_1_scf including peak assignment[139]

FT-IR Peaks [cm ⁻¹]					
Peak assignment	acryl_1	acryl_4	acryl_5	acryl_6	acryl_1_scf
-OH, stretch					3389
CH, stretch (aliphatic)	3000-2800	3000-2800	3000-2800	3000-2800	3000-2800
C=O, stretch	1731	1734	1733	1733	1736
C=C, stretch	1645	1647	1645	1698	1664
C=O, stretch of carboxylic acid salt					1574
HCH, bend	1450 1380, 1336	1460 1386	1453 1380	1451 1380	1459, 1413 1366
HCH, bend	1242	1229	1235	1236	1262
C-O-C, stretch	1159	1161 1132	1159	1160	1165
C-O-C, stretch	1117 1062 1034	1030	1117 1051	1118 1064 1034	1132-1018
C=CH, deformation	961 907	974	968	963 906	974
	829	874	839	829	844
	768	762	768	768	
-(CH₂)_{n>3}	729		729	729	725

Table_A 3 summarizes the results of the characterization of polyether_1-3 by FT-IR-spectroscopy.

Table_A 3: List of FT-IR bands of polyether_1, polyether_2 and polyether_3 including peak assignment [139]

Peak assignment	FT-IR Peaks [cm ⁻¹]		
	polyether_1	polyether_2	polyether_3
-OH, stretch	3425	3479	3517
CH, stretch (aliphatic)	2939	3000-2800	3000-2800
C=O, stretch	1710	1723	1721
C=C, stretch	1641	1641	1638
HCH, bend	1458	1460	1455
	1366	1381, 1318	1379, 1318
HCH, bend	1249	1279, 1254	1252
C-O-C, stretch	1171	1161	1156
	1129	1133	1131
		1104	
	1045	1019	1015
C=CH, deformation	945	942	984
		911	910
	861	847	844
	819		816
	766		762
-(CH₂)_{n>3}	659		656

-Appendix-

The UV-doses, which were applied during pre-crosslinking and UV-release in experiments displaying the impact of the PI-concentration on PSA tape performance, are listed in Table_A 4.

Table_A 4: UV-doses for pre-crosslinking and photo triggered release applied in the experiments which displayed the impact of the PI concentration on PSA tape performance

multifunctional acrylate	PI concentration	UV-dose [mJ/cm ²]	
		pre-crosslinking	release
DTMPTA	0.5	80	7750
	0.75	80	7750
	1	1550	7750
	5	/	/
DPEPHA	0.5	80	1000
	0.75	80	1000
	1	200	1550
	5	1550	7750